Evaluation of Electroless Nickel-Phosphorus (EN) Coatings

A Thesis Submitted to the College of

Graduate Studies and Research

in Partial Fulfillment of the Requirements

for the Degree of Doctor of Philosophy

in the Department of Mechanical Engineering

University of Saskatchewan

Saskatoon

By

Ray Taheri

Spring 2003

Permission to Use

In presenting this thesis in partial fulfillment of the requirements for a Postgraduate degree from the University of Saskatchewan, I agree that the Libraries of this University may make it freely available for inspection. I further agree that permission for copying of this thesis in any manner, in whole or in part, for scholarly purposes may be granted by the professor or professors who supervised my thesis work or, in their absence, by the Head of the Department or the Dean of the College in which my thesis work was done. It is understood that any copying or publication or use of this thesis or parts thereof for financial gain shall not be allowed without my written permission. It is also understood that due recognition shall be given to me and to the University of Saskatchewan in any scholarly use which may be made of any material in my thesis.

Requests for permission to copy or to make other use of material in this thesis in whole or part should be addressed to:

Head of the Department of Mechanical Engineering
University of Saskatchewan
Saskatoon, Saskatchewan
57 Campus Drive
Saskatoon, SK,
Canada, S7N 1L6

Abstract

The utilization of Electroless Nickel-Phosphorus (EN) coatings has witnessed a staggering increase during the last two decades. Many outstanding characteristics of the EN coating method have generated a lot of interest in various industries including oil and gas, electronic, chemical, automotive, aerospace, and mining. Some of the highlighted characteristics of EN coatings are superior corrosion and wear resistance especially in environments containing H_2S and CO_2, superior mechanical properties, uniform coating thickness, excellent surface finish properties, superb adhesion characteristics, and wide range of thickness.

The EN coating process is based on a redox reaction in which a reducing agent is oxidized and Ni^{+2} ions are reduced on the surface of the substrate materials. Once the first layer of Ni is deposited, it acts as a catalyst for the process. Consequently, a linear relationship between coating thickness and time usually occurs. If the reducing agent is sodium hypophosphite, the deposit obtained will be a nickel-phosphorus alloy.

The objective of this research was to evaluate various properties of three types of EN coatings, namely, low, medium, and high phosphorus. In the first phase of this work an automated prototype EN bath was designed and engineered. As a result, three types of EN coatings were deposited on various substrates. In the second phase of this research, various qualitative and quantitive methods were implemented to evaluate various properties of EN coatings. Also, the effects of various coating parameters including coating thickness and phosphorus content on properties of EN coatings were comprehensively investigated. Furthermore, the effect of post heat treatment on various properties of EN coatings was studied. Heat treatment on EN deposits in the range of 300-400 °C for one hour caused the hardness to increase due to the formation of various types of nickel phosphide (Ni_xP_y).

The results of this study showed that various properties of EN coatings are directly related to the phosphorus content of the coatings. EN coatings with lower phosphorus content are crystalline, hard and brittle. As a result, they have superior wear resistance. On the other hand, EN coatings with higher phosphorus content are amorphous with superior corrosion resistance.

EN coatings in general have excellent adhesion properties. However, the degree of adhesion is affected by several parameters including coating thickness, phosphorus content, post heat treatment, and ductility of the substrate. Moreover, it was shown that due their brittle nature EN coatings in general and heat-treated low phosphorus EN coating in particular have a detrimental effect on fatigue properties of their substrates.

It was also shown that EN coatings in general, improve the kinetic coefficient of friction. In other words, EN coatings exhibit a self-lubricating behavior. Also, it was shown that EN coatings completely follow the surface profile of their substrate unlike conventional electroplating.

Corrosion and wear studies on EN coatings revealed that EN coatings are excellent candidates for materials subjected to excessive corrosion and wear in a potash brine environment.

Finally, the microstructure study of EN coatings using TEM and STEM electron microscopy revealed valuable information regarding the phase transformation during the heat treatment. It was shown that heat treatment at 400°C for one hour caused the precipitation of various nickel phosphide particles. As a result, significant changes in various properties of EN coatings occurred.

Acknowledgements

The author would like to express his attitude of gratitude toward his supervisor, Prof. Spiro Yannacopoulos for his non-stop guidance, support, and inspiration throughout the course of the last six years. Also, the author would like to thank Professors Barry Hertz[1], Colin Sargent[2], Leon D. Wegner[3], and I.N.A. Oguocha[4] for their guidance and support during the completion of this work.

The author wishes to express his appreciation to Mr. H.J. Steinmetz[5] and other lab technicians, departments of Mechanical and Chemical Engineering, University of Saskatchewan, for their valuable technical assistances in various segments of this work.

Finally, the author would like to acknowledge the Potash Corporation of Saskatchewan (PCS) and the Natural Sciences and Engineering Research Council (NSERC) for their financial support.

May God bless them all.

[1] Prof., Department of Mechanical Engineering, University of Saskatchewan
[2] Prof., Department of Mechanical Engineering, University of Saskatchewan
[3] Prof., Department of Civil Engineering, University of Saskatchewan
[4] Prof., Department of Mechanical Engineering, University of Saskatchewan
[5] Advance machine shop, Department of Mechanical Engineering, University of Saskatchewan

Dedication

I would like to dedicate my thesis to my family especially my mother whose unbelievable endurance, unconditional love, and untouchable devotion have been monumental. Also, I would like to dedicate this work to anyone who has ever taught me anything. Finally, I would like to dedicate this work to all those who have devoted their lives to bring the faded light of ambiguity to the complete shininess of clarity.

"He who has ever taught me anything shall always remain my master"

Imam Ali

Table of Contents

List of Tables

List of Figures

Nomenclature

C_x	Concentration at distance x
C_{Red}	Concentration of reducing agent
C_O	Concentration at initial stage,
$C_{Ni^{2+}}$	Concentration of nickel in the solution
C_s	Concentration of solute
n_1	Agitation factor
D_o	Temperature independent pre-exponential ($\frac{m^2}{S}$)
a	Acceleration
AS	As-plated
ATC	Automatic Temperature Compensation
C&W	Corrosion and Wear
CIDV	Crack Initiations Deflection Value
CORR	Corrodkote corrosion (test)
CTE	Coefficient of Thermal Expansion
D	Deposition rate
DSC	Differential Scanning Calorimetric
E	Modulus of Elasticity
E_C	Activation Energy for Crystallization of EN Deposits (J)
EDS	Energy Dispersive Spectroscopy
EIS	Electro Impedance Spectroscopy
EN	Electroless Nickel Phopshorus

EP	Electroplating
F_1	Wetting force at 2s
FCC	Face Centered Cubic
F_{max}	Maximum wetting force
g	Gravitational acceleration constant (9.81 ms^{-2})
HP	High phosphorus
HT	Heat-treated
HV	Vickers Hardness
KCOF	Kinetic Coefficient of Friction
LP	Low phosphorus
MP	Medium phosphorus
O/V	Bath load
PIPS	Precision Ion Polisher System
P_{max}	Maximum Hertzian contact Stress
PM	Powder Metallurgy
Q	Activation energy for diffusion ($\frac{J}{mol}$ or $\frac{eV}{atom}$)
R	Gas constant (8.31 $\frac{J}{mol-K}$ or $8.62\times10^{-5}\frac{eV}{atom-K}$)
R_a	Surface roughness
Red	Type of reducing agent
RT	Room Temperature
R_z	Surface roughness
s	Second

SD	Saline Droplets corrosion (test)
SEM	Scanning Electron Microscope
STEM	Scanning Transmission Electron Microscope
T	Temperature
TEM	Transmission Electron Microscope
T_p	Temperature where the maximal transformation rate is experienced during DSC scan (K)
TWI	Taber Wear Index
T_{zero}	Zero crossing time
W	Load
Φ	DSC heating rate (K/min)
μ	kinetic COF

1 Introduction

1.1 Background

Electroless nickel plating (EN) is an autocatalytic chemical reduction process in which the reducing agent is oxidized and Ni^{2+} ions are deposited (reduced) on the substrate surface. Once the first layer of Ni is deposited, it acts as a catalyst for the process. For metals that catalyze the electrochemical reaction (e.g. Ni, Co, Cu, and Ag), a linear relationship between coating thickness and time is often obtained [Barker, 1993]. Formaldehyde and sodium hypophosphite are the most widely used reducing agents in electroless plating, whereas borane and hydrazine are employed in special applications. EN coating deposition initiated on the substrate has been reported Homma *et al*. [1990] to proceed in three dimensions (3-D) during the plating process. The 3-D growth of the deposit depends on the rate of plating on each part of the substrate surface. The EN deposition process starts only on the catalytic surface and it involves the diffusion of chemicals to the deposited surface and by-products away from the surface. Hydrogen is one of the by-products evolved from the deposit surface during the electroless plating process.

EN coatings have wide industrial applications owing to their excellent mechanical, physical, electrical, as well as corrosion and wear resistance properties. Other outstanding characteristics of EN coatings include the ability to be applied to a variety of substrate materials and the ability to plate uniformly on intricate part geometries.

1.2 Objectives

The main objectives of this research are to study, evaluate, and compare the various properties of three types of electroless nickel-phosphorus (EN) coatings, namely, low, medium, and high phosphorus. Various conventional techniques such as Differential Scanning Calorimetry (DSC), X-ray diffraction analysis, Energy Dispersive Spectroscopy (EDS), X-ray diffraction pattern analysis, X-ray mapping, three-point bending, fatigue, etc., were implemented to conduct this study. Also, several

apparatuses including the EN bath, three-point bending, reciprocating corrosion and wear, slurry jig, friction ramp, etc, were designed and built in order to conduct the evaluation of various properties of EN coatings, including adhesion, corrosion and wear, and tribological properties. The work conducted can be divided into two phases.

In the first phase, comprising early stages of this research, an automated prototype EN bath was designed and built. As a result, three types of EN coatings had been deposited on various substrates under a fully controlled bath condition; temperature, pH, filtration, agitation, etc.

In the second phase of this research various physical, mechanical, tribological, corrosion and wear, and microstructural properties of three types of EN coatings were comprehensively investigated. In the physical properties evaluation part of this work, coefficient of friction, surface morphology, elemental analysis (X-ray diffraction and EDS analysis), and phase transformation characteristics during heat treatment (DCS analysis) were studied. In evaluating the mechanical properties of EN coatings, fatigue behavior, hardness, tensile strength, and bending characteristics were studied. Corrosion and wear (C&W) resistance of various EN coatings were studied by means of a reciprocating wear experiment in saturated potash brine as well as a slurry erosion–corrosion experiment. Finally, the microstructures of three types of EN coatings (as-plated and heat-treated) were studied using optical microscope, SEM, and TEM. Various methods including X-ray diffraction pattern, X-ray spot and mapping analysis were conducted to study the microstructure of EN coatings and to identify the existing phases. The experimental program is schematically shown in Figure 1.1.

1.3 Thesis outline

The material in this thesis is divided into five chapters. Chapter One, introduction, Chapter Two, a comprehensive literature review on EN coatings, discusses history, mechanisms, and various properties of EN coatings. Apparatuses and experimental procedures are discussed in Chapter Three. Chapter Four is allocated to present the results obtained and discussion. Chapter Five presents the conclusions obtained, and includes recommendations and possible future research work.

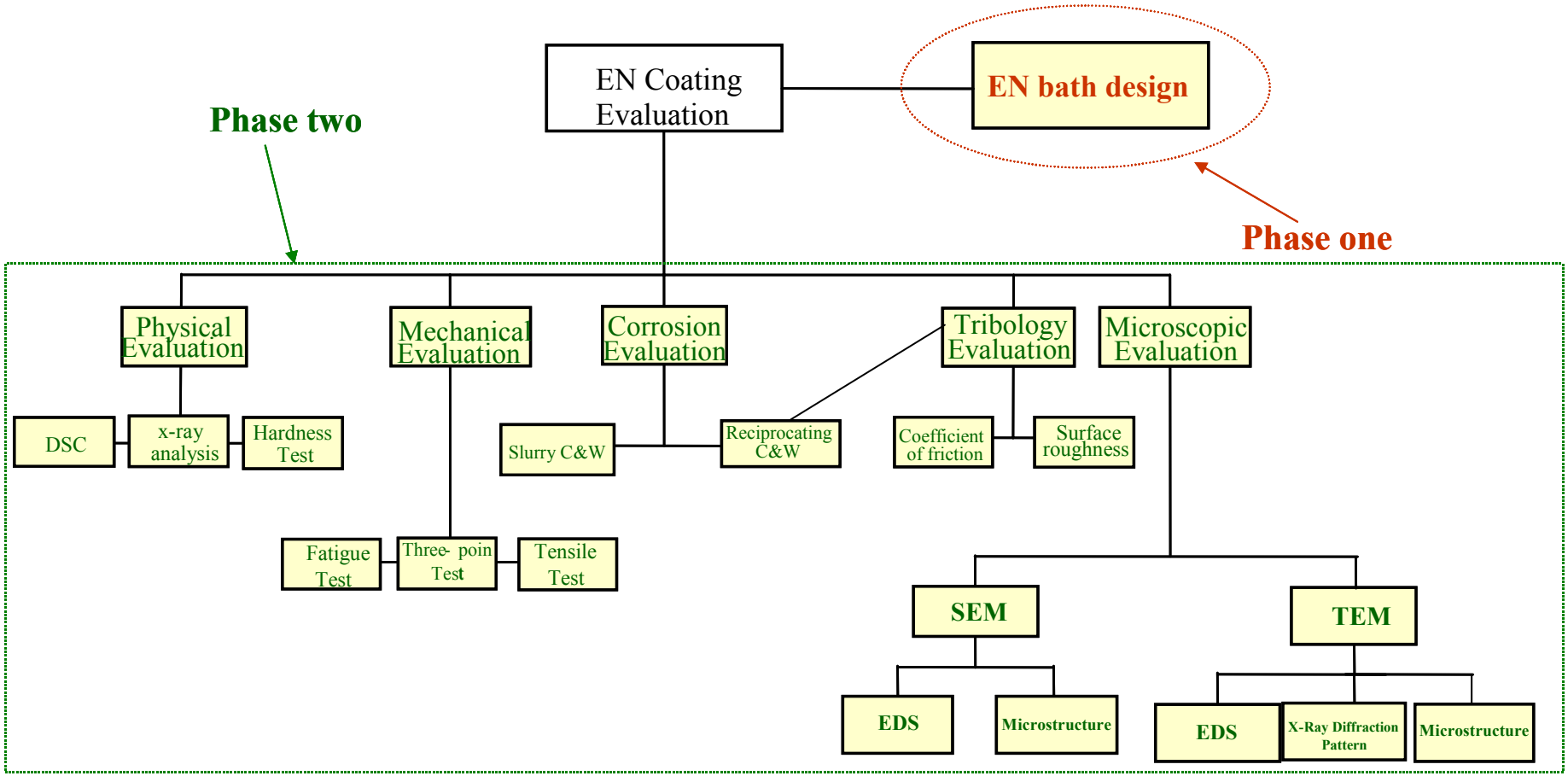

Figure 1.1. Outline of the research study on EN coatings.

2 Literature Review

2.1 Background

Electroless Nickel-Phosphorus (EN) coatings have been used increasingly in various industries since the early 1980's. Some of the outstanding characteristics of these coatings are superior corrosion and wear resistance, excellent uniformity, wide range of thickness as well as mechanical and physical properties, good solderability, and surface lubricity [Baudrand, 1978]. They are widely used either as protective or decorative coatings in many industries, including petroleum, chemical, plastic, optics, printing, mining, aerospace, nuclear, automotive, electronics, computer, textile, paper, and food [Parker, 1972]. In addition, compared to conventional electroplating methods, EN coatings can be applied on different substrates (conductive and non-conductive) since no external current is applied to the component [Khoperia et al., 1997;Gemmler et al. 1990; and Gawne and Ma, 1987].

Although EN coatings are fairly new, the discovery of the fact that nickel could be deposited on a surface from an aqueous solution of its salt by reduction with hypophosphite was made by Waltz in 1844 [Dang and Moller, 1993]. Due to the poor quality of the reducing agents that leads to rough deposits with inferior properties, Waltz's idea was not developed for a whole century. In 1944, the first laboratory experiment reported on EN was completed by Brenner and Riddel, who were later given credit for introducing the EN method to the world [Mandich and Krulik, 1993]. Since then, there have been many advances in the EN method. Nowadays, EN is no longer a single type of coating but an entire family of coatings [Stevenson, 1992].

Figure 2.1 illustrates the EN family tree. As shown, there are various types of EN coatings, including ternary alloy and composite coatings. The diversity of the EN method has resulted in a wide range of its applications in various industries.

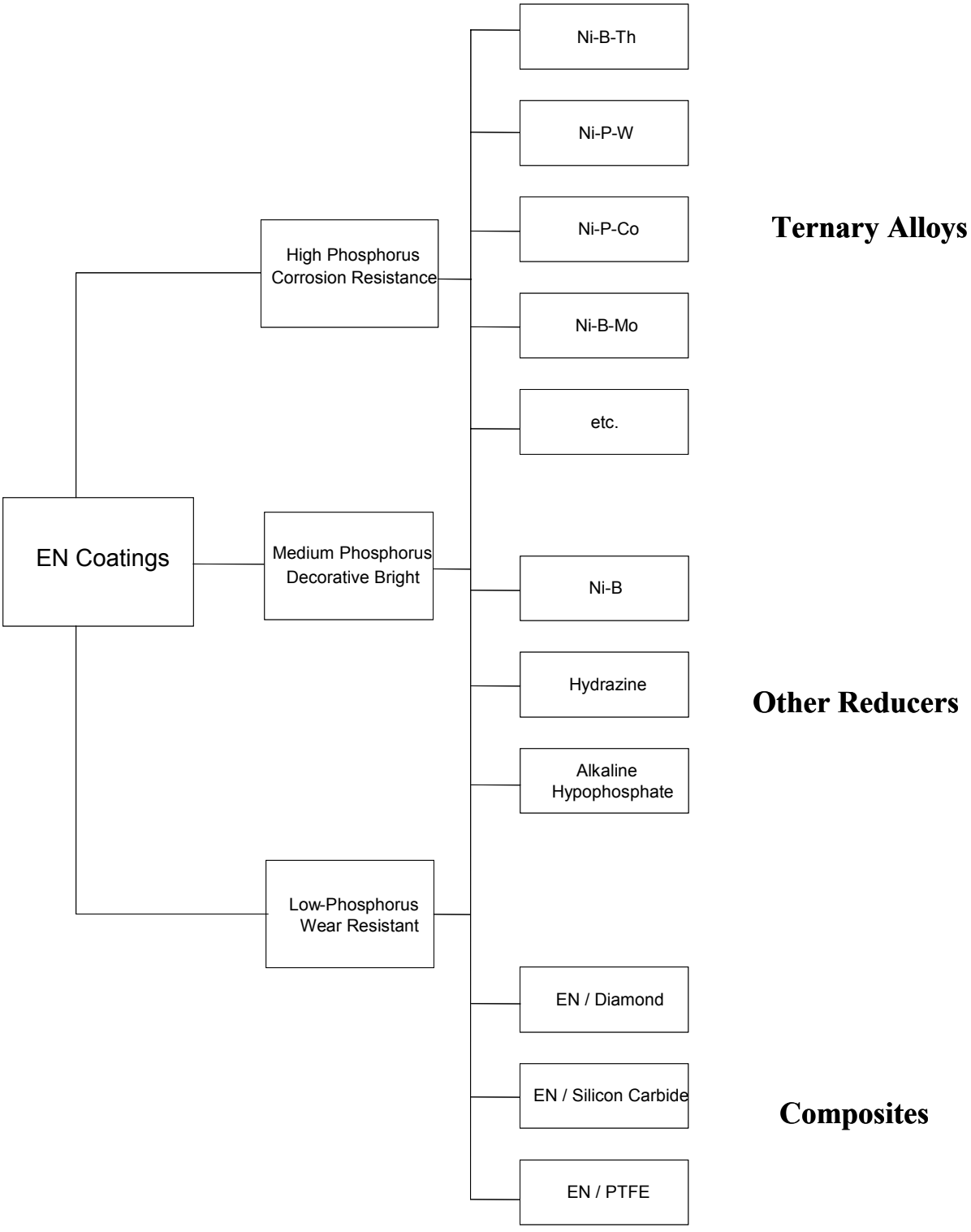

Figure 2.1. Electroless plating family tree [Stevenson, 1992].

2.2 Chemical reactions

Electroless Nickel deposit, EN, is defined as the autocatalytic deposition (reduction) of Ni ions in the presence of a reducing agent (hypophosphite, aminoborane or borohydride). It is often mistaken for two other commercial nickel-plating methods, immersion and vapor decomposition of nickel carbonyl. Immersion deposition (at 70°C) provides a poor adherent and non-protective coating while vapor decomposition (at 180°C) is expensive and hazardous [Baudrand, 1978]. Consequently, EN has gained wide acceptance in many industries.

Hypophosphite baths are the most common types of commercially used EN baths. The mechanism of the electroless Ni-P deposition reactions taking place in the hypophosphite bath [Lukes, 1964; and Donahue and Yu, 1970] is not well understood, but it has been postulated that it occurs in microcells of alternating anodic/cathodic polarity on the surface of the substrate. However, the occurrence of the following reactions is most definite [Reidel, 1997]:

$$3NaH_2PO_2 + 3H_2O + NiSO_4 \longrightarrow 3NaH_2PO_3 + H_2SO_4 + 2H_2 + Ni \qquad (2.1)$$

$$2H_2PO_2^- + Ni^{++} + 2H_2O \longrightarrow 2H_2PO_3^- + H_2 + 2H^+ + Ni \qquad (2.2)$$

$$Ni^{++} + H_2PO_2^- + H_2O \longrightarrow Ni^o + H_2PO_3^- + 2H^+ \qquad (2.3)$$

$$H_2PO_2^- + \frac{1}{2}H_2 \longrightarrow H_2O + OH^- + P \qquad (2.4)$$

$$3H_2PO_2^- \longrightarrow H_2PO_3^- + H_2O + 2OH^- + 2P \qquad (2.5)$$

Reaction (2.3), the simplified form of reactions (2.1) and (2.2), corresponds to nickel reduction while reaction (2.5) (a simplified form of reaction 2.4) corresponds to phosphorus reduction.

The aforementioned reactions can be described as the following separate reactions [Mainier and Araujo,1994]:

$$H_2PO_2^- + H_2O \longrightarrow H^+ + HPO_3^{-2} + 2H \quad (2.6)$$

$$Ni^{2+} + 2H \longrightarrow Ni + 2H^+ \quad (2.7)$$

$$H_2PO_2^- + H \longrightarrow P + OH^- + H_2O \quad (2.8)$$

$$H_2PO_2^- + H_2O \longrightarrow H^+ + HPO_3^{-2} + H_2 \quad (2.9)$$

$$Ni^{2+} + H_2PO_3^{2-} + \longrightarrow NiHPO_3 \quad (2.10)$$

Reactions (2.6) to (2.8) are responsible for the formation of the Ni-P alloy coating. In reactions (2.7) and (2.8), the H_{ads}[1] produced is consumed and Ni and P are deposited. Not all of the reactions occurring in the bath are favorable to EN deposition. Reactions (2.9) and (2.10) are deleterious to the deposition. In reaction (2.9), hypophosphite forms molecular hydrogen instead of atomic hydrogen, which diminishes the reducing power. As a result of reaction (2.10), nickel precipitates as nickel orthophosphite. This causes a reduction in the concentration of nickel ions in the bath. Also, the nickel orthophosphite precipitation occurring on the coating surface results in a defective and rough surface [Mainier and Araujo, 1994]. The unwanted occurrence of the reactions (2.9) and (2.10) causes a reduction in the efficiency of the EN coating deposition process.

The vast majority of EN coatings are deposited by catalytic reduction of nickel ions with sodium hypophosphite (NaH_2PO_2). From published tables of standard electrode potentials, the hypophosphite ion ($H_2PO_2^-$) has a redox potential of –0.5V and so, theoretically, is strongly reducing to nickel ions (-0.25V) under standard conditions [Barker, 1993 and Gawne and Ma, 1987]. Curiously, at normal bath conditions there is no reduction of nickel ions by hypophosphite despite the significant thermodynamic driving force derivable from the standard electrode potentials [Gemmler et al., 1990]. This is due to the fact that hypophosphite ions possess a remarkable inertia towards electrochemical oxidation in aqueous solutions [Hickling and Johnson, 1967 and

[1] Hydrogen adsorbed in form of atoms prior to the formation of hydrogen molecule.

Salvago and Cavalotti, 1972]. However, on specific surfaces that act as catalysts, nickel ions are reduced by hypophosphite and this is the basis for the high throwing power of the EN process. Initiation of deposition occurs readily with metals such as iron, nickel, and cobalt. Once the initial nickel layer has deposited on the catalytic substrate, it acts as a catalyst for the process and the deposition continues to propagate unaided. This is referred to as autocatalysis of the deposition reaction [Barker, 1993]. This unique property of EN plating makes it possible to coat internal surfaces of pipes, valves, nuts and bolts, and other complex geometries that are very difficult or impossible to be coated by conventional electroplating techniques.

In practice, the stoichiometric values are different than what is shown in the aforementioned reactions [Yusis et al., 1989]. This is due to the complexity of the simultaneously occurring reactions during the EN coating. Usually, 10 kg of sodium hypophosphite are required to reduce 2 kg of nickel for an average efficiency of 37% [Gawrilw, 1979].

As can be deduced from reactions (2.3) to (3.5), the result of the EN coating is not pure nickel, unlike for electroplating, but a nickel-phosphorus alloy. The phosphorus content of the deposit defines the physical, mechanical, and corrosion resistance properties of the coating. There are three types of EN coatings commercially available, namely, low, medium, and high phosphorus.

Table 2.1 shows some of the general properties of EN coatings. One of the unique characteristics of the EN process is the dependence of the microstructure on phosphorus content. Duncan has reported that the as-deposited Ni-P alloy possesses a non-equilibrium phase structure [Duncan, 1996]. Generally, it is accepted that a microcrystalline, amorphous, or a co-existence of these two phases can be obtained depending on the phosphorus content [Barker, 1993, 1996; Hur et. al., 1990; Allen and Vander, 1982; Park and Lee, 1988].

Compared to electroplating deposition, layers obtained via the EN process have a very homogeneous distribution regardless of the substrate geometry [Okinaka and Osaka, 1994]. A more detailed discussion on the microstructure of the EN coating will be

presented later (section 3.1.1). In addition to a source of nickel (nickel chloride or sulfide) and a reducing agent (sodium hypophosphite), many other components are required for the occurrence of deposition in the EN bath. A list of the components commercially used in the EN technique is shown in Table 2.2.

One of the most important steps in understanding the EN method is the study of the effective parameters, such as temperature, pH, and bath composition.

Table 2.1. General properties of EN coatings.

Properties	**Value**
Phosphorus Content	5-15% wt.
Specific Gravity	7.75 to 8.25 g/cc
Hardness (as plated)	45 to 50 Rc
Hardness (heat-treated)	60 to 70 Rc
Ductility	Will pass 180° bend test
Color	Bright deposit resembling polished stainless steel

Table 2.2. EN bath components and their function [Reidel, 1997].

Component	**Function**
Nickel Ion	Source of Metal
Hypophosphite	Reducing Agent
Complexants	Stabilizes the solution
Accelerators	Activate Hypophosphite
Buffers	Controlling pH (longer term)
pH regulators	Regulates the pH of the solution
Stabilizer	Prevents solution breakdown
Wetting agents	Increases wettability of surfaces

2.3 Effective Parameters

There are numerous parameters affecting the EN process. The following function, suggested by Riedel [1991], who is one of the pioneers in this field, describes the deposition rate as a function of effective parameters of the EN method:

$$D = F(T, pH, C_{Ni^{2+}}, Red, C_{Red}, O/V, n_1, ...) \quad (2.11)$$

where:

D= Deposition rate

T= Temperature

pH= solution pH

$C_{Ni^{2+}}$ = Concentration of nickel in the solution

Red= Type of the reducing agent

C_{Red} = Concentration of reducing agent

O/V= Bath load

n_1 = Agitation factor

2.3.1 Effect of Temperature

Temperature is the most important parameter affecting the EN deposition rate. Most of the reactions involved in the deposition process are endothermic. As a result, by increasing the temperature the deposition rate increases. Figure 2.2 illustrates the effect of temperature on the deposition rate [Fields, 1984]. As the figure shows, the deposition rate increases with increasing bath temperature. Most of the acidic baths are operated at 80-90°C while the alkaline baths can be operated at lower temperatures (as low as 40°C). This is why alkaline baths are used for coating plastic substrates.

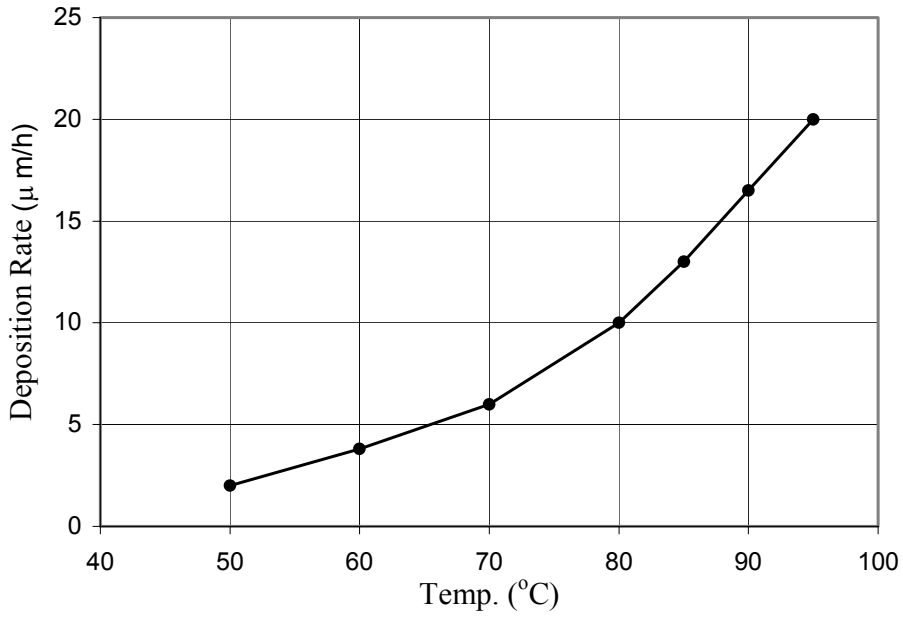

Figure 2.2. Effect of solution temperature on the deposition rate [Fields, 1984].

2.3.2 Effect of pH

Many of the reactions involved in the EN process are sensitive to changes in the pH of the solution. By increasing the pH the nickel-reduction reaction (2.3) is accelerated. On the contrary, by increasing the pH of the solution, the phosphorus reduction is retarded. This is due to the production of hydroxide ions as a result of the phosphorus reduction reaction. Therefore, increasing the pH of the solution decreases the phosphorus content of the coating. Also, since the nickel reduction reaction predominantly controls the deposition rate, increasing the pH of the solution increases the deposition rate. Figure 2.3 illustrates the effect of pH of the solution on both deposition rate and phosphorus content [Fields, 1984].

Raising the bath pH has the following effects [Reidel, 1997];

1. Increasing the deposition rate in an almost linear manner.

2. Modification of the hypophosphite reaction from catalytic to homogeneous. A consequence of this can be spontaneous decomposition of the solution with nickel deposition.

3. Lowering the solubility of the nickel phosphate. Deposition of this unwanted component may initiate decomposition and often leads to rough deposits.

4. Reducing the phosphorus content of the deposit.

Lowering the pH can lead to [Reidel, 1997];

1. Prevention of the deposition of basic salts and hydroxides

2. Lowering the reducing power of the hypophosphite

3. More effective buffering action of species in the bath

At a pH below 4 the deposition occurs at a retarded rate causing a defeated deposition.

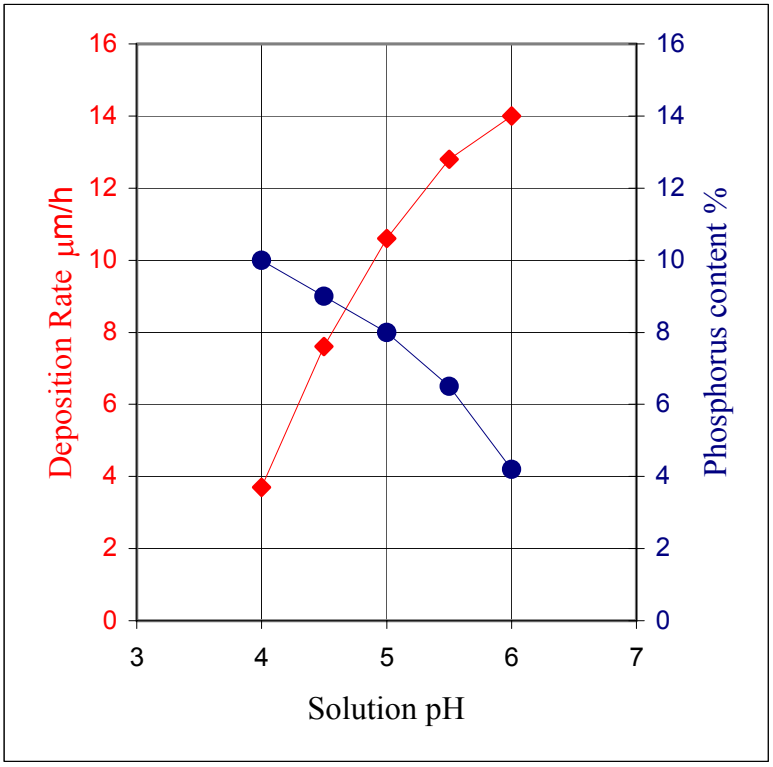

Figure 2.3. Effect on solution pH on deposition rate and phosphorus content of the coating [Fields, 1984].

2.3.3 Effect of Bath Composition

The Ni concentration as well as the $\frac{Ni^{++}}{H_2PO_2^-}$ ratio are two important parameters affecting deposition rate. According to the result of the study done by Riedel [1991]:

a) The concentration of hypophosphite should lie between 0.15 and 0.35 mol/l, and

b) The optimum $\frac{Ni^{++}}{H_2PO_2^-}$ ratio should be maintained between 0.25 and 0.6, preferably between 0.3 to 0.45.

As the following reaction shows, each mole of Ni ion consumes 3 moles of hypophosphite.

$$3NaH_2PO_2 + 3H_2O + NiSO_4 \longrightarrow 3NaH_2PO_3 + H_2SO_4 + 2H_2 + Ni^o \quad \ldots\ldots(2.12)$$

Therefore theoretically, the ideal $\frac{Ni^{++}}{H_2PO_2^-}$ ratio would be 0.33, which is not very far from the measured value of 0.3 to 0.45. As illustrated in Figure 2.4, the highest deposition rate can be obtained when the $\frac{Ni^{++}}{H_2PO_2^-}$ ratio is about 0.45 [Gutezit and Kring, 1959].

If the $\frac{Ni^{++}}{H_2PO_2^-}$ ratio is too low, the lack of Ni ions in the solution causes a brownish coating on the specimen. Also, the lower the value of the $\frac{Ni^{++}}{H_2PO_2^-}$ ratio, the higher is the concentration of the hypophosphite ions and the danger of solution decomposition increases. On the other hand, if the $\frac{Ni^{++}}{H_2PO_2^-}$ ratio is too high, the phosphorus content of the deposition decreases. Also, the coating deposition rate would become rather slow.

Figure 2.5 shows the effect of nickel concentration on the deposition rate [Solowjewe, 1959]. As shown, an optimum amount of nickel concentration is required to obtain the maximum deposition rate in the bath.

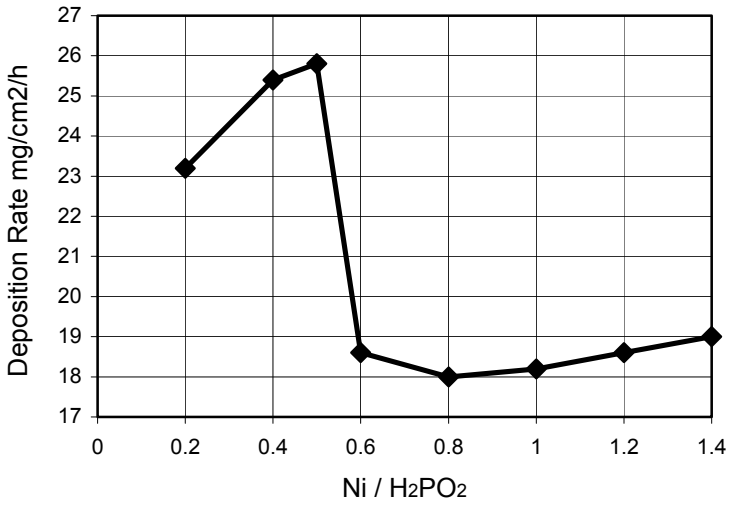

Figure 2.4. Dependence of deposition rate in an acetate-containing solution on the Ni ion: H_2PO_2 ratio. $Na_2H_2PO_2$=0.224 mol/ l Acetate ion = 0.12 mol/l Initial pH=5.5 [Gutzeit and Kring, 1995].

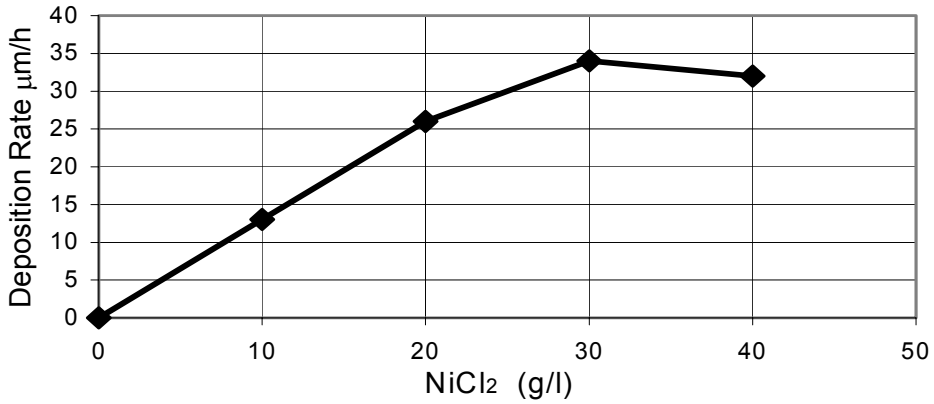

Figure 2.5. Dependence of deposition rate on nickel chloride concentration [Solowjewe, 1959].

As illustrated in Figures 2.4 and 2.5, there is a correlation between the bath composition and the deposition rate. This is why accurate control of the replenishment process is required. Most of the commercially available EN solutions come with replenishment instructions. An analytic titration method with EDTA (ethylene diamine tetra acetic acid) is commonly used to estimate the concentration of nickel as well as hypophosphite and orthophosphite in the bath.

2.3.4 Effect of Bath Loading

Bath loading is a term used to define the ratio of the surface of the working piece to the volume of solution in the tank. Commercial baths are operated in a bath loading range of 0.1 to 1.0 $\frac{\mathrm{dm}^2}{l}$ depending on the bath solution [Reidel, 1997].

Figures 2.6 and 2.7 show the effect of bath load on the deposition rate. As shown, the deposition rate decreases with increasing bath load. Therefore, an optimum bath load is required to provide the acceptable deposition rate as well as bath efficiency.

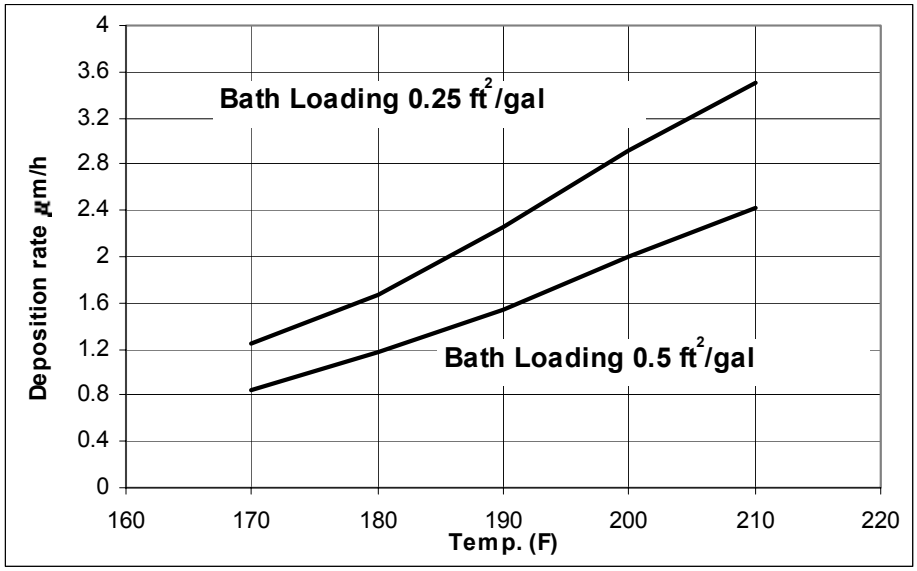

Figure 2.6. Effect of bath load and temperature on deposition rate [MFPP-Process Guide].

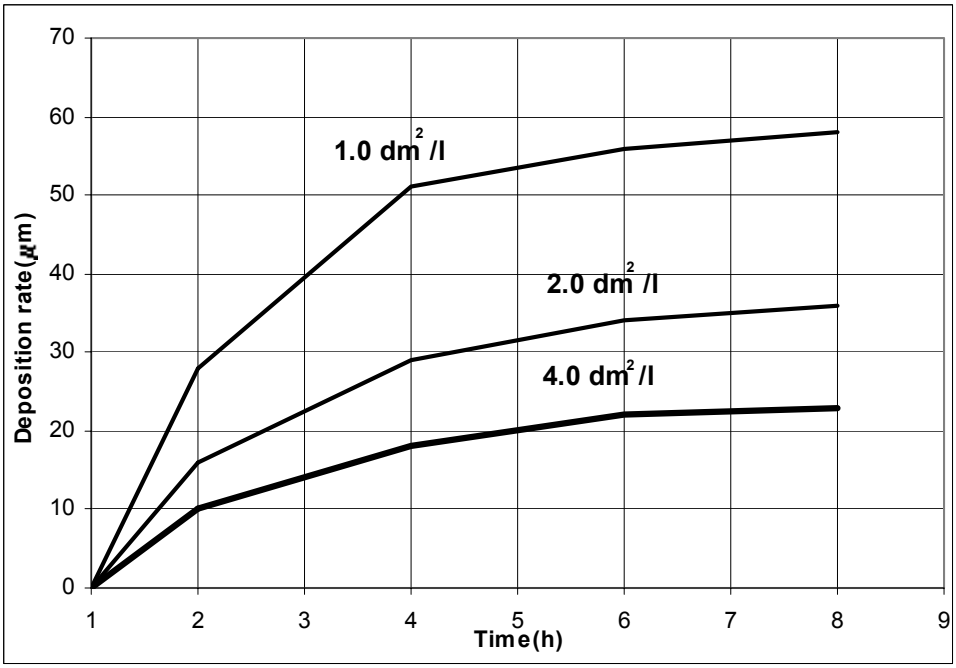

Figure 2.7. Effect of bath load on deposition rate [Grunwald, 1983]

2.3.5 Effect of Bath Age

Electroless nickel baths have a finite life. Bath age is defined in terms of the number of times the entire nickel ion content (g/l) is consumed and replenished. Each such replenishment is called a *turnover*. Typically, a bath contains 6 g/l Ni ion. By the time the amount of Ni ions replaced reaches 30 to 80 g/l, after turnover reaches 5 to 13, the whole bath has to be discarded. By increasing the amount of Ni replaced, the deposition rate and, consequently, the efficiency of the bath decrease.

Bath age has a profound effect on the EN deposit composition as well as other EN properties such as internal stress, ductility, corrosion resistance, and fatigue resistance. Riedel [1997] and Duncan [1983] have separately studied the effect of bath age on the properties of EN coatings. Both of these studies show that after 4 to 5 turnovers, the deposition rate is reduced. Figure 2.8 shows that as the EN bath gets older, the deposition rate decreases. On the other hand, the phosphorus content of the coating increases with bath age [Linka and Riedel, 1986].

The effect of bath age on the properties of EN deposits is minor when up to 5 to 6 turnovers (Figure 2.9). As the bath solution exceeds its sixth turnover the properties of the deposit are deleteriously changed. Some studies have shown that even the phosphorus content stays constant for up to 6 turnovers [Riedel, 1997].

Figure 2.9 shows the effect of bath age on corrosion resistance of high phosphorus EN coating. As shown, after five turnovers the cyclic corrosion resistance of the EN deposit significantly drops. Thus, as a rule of thumb in most of the commercial plating shops, the bath content is replaced with a new solution after the fifth turnover. The bath age also has a pronounced effect on the deposition rate. As shown in Figure 2.10, as the bath gets older the plating rate decreases.

This is due to decomposition of chemicals in the bath including the complexants[2] and accelerators[3].

[2] Complexants prevent excess free Ni ion concentration so stabilizing solution and preventing Ni phosphite precipitation. Also, they act as a pH buffers.

[3] Accelerators activate hypophosphite ions and accelerate deposition.

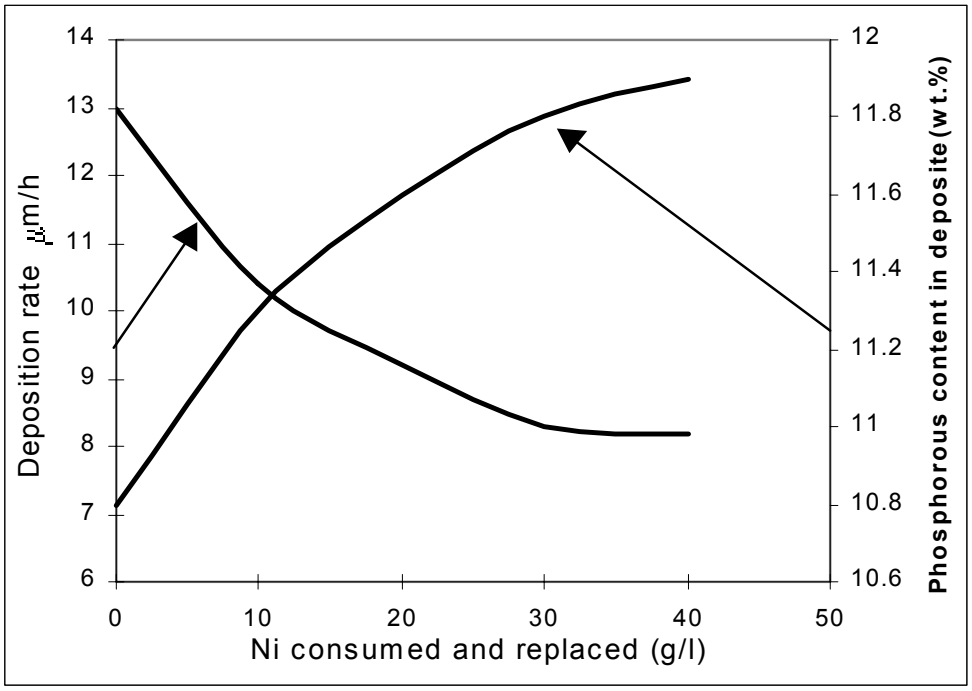

Figure 2.8. Dependence of deposition rate and phosphorous content of the EN coating on the bath age[Linka and Riedel, 1986].

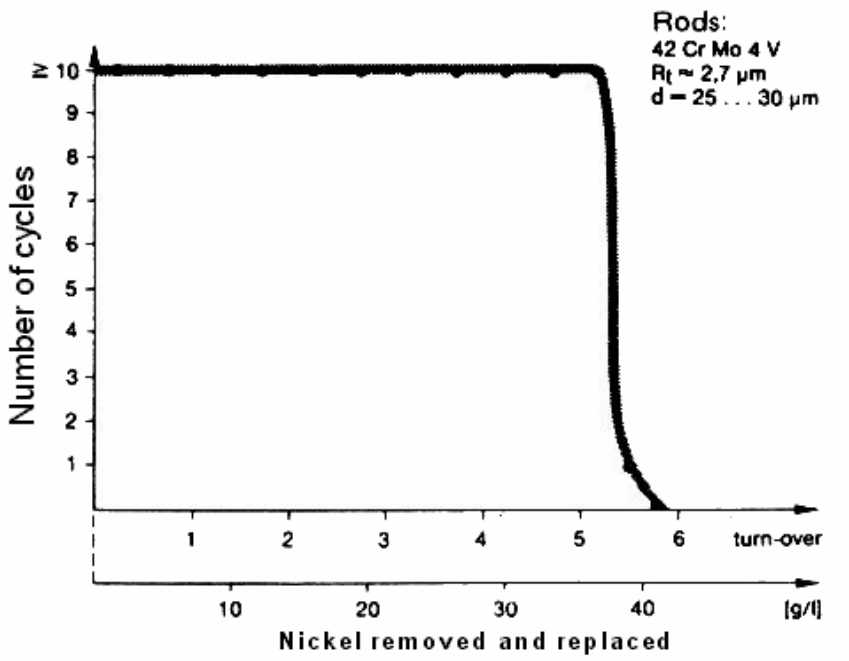

Figure 2.9. Corrosion resistance of Ni-P (12% wt.) deposits of 28 ±1µm thickness in Kesternick[4] test as function of bath age [Linka and Riedel, 1986].

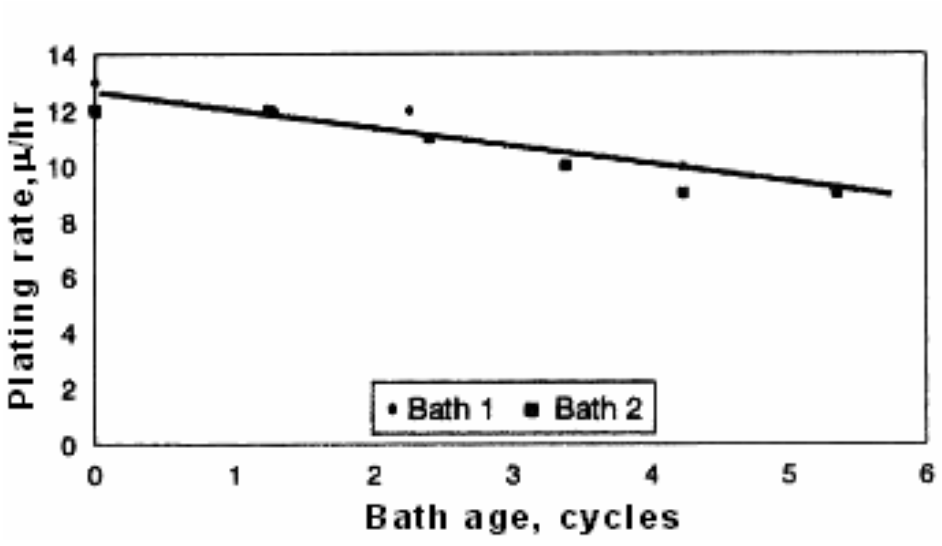

Figure 2.10. Dependence of deposition rate on bath age [Duncan, 1983].

[4] The Kesternick test is a moist sulphur dioxide corrosion test in which the panels are exposed for 8 hours to the corrosive atmosphere and then washed and dried for 16 hours (one cycle is then 24 hours).

2.4 Properties of EN coatings

2.4.1 Microstructure of EN deposits

The properties of EN coatings are directly attributed to their microstructural characteristics. The phosphorus content of EN deposits controls their microstructure and properties [Park and Lee, 1988; A. W. Goldstein et al., 1972; and E. Vafaei-Makhsoos et al., 1978]. The detailed structure of EN deposits is not well understood but as-plated EN coatings have been reported to be either crystalline, amorphous, or a co-existence of both . In spite of some contradictory results in the existing literature, the general trend in the understanding of EN deposits is that as-plated EN coatings containing 1-5 wt% phosphorus (low phosphorus) are crystalline; those containing 6-9 wt% phosphorus (medium phosphorus) consist of mixed crystalline and amorphous microstructures; whereas those containing 10-13 wt% phosphorus (high phosphorus) are amorphous and crystallize on heat treatment to nickel and various forms of nickel phosphides. The degree of crystallinity affects resultant properties and is a complex function of a number of factors [Allen and VanderSande, 1983], namely: phosphorus content, heating rate, heat treatment temperature and time at heat treatment temperature, and previous thermal history.

Furthermore, studying the microstructure of the deposits helps us to understand the mechanism of deposition and to evaluate the properties of EN coatings. The Ni-P phase diagram was originally developed by Konstantinov in 1908, long before the discovery of the EN method. Many years later, the Ni-P phase diagram was modified (Figure 2.11a) [Hansen, 1943; and Koeneman and Metcalfe, 1958]. Below the melting point, the conventional diagram shows only two phases for the alloy: Ni_3P, an intermetalic compound containing 15 wt.% phosphorus, and α phase, which is a solid solution of 0.17 wt.% phosphorus in nickel. The region between these two phases consists of a mixture of α and Ni_3P. The conventional Ni-P phase diagram can be used to describe the microstructure of the alloys in their equilibrium condition (e.g., the solidified alloys after melting or the EN coating after heat treatment). Mistakenly, many authors have used the conventional Ni-P phase diagram to explain the behavior

of the as-deposited EN coating [Gawrilov, 1979 and Reidel, 1991], although the as-deposited EN is not in its equilibrium state [Duncan, 1996]. Therefore, the prediction of the microstructure of the as-deposited EN from the conventional phase diagram (e.g. Figure 2.11a) is not accurate. As the non-equilibrium Ni-P phase diagram shows, there are two additional phases not contained in the equilibrium phase diagram. Phase β is a crystalline solution of phosphorus in nickel (same as α but with 4.5 wt.% P). The second phase is γ, which is a totally amorphous phase with 11-15 wt.%. phosphorus. Between these phases, region 4.4-11 wt.%, β and γ co-exist.

Zhang and Yao [1999] conducted a comprehensive study on the microstructure of EN coatings. They also studied the effect of heat treatment on the transformation of amorphous to crystalline microstructure of EN coatings. Figure 2.12 shows the TEM images and electron diffraction patterns of electroless Ni-l.5wt.%P deposits under different heat treatment conditions. The diffraction pattern shows continuous well defined rings which are characteristic of a microcrystalline structure for deposits after 200°C one hour annealing. All rings were determined to be from f.c.c. nickel, and there was no evidence of any nickel phosphide. The grain size was about 10 nm. Annealing at 400°C for one hour gave rise to the precipitation of b.c.t. Ni_3P, which was determined from XRD. Due to the fine size of Ni and Ni_3P the diffraction pattern appears to be several discontinuous rings Figure 2.12(d). Increasing annealing temperature to 600°C resulted in coarsening of microstructure, Figure 2.12(e).

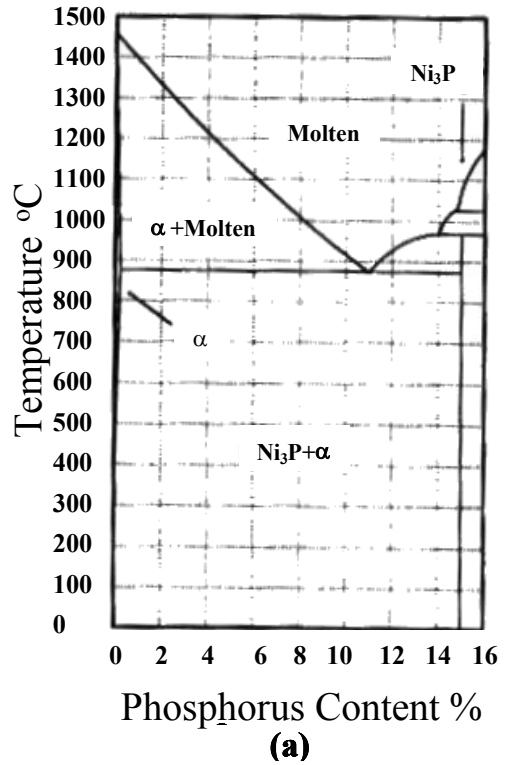

(a)

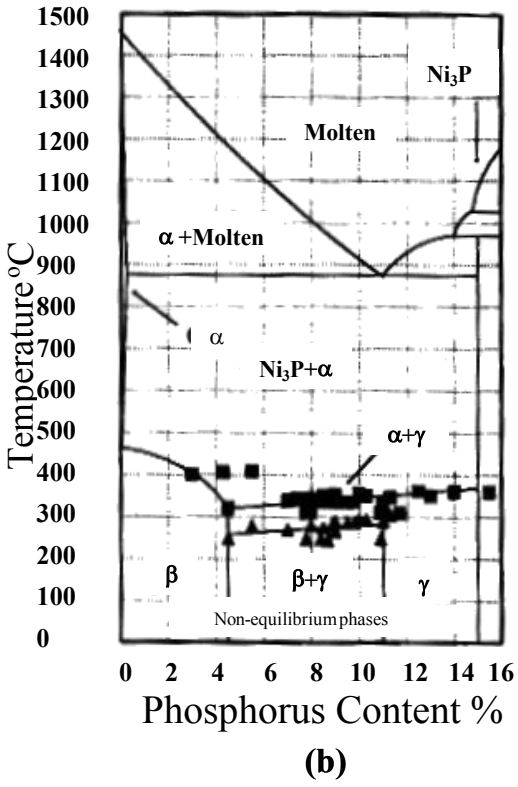

(b)

Figure 2.11. Ni-P binary phase diagram.
(a) Ni-P conventional phase diagram, (b) Non-equilibrium Ni-P phase diagram.

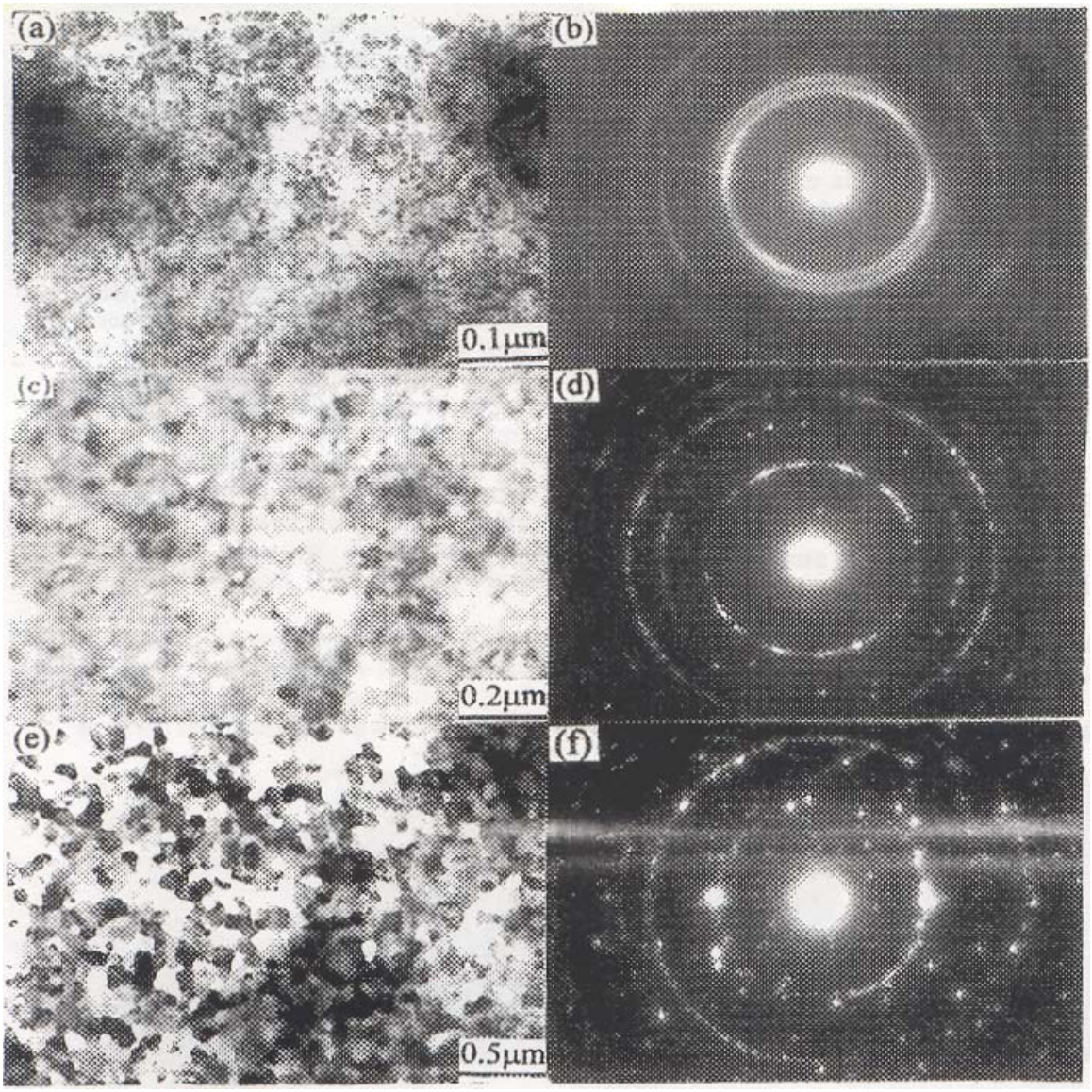

Figure 2.12. TEM micrograph of low phosphorus EN coating, 1.5 wt.% P, after various heat treatment process
(a) and (b) 200°C for one hour, (C) and (d) 400°C for one hour, and (e) and (f) 600°C for one hour [Zhang and Yao,1999].

2.4.2 Magnetic Properties

One of the interesting characteristics of the EN deposit is its diversified magnetic properties. Figure 2.13 illustrates the magnetic properties of EN coatings. As shown, the coating with less than 4 wt.% phosphorus (crystalline β phase) is ferromagnetic. Increasing the phosphorus content of the coating results in an increase in the amount of the γ phase in the microstructure, whereas the magnetic properties decrease drastically. At 11wt.% phosphorus, the EN deposit is totally non-magnetic. The wide range of application of this method of coating in the computer and electronics industry is due to the superior magnetic properties of low phosphorus EN deposits.

Table 2.3 shows the effect of phosphorus content on the magnetic properties of the EN deposit. It can be seen that the-heat treated EN coating has the highest coercivity[5] of all. Similar results were presented by the NACE researchers [1981], Figure 2.14. Based on the results obtained, magnetic properties of EN coatings are greatly affected by the phosphorous content. The ferromagnetism associated with high purity nickel decreases significantly with an increase in phosphorus content. Deposits with over 11 wt. % P are essentially non-magnetic. This condition can be maintained even after a short period of heat treatment at 260ºC. However, as soon as the precipitation of nickel phosphite particles occurs, the ferromagnetism increases.

[5] Coercivity is a physical property of materials defining the degree of magnetism. Generally, 80k A/m (1,000 Oe) to be a border, separates the high coercivity (it is called Hi-Co) and the low coercivity (it is called Lo-Co).

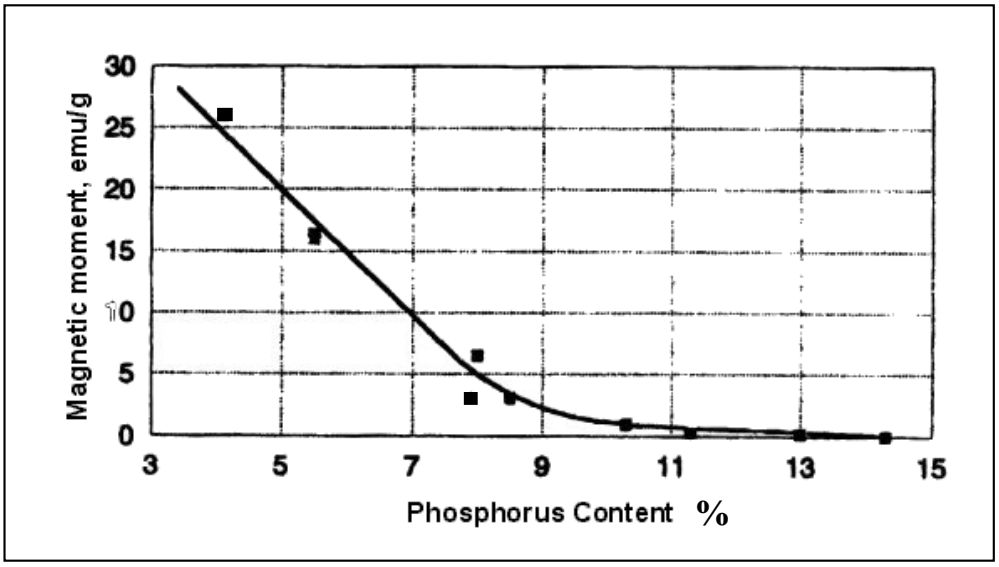

Figure 2.13. Effect of phosphorus content on the magnetic properties of the EN deposit [Duncan, 1996].

Table 2.3. Magnetic properties of EN [Stevenson, 1992].

Coercivity (Oe)	**Composition**
100-300	Any heat-treated
30	3.5wt.% P
20-80	3-6wt.% P
2	7.0wt.% P
1.4	8.6wt.% P
1-2	7-9wt.% P

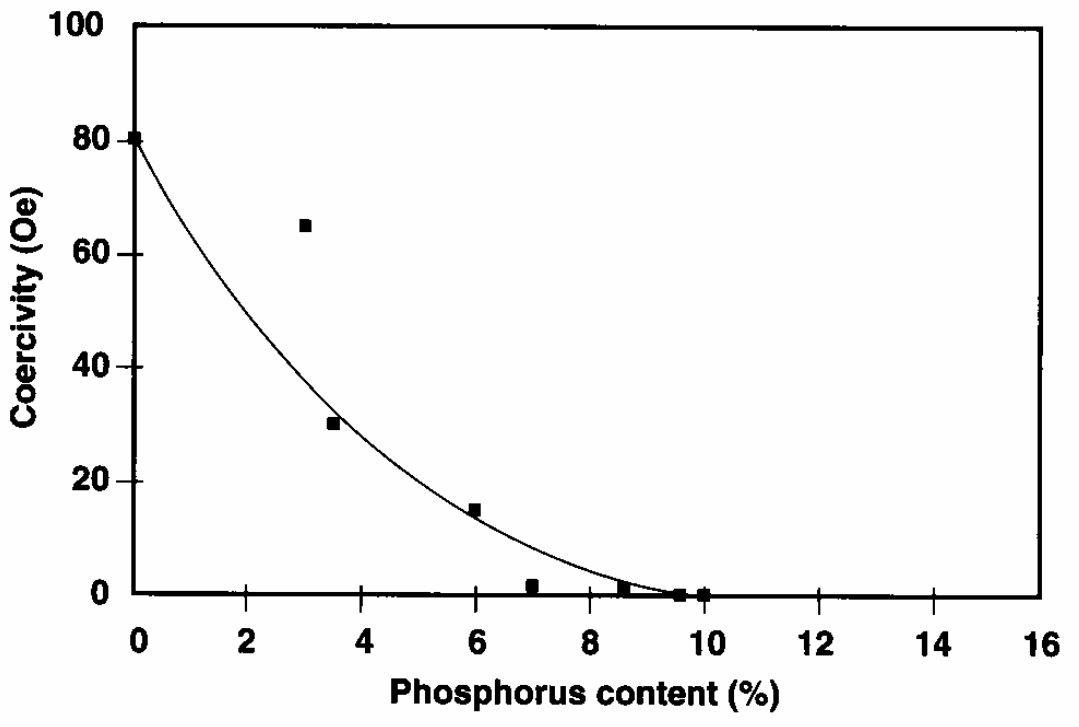

Figure 2.14. Effect of phosphorus content on the magnetic properties of EN coatings [NACE, 1987]

2.4.3 Electrical Resistivty

The resistivity of pure nickel is 7.8×10^{-6} Ω-cm. However, that of electroless nickel phosphorus coating can be ten times higher. The high resistivity of EN deposits is caused by the co-deposition of phosphorus. Thus, the resistivity increases with increasing phosphorus content, Figure 2.15.

The high resistivity of high-phosphorus EN coating is an important property when a magnetic metallic coating with low conductivity is required. Also, post heat treatment has a deleterious effect on the electrical resistivity of EN deposit as shown in Figure 2.16. A high annealing time and temperature result in a large drop in the electrical resistivity of the EN deposit.

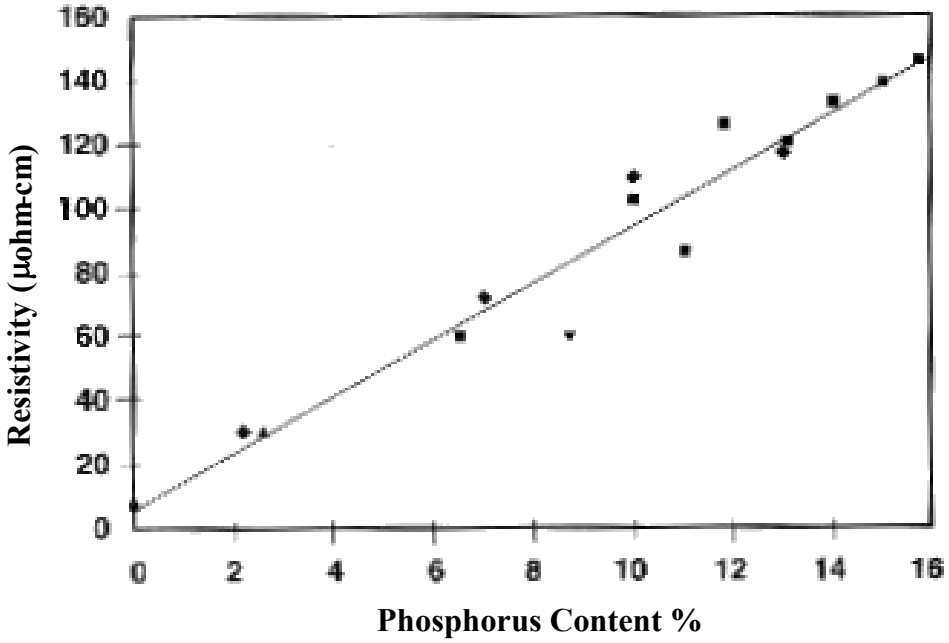

Figure 2.15. Dependence of resistivity of the EN on phosphorus content [Parkinson, 1997].

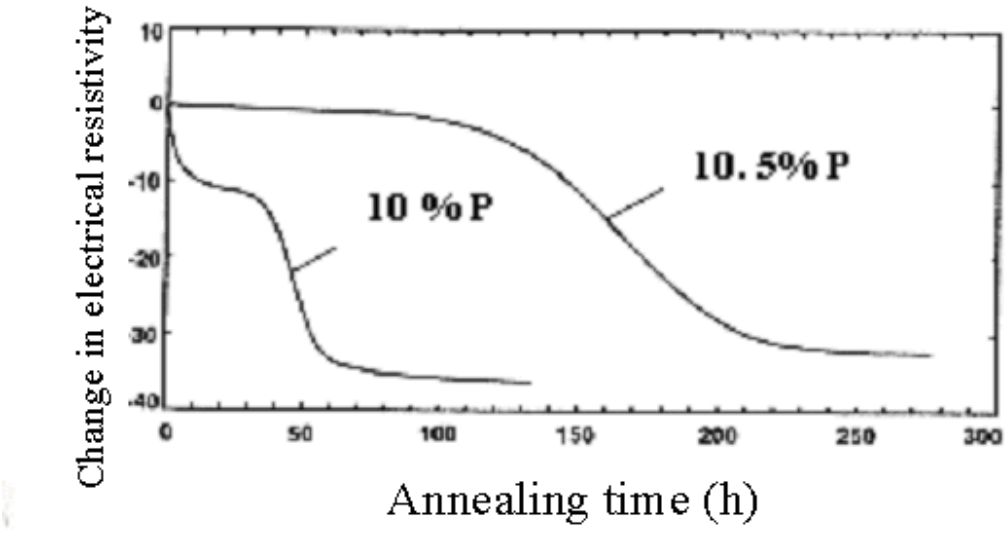

Figure 2.16. Dependence of electrical resistivity on annealing time [Baudrand, 1978].

2.4.4 Wettability and solderability

EN coatings are widely used in the electronics industry. Typical examples of applications of EN coatings include metal finishing of printed circuit boards [Gallory and Hajdu, 1990], filling of via-holes in multilevel interconnection [Wong et al., 1994 and Queau, et al., 1994], fabrication of multi-chip modules, [Baudrand, 1995], and formation of solder bump in tape-automated-bonding technology [Simon et al., 1995]. One of the important characteristics of surfaces used in circuit boards and other electronic devices is their solderability[6]. The solderability of the surfaces coated with EN coatings have been studied by many researchers [Chow et al., 2001; Young et al., 2201; and Chen et al., 2000]. Solderability of EN coatings was measured by Chow and co-workers. They measured three important parameters, namely, zero crossing time, T_{zero}, maximum wetting force, F_{max}, and wetting force at 2s, F_1, shown in Table 2.4. Based on the results obatined, Ni-B has the highest solderability properties compared with the other two EN coatings, namely, low and high phosphorus, (LP and HP).

However, as shown in Figure 2.17, if soldering is performed in a significantly high speed manner, with a soldering time of smaller than 1 s, EN LP will show better solderability properties than EN-B even though EN-B has higher wetting forces F_{max} and F_1.

Another interesting fact revealed in this study is that conventionally it has been accepted that wettability of a surface is directly related to the thickness of the oxide layer formed on the surface. In other words, coatings with a thinner oxide film show a better wettability. Based on the study conducted by Chow et al., the oxide film formed on EN-B is thicker than that of EN-LP and EN-HP. This is in contrast with the results of wetting balance measurement which ranks the EN coatings tested in the order of EN-B > EN-LP > EN-HP, Table 2.4. In order to solve the puzzle, Chow and co-workers conducted a surface morphology study using an Atomic Force Microscope

[6] Solderability is a scientifically measured quality of a surface to be completely wetted by solder.

(AFM), Figure 2.18. As shown, three types of EN coated surfaces had different surface morphologies and their nodule sizes decreased in the following order:

EN-HP > EN-LP > EN-B. As a result, EN-B has a larger surface area per unit volume compared with that of EN-LP and EN-HP. Since a larger surface area guarantees a better wettability, EN-B shows a better solderability.

Table 2.4. Solderability properties of EN coatings [Chow et al., 2001].

Coating Type	T_{zero} (s)	F_{max} (mN)	F_1 (mN)
EN-LP	0.30±0.01	0.29±0.07	0.11±0.03
EN-HP	0.00±0.01	0.31±0.06	0.31±0.05
EN-B	0.01±0.01	0.45±0.11	0.36±0.10

EN-LP: Low phosphorus, EN-HP: High phosphorus, EN-B: Low phosphorus, Nickel- Boron

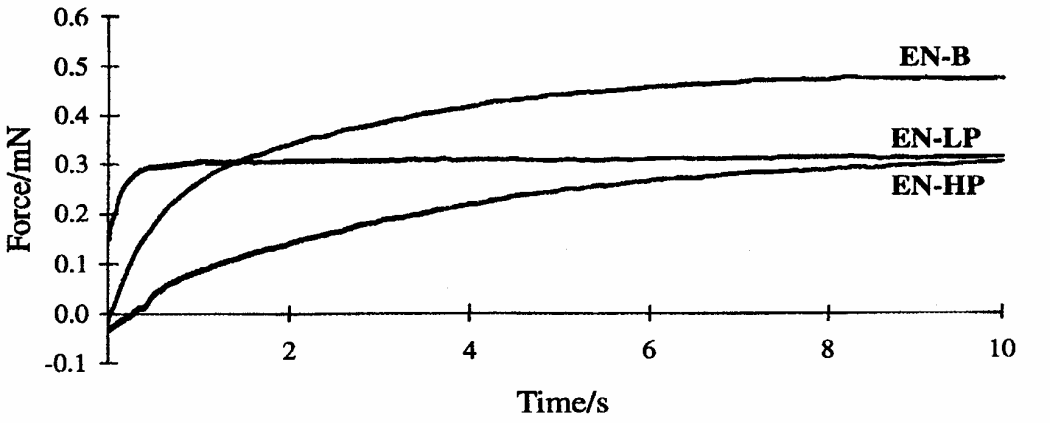

Figure 2.17. Wetting curves of EN-Hp, EN-LP, and EN-B samples [Chow et al., 2001].

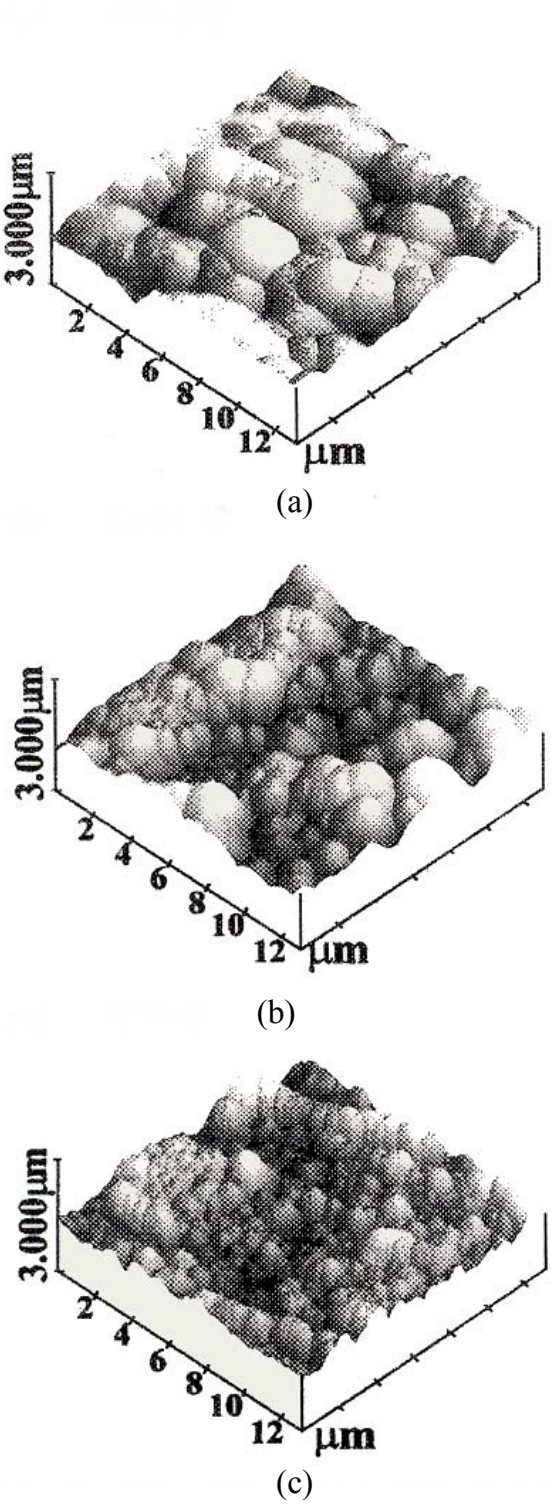

Figure 2.18. The AFM images of EN coated surfaces.
(a) EN-HP, (b) EN-LP, and (c) EN-B [Chow et al., 2001].

2.4.5 Thermal properties

The coefficient of thermal expansion (CTE) is one of the important characteristics of coatings. If there is a significant difference between the thermal expansion coefficients of the coating and the substrate, the coating might fail due to poor adhesion or cracking caused by residual thermal stresses at high working temperatures. The residual thermal stresses created at the substrate-coating interface cause initiation and propagation of cracks which may lead to failure. However, unlike many of the conventional coating methods, EN coatings have a wide range of thermal expansion coefficients depending on the phosphorus content. The coefficient of thermal expansion of EN coatings varies from 22.3 μm/m/°C at 3wt.% phosphorus to 11.1μm/m/°C at 11wt.% phosphorus [Duncan, 1997]. Therefore, whenever thermal expansion is a main concern, it is possible to minimize the residual thermal stresses by controlling the phosphorus content. Figure 2.19 shows the dependence of the thermal expansion coefficient of EN deposit on the phosphorus content [Baudrand, 1978].

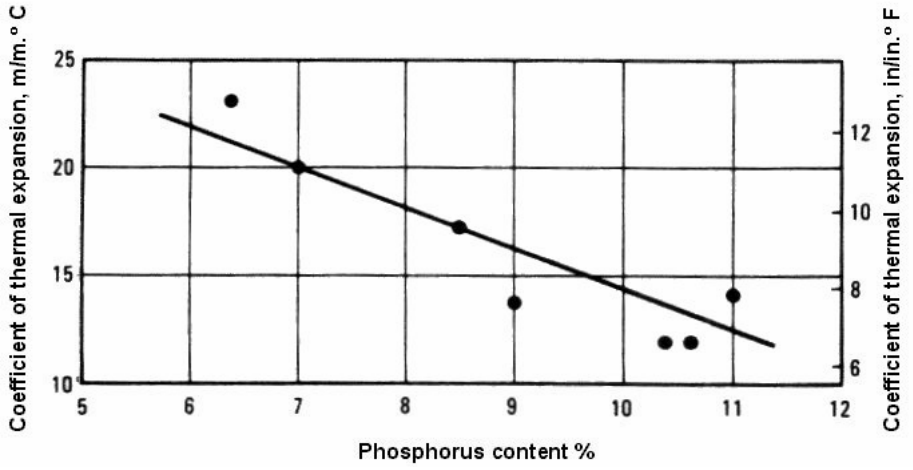

Figure 2.19. Effect of phosphorus content on the thermal expansion coefficient [Baudrand, 1978].

2.4.6 Porosity

Many of the EN coatings properties, such as adhesion and corrosion resistance, are directly related to their porosity. The porosity of EN coating is related to many parameters. These include substrate surface characteristics such as roughness and morphology, substrate pre-treatment, coating thickness, agitation, and filtration. There are many methods for measuring and evaluating the porosity of a coated surface. The following are some of the common porosity measurement methods;

1. Ferroxy test [Tomlison and J. P. Mayor, 1988; and Munemass and Kumakiri, 1991], ASTM B765-1993.

2. Neutral salt spray test (NSS) [International Standard ISO 9227, 1990].

3. Acetic acid spray test (AAS) [International Standard ISO 9227, 1990].

4. Copper acceleration acetic acid salt spray test (CASS) [International Standard ISO 9227, 1990].

5. Saline droplets corrosion test (SDS) [International Standard ISO 4536, 1985].

6. Corrodkote corrosion test (CORR) [International Standard ISO 4541, 1978].

7. Moist SO_2 test [ASTM Standard G87, 1998].

8. Nitric acid vapor test [ASTM Standard B 735-84, 1984].

9. Sulfur test [Annual Book of ASTM Standards vol. 03.04, 1983].

Figure 2.20 shows different types of pores that may be created during the EN process [Nahle et al., 1998]. The porosity of EN coated surfaces is an important criterion defining the quality of the coating, especially when the thickness of the coating is below 10 μm. Some studies show that the open pores on EN coated surfaces participate in a galvanic reaction in which the coating surface is the cathode and the small pore area acts as the anode. As a result of the severe galvanic corrosion, the uncoated area of the pore corrodes drastically [Leisner and Benzon, 1997]. On the

other hand, based on some other studies conducted in the presence of carbon dioxide and hydrogen sulfide, the existence of man-made pits did not cause any acceleration of the corrosion rate [Stevenson, 1996]. As the EN deposition progresses, the porosity of the coating is reduced. This means that the pores with less depth are filled with the Ni-P alloy. Therefore, in many cases, a minimum thickness of 25 μm is recommended for obtaining a coating with the least amount of pores and highest corrosion and wear resistance [Deng and Hong, 1993; and Das, and Chin, 1959]. The result of salt spray and electrochemical measurement of the porosity of an EN deposit are shown in Figures 2.21 and 2.22 [Das, and Chin, 1959]. As shown, the porosity of an EN coating reaches its minimum value at a thickness of 25 μm. Also, Table 2.5 shows the effect of EN coating thickness on coating porosity. It can be seen that both ferroxy and salt spray fog tests are not appropriate for measuring the porosity of very thin EN coatings. In such cases, the electrochemical porosity measurement method gives more accurate results [Das, and Chin, 1959].

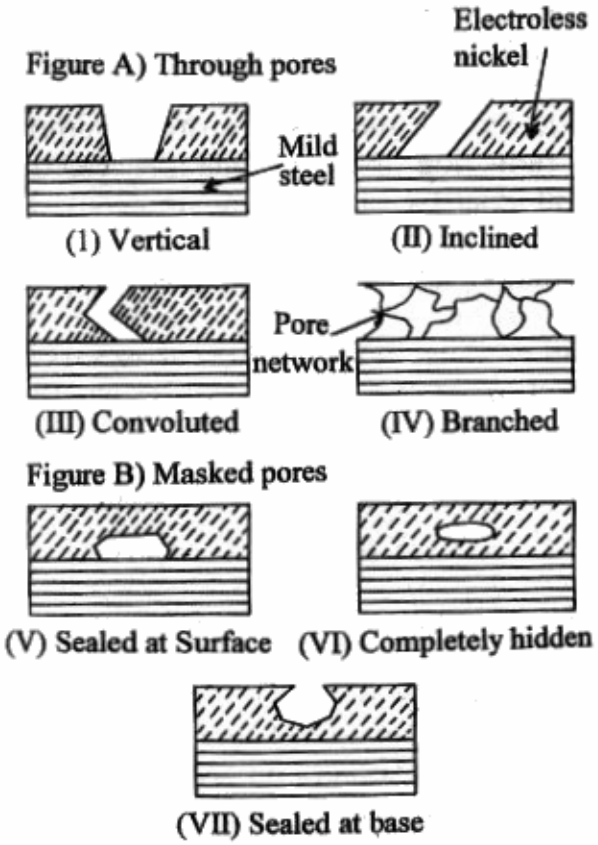

Figure 2.20. Different types of EN pores [Leisner and Benzon, 1997].

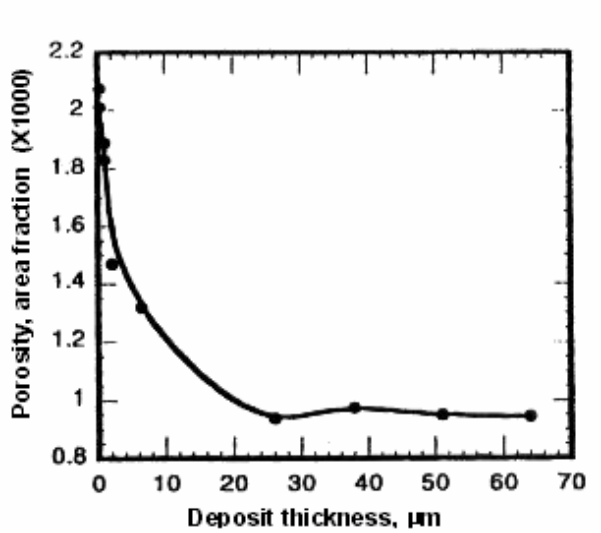

Figure 2.21 Dependence of porosity of coating on deposition thickness [Das, and Chin, 1959].

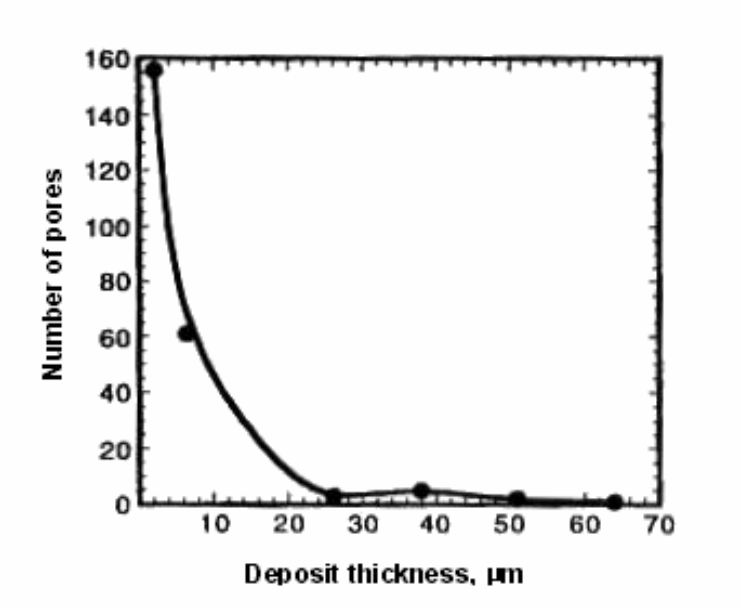

Figure 2.22 Dependence of porosity of coating on deposition thickness [Das, and Chin, 1959].

Table 2.5. The results of the ferroxy and salt fog spray porosity measurement [Das, and Chin, 1959].

EN Deposit thickness μm	**Ferroxy Test No. of spots on 8 cm^2**	**Salt Fog Test No. of spots on 8 cm^2**
0.42	-	-
1.05	-	-
2.1	11	156
6.4	0	61
26	0	3
38	0	5
51	0	2
64	0	1

2.4.7 Adhesion properties

Coatings with poor adhesion do not provide good protection. The adhesion evaluation of EN and electrodeposited nickel remains an unsolved problem [Reidel, 1997]. Most of the methods applied such as pull-off test, ring-shear test, peel test, and three-point bend test give semi-quantitative or qualitative results only.

Figure 2.23 is a schematic illustration of the three most common types of adhesion measurement methods. In general, EN coatings have superior adhesion compared with the nickel electrodeposition method. This is due to the existence of a stronger metal-to-metal bonding during the EN deposition. The adhesion properties of EN coatings have been investigated by many researchers [Reidel, 1997; Dickinson, 1954; and Wesley, 1950]. Dickinson [1954] found adhesion values greater than 350 $\frac{N}{mm^2}$ for EN coatings on unalloyed steel or brass substrate, while Wesley [1950] reported a value of 415 $\frac{N}{mm^2}$ for acidic and 219 $\frac{N}{mm^2}$ for alkaline bath prepared coatings.

Also, Safranek [1959] measured the adhesion strength of Ni-P coating on iron and copper alloys and reported values of 350-450 $\frac{N}{mm^2}$, while the adhesion of EN deposit on pure iron substrate was reported as 210-350 $\frac{N}{mm^2}$. Lower values have been found for the adhesion of EN deposit on aluminum substrates [Dini, 1974]. Others have reported values of 60-380 $\frac{N}{mm^2}$ [Hammond, 1963] and 350-420 $\frac{N}{mm^2}$ [Simon and Thoma, 1985] for steel, and 160-200 $\frac{N}{mm^2}$ for stainless steel [Tlusi, 1986]. The low value of adhesion reported for EN deposition on stainless steel is due to weak adhesion of the electrodeposited nickel on the substrate during the nickel strike.

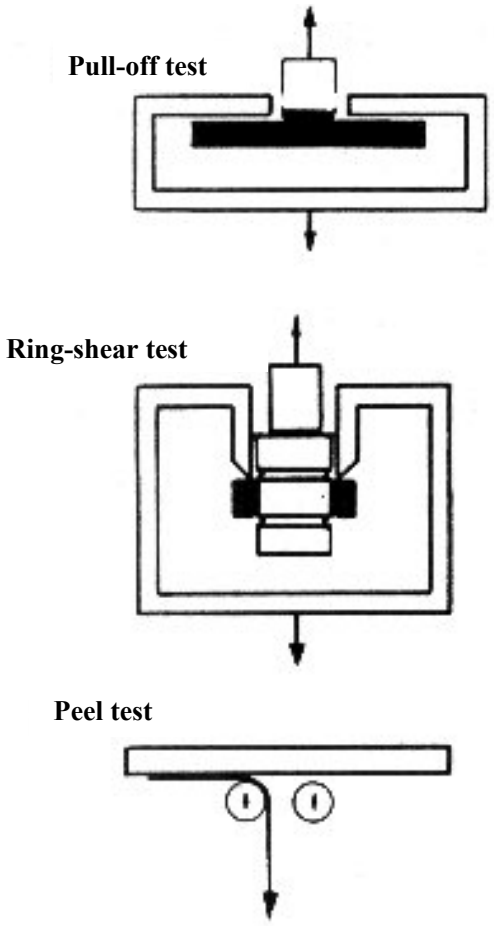

Figure 2.23. Three quantitative methods to measure adhesion of coatings [Heymann and Doner, 1983].

2.4.8 Internal stress

EN deposits contain internal stresses. These stresses are caused by atomic and crystallographic defects such as dislocations. There are numerous theories offered to explain the internal stresses in EN deposits [Bozordat, 1925 and Hosthersall, 1948]. The mechanical and corrosion resistance properties of EN coatings are correlated to the state of the internal stress, which has been studied by many researchers. Although the results obtained are in conflict in some cases, they all agree on the significant effect of internal stress on the mechanical properties of EN deposits. Duncan [D1981] has correlated the effect of phosphorus content on the internal stress (Figure 2.24). It can be seen that as the phosphorus content increases, the nature of the internal stress is changed from tensile to compressive. At about 11wt.% phosphorus, the coating obtained seems to be free from stress. Additionally, in a recent work, Duncan has suggested a regime for the internal stress in the EN deposit [Duncan, 1996]. According to this proposed theory, the existing internal stress is directly related to the microstructure. As explained earlier, at the phosphorus contents between 4 and 7.5 wt.%, the microstructure of an EN deposit consists of two phases, β and γ. Due to the existence of these two phases, the microstructure is in its most incoherent state and, therefore, very brittle. Thus, the existing internal stress has its maximum tensile value. Below 4 or above 11 wt.% phosphorus, the microstructure is either β or γ. Either of these two microstructures is more coherent than the microstructure containing both β and γ, Figure 2.25. As a result, the internal stress of either β or γ when present alone, is compressive.

The Duncan's new finding [1996] consistently explains many of the characteristics of EN coatings, such as wear resistance, tensile strength, and ductility. The internal stress of the EN deposit is also a function of the bath age. Many studies have shown that as the EN bath gets older, the internal stress tends to become more tensile [Reidel, 1997] explaining the fact that the solution needs to be discarded after 5 to 6 turnovers.

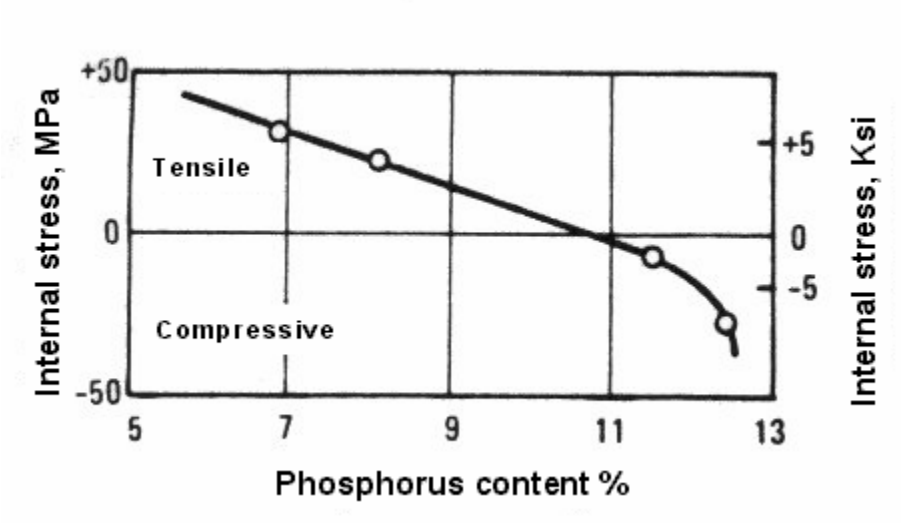

Figure 2.24. Effect of phosphorus content on internal stress of EN deposit [Baudrand,1978].

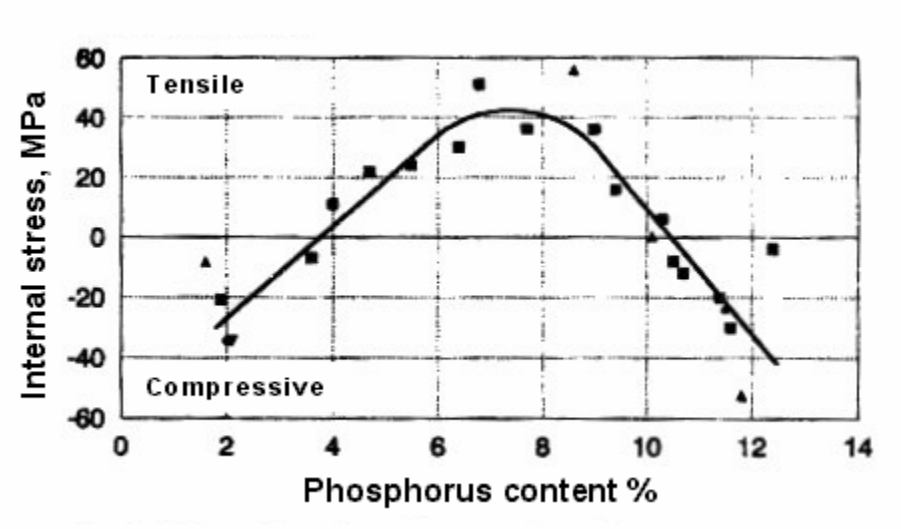

Figure 2.25. Dependence of internal stress of EN deposit on phosphorus content [Duncan, 1996].

Reidel has reported the dependence of internal stress on the bath age, Figure 2.26 [Reidel, 1997]. After the fifth turnover, the nature of the internal stress significantly changes from compressive to tensile. The results of a broad investigation conducted by Kerr et al. [Kerr, Barker, and Walsh, 1997] agree with this finding. Based on the latter study, the acceptable life of commercial EN baths has been limited to previously stated six turnovers.

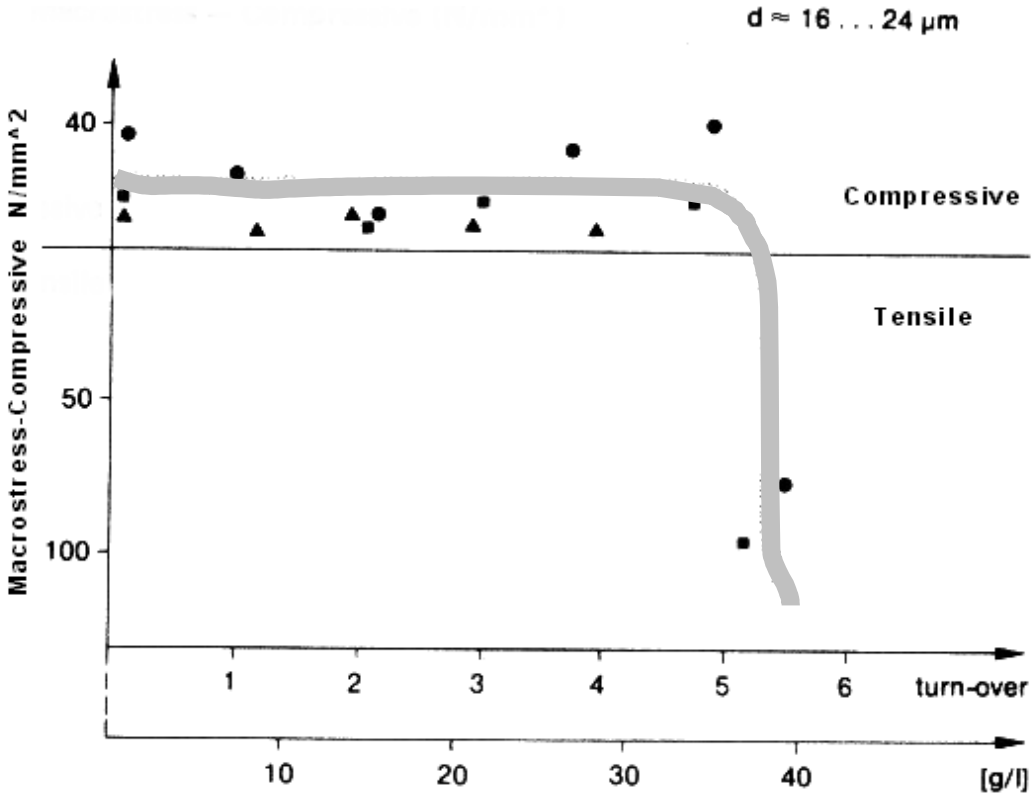

Figure 2.26. Effect of bath age on internal stress of 12wt.% phosphorus EN coating [Reidel , 1976].

2.4.9 Hardness

One of the outstanding characteristics of EN coatings is their high hardness, especially after heat treatment. There are three major parameters affecting the hardness of these coatings, namely, phosphorus content, time, and the temperature of the applied post heat treatment. The hardness of an EN deposit is especially important when superior wear resistance is required.

2.4.9.1 Effect of phosphorus content on the hardness of EN deposits

The hardness of EN deposits, as with many other properties, is directly affected by the phosphorus content. As Figure 2.27 shows, increasing the phosphorus content of the deposit lowers the hardness of the coating. The maximum hardness is obtained at around 4wt.% phosphorus where the microstructure consists of the single β phase. As the phosphorus content increases, the amount of the β phase decreases while the amount of the γ phase increases. This causes a reduction in the hardness since the γ phase is a softer phase compared to the β phase. The minimum hardness value is obtained when the microstructure consists of the single γ phase at 11wt.% phosphorus.

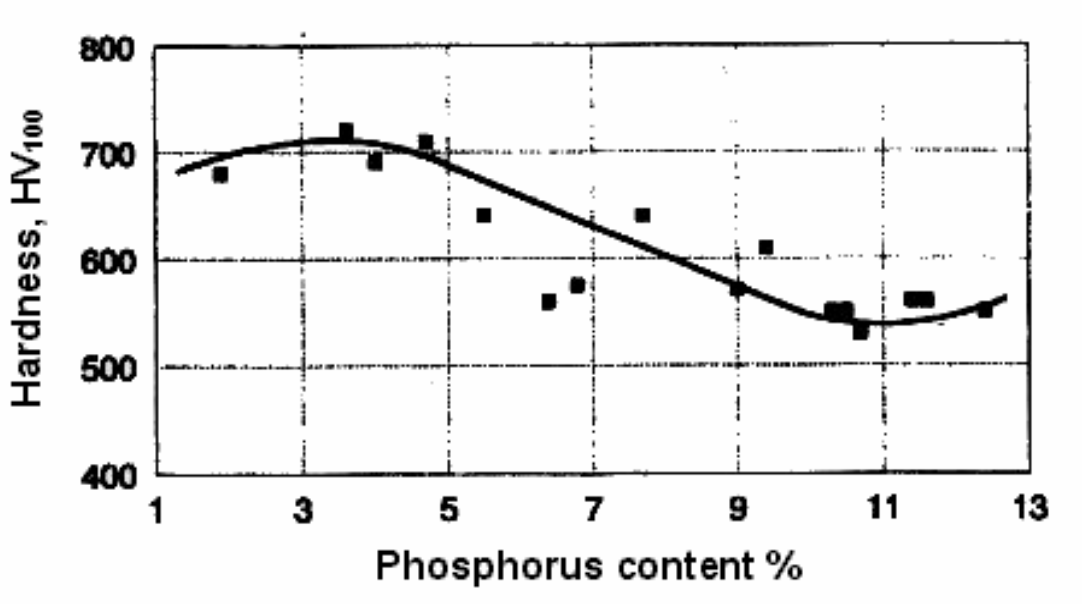

Figure 2.27. Dependence of hardness of EN deposit on phosphorus content [Duncan, 1996].

2.4.9.2 Effect of Heat Treatment on Hardness

Post heat treatment has a significant impact on the hardness of the EN deposit. As a matter of fact, one of the outstanding characteristics of EN coatings is the possibility of obtaining very high hardness values (980-1050 VHN) through an appropriate heat treatment. This provides a unique wear and erosion resistance. The parameters of the post heat treatment (time and temperature) are defined by the phosphorus content. If the phosphorus content stays in one phase region, i.e., below 4.5 or above 11, there would be only one reaction in which the β or γ phase is transformed to α and Ni_3P. This transformation occurs at 400°C for low phosphorus and 330-360°C for high phosphorus content alloys [Duncan, 1996]. However, in the region between 4.5 and 11wt.% phosphorus, there is another transformation in which β is transformed to α nickel. This transformation occurs at 250-290°C and causes the precipitation of fine particles throughout the coating. Figures 2.28 and 2.29 show the effect of heat treatment temperature on the hardness of EN coating. Many sources also reported that the maximum hardness is obtained after a heat treatment at 400°C for one hour [Baudrand, 1978 and Reidel, 1997].

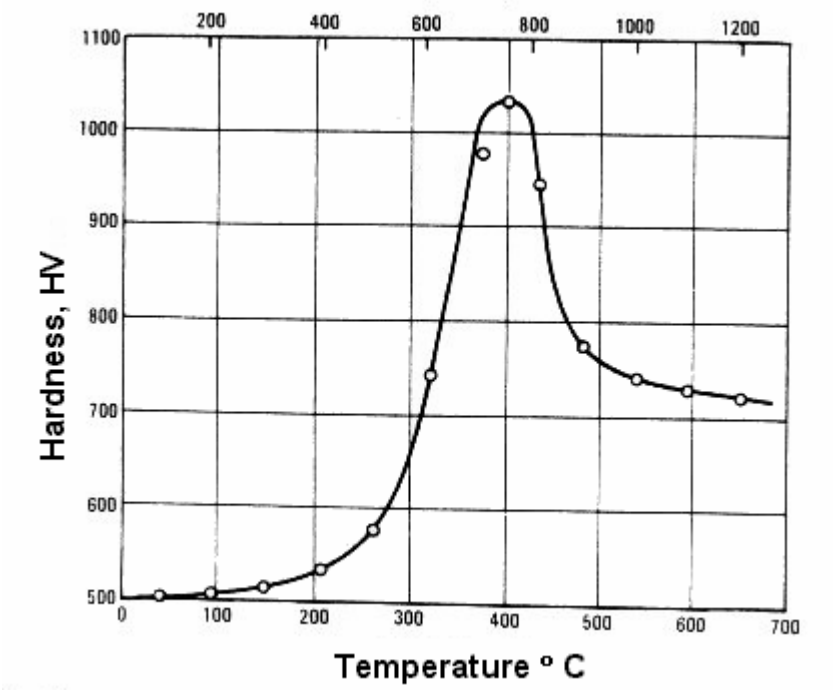

Figure 2.28. Effect of heat-treatment temperature (one hour) on hardness of 10.5% P EN coating [Baudrand, 1978].

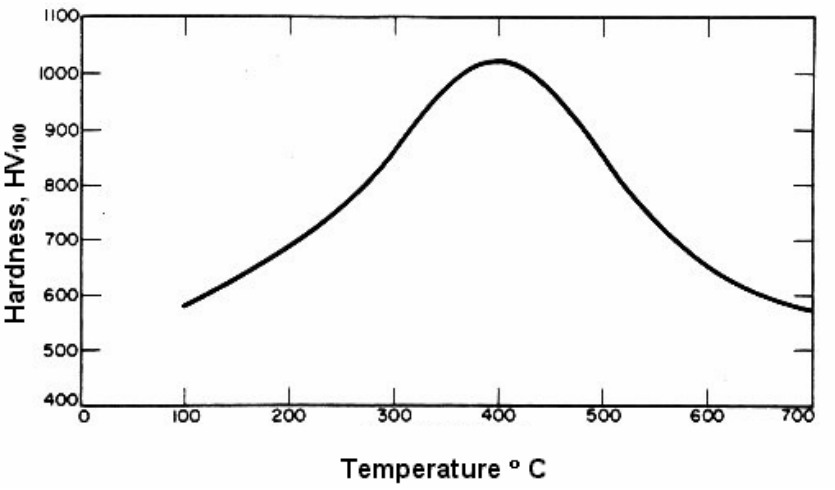

Figure 2.29. Hardness versus temperature (1 h, 9wt.% phosphorus coating) [Baudrand, 1978].

2.4.10 Wear resistance

One of the unique characteristics of EN deposition is the superior wear resistance of the coatings. Theoretically, there is a correlation between wear resistance and hardness of a surface. However, the wear properties of a surface are affected by numerous parameters such as the nature of the applied stress and the surface morphology. The wear resistance of EN deposits depends on both phosphorus content and the type of post heat treatment applied. It was explained previously that the hardness reaches its highest value when the γ phase first forms at approximately 4wt.% phosphorus whereas it reaches its lowest value when the last remaining β phase disappears. The same conclusion is true for explaining the wear resistance properties of EN coatings.

Figure 2.30 shows the dependence of wear resistance on the phosphorus content [Duncan, 1996]. The great consistency between Figure 2.27 and Figure 2.30 is evidence to the accuracy of Duncan's new theory. Figure 2.31 also shows the effect of heat treatment temperature on wear resistance of an EN coating. As shown, the higher the hardness, the lower is the weight loss due to wear [Baudrand, 1978]. Figure 2.32 illustrates the effect of post heat treatment on the wear resistance of the EN deposit.

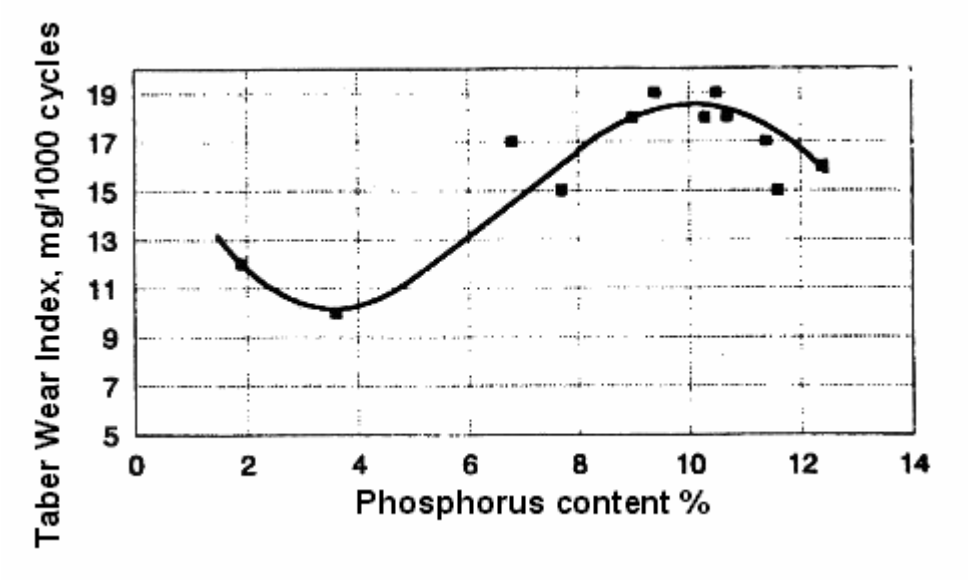

Figure 2.30. Effect of phosphorus content on wear resistance [Duncan, 1996].

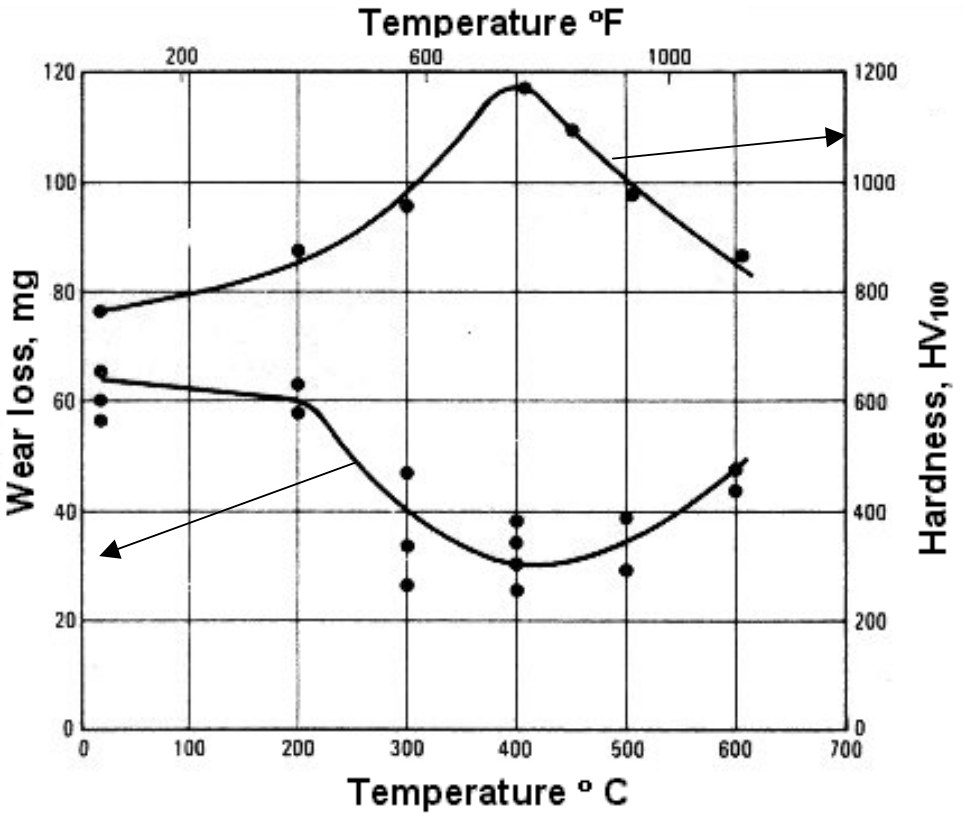

Figure 2.31. Effect of heat-treatment temperature on the wear resistance properties [Baudrand, 1978].

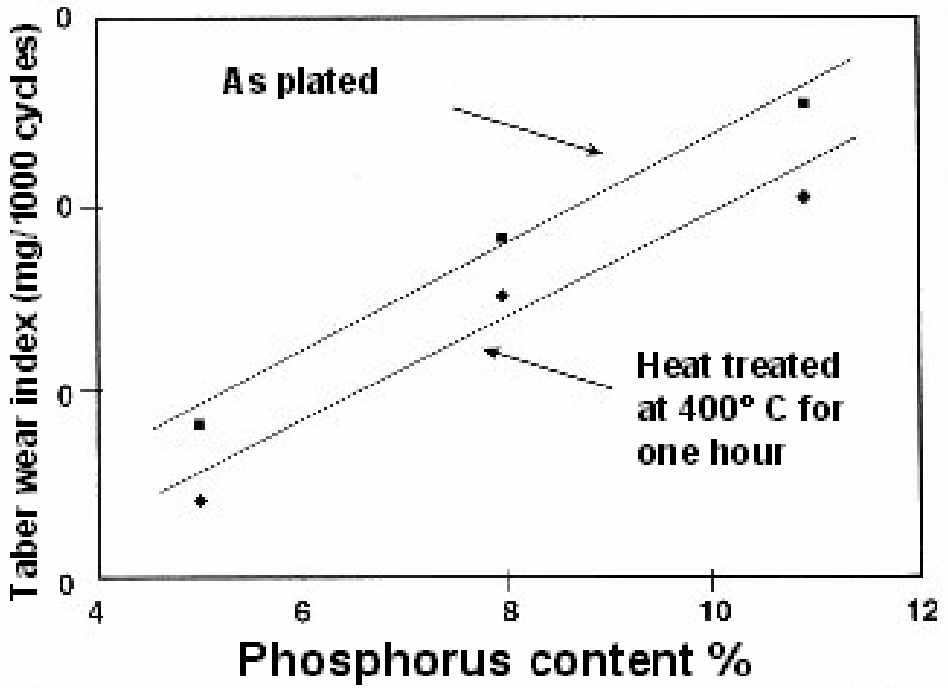

Figure 2.32. Effect of phosphorus content of the EN deposit on the wear resistance of as-plated and heat-treated sample [Parkinson, 1997].

2.4.11 Tensile strength

The tensile strength of EN deposits is related to their phosphorus content and, consequently, the microstructure. Generally, an amorphous microstructure has a high tensile strength and strain due to the absence of defects and high stress areas normally located in the grain boundaries. As a result, by increasing the phosphorus content a high tensile strength and strain can be achieved. This is illustrated in Figures 2.33 and 2.34 [Baudrand, 1978 and Duncan, 1996]. Figure 2.35 shows the effect of phosphorus content on the elongation properties of an EN deposit. As illustrated, between 4.5 and 11wt.% phosphorus (when the microstructure consists of both β and γ) the ductility is at its lowest value. As the phosphorus content falls below 4% or rises above 11wt.%, the EN deposit becomes more ductile. This observation completely agrees with that obtained for the internal stress (see Figure 2.25, and Figure 2.35). The high internal tensile stress value of the deposit leads to a decrease in its ductility.

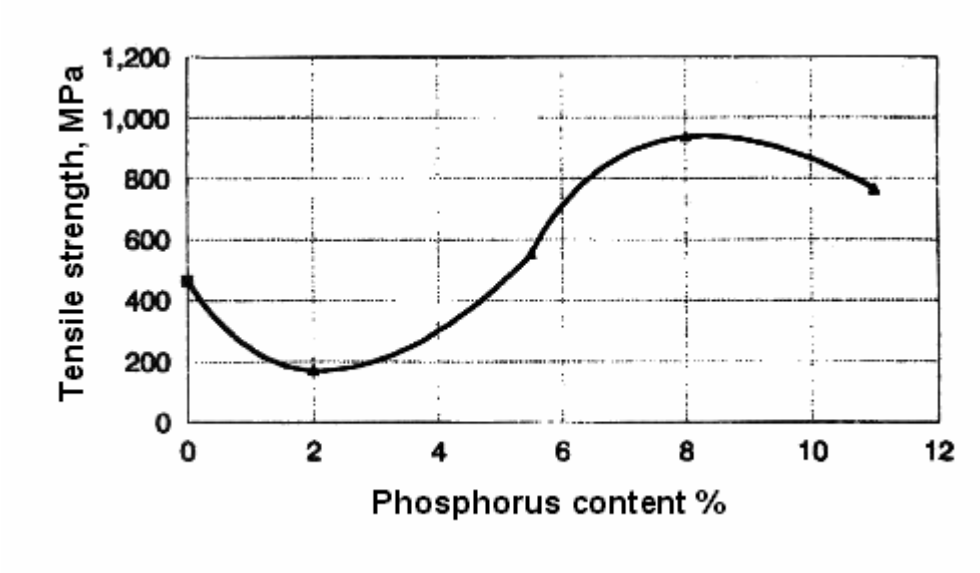

Figure 2.33. Dependence of tensile strength on phosphorus content of EN deposition [Duncan, 1996].

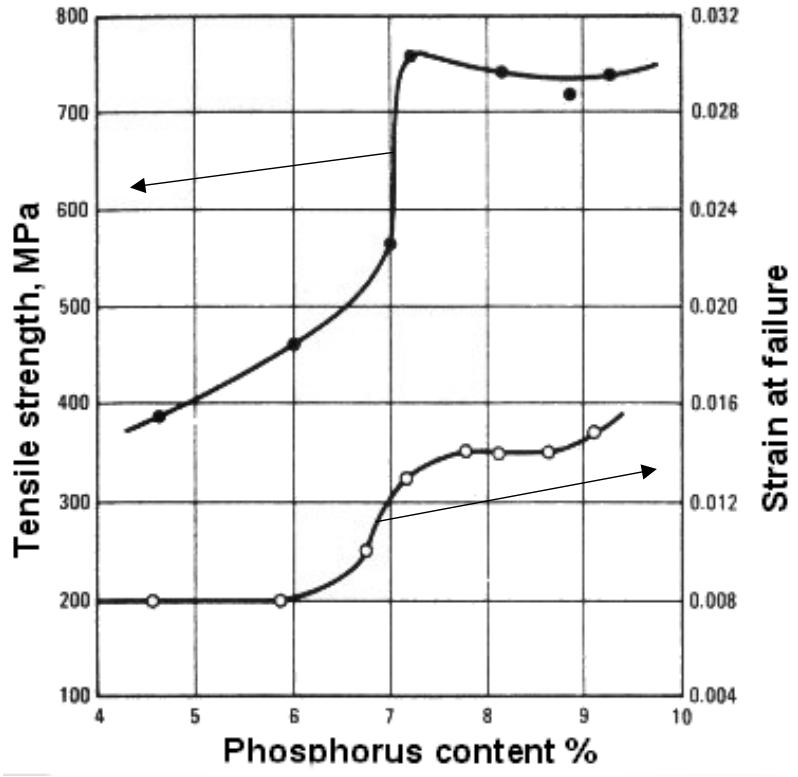

Figure 2.34. Dependence of tensile strength and strain on phosphorus content of EN deposition [Baudrand,, 1978].

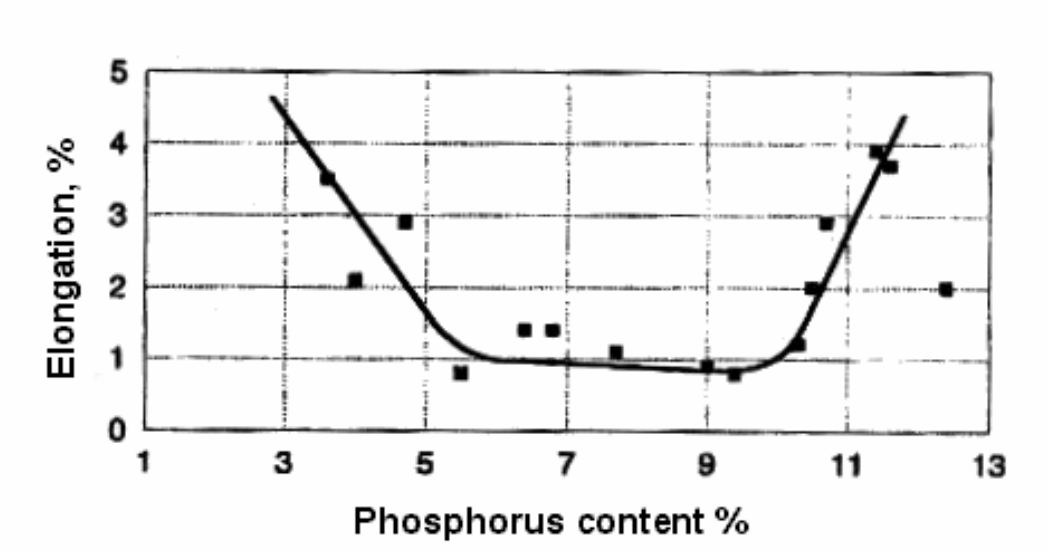

Figure 2.35. Dependence of elongation on phosphorus content of EN deposition [Duncan, 1996].

2.4.12 Fatigue properties

Fatigue and corrosion fatigue properties of EN coatings have been studied by many researchers [Pertuz et al., 1999; Chitty, 1998; Puchi et al., 1996; Prasad et al., 1994; and Yamasaki et al., 1981]. However, in many cases the results obtained are controversial. A detailed discussion of the parameters affecting the fatigue properties of EN coatings will be presented in Chapter Four (4.3.2).

The general belief concerning this topic is that due to their tendency to crack under cyclic loads, electroless nickel phosphorus coatings can cause a significant reduction of the fatigue properties of steel substrates, although the magnitude of reduction in fatigue strength would depend upon composition, heat treatment, and coating thickness [Chitty, 1999]. Chitty and his colleagues found that EN coatings had a detrimental effect on corrosion fatigue properties of AISI 1045 substrate in 3% sodium chloride solution. Moreover, based on other studies [Safranek, 1959; Wu, 1995; and Zhang, 1995], the reduction in fatigue strength could range between 10-50%. Also, a study conducted by Yamasaki et al., [1980] shows that EN coatings deteriorate the cyclic stress properties of the substrate. The effect is dependent on the pH of the EN solution and phosphorus content of the coating. As shown in Figure 2.36, a coating with a higher phosphorus level (amorphous at pH below 4.7) has better fatigue resistance compared with that of a low phosphorus (crystalline at pH above 4.7) EN coating. This is directly related to the brittleness of the EN coatings with lower phosphorus content. Figure 2.37 shows variation of fracture strain of Ni-P, 7 wt.% P, after cyclic stressing at σ_a= 275 MPa. This figure shows a typical fatigue behavior of a metal.

Puchi et al. [1996] also studied the effect of EN coatings on the fatigue properties of their substrates. Their results indicated that EN coating, 10 wt.% P, improves the fatigue properties of AISA 1010 and 1045 substrates. Figures 2.38 and 2.39 show the results obtained by Puchi and his colleagues.

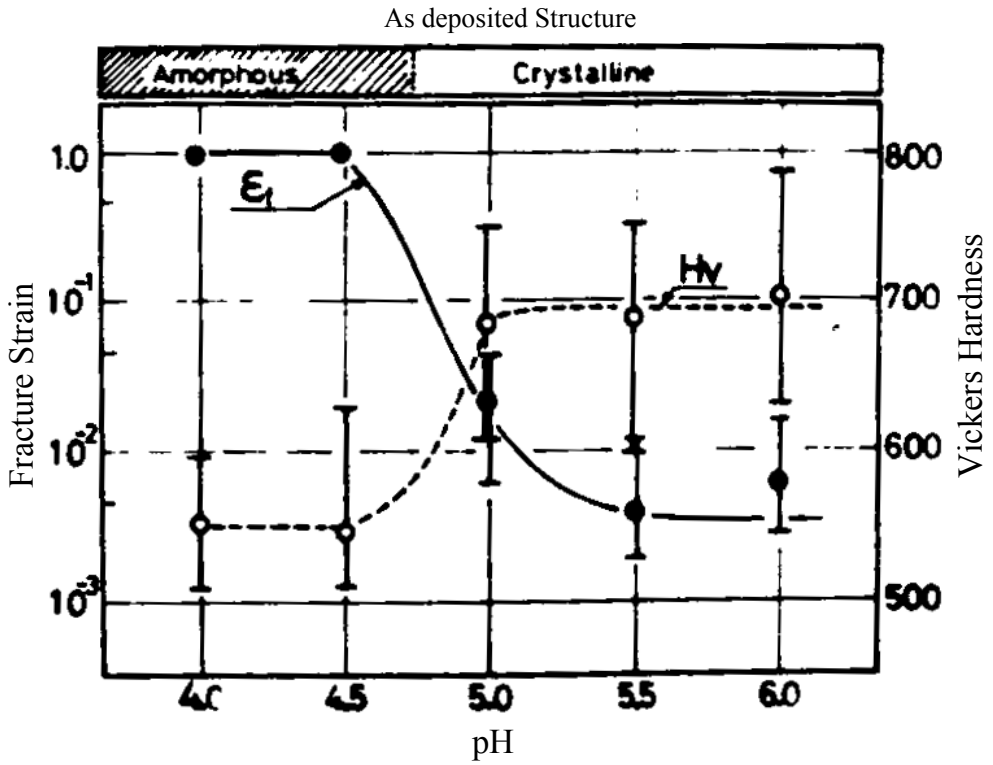

Figure 2.36. Effect of pH on the fracture strain and Vickers hardness of EN coatings.

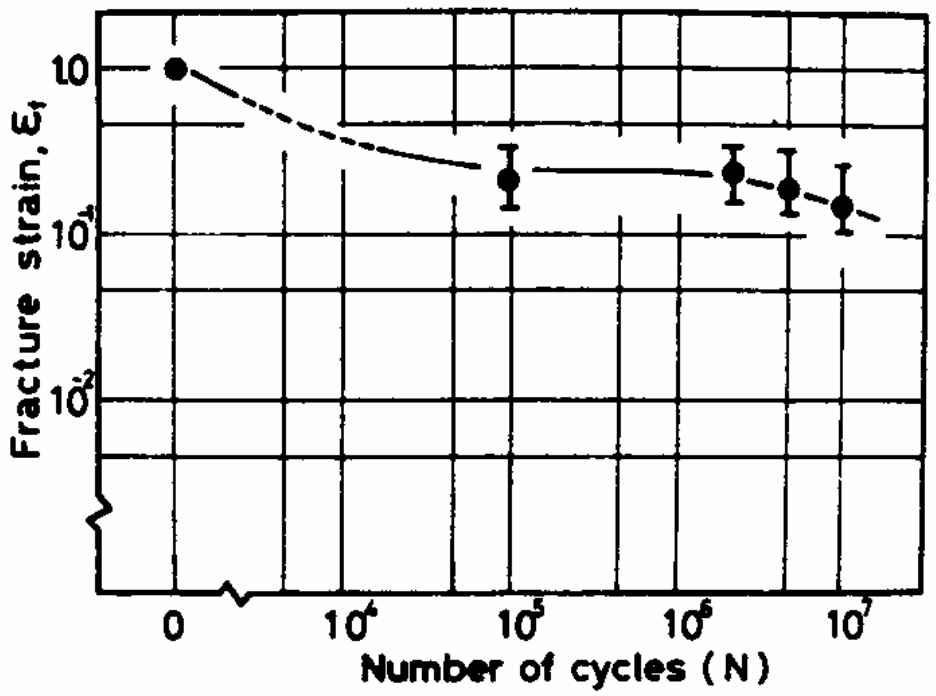

Figure 2.37. Variation of fracture strain of Ni-P, 7 wt.% P, after cyclic stressing at σ_a= 275 Mpa [Puchi et al., 1996].

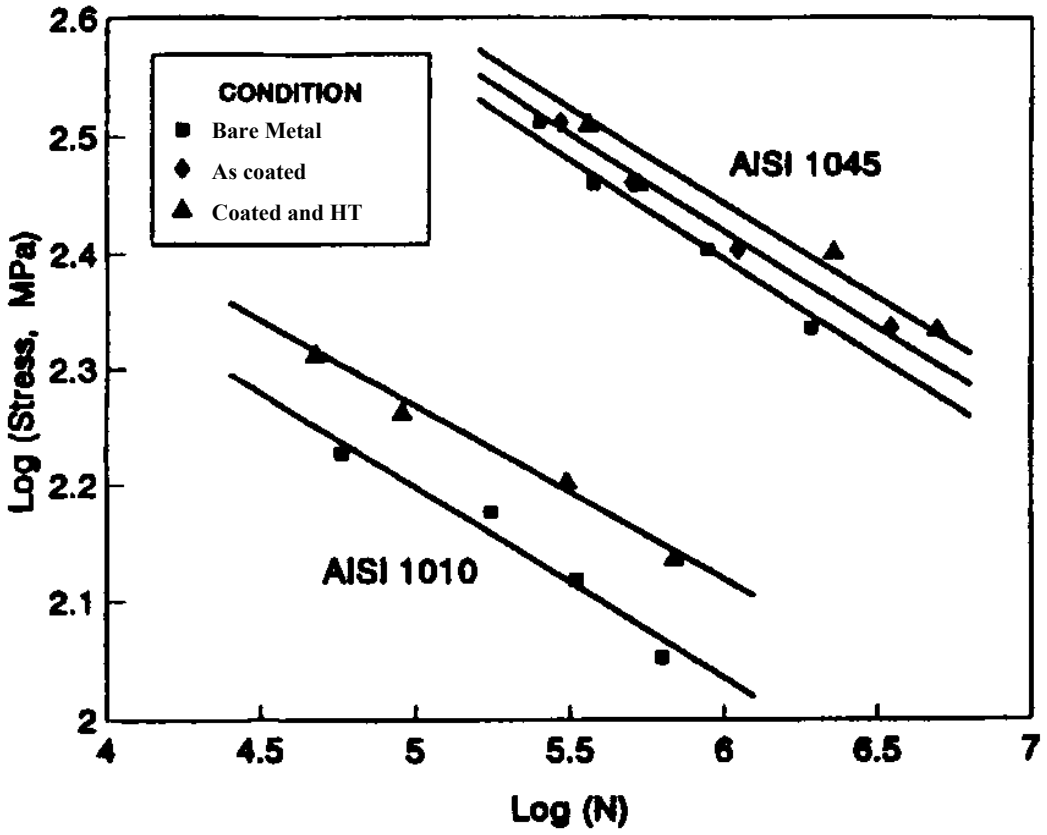

Figure 2.38. Stress amplitude vs. number of cycles of failure for AISA 1010 and 1045 steel under different conditions [Puchi et al., 1996].

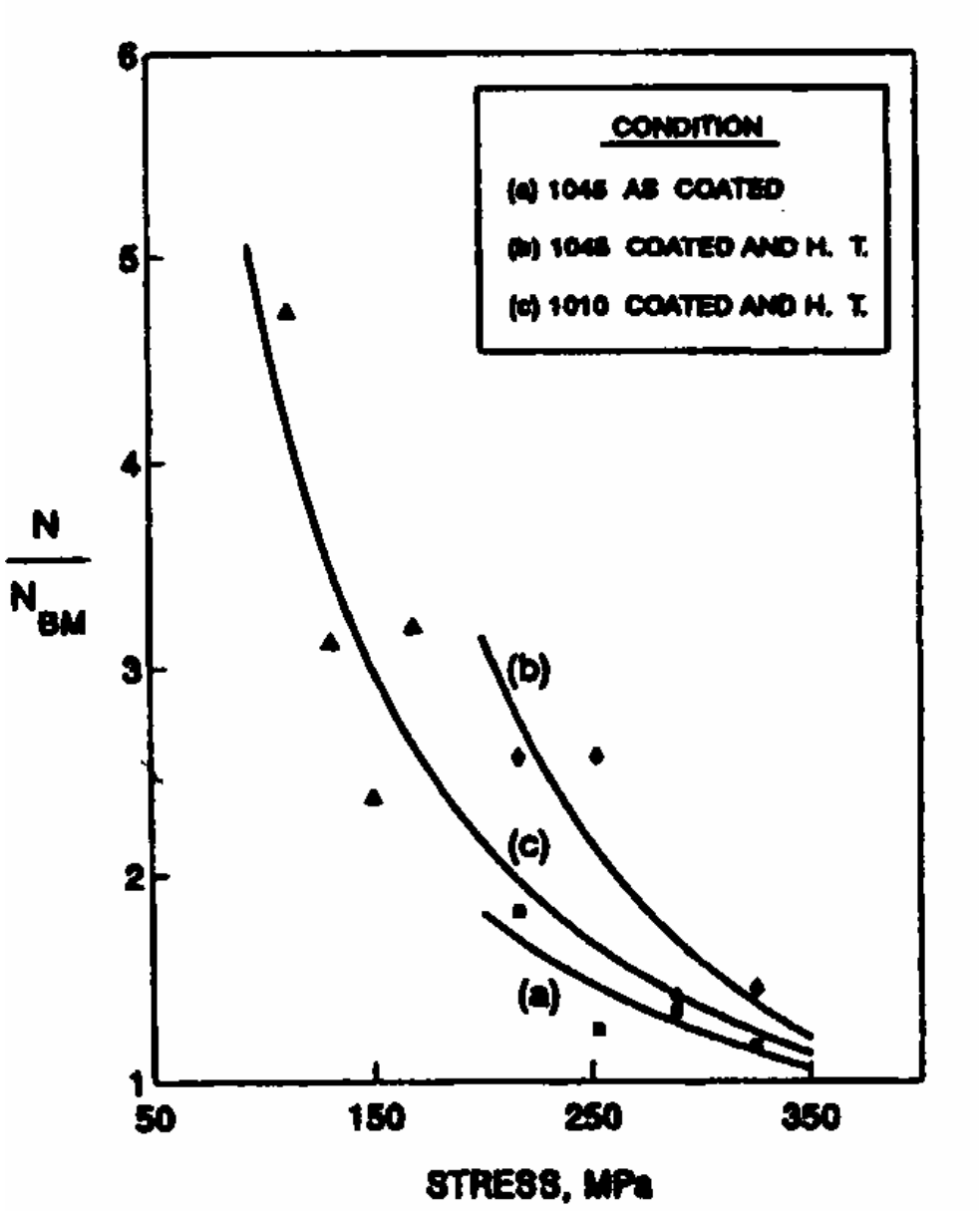

Figure 2.39. Number of cycles to failure EN coatings, as-plated and heat-treated, on AISI 1001, and 1045 substrates vs. stress [Puchi et al., 1996].

Furthermore, Prasad et al. [1994] studied the effect of the agitation factor in the fatigue properties of EN coating. They found that using an ultrasonic agitation system was significantly beneficial in improving the fatigue properties of the coating, Figure 2.40. They correlated the improving effect of an ultrasonic agitation bath on the fatigue properties of EN coatings to the superior surface properties of EN coatings deposited in an ultrasonic bath. Based on his results, EN coating deposited in a bath with an ultrasonic agitation system had lower roughness values, Ra, compared with that deposited in a still bath. Figure 2.41 shows the perthometer[7] traces for EN coated surfaces deposited in ultrasonic and still baths.

[7] Perthometer technique is a modular computer-controlled method for measuring and analyzing roughness, contour, and topography.

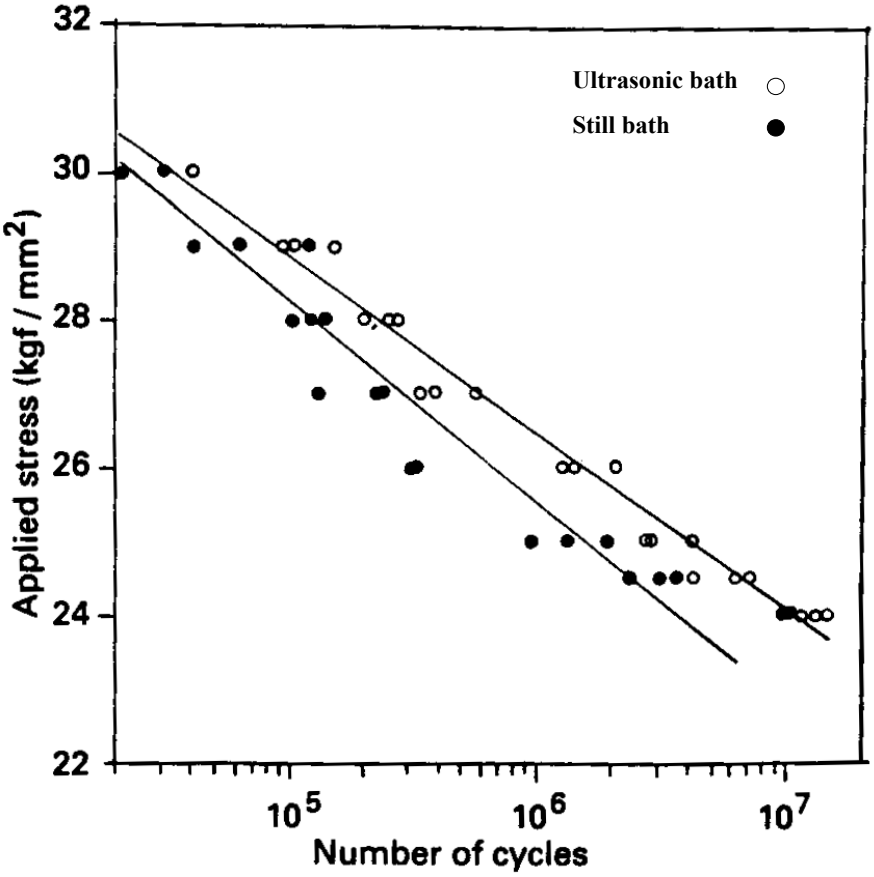

Figure 2.40. Fatigue life of nickel coating at different stresses [Prasad et al., 1994].

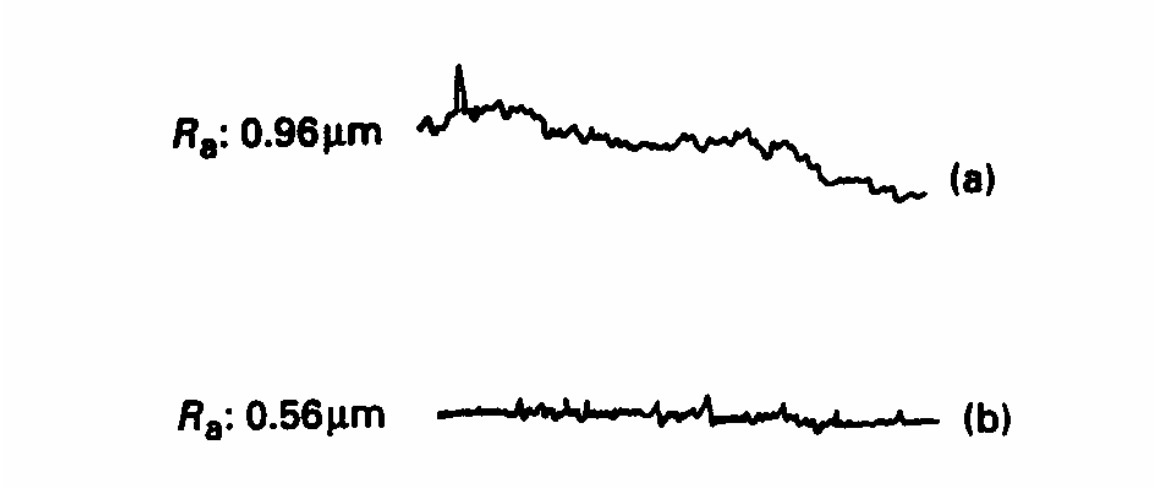

Figure 2.41. Perthometer traces for EN coated surfaces
(a) still bath, (b) ultrasonic bath [Prasad et al. 1994].

2.4.13 Corrosion Resistance Properties

2.4.13.1 DC methods and weight loss measurement

EN coatings have excellent corrosion resistance in many industrial environments. The corrosion resistance is attributed to their phosphorus content. The EN coating shows superior corrosion resistance compared with electroplated (EP) nickel. Table 2.6 shows a comparison between the pitting resistance of EN and (EP) after a salt spray exposure [Weil et al. 1989]. It can be seen from Table 2.6 that EN has a better pitting resistance than EP. The corrosion resistance of EN coatings is a rather complicated phenomenon. The general concept that high phosphorus coatings are more corrosion resistant than low phosphorus coatings cannot be generalized for all industrial environments. However, as a rule of thumb, coatings with high phosphorus content have amorphous microstructures. This provides a better corrosion resistance due to the absence of grain boundaries. There are several factors affecting the corrosion properties of EN coatings. These include phosphorus content, coating thickness, porosity, type of heat treatment, and induced tensile stress of substrates caused by machining or surface finishing operations [Jafar et al., 1996].

Figure 2.42 illustrates the effect of phosphorus content on the corrosion resistance of an EN deposit in 10% HCl. The highest corrosion rate is obtained when the microstructure consists of both the β and γ phases. Similar results have been obtained by measuring the time to failure in nitric acid as illustrated in Figure 2.43 [Duncan, 1996].

Table 2.6. Pitting rating and corrosion potential of EN and EP [Weil et al. 1989].

Phosphorus Content	Rating *		Corrosion Potential mv. vs. SCE.		Corrosion current μA/cm2	
	EN	EP	EN	EP	EN	EP
Low	4/4	2/2	0.44	0.55	1.55	0.66
Med.	1/1	2/2	0.57	0.50	0.19	1.2
High	1/2	2/2	0.50	0.73	0.62	0.7
Med+Low	1/2	1/1	0.58	0.41	0.28	0.37
High+Low	2/2	0/1	0.46	0.27	1.42	0.12
High+Med	0/1	2/2	0.42	0.54	0.66	0.43

* The first number indicates the number of pits that penetrated to the steel substrate and the second number indicates the total number of pits.

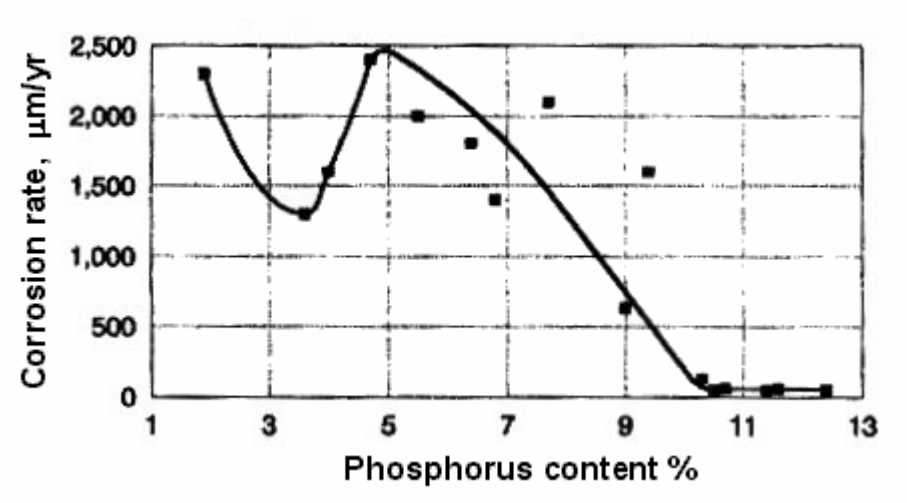

Figure 2.42. Effect of phosphorus content on corrosion rate of EN deposition in 10% HCl [Duncan, 1996].

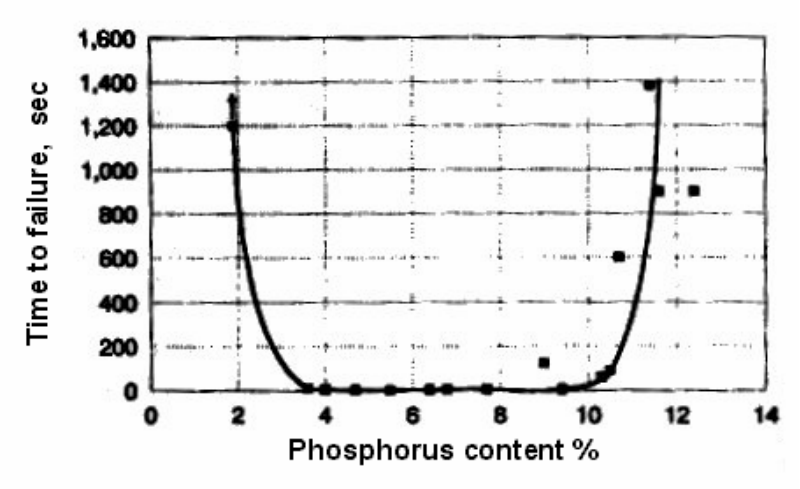

Figure 2.43. Effect of phosphorus content on nitric acid resistance [Duncan, 1996].

Figure 2.44 shows the effect of phosphorus content on the corrosion potential of the powder metallurgy (PM) specimens in 1.0 MHCl solution. A few conclusions can be made from Figure 2.44. Firstly, reducing the porosity of the coating results in lower corrosion potentials. Secondly, heat treatment has a deleterious effect, decreasing the corrosion resistance of the coating. In addition, the corrosion resistance of EN deposits is directly related to their thickness. It was explained previously that the porosity of an EN coating is a function of many parameters of which thickness is one. As the coating thickness increases, the density of pores also increases resulting in reduced corrosion resistance.

Figures 2.45 and 2.46 show the effect of coating thickness on the corrosion resistance of EN deposits in 0.5 M H_2SO_4. Figure 2.45 shows that the presence of 3 μm EN coating reduces the I_{corr}= 243 μAcm^{-2} for pure iron to 73 μAcm^{-2}. Furthermore, the I_{corr} drops to 40 μAcm^{-2} when the EN coating thickness exceeds 5 μm. Figure 2.46 shows that thicker coatings passivate at lower currents and, consequently, have a better corrosion resistance. This is related to the reduction in the porosity of the coating due to increased thickness shown in Figures 2.21 and 2.22.

As mentioned previously, coatings with high phosphorus show better corrosion resistance than those of low phosphorus content coatings due to their amorphous microstructure. However, in hot concentrated caustic soda (NaOH) environments, EN coatings show a reverse corrosion behavior [Tracy et al., 1986]. Fills and Duquette [1985] studied the effect of phosphorus content on various environments. Also, Wronkowska [Wronkowska, 1993] studied the characteristics of the passive layer formed on EN coated surfaces in 0.1N potassium hydroxide. The results of these studies show that the top passive layers on low and medium phosphorus EN coatings are NiO and NiO_2 as shown in Figure 2.47. The multi-layered passive film shows good stability that leads to high corrosion resistance.

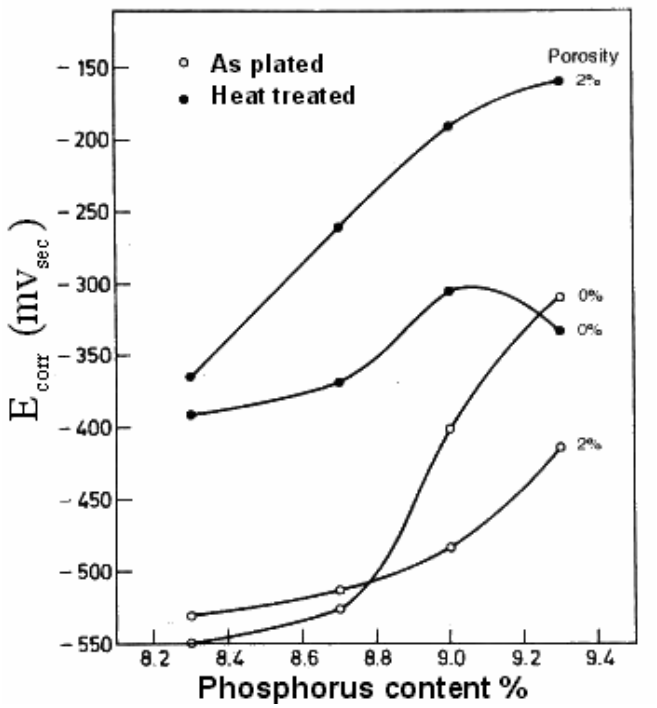

Figure 2.44. Effect of phosphorus content on the corrosion potential [Singh et al., 1995].

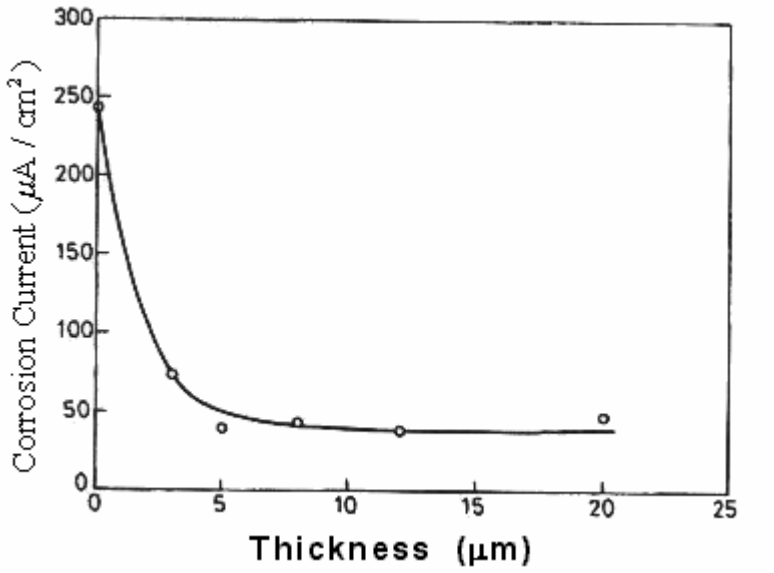

Figure 2.45. Dependence of corrosion current on coating thickness [Doong et al., 1986].

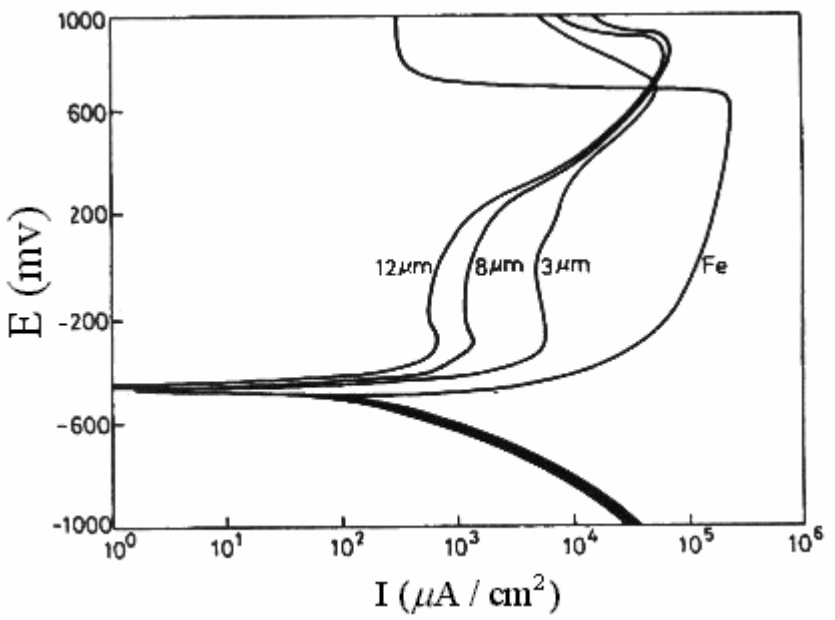

Figure 2.46. Effect of coating thickness on Corrosion potential [Doong et al., 1986].

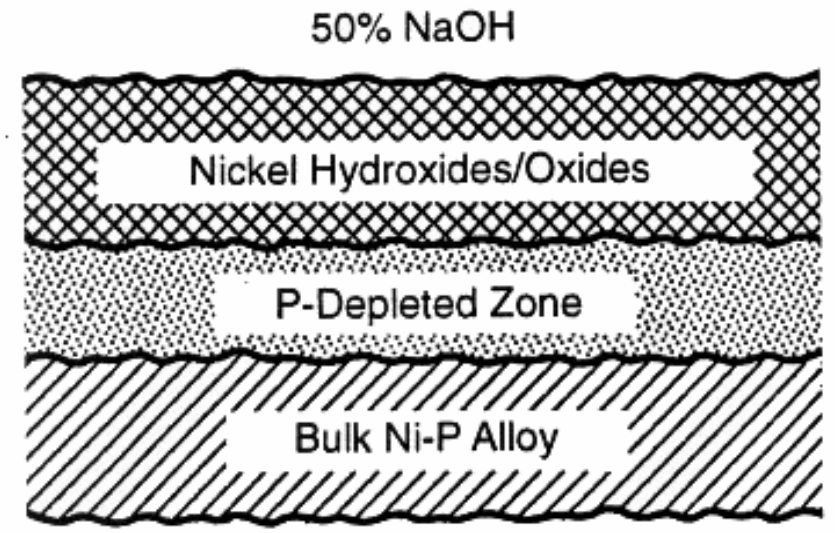

Figure 2.47. Schematic surface cross-section of EN coating in alkaline solutions [Tracy et al., 1986].

This type of passive film is observed only in low and medium phosphorus content EN deposits in hot alkaline environments [Wronkowska, 1993]. Table 2.7 shows the corrosion rates calculated for different types of EN coating. C. Kerr and co-workers [1997] studied the effect of coating thickness on Tafel analysis of high phosphorus EN coating in 0.125 M H_2SO_4 at 22°C. As shown in Table 2.8, there is a direct correlation between the coating thickness and its corrosion resistance. The thicker the coating is, the higher the E_{cor} would be. However, based on this study there is a significant increase in corrosion resistance of high phosphorus EN coating when the thickness exceeds18 μm.

Table 2.7. Electrochemical results of the test conducted by Wronkowska [Tallet, 1986].

	Corrosion Rate (μm/y)			
Techniques	Ni	LPEN	MPEN	HPEN
EIS	0.69	1.43	0.55	4.35
Linear Polarization	0.73	2.29	0.70	2.17
Tafel Polarization	0.71	1.10	0.68	2.67
$\beta\alpha$ (A)	0.166	0.155	0.237	0.193
βc (A)	0.352	0.161	0.126	0.150

Table 2.8. Tafel analysis of electroless nickel deposits of various thickness [Kerr et al., 1997].

Deposit thickness (μm)	**Corrosion potential E_{cor} vs. SCE (v)**	**Corrosion current i_{cor} (μA cm^{-2})**
0	-0.539	61
1	-0.447	30
3	-0.425	30
6	-0.423	30
12	-0.388	9
18	-0.230	5
24	-0.205	7

Amorphous Cu-Ni-Sn-P alloys prepared by splat quenching are good filter materials [Data et al., 1984 and Bangwei et al., 1994]. It is apparent that if a Ni-Cu-Sn-P coating can be produced through the EN deposition method, it will be attractive since it can be used in several applications in various industries. Although deposition of nickel phosphorus coatings containing two or more extra alloying elements such as Cu and Sn is more complex than normal EN coatings, it is feasible. The corrosion resistance of EN alloys has been studied by Zhang and co-workers [2000]. Table 2.9 shows the results of a study conducted by Zhang et al. As shown, all the deposited samples showed significantly higher corrosion resistance compared with stainless steel sample, smple No. 6. It can be concluded from their study that in 5% HCl, 50% NaOH, and 10% NaCl all the coatings showed nearly similar corrosion resistance. However, samples 1 and 2 showed superior corrosion resistance compared with other samples in 0.5 molar H_2SO_4. Based on a previous study conducted by the same group, [Haowen et al., 1999], as long as the deposits were amorphous, the addition of Sn to Ni-P coating did not improve the corrosion resistance of the coating. Moreover, Zhang and co-workers studied the effect of the immersion time on the corrosion rate for various types of complex EN coatings. Figures 2.48 to 2.50 illustrate the results obtained. As seen, in all the solutions except 0.5 molar H_2SO_4, coated specimens showed superior corrosion resistance compared with stainless steel. A very interesting point revealed as the result of this study was that all of the coated samples after few days of immersion in 50% NaOH solution showed passivation behavior, Figure 2.51. In other words, after initiation of corrosion in the first few days of immersion the corrosion, as measured by weight loss, stops. However, for the stainless steel sample weight loss increases as time passes.

Table 2.9. The corrosion rates per year of the various types of EN alloyed deposits in different types of solution[a] [Zhang et al., 2000].

Sample No.	**1**	**2**	**3**	**4**	**5**	**6 (Stainless Steel)**
Ni content at.%	90.0	81.6	82.91	74.08	80.24	1Cr18Ni9Ti
P content at.%	8.2	15.68	12.26	22.48	11.01	
Sn content at.%		0.5	1.42	1.59	3.66	
Cu content at.%	1.8	2.22	3.41	1.85	5.09	
Structure[b]	c	a	a	a	a	c
	Corrosion rate, mg (cm^2 year)$^{-1}$					
0.5 M H2SO4	2.6	3.0	7.8	20.9	14.3	11.3
5% HCl	514.9	599.6	501.9	740.4	280.3	2923.5
50% NaOH	1.3	2.6	1.3	1.3	1.3	10.4
10% NaCl	0	0	3.9	1.3	3.9	10.4

[a] The values for corrosion rates are calculated from the weight loss data for immersion for 7 days.
[b] a: amorphous, c: crystalline.

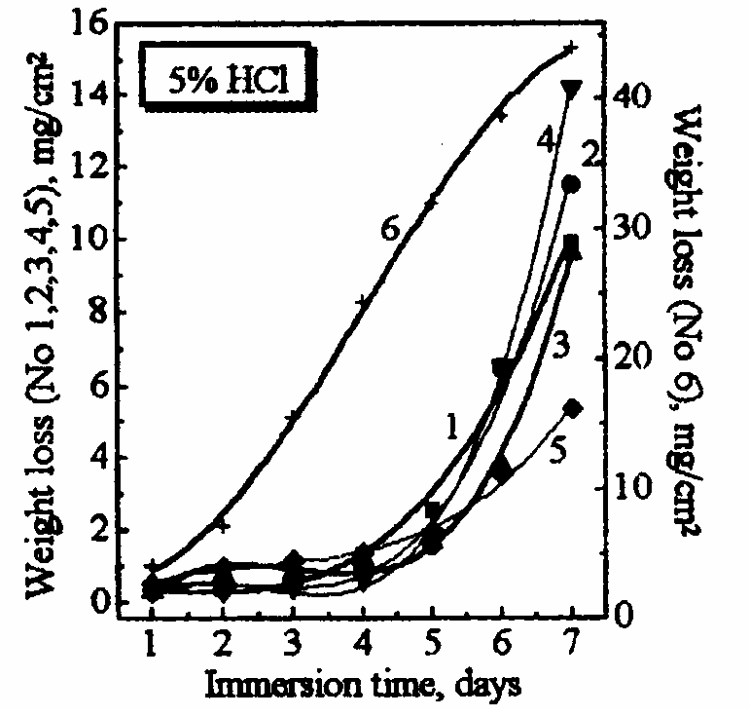

Figure 2.48. Weight loss vs. immersion time in 5% vol. HCl for various Ni-Cu-Sn-P deposited alloys (legend in Table 2.9) [Zhang et al., 2000].

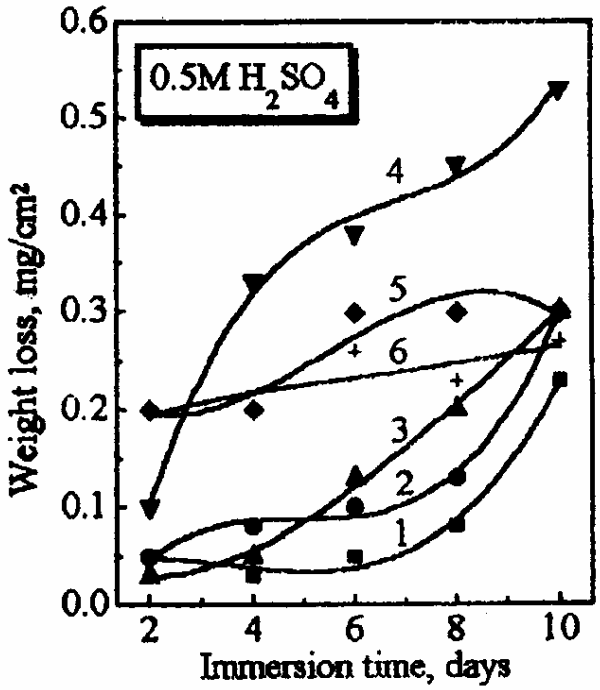

Figure 2.49. Weight loss vs. immersion time in 0.5 molar H_2SO_4 for various Ni-Cu-Sn-P deposited alloys (legend in Table 2.9) [Zhang et al., 2000].

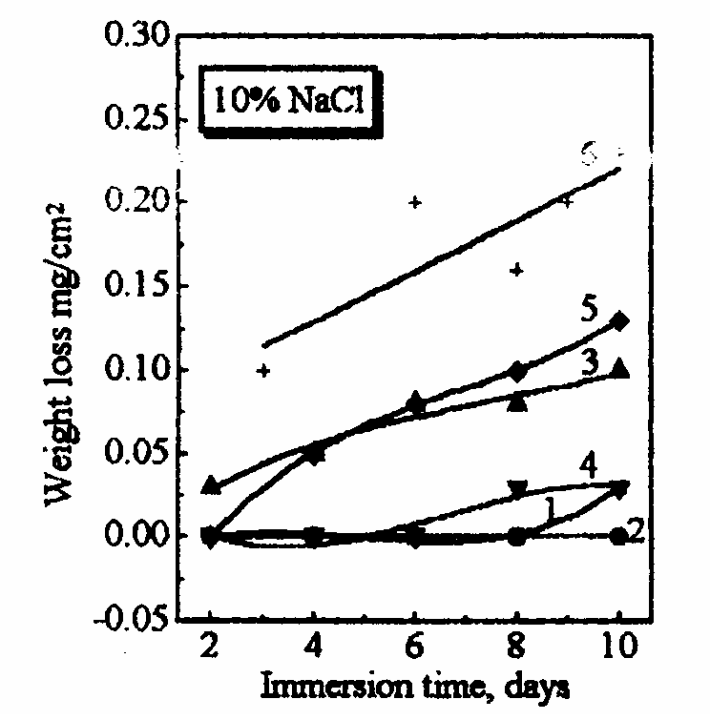

Figure 2.50. Weight loss vs. immersion time in 10% NaCl for various Ni-Cu-Sn-P deposited alloys [Zhang et al., 2000].

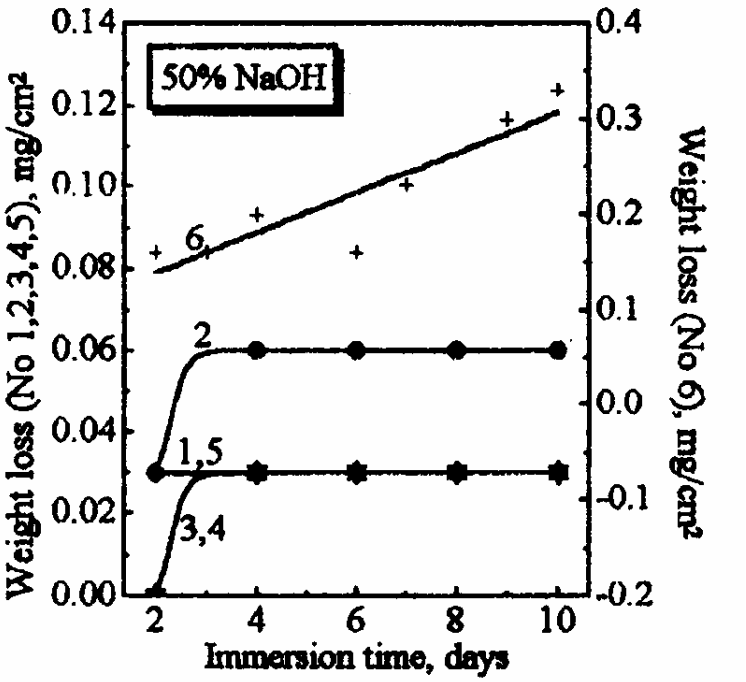

Figure 2.51. Weight loss vs. immersion time in 50% NaOH for various Ni-Cu-Sn-P deposited alloys [Zhang et al., 2000].

2.4.13.2 AC methods

In many cases, coating failure occurs in only a small portion of the exposed area. In other words, the area on which electrochemical reactions occur is significantly smaller than the exposed area. Therefore, the magnitude of the corrosion current does not indicate the corrosion rate, which results in inaccuracy of corrosion evaluation. Also, the applied potential when using the DC method may damage the coating being examined [Eggers, 1998]. That is why the AC method (electrochemical impedance spectroscopy) has been widely used during the past. Many studies have shown that changes in a coating system can be monitored with the electrochemical impedance spectroscopy technique (EIS) [Walter, 1981; Mansfeld et al., 1982; and Padget and Moreland, 1983]. The EIS technique can also be considered a unique method for a better understanding of the mechanisms of corrosion attack in coated and bare metals. In the EIS method, an alternating voltage is applied to the corroding metal, and the impedance, Z, is measured because both the magnitude and the relative phase angles of the voltage and current have to be accounted for. Applying an alternating potential introduces a new parameter, the frequency of the signal. In the EIS technique, the impedance is measured for a wide range of frequencies from a few mHz to hundreds of kHz [Fildes et al., 1995]. Since the impedance in the alternating signal is represented by a complex number, there are two associated quantities, the real and the imaginary component. Thus it requires the use of vector analysis methods [Fildes et al., 1995].

Tallet at el. [1988] studied the corrosion resistance of EN coatings. Two plating baths were used to deposit EN coatings, bath I and II. Table 2.10 shows the composition and condition of these two baths. Table 2.11 shows a summary of the results obtained in this study. As seen, in most of cases the deposit from bath I exhibited a good corrosion resistance in diluted food acidulants. For example, the resistance polarization in 5 vol.% tartaric acid was 4.8×10^4 ohm compared to 1.3×10^4 ohm for deposit from bath II.

Furthermore, EIS studies on corrosion resistance of EN coatings, Figure 2.52, shows that the medium phosphorus EN (MPEN) deposit provides superior corrosion resistance compared to the other two types of EN coatings, high phosphorous EN (HPEN) and low phosphorus EN (LPEN) coatings. As shown, in some cases the LPEN coating shows superior corrosion resistance compared to that of the HPEN coating (e.g. 50 Vol.% acid citric and tartaric). This may be attributed by the nature of the oxide film formed.

Table 2.10. Compositions and conditions of the EN baths [Tallet, 1986]..

Chemical	Bath I (M)	Bath II (M)
Nickel Chloride	0.10	0.10
Sodium Hyphosphite	0.28	0.10
Acetic Acid	0.20	0.20
pH	4.61-4.97	4.66-4.67
Temperature (°C)	80±2	80±2

Table 2.11. Comparison of the corrosion resistance of HPEN and LPEN in weak acidic environments [Tallet, 1986].

	Corrosion Data in Succinic Acid			
	1% wt.		5% wt.	
	E_{corr} v	R_p *Ohm*	E_{corr} v	R_p *Ohm*
Bath 1	-0.392	3.00×10^3	-0.472	8.73×10^3
Bath 2	-0.359	3.25×10^3	-0.390	4.24×10^3
	Corrosion Data in Citric Acid			
	5% wt.		50% wt.	
	E_{corr} v	R_p *Ohm*	E_{corr} v	R_p *Ohm*
Bath 1	-0.304	2.70×10^3	-0.432	1.99×10^3
Bath 2	-0.299	1.72×10^3	-0.320	4.99×10^3
	Corrosion Data in Tartaric Acid			
	5% wt.		50% wt.	
	E_{corr} v	R_p *Ohm*	E_{corr} v	R_p *Ohm*
Bath 1	-0.366	4.8×10^3	-0.402	1.15×10^3
Bath 2	-0.520	1.3×10^3	-0.369	6.5×10^3
	Corrosion Data in Malic Acid			
	5% wt.		25% wt.	
	E_{corr} v	R_p *Ohm*	E_{corr} v	R_p *Ohm*
Bath 1	-0.402	6.453×10^3	-0.246	1.03×10^3
Bath 2	-0.334	5.019×10^3	-0.725	2.05×10^3

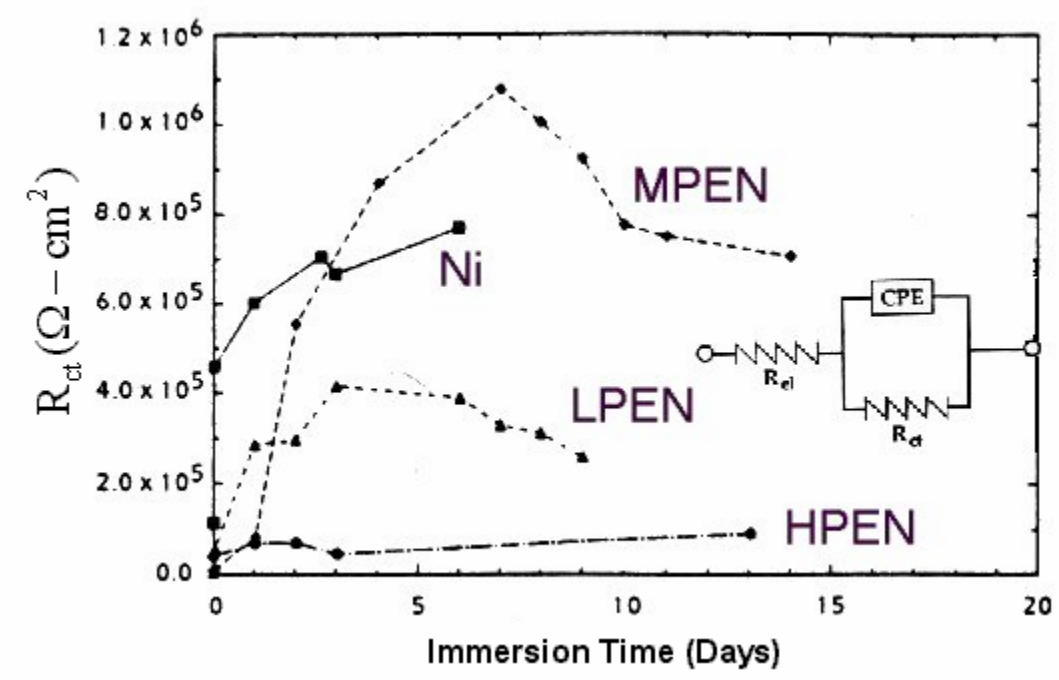

Figure 2.52. Effect of immersion time on R_{ct} in 50% caustic soda [Tallet, 1986].

2.5 EN Composite coatings

The ability to co-deposit particulate substances in an EN coating matrix created a new branch of EN coatings, namely, EN composite coatings. The co-depositing particulate materials are added in the EN bath in powder form. These materials are either a hard substance such as silicon carbides, aluminum oxides, diamond, and tungsten to improve the wear resistance of the EN coatings or dry lubricants such as fluoropolymers (PTFE) [Tulsi, 1983 and Nishiro et al., 1994], molybdenum disulfide, and graphite (Henry, 1990, Xam-Hua et al., 1992, and Feldstein, 1985) to reduce the coefficient of friction. The fact that filmability of molybdenum disulfide is about 80 times higher than that of graphite [Puipee and Eudeline, 1989] has made the nickel-phosphorus-molybdenum disulfide composite coating an excellent candidate where high wear resistance is required. Noomir-Vaghefi et al. [1997] have studied the wear properties of nickel-phosphorus-molybdenum disulfide. Based on their study, the existence of molybdenum disulfide particles in the EN coating matrix improves the wear properties of the EN coating by reducing the coefficient of friction.

Another common substance used in EN composite coating is diamond. Reddy et al. [2000] studied the wear resistance of a nickel-phosphorus-diamond composite. Moreover they studied the effect of various parameters including diamond particle size and coating thickness to particle size on wear resistance EN diamond composite coatings. They found that the larger size diamond particles are less firmly held by the thinner EN coatings while very fine diamond particles do not significantly affect the wear resistance of the thicker EN coatings. As a result, an optimum coating thickness to particle size ratio is required in order to provide the best wear resistance.

Yu et al. [2000] studied the corrosion properties of Ni-P-CeO_2, Ni-P-SiO_2, and Ni-Sn-P coated on a plain carbon steel substrate. Table 2.12 shows the result of this study. As shown, the corrosion resistance of Ni-P-CeO_2 and Ni-P-SiO_2 in salt water is about the same, however, the tarnish resistance in H_2S of the Ni-P-CeO_2 coatings is a little worse than that of Ni-P-SiO_2 coating. An over all comparison among the three

coatings, Ni-P-CeO_2, Ni-P-SiO_2, and Ni-Sn-P, shows that Ni-Sn-P has superior corrosion resistance.

Table 2.12. Results of the acceleration corrosion and tarnishing tests [Yu et al., 2000].

Type of Coating	**Salt water dipping (h)[a]**	**H_2S tarnish (min)[b]**
Uncoated carbon steel	1.5	20
Ni-Sn-P	12	330
Ni-$PceO_2$	28	500
Ni-P-SiO_2	29	670

(a) Time (h) needed until the solution became faint muddy.
(b) Time (h) needed until the solution became faint tarnish.

3 Apparatuses and Experimental Procedures

This chapter discusses the apparatuses and experimental procedures. The work conducted in this research can be divided into two phases; namely, design and construction of an automated prototype EN bath ,phase one, and evaluation of three types of EN coatings (high, medium, and low phosphorus in as-plated and heat-treated condition) phase two. Following is the outline of the research conducted in this thesis:

1. Design and engineering of the EN bath

2. EN coating evaluation

    2.1. Physical evaluation
        2.1.1. Hardness
        2.1.2. Differential Scanning Calorimetry (DSC)
        2.1.3. X-ray diffraction compound analysis

    2.2. Tribological evaluation
        2.2.1. Surface roughness
        2.2.2. Friction coefficient

    2.3. Mechanical evaluation
        2.3.1. Three-point bending (adhesion)
        2.3.2. Fatigue
        2.3.3. Tensile

    2.4. Corrosion resistance evaluation
        2.4.1. Reciprocating corrosion and wear
        2.4.2. Slurry corrosion and wear

2.5. Microscopic evaluation

2.5.1. SEM

2.5.1.1. Microstructure

2.5.2. TEM

2.5.2.1. Microstructure

2.5.2.2. Energy dispersive spectrometry (EDS)

2.5.2.3. X-ray diffraction pattern

3.1 Electroless nickel phosphorus bath

In order to completely monitor and control the coating parameters such as bath pH, temperature, agitation factors, and chemical composition during the coating process, a computer automated prototype EN bath was designed and built. Unlike many conventional baths used in industries, in which replenishment is accomplished by adding fresh solution to the main bath, in the bath designed the replenishing solutions were added to a secondary mixing chamber. This prevented localized variations in temperature and pH, one of the major reasons for various types of coating defects. Furthermore, the computerized control system allowed the operator to control pH and temperature in a constant or in an intermittently increasing or decreasing value, accurately ($\pm$ 0.2 pH and $\pm$ 0.3°C).

As shown in Figure 3.1 the EN bath designed consisted of the following main components, namely: two rectangular tanks, filters, solenoid valves, gate valves, T-type thermocouples, magnetic stirrer, 500 W quartz heater, pH probe quipped with an ATC (automatic temperature compensation), circulation pump, and a computer-controlled data acquisition (Labmate) system.

3.1.1 Design specification

3.1.1.1 Tank

The bath designed included two rectangular shaped tanks made from Lexan^{TM}, which is a type of polycarbonate with superior mechanical properties. Tank 1 (coating bath) was connected to Tank 2 (the backup and storage tank) by two MasterFlex^{TM} silicone tubes, Figure 3.1. The maximum capacity of each of these tanks was7 liters. However, the coating tank could be operated within the range of 3.5 to 7 liters of solution. This provided a wide range of substrate size (70 to 800 cm^2). Figure 3.2 shows a schematic illustration of the apparatus. Also, Figure 3.3 shows the 3-D solid modeling of the EN bath designed.

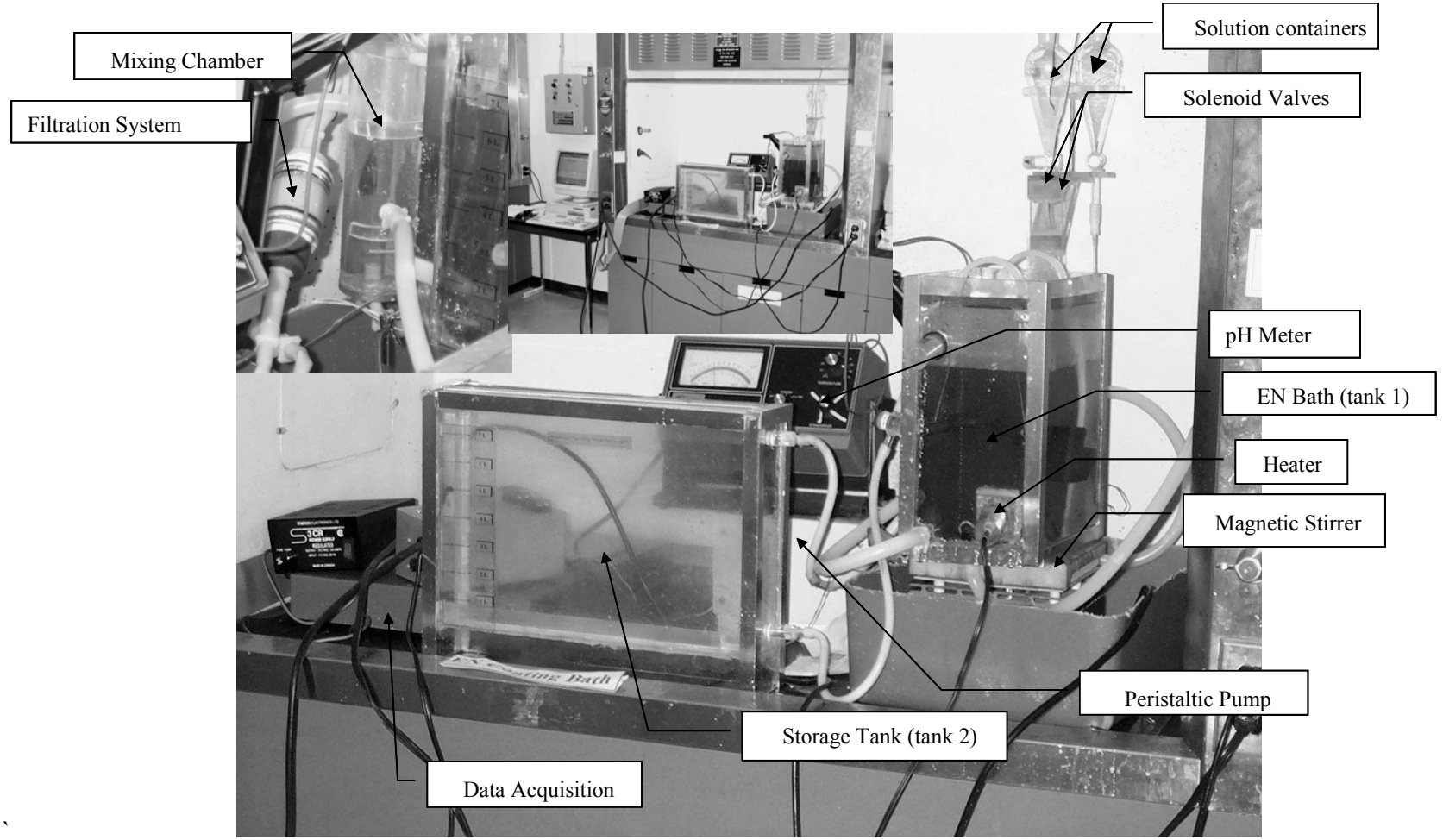

Figure 3.1. Photograph of the designed EN bath

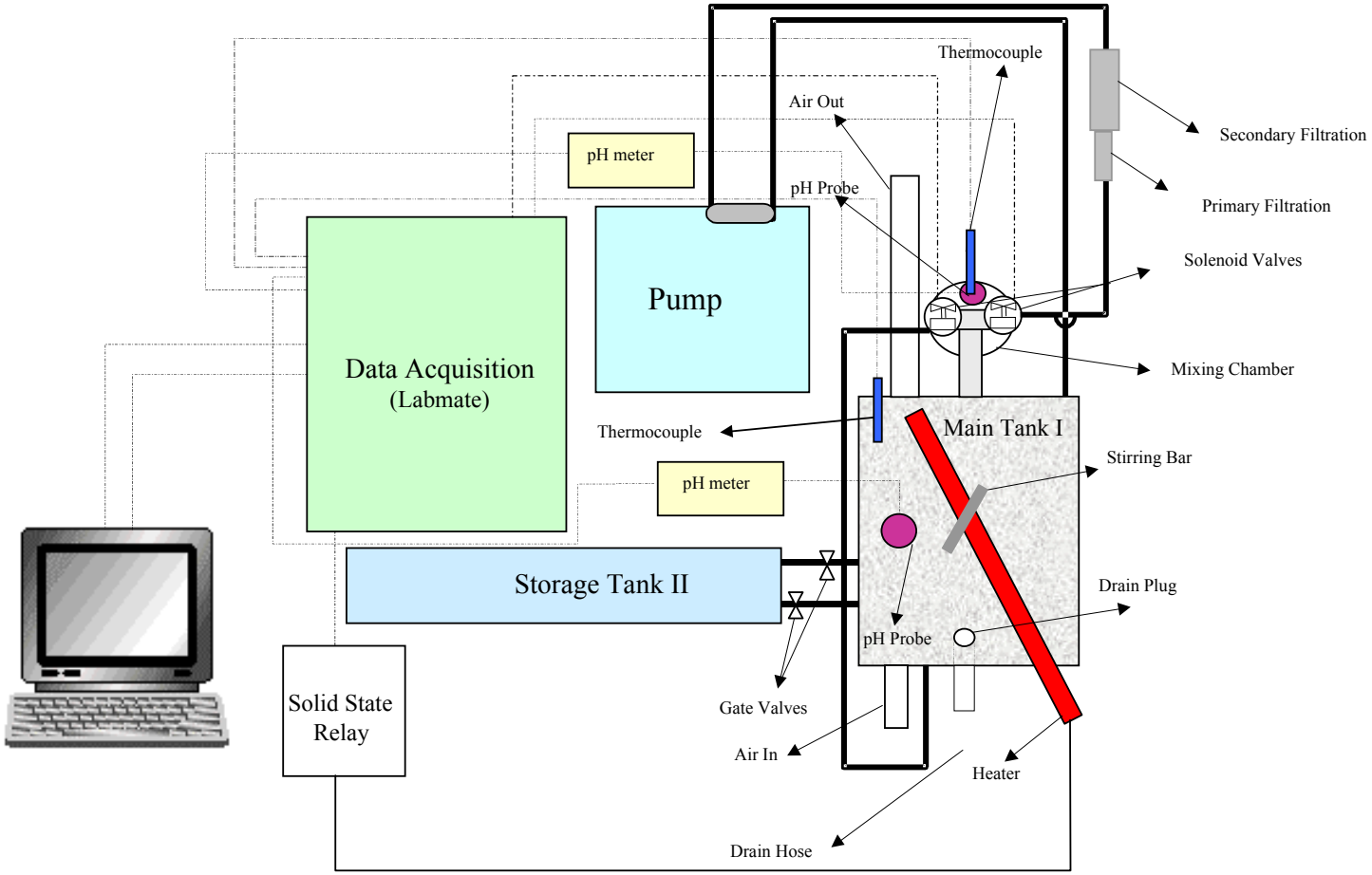

Figure 3.2. Schematic view of the experimental setup.

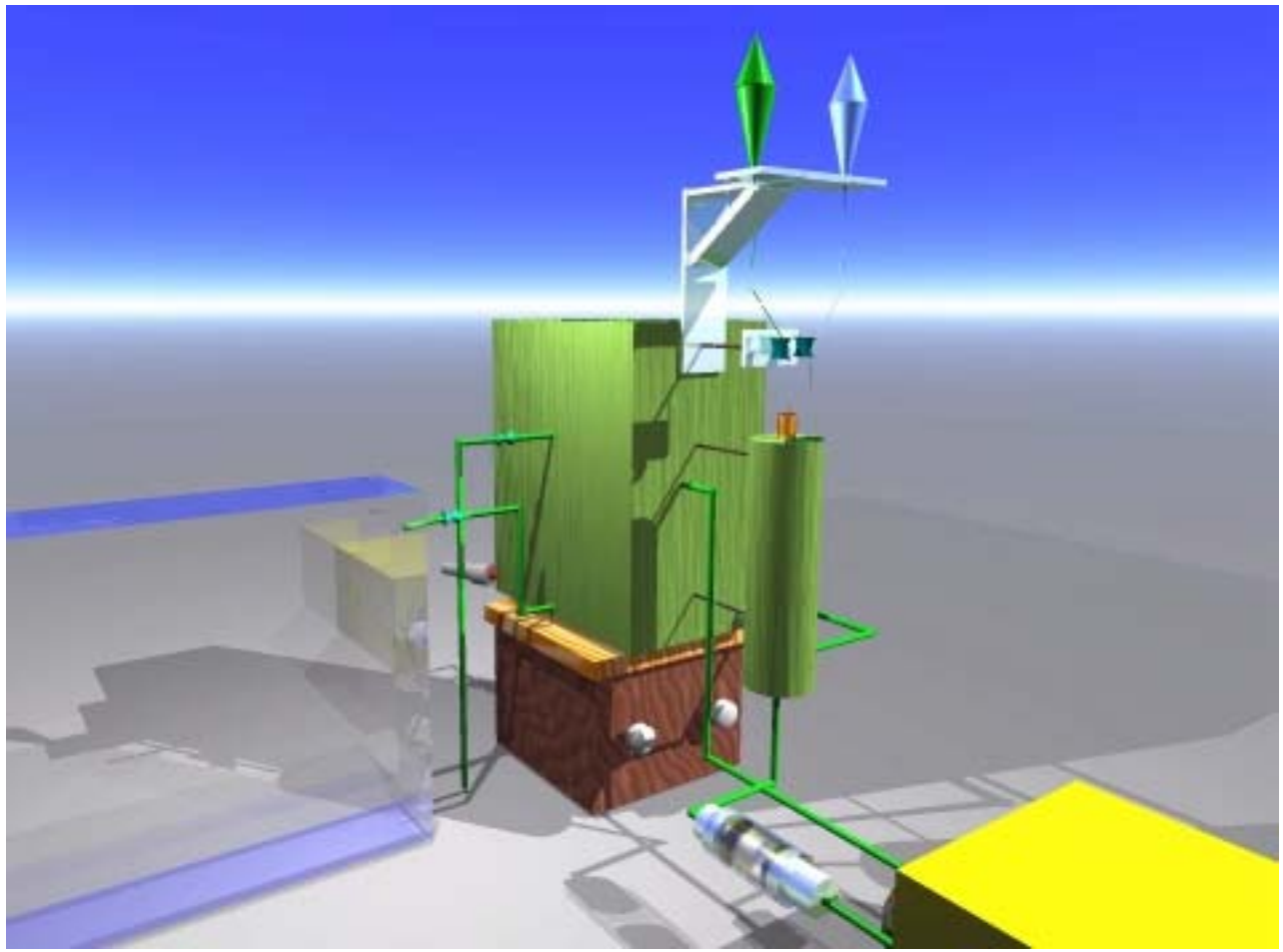

Figure 3.3. 3-D solid-model view of the EN bath.

3.1.1.2 Temperature control system

The temperature control system consisted of a 500 W quartz electric heater, two T-type thermocouples which were mounted inside 3 mm-diameter glass tubes filled with high thermally conductive zinc oxide paste, and a solid state relay. The thermocouples were connected to the main control device, which is a 700 series Scimetric Instruments data acquisition with several digital and analog input and output channels. The control system monitored the temperature in both the coating tank (Tank 1) and the mixing chamber. If the temperature difference between these two exceeded 5° C (this may only occur when there is a problem with the circulation system due to either pump failure or plugged filter) the system alerted the operator. The heater was connected to a solid state relay operated by the control system as illustrated in Figure 3.2. As a result, the bath temperature could be maintained in a fixed narrow range ($\pm 0.3^{o}$C) or could be changed according to a user defined function.

3.1.1.3 PH control system

The pH of the plating solution decreased with time due to hydrogen evolution. To control the bath pH, two conventional gel pH probes, mounted in Tank 1 and the mixing chamber, continuously measured the instantaneous pH value of the solution. Whenever the bath pH fell below the set limit, a few droplets of diluted ammonia were allowed into the bath by means of one of the two electronically controlled pinch valves. A computer program estimated the required amount of ammonia to be fed into the bath. Also, the solution replenishment was accomplished by means of the other pinch valve. The required amount of fresh solution was added to the mixing chamber in order to balance the concentration of nickel and hypophosphate ions in the solution. The ammonia and the replenishing solution were added into the mixing chamber but not to the coating tank directly. This prevented any rapid chemical composition changes in the bath. However, there was a time delay for the system to reach its steady state condition. To eliminate the error due to the instability of the bath pH during the delay period, the control system terminated the replenishing module

immediately after any of the pinch valves had opened. The replenishing module was activated when the pH levels in the mixing chamber and Tank 1 were approximately equal (±0.2). The estimated time for the system to reach its steady state condition varied between 30 seconds to 1 minute depending on the solution volume and the flow rate.

3.1.1.4 Bath agitation

Bath agitation was another important factor in the EN process. Agitation in the bath creates a uniform solution and prevents any localized temperature spikes. There were several types of agitation systems used in industry. These include air agitation, ultrasonic, and magnetic stirring. In the present bath an adjustable magnetic stirrer and a 3" long Teflon stirring bar were used to create a moderate solution agitation. It was crucial to keep the bath agitation at an optimum level. A strong agitation prevents a complete reaction between the solution and the substrate. On the other hand, a very mild agitation leads to localized temperature or pH changes.

3.1.1.5 Bath filtration

An effective level of filtration was required in the EN process to obtain a smooth and uniform coating. Debris in the solution might seat on the coated surface and cause various types of coating defects. The most common types of filtration systems used in the commercial EN baths are filter bags (up to 500 mesh). However, in the present system a more sophisticated filtration system was desirable. This system consists of a polyethylene tube (80 mm long, 45 mm outside diameter), at the entry level of which two 304 stainless steel screens (100 and 200 mesh) were mounted, as illustrated in Figure 3.4 (a,b,c). The screens were previously passivated in 50 vol.% nitric acid for a period of six hours in order to make them inert to the EN coating. Most of the particles were stopped at this level. However, small size particles might pass through the primary filtration. That was why the middle of the filtration tube had been partially filled with dense fiberglass wool. With the combination of these two filtration systems, the circulated solution can be effectively filtered to 0.5 micron. The flow circulation was accomplished by an adjustable MasterFlex^{TM} peristaltic pump. It

was recommended that the circulation flow rate (per hour) should be ten times greater than the tank volume [Beck and Arnold, 1997]. Therefore, the circulation flow rate required for the present tank would be 35 to 70 liters per hour, which can easily be provided by the pump used.

3.1.1.6 Bath ventilation

A ventilation system was required in the EN process to vent hydrogen and any other hazardous gases or foams produced during the coating process. The entire setup was housed inside a fume chamber. Also, air-in and air-out hoses were installed at the top of Tank 1 to facilitate the ventilation action, Figure 3.1.

3.1.1.7 Bath Calibration

Equipment calibration was an inevitable but nevertheless time consuming part of any experimental study. In order to attain an accurate measurement with the least amount of error, all the measuring devices needed to be calibrated. In the new bath, three quantities needed to be measured, namely, temperature, pH, and the volume of replenishing solution added into the bath. Temperature measurement in the bath was accomplished by means of two sets of thermocouples connected to the data acquisition system (Labmate). In thermocouples the potential difference produced was proportional to the temperature. Although the Labmate converted the input potential to temperature, it was required to define an error factor in order to minimize the measurement error. Such a factor, which was proportional to the read temperature, was obtained by placing an accurate thermometer (± 0.1 °C) close to the thermocouples in the bath and measuring the temperature. Then, the relationship between the input voltage and temperature was obtained using Maximum likelihood method. It was observed that the accuracy of the temperature measured by Labmate was ±0.3 °C, which was accurate enough to satisfy the requirements for the coating process.

In terms of pH measurment, two pH meters equipped with an automated temperature compensated (ATC) system were used (siher Acuument pH meter Model 620). As in

the case of temperature, the input potential received by the Labmate was converted to pH. Since pH was a function of temperature, in order to compensate for the effect of temperature during the calibration of the pH meter, buffer solutions with known pH at different temperatures were used. The function correlating input voltage, pH, and temperature was obtained.

In controlling the bath pH and replenishing the bath solution, it was required to measure the volume of the solution added to the mixing chamber. Since the solution containers were conically shaped, Figures 3.1 and 3.3, the amount of solution added into the mixing chamber was a function of time (the period of time that the solenoid valves are open), the height of the solution in the containers (the total period of time that the valves have been open), and the density of the solution.

3.1.1.8 Software specification

A fully customized computer program was written in QBasic language to monitor and control the system variables. The program was capable of receiving several input variables and controlling temperature, pH, and bath composition accordingly. The bath temperature and pH could be maintained at predetermined values (±0.5 °C and ± 0.01 pH); in addition they could be changed according to a given function of time by the user. The software developed was also capable of dividing the entire coating process into a maximum of four segments. In each segment, the system variables could be monitored and controlled independently. This feature enabled the user to accomplish up to four different layers of coatings in four different temperature and pH ranges. As a result, a multi-layer coating with different phosphorus content (different properties) could be deposited on a single substrate.

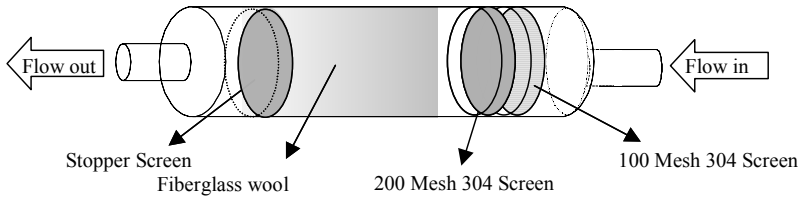

(a)

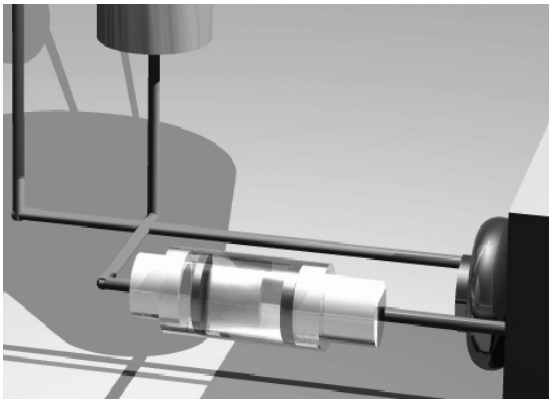

(b)

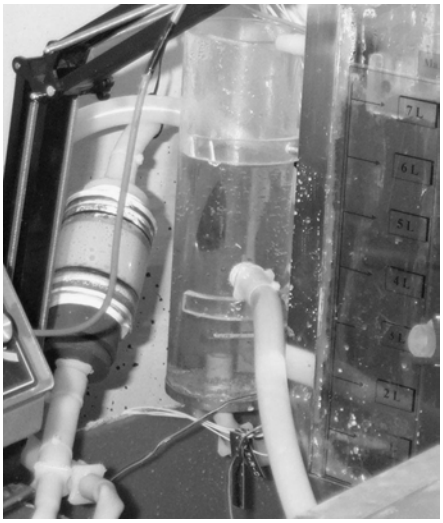

(c)

Figure 3.4. Filtration System; (a) Schematic, (b) 3-D solid modeling view, (c) Photograph.

3.2 Surface preparation

All the samples were subjected to the following pre-treatment and plating procedure[1]:

1. Ultrasonic cleaning in industrial cleaning solution at 60 °C for 30 min.
2. Rinsing with tap water at room temperature (RT) for 2 min.
3. Cleaning in 20 vol. % H_2SO_4 at RT for 30 s.
4. Rinsing by immersion in de-ionized water at RT for 2 min.
5. Cleaning in 5 vol. % H_2SO_4 at RT for 30 s.
6. Rinsing by immersion in de-ionized water at RT for 2 min.
7. Electrocleaning in 40 g/l potassium carbonate solution at RT for 30 s. The current density applied was 0.5 A/cm^2. In order to provide a better scrubbing action on the surface of the specimens during electrocleaning, periodic starts and stops were introduced (5 s on and 1 s off).
8. Rinsing by immersion in de-ionized water at RT for 30 s.
9. EN coating process.
10. Rinsing by immersion in 60 °C water for 1 min.

Also, the following tips are important in order to obtain a high quality coating.

1. Using distilled water rather than tap water in the rinsing stages is beneficial. However, due to economic factors, using distilled water through all of the rinsing

[1] The surface preparation procedure was adapted from the methods recommended by Riedel [1991] and EN solution supplier, Enthon Omi™.

stages might not be feasible. In such a case, using distilled water in the last rinsing stage, right after electrocleaning, is desirable.

2. For more complex shapes with various angles, it is important to provide a uniform current density during the anodic and cathodic electro-cleaning. Using a single electrode does not provide a homogeneous hydrogen or oxygen evolution on the entire exterior surface of the work piece. It was found that the best way to provide such a uniform current is by immersing the specimen(s) in a conductive container and using the body of the container as the cathode (in an anodic cycle) or as the anode (in a cathodic cycle). Therefore, as long as the component is completely immersed in the solution, the oxygen or hydrogen evolution reaction occurs on the surface of the component uniformly.

3. Minimizing the lag time between each stage is very crucial since the specimen immersed in the acid is very susceptible to oxidation in air and the oxide film formed deleteriously affects the properties of the EN deposit. Therefore, an appropriate floor setting is required for industrial capacity plating shops.

4. It is very important to use distilled water for the electrocleaning solution. The presence of contaminants and debris drastically affects the adhesion and porosity properties of EN deposits. Also, it is strongly recommended to use distilled or de-ionized water with very high resistivity (30 MΩ-cm or higher) for the make-up solution.

5. Application of agitation during rinsing is very beneficial in removing the remaining acid trapped in blind spots in more complex shapes.

Table 3.1 shows the phosphorus content, bath pH, temperature, solution, and coating rate for three types of EN coatings.

Table 3.1. EN coating composition and EN bath operating conditions.

EN Coating	**Wt. % P***	**pH**	**Temperature °C**	**Bath Solution**	**Coating Rate (μm/h)**
Low phosphorus	4.5±0.4	6.2±0.2	85±0.3	NI-429 (200 ml/l)	9.4±0.5
Medium phosphorus	7.5±0.5	5.0±0.2	88±0.3	EN-435A (60 ml/l) EN-435B (150 ml/l)	9.0±0.5
High phosphorus	11.25±0.5	4.8±0.2	87±0.3	NI-425A (60 ml/l) NI-425B (180 ml/l)	16.6±0.5

*Average of 10 readings taken along the coating cross-section.

In various experiments including DSC, X-ray diffraction analysis, and TEM the stripped-off EN coatings were required to conduct the test. In such cases, AISA 304 stainless steel was used as the substrate. The following cleaning and coating procedure sequence was followed:

1. Ultrasonic cleaning in industrial cleaning solution at 60 °C for 30 min.
2. Rinsing with tap water at room temperature (RT) for 1 min.
3. Cleaning in 20 vol. % H_2SO_4 at RT for 30 s.
4. Rinsing by immersion in de-ionized water at RT for 2 min.
5. Cleaning in 5 vol. % H_2SO_4 at RT for 30 s.
6. Rinsing by immersion in de-ionized water at RT for 2 min.
7. Electroplating in coating solution at optimum EN coating temperature suggested by the supplier (Table 3.1), using 0.2 A/cm^2 current for 30 s.
8. The EN coating process.
9. Rinsing by immersion in 60 °C water for 1 min.

During this coating procedure since, the first layer of the plating is being formed through an electroplating process, there is a poor bonding between the coating and the substrate, unlike in EN coating. As a result, the entire coating can be removed simply by bending the stainless steel coated thin plate. The electroplated portion of the coating, <0.1 μm, can be easily removed by applying a quick polishing process using 1μm aluminum oxide paste.

Figure 3.5 shows the relation between coating thickness and time for various types EN coatings with different phosphorus contents. As shown there is an almost linear correlation between the coating thickness and time. This is due to the fact that the replenishment has been done accurately during the deposition process. As a result, the pH and Ni^{++} concentration has been kept in a steady range. Furthermore, the solution

temperature which directly affects the deposition rate has been kept at a desirable value during the process. Figure 3.6 shows the range of temperature and pH changes during the coating process. Temperature and pH values of the EN bath during the coating process were recorded by the data acquisition system in an interval base, every second. As shown, the temperature in the main tank and mixing chamber have been steadily kept at the preset value. In terms of the temperature in the mixing chamber there are some rapid fluctuations during the replenishment stages. This is due to the fact that the replenishment solutions are at room temperature. Therefore, adding the replenishment solutions to the mixing chamber causes a rapid drop (few degrees) in the temperature. However, after a short period of time the temperature in the mixing chamber comes back to the preset value. The noticeable point in Figure 3.6 is that the fluctuation of the temperature in the mixing chamber does not affect the temperature in the main tank (coating tank). As mentioned previously, this advantage of the bath design eliminates the detrimental effect of the localized temperature changes, one of the sources of superficial defects, due to adding the replenishment solutions directly into the coating tank.

As was mentioned previously, during the deposition process due to the production of H^+, the pH of the tank decreases continuously. As a result, there is an inevitable need for controlling the pH in the coating tank. This is achieved by adding ammonium solution to tank. Figure 3.6 also shows the fluctuation in pH in the coating tank. As shown, although pH fluctuates during the deposition process, this fluctuation is within the acceptable range suggested by the EN solution producer (±0.5 pH unit).

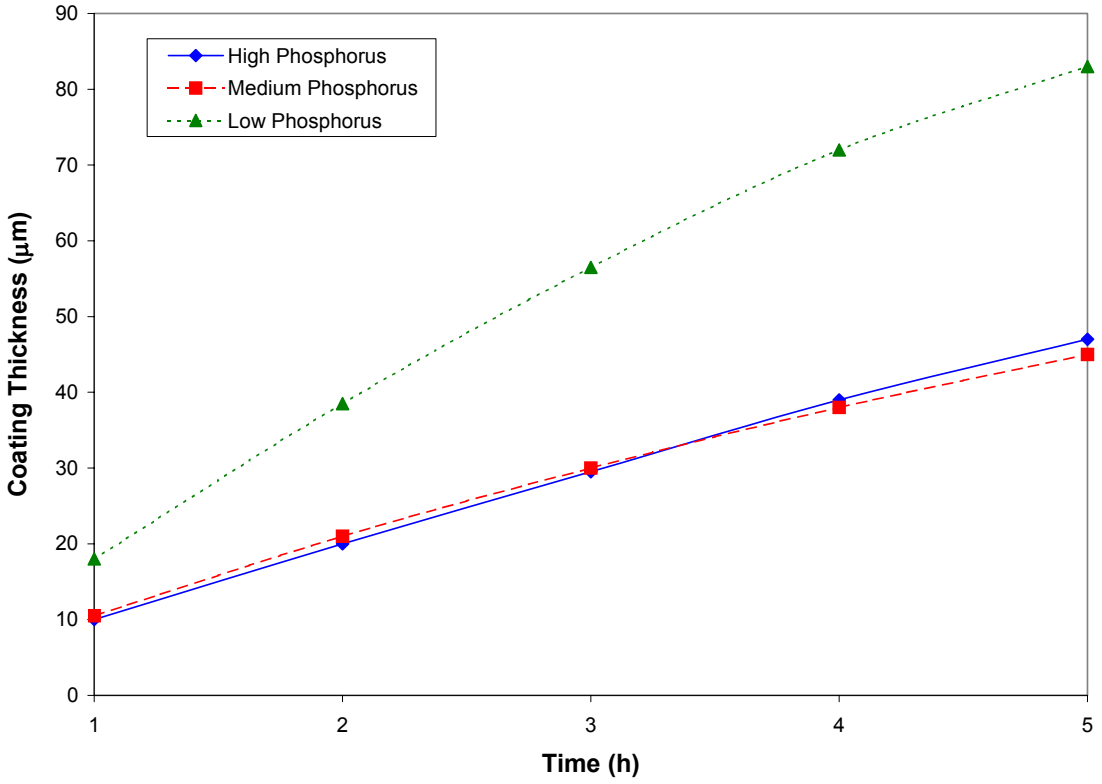

Figure 3.5. Relation between coating thickness and time for three types of EN coatings; low, medium, and high phosphorus content.

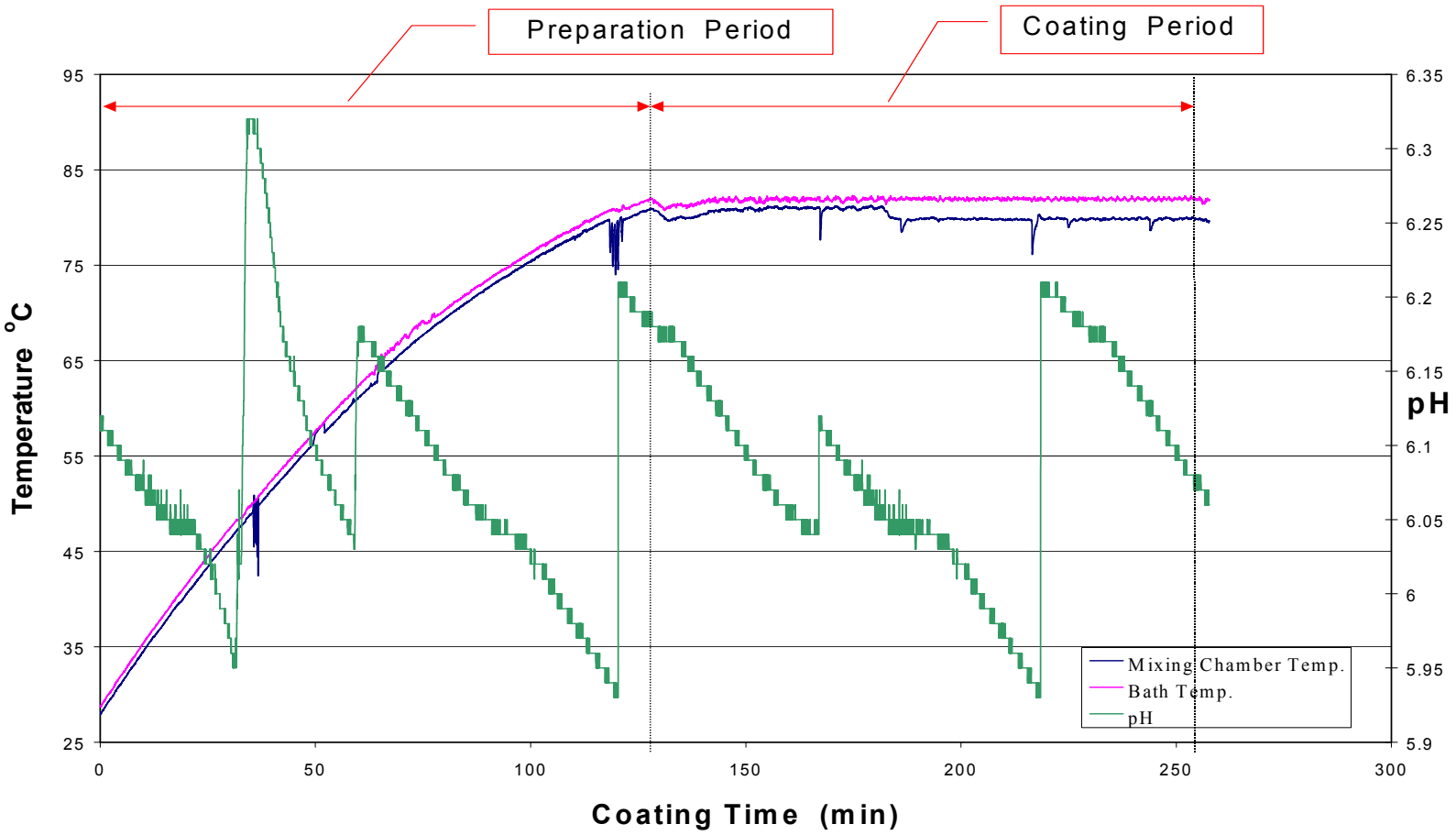

Figure 3.6. Temperature and pH value tolerance during the EN coating process.

3.3 Heat treatment

Heat treatment of EN alloys can cause significant changes in properties and structure. The hardness and wear resistance of EN deposits can be increased by heat treatment [Barker, 1993; Wing, 1997; Apachitei et al., 1998; and Parkinson, 1995]. It is well known that heating an EN deposit to temperatures of 300-400 °C for 1 hour causes the hardness to increase due to the formation of nickel phosphide (Ni_3P).

Heat-treatment was conducted in a tube furnace with an accuracy of ±1°C. A nitrogen atmosphere was used to eliminate the formation of oxide films. In many cases the coated specimens were wrapped in several layers of thin aluminum foil. As a result, no discoloration caused by the formation of the oxide film was detected on the surface of the specimens. After the heat treatment, the specimens were air-cooled.

3.4 Hardness test

Hardness measurements were taken using a Buehler Vickers Microhardness Tester (Micromet II) with a diamond indenter. The load chosen varied between 25 to 100 grams depending on the coating thickness. In all cases the depth of indentation was less than one-fifth of the coating thickness in order to eliminate the effect of the substrate mechanical properties. The values reported represent the average of at least five microhardness readings, standard deviation of the readings ranged between 4 to 8 (< ± 2% of the read values).

3.5 Differential Scanning Calorimetry (DSC)

Differential scanning calorimetry independently measures the rate of heat flow to a sample and a standard that are at the same temperature. Differential thermal analysis is the measurement of the difference in temperature between a sample and a reference as heat is applied to the system. This method is sensitive to endothermic and exothermic processes including: phase transitions, dehydration, and decomposition, redox, or solid-state reactions. DSC is a very useful method to study the physical and thermal properties of heat-dependent reactions such as precipitation processes.

In order to study the effect of heat treatment on the phase transformation of various types of EN coatings, a comprehensive DCS study was conducted. The crystallization temperature of the EN deposits (separated from the substrate) was measured using a Mettler TA4000 thermal analyzer equipped with a DSC-20 cell at a heating rate of 10 °C/min. The DSC scans were initiated at 40 °C and completed at 540 °C. The output was in milliwatts (mW). The net heat flow to the reference pan (i.e., relative to the sample) was obtained by subtracting the baseline data from the heat data of the test samples and recorded as a function of temperature. The baseline data were obtained by scanning an empty reference pan through the same temperature range as the test samples. The sample and reference pans were constructed with high purity annealed aluminum. The utility program supplied with the thermal analyzer was used to calculate the specific heat capacity and enthalpy of reaction data and the volume fractions of phases transformed. At least two samples of each material were scanned to ensure reproducibility. The results obtained were found to be reproducible.

3.6 X-ray diffraction

The X-ray diffraction method is a powerful technique widely used for studying the microstructure, phase identification, compound analysis of materials. The structure and compound analysis of EN coatings, as-plated and heat-treated, were investigated using a Rigaku d/max 2200 X-ray diffractometer with monochromatic Cu kα radiation. In order to increase the accuracy of the detection of the peaks, the coating samples were ground into the form of a very fine powder (<20μm). Acetone was used to bond the coating powder to the glass holder.

3.7 Surface roughness measurements

The surface roughness of the substrate samples before and after EN coating was measured by means of a Mitutoyo 211 surface roughness tester. It was decided to use

the Ra[2] and Rz[3] to describe the surface roughness. All the reported data represents the average of at least ten surface roughness measurements.

3.8 Friction test

The kinetic coefficient of friction (KCOF) of EN coatings was measured using a simple adjustable ramp apparatus equipped with a tape-ticker device. The ramp apparatus consisted of a U-shaped polycarbonate channel mounted on the inclined wooden base of the ramp, Figure 3.7. The use of the U-channel was to ensure that the samples travel in a straight line without wandering on the ramp or even falling off the ramp before they reached the desired destination. The ticker device was used to measure the acceleration of the specimens as they traveled down the ramp. The working principle of the ticker is very simple. An electric spark capable of indenting a heat-sensitive ticker tape is generated between its tips at a rate of 60 sparks per second. The tape is attached to the specimen. As the specimen slides down the ramp, the tape is pulled through the energized ticker device which, in turn, indents it with a series of burn marks. The distance between two ticker marks, therefore, represents the distance traveled by the specimen in 1/60 s. As a result, the velocity as well as the acceleration of the specimen can be calculated. The relationship between kinetic COF (μ) and acceleration (a) is given in Equation 3.1.

$$\mu = \frac{gSin(\theta) - a}{gCos(\theta)} \quad \text{.....(3.1)}$$

---

[2] Ra is defined as;

$$\frac{1}{L}\int_0^L |Z(x)dx|$$

where;
L= measured length
Z(x)= the profile of the mountains and valleys

[3] Rz is defined as the average value of the absolute values of the heights of five highest profile peaks and the depths of five deepest profile valleys within the measuring length

where;

μ= is kinetic COF

a=is the acceleration of the specimen down the ramp

g= is gravitational acceleration constant (9.81 ms^{-2})

θ= is the ramp angle

In order to study coefficient of friction for various ramp surface roughness values, strips of emery papers (600 and 400 grid) were carefully glued to the ramp surface using 3M photo adhesive spray glue. Thus, the experiment was conducted under three ramp surface roughness values (Ra=0.254 μm for bare polycarbonate surface, Ra=4.928 μm for polycarbonate surface covered with 600 grid emery paper, and Ra=13.517 μm for polycarbonate surface covered with 400 grid emery paper).

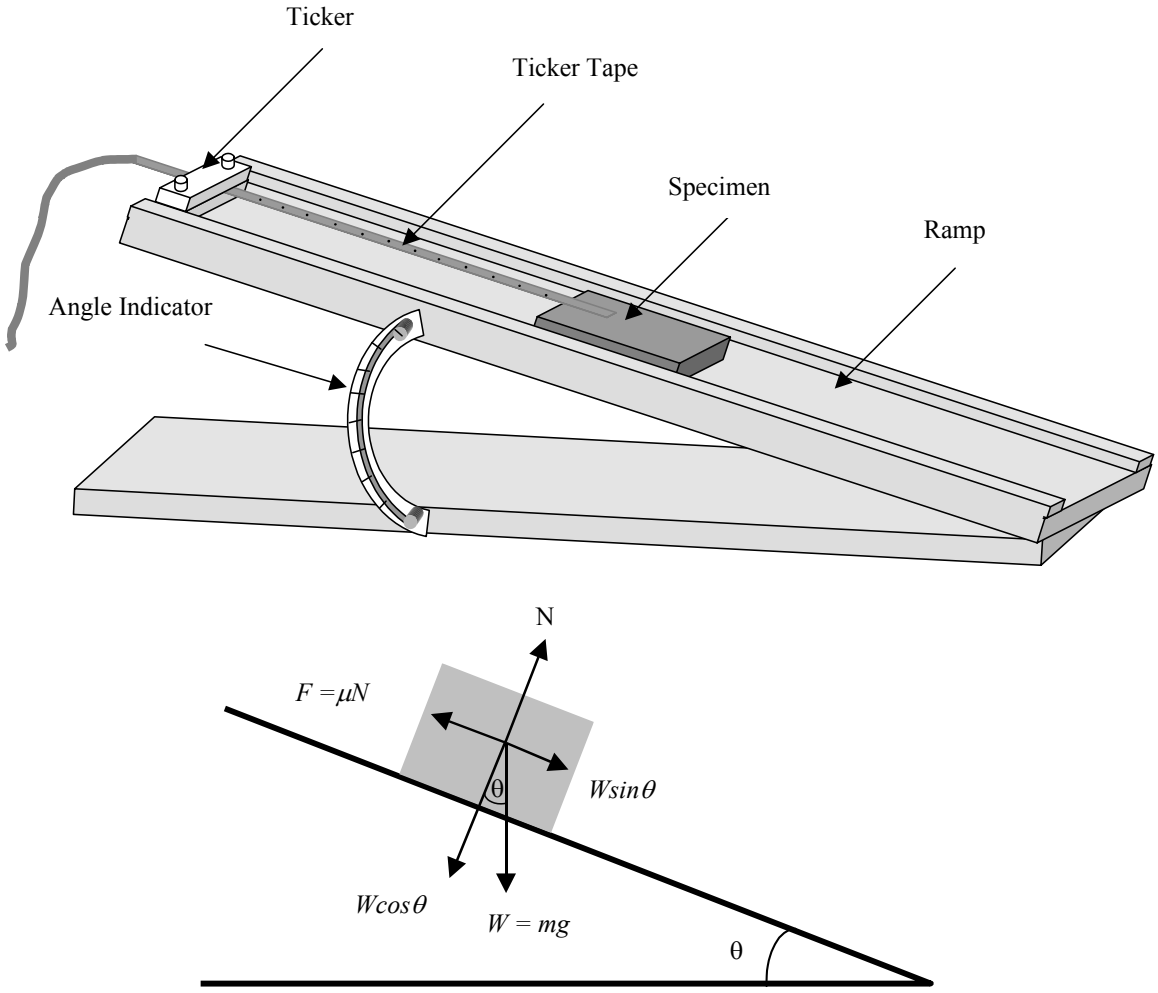

Figure 3.7. Schematic illustration of the friction experiment set-up.

3.9 Three-point bending test

The adhesive properties of coatings are important parameters affecting their quality. The quality of a coating is determined by the extent of bonding with the substrate. In the case of metallic coatings applied on metal substrates, a complete metal-to-metal bonding must form between the deposit and base metal. Most of the methods used to evaluate adhesive properties of coatings give semi-quantitative or qualitative results only. These methods involve attaching some type of equipment to the surface of the deposits by means of either soldering or grinding away part of the coating, which introduces unreasonable effects; or they involve using specially-shaped test pieces which cannot be used for an actual sample from a production line [Riedel, 1991]. Thus, due to the complicated nature of adhesion the measurement of the bonding properties of EN coatings remains a problem to which no satisfactory solution has yet been found [Riedel, 1991]. Among several methods applied to evaluate the adhesive properties of coating, pull-off, ring-shear, peel, and three-point bending tests are widely used.

Adhesion properties of EN coatings were investigated by means of a three-point bending test. In order to progressively monitor the initiation and propagation of the cracks during the bending tests, an apparatus equipped with a traveling microscope was designed and constructed. The apparatus comprises a fixture in which a traveling optical microscope (50X) and a high-intensity halogen lighting system are mounted on the lower jaw of a model 1122 Instron tensile testing machine. Figure 3.8 shows the experimental setup. The Crack Initiation Deflection Value, CIDV, was recorded when the first crack was detected on the surface. The initiation of the cracks was accompanied by a snapping sound that made it easier to determine the exact time of coating failure. Figure 3.9 shows a schematic illustration of the apparatus. The experimental parameters, such as dimensions of the fixture, holders, specimen displacement velocity, and applied load were, adapted from the ASTM (D790) for the three-point bending test [Annual ASTM Standards, 1998]. The support span distance was 126 mm and the loading nose radius was 3.2 mm, as suggested by the ASTM standard. An overhang length of 10% of the span distance was allowed on each end of

the specimens. A span-to-depth ratio of 40:1 was selected in order to eliminate shear effects. The lower jaw of the Instron machine was moved vertically with a constant velocity of 0.2 mm/min during the bending test. A load cell with a maximum capacity of 5000 N was used. A strip chart recorder was used to measure the applied load during the test. The midspan deflection was measured as a function of lower jaw displacement. Test specimens were machined as flat bars 160mm×2.54mm×3.2 mm, according to ATSM D790. Two types of EN coatings, namely, high (11.3 wt.%) and low (4.5 wt.%) phosphorus content, were deposited on two types of substrates, AISI 1018 and 1045 plain carbon steels, in various thicknesses from 10 μm – 50 μm. Table 1 shows the bath composition, condition and phosphorus content of the coatings applied. Heat-treatment was conducted at 400°C ±1° for one hour in a N_2 atmosphere. In order to eliminate the formation of the oxide layer on the outer surface of the specimens, coated samples were wrapped in several layers of thin aluminum foil. As a result, no discoloration caused by the formation of an oxide film was detected on the surface of the specimens.

Figure 3.8. Experimental setup for the three-point bending test.

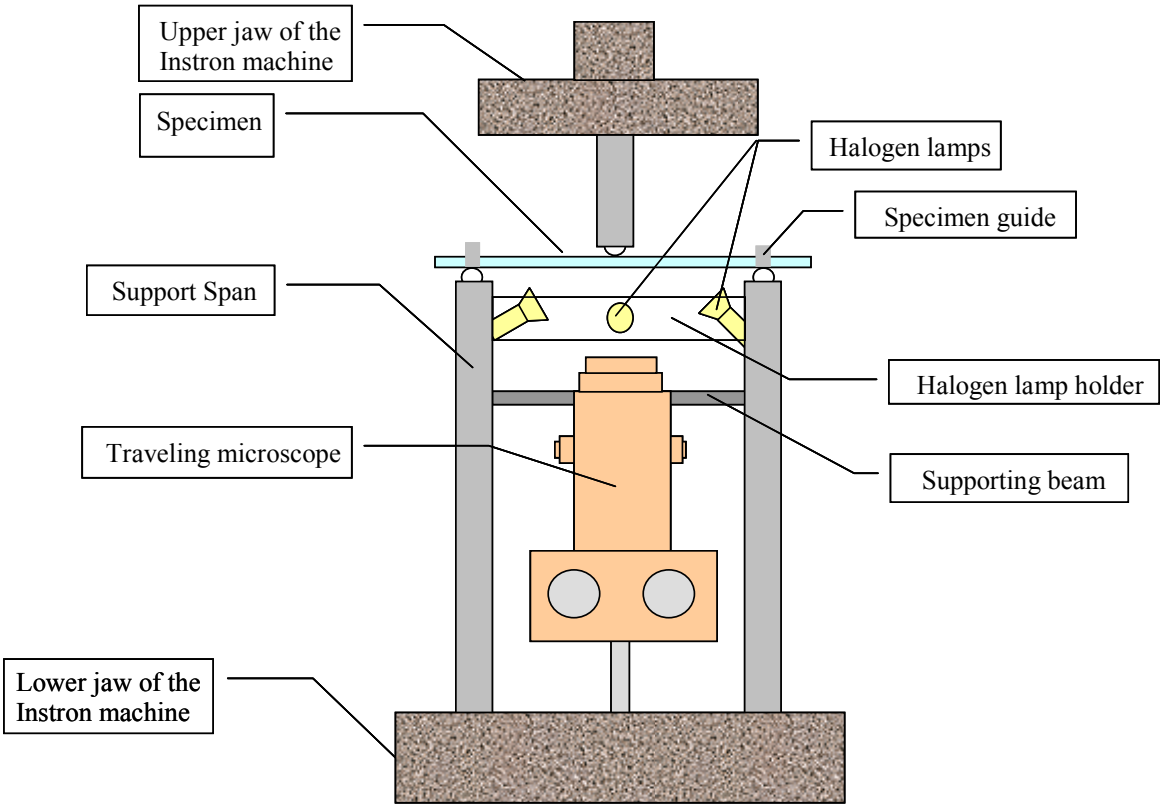

Figure 3.9. Schematic illustration of the three-point bending test apparatus

3.10 Fatigue testing

Fatigue properties of EN coatings have been studied by many researchers. However, in several cases the results obtained are in contradiction. Safranek (1959) suggested that high strength steel with a tensile strength greater than 1400 N/mm^2 can be coated with EN coating without loss of fatigue strength. Also, results obtained by Izumi (1975) and Reinhardt (1979) show no significant changes on the fatigue strength of steel substrates coated with EN coatings. Other studies show that EN coatings depending on the type of bath, phosphorus content, and post heat treatment characteristics, can cause a 10-46 % reduction in fatigue strength of the substrate [Narcus, 1967 and Spähn, 1964]. The results of a study conducted by Wu and co-workers (1995) also show EN coatings have a deleterious effect on fatigue behavior of quenched and tempered 0.3C-1.09Cr-0.24 Mo alloy. On the contrary, some other studies show that EN coatings increase the fatigue strength of various substrates [Kehrer et al., 1982 and Puchi et al., 1996].

The contradiction in results presented in the aforementioned studies is due to the fact that there are numerous coating parameters affecting the fatigue properties of the substrates simultaneously. Firstly, EN coatings can affect the surface properties of their substrates, which in itself has a profound effect on fatigue properties of a material. Secondly, EN coatings, depending on the phosphorus content and post heat treatment, may be hard and brittle. The brittle nature of EN coatings may have a significant effect on the initiation and propagation of fatigue cracks. Furthermore, EN coatings contain internal stresses in general. Depending on the bath conditions and phosphorus content of the coating the internal stress can be compressive or tensile. Gawne and Ma (1987) reported that for some EN coatings containing more than 8.8 wt.% P the internal stress is compressive in the order of 2-50 MPa. Also, Weil (1990) and Parker (1971) suggested that the transition from tensile to compressive internal stress occurs at about 10 wt.% P (Section 2.4.8). Generally, coatings with tensile internal stress are more susceptible to fatigue crack initiation and propagation compared with those with compressive internal stress. Finally, the effect of EN coatings on fatigue properties of their substrates varies depending on the mechanical

properties (strength, ductility, and fatigue properties) of their substrates. For example, fatigue properties of a harder and more brittle substrate (similar to the coating) may not be affected by EN coatings as much as that of a more ductile substrate, for example low carbon steel.

A Krouse rotational fatigue apparatus, ASTM E466 [Annual ASTM Standards, 1998]. , was used to conduct this work. The machine was set at 5000 rpm, as suggested by the ASTM standard and manufacturer's manual. Using a rounded tip micrometer, the smallest measured diameter of each specimen was measured with an accuracy of ±0.001 in. Equation 3.2 shows the correlation between stress and moment.

$$\sigma = \frac{MC}{I} = \frac{M(\frac{D}{2})}{\frac{\pi}{64}(D^4)} = \frac{32M}{\pi D^3} \quad \text{.....(3.2)}$$

σ = Stress, MPa

M= Moment, Nmm

D = Smallest measured diameter (mm)

It was critical to determine an appropriate applied load in order to obtain the recorded number of cycles at failure within a reasonable range. Lower load values would have unreasonably prolonged the test whereas higher load values would have narrowed the range of variation of the number of cycles recorded for various specimens. After many preliminary tests with various loads, the value of 448 MPa (65 ksi) was chosen for the stress to be applied during the test. Consequently, the required moment values (M) were calculated using Equation 3.2. The fracture surfaces of the specimens were studied using both optical microscopy and SEM.

3.11 Tensile testing

The tensile test experiment was conducted using a model 1122 Instron machine with 5 kN maximum load. The instant load, stress, and instant elongation were recorded

using a computer data acquisition system. Also, both load and stress versus elongation were plotted using the Instron software. The fracture surfaces of the specimens were studied using both optical microscopy and SEM.

3.12 Corrosion and wear (C&W) test in potash brine

3.12.1 Background

Potash Corporation of Saskatchewan (PCS) Mines, processes and distributes granular potash, a billion-dollar export fertilizer product, around the world. This fertilizer is an important component in maintaining and improving the food producing capacity of the world's agricultural land, and will become even more important as the world population strains its food supply. Between the time the potash is mined and exported, it undergoes many beneficiation and refining processes during which the conveyance and transport systems, compactors, dryers, grinders, digesters, and receptacles may come into close contact with pulverized potash, hot brines, and slurries. The temperatures, particulate slurries and highly concentrated chloride environments involved in potash mill operations provide conditions for erosive wear, erosion-corrosion, and high susceptibility to other forms of localized corrosion.

In potash production (mining and processing), handling, and storage, materials used for constructing the plant and equipment play a major role in ensuring their durability. Potash plants handle very corrosive raw materials and several corrosive intermediates and by-products. The problem of protecting the equipment and structures used in mining, processing, transporting, and storing potash granules also impacts on the final consumers. According to a recent study by Strathdee [1996], the potash industry suffers extensive financial loss due to corrosion and wear of mining equipment. To remain competitive, these costs are passed on to the final consumers.

During potash production, many types of corrosion problems are encountered under the prevalent conditions of high pressures and temperatures, high fluid velocities, abrasion, erosion, and the presence of very corrosive chemicals and by-products handled [Strathdee, 1996; Fontana, 1986; Lyons, 1979; and Prabhu-Gaunkar, 1998].

Equipment used in potash production and handling usually comprises different types of heat exchangers, scrubbers, boilers, crystallizers, dry screens, compactors, rod and cage mills, dryers, cooling towers, pipelines, pumps, compressors, fans, valves, conveyors, as well as the structures supporting these units [Strathdee, 1996]. Carbon steels, low alloy steels, and cast irons are among the cheapest materials often used along with suitable corrosion protection measures. Specialty steels, stainless steels, and corrosion-resistant nickel alloys are used in some highly corrosive situations. Corrosion failures have been reported, particularly in materials serving under highly hydrodynamic conditions, such as pumps, their impellers, agitators, etc. [Strathdee, 1996]. Development and use of specially engineered alloys for the potash industry is an ongoing process. Some of the most expensive materials are used in components of pumps, valves, agitators, pipe sections, and tank walls where condensates form, etc., without the use of any corrosion protection measures [Horne and Houlle, 1993]. In addition, the atmosphere in potash mills is usually highly aggressive due to leakage of chemicals, potash dusts, and pollutants, which give rise to serious corrosion problems of supporting structures. These are generally protected by special paint formulations containing inhibitors [Burke, 1959]. The use of polymeric and ceramic materials in the potash industry is quickly gaining wide acceptance, especially polymers in areas such as pipelines and vessel linings where mechanical strength and elevated temperature resistance are not strong factors.

Metallic and concrete structures that support production equipment such as compressors, pumps, pressure vessels, storage tanks, pipelines, and heat exchangers are susceptible to corrosion due to spillages of corrosives, stagnation of products, and the surrounding aggressive atmosphere. Failures have been reported at rivets, welds, and other critical places. The structures are protected using special coatings and linings that use inhibitors in the primer coats. Fitzsimmons and Henry (1990) have discussed the maintenance of concrete structures using urethane, epoxy, acrylic, and asphalt, in suitable paint systems.

A large amount of money is spent annually on materials-related maintenance at potash mills due to erosion-corrosion and other forms of corrosion damage. The results of a

1991 study of materials-related mill maintenance for Saskatchewan Potash Producers with conventional mills show that the corrosion problem is very severe in such components as compactors, conveyors, pumps, valves, and piping used in the processing and conveyance of potash slurries [Nicholls, 1996]

3.12.2 Reciprocating Corrosion and Wear testing

Corrosion and wear resistance of EN coatings in saturated potash brine was investigated by means of the reciprocating corrosion and wear test. An apparatus was designed and engineered to conduct this study [Hedayat at al., 1997]. Figure 3.10 shows the experimental set up. Also, Figure 3.11 shows the schematic illustration of it. Three types of EN coatings, namely, low, medium, and high phosphorus were deposited on $38.1 \times 38.1 \times 6.35$ mm AISA 1018 coupons. The coating thickness was 85± 2 μm. The reciprocating motion frequency was set at approximately 1 Hz. The ball used to apply the load was made from hardened steel, 69 RC. The maximum stress calculated was 1 GPa[4]. The wear scar areas were measured after each set of

---

[4] Circular point contact stress between the ball and flat specimen can be obtained using the following equation [Williams, 1994]:

$$P_{max} = \left(\frac{6WE^{*2}}{R^2 \pi^3} \right)^{\frac{1}{3}}$$

Where,

$$\frac{1}{E^*} = \frac{1-\nu_1^2}{E_1} + \frac{1-\nu_2^2}{E_2} \quad , \quad \frac{1}{R} = \frac{1}{R_1} + \frac{1}{R_2} \text{, and W= Load N}$$

$$\frac{1}{E^*} = \frac{1-\nu_1^2}{E_1} + \frac{1-\nu_2^2}{E_2} \Rightarrow E^* = 115 \text{ GPa}$$

$$\frac{1}{R^*} = \frac{1}{R_1} + \frac{1}{R_2}, R_1 = 9.5 \text{ mm and } R_2 = \infty \Rightarrow R^* = 9.5 \text{ mm}$$

$$P_{max} = \left(\frac{6WE^{*2}}{R^{*2}\pi^3} \right)^{\frac{1}{3}} = \left(\frac{6 \times 29.63 \times (115 \times 10^9)^2}{(9.5 \times 10^{-3})^2 \times (3.14)^3} \right)^{\frac{1}{3}} = \left(\frac{2.35 \times 10^{24}}{2.79 \times 10^{-3}} \right)^{\frac{1}{3}} = (0.84 \times 10^{27})^{\frac{1}{3}} = 0.94 \times 10^9 \approx 1 \text{ GPa}$$

tests, intervals of 15000, 30000, 45000, 90000, 180000, and 540000 cycles, using an image analyzer. Also, the scar depths were determined using an optical microscope.

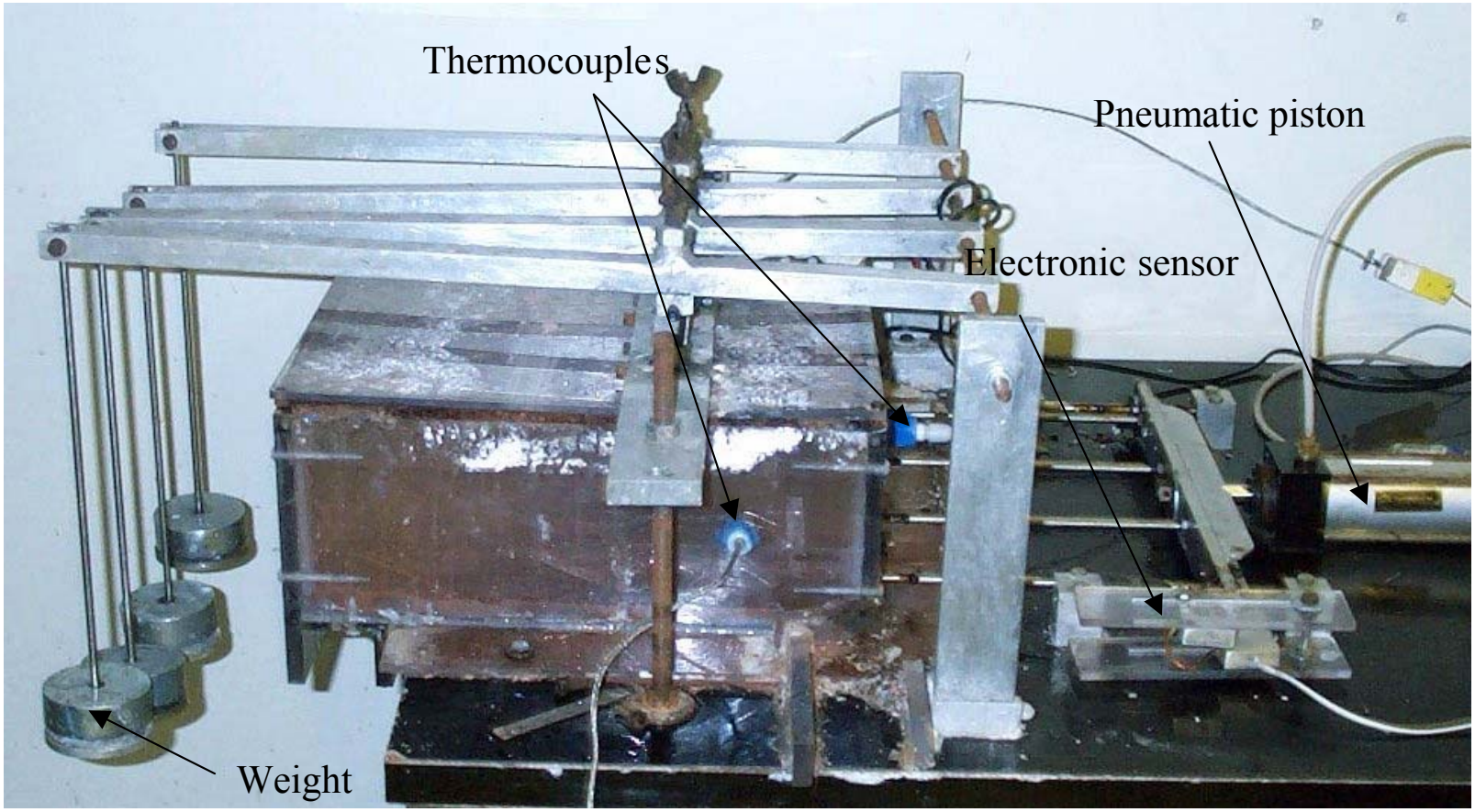

Figure 3.10. Photograph of reciprocating corrosion and wear experimental set up.

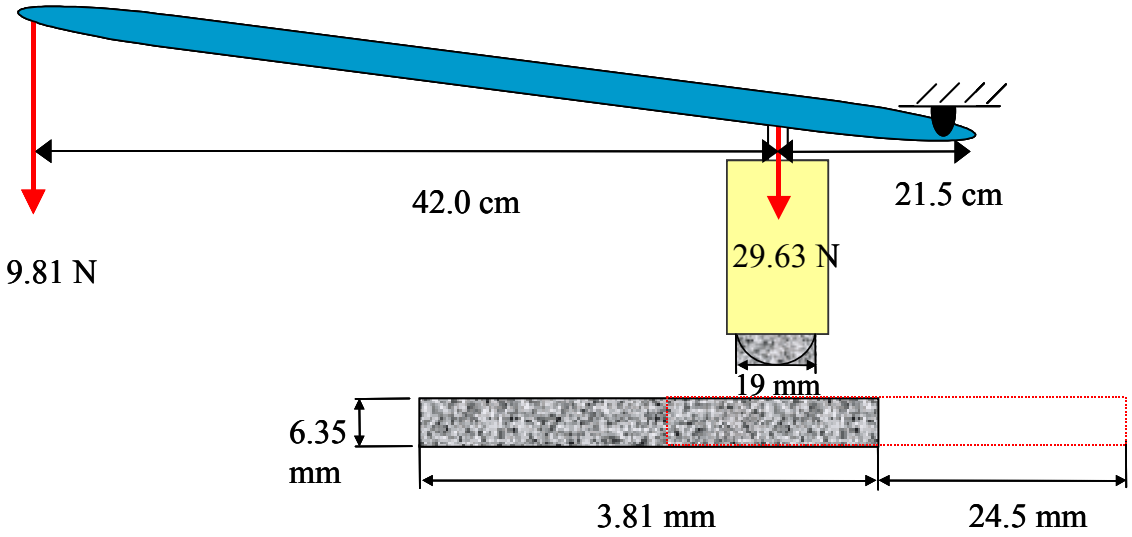

(a)

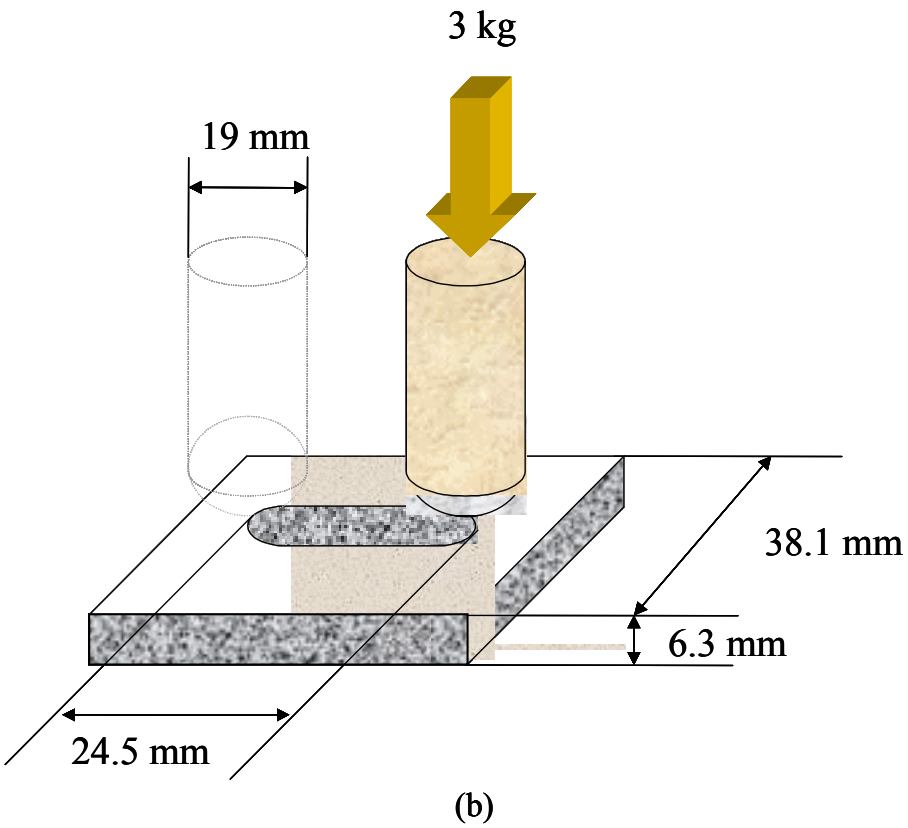

(b)

Figure 3.11. Schematic illustration of reciprocating corrosion and wear set up.

3.12.3 Erosion-corrosion testing

The erosion-corrosion behavior of EN coatings in potash brine was studied by means of a slurry experiment. A previously designed and built apparatus was modified to simulate the actual flow and impingement regime in the potash industry at room and high temperature (85°C). Figure 3.12 shows the experimental set up. The redesigned jig could hold 8 samples (1.5"x1.5") during each set of runs. A reference coupon, made from AISI 1018 carbon steel, was used during each run to monitor and compensate for the occurrence of any abnormal corrosion and wear. Figure 3.13 shows the Autocad drawings of the jig. Also, Figure 3.14 shows the photographs of the slurry experiment setup located at the PCS pilot plant, Saskatoon, Saskatchewan. The over-saturated potash brine at 85^{o}C was circulated by means of a motor pump through the main pipe and drawn back to the tank. At the beginning of each run 30 to 40 pails (20 liter) of potash (mixture of fine and coarse grains) were added into the tank, so that the solution was over-saturated and the solids level was at 10-15 %vol. or 20-30 wt.%. Potash grains were periodically added into the tank to keep the over-saturated solids at a certain particle size. Approximately 7-9 pails of coarse potash were added into the main tank daily, 4-5 pails in the morning and 3-4 pails in the evening. The tank was heated by steam to keep the brine temperature at 85±5^{o}C. Condensed water was accumulated in the solution. Table 3.2 shows the specimen specifications and experimental parameters.

In order to determine the variation of particle size with time during the erosion-corrosion experiment slurry samples were taken from the jig and the circulation system at 10 minutes, 2 hours, and 17 hours after adding the fresh potash into the system. As shown in Figure 3.15, during the experiment the particle size of the majority of the gains remained constant at around 0.5 mm. Furthermore, the ratio of the particles added to the tank to the existing particles in the tank was very small at $\frac{4}{30}$. Also, as shown in Figure 3.15, within a short time after adding a new batch of potash into the system, 10 minutes, more than 85% of the particles were within 0 to 1

mm. As a result, it can be concluded that the variation of the average of particle size in the tank is negligible.

The experiment was conducted for approximately 960 hours, 4 periods of 240 hours. Every 240 hours, the specimens were removed, cleaned, and the exposed surfaces were studied using an optical microscope. The cleaning procedure involved 30 minutes of ultrasonic cleaning at 40°C followed by immersion in 50 HCl solution for 10 s and rinsing with cold water. At the end of each test, the existence of any open micro-pits or other superficial defects was investigated using the Ferroxyl method[5].

[5] Ferroxyl method employs 30 drops of potassium ferrocyanide mixed with 75 ml saturated potash gel (gelatin added).

Figure 3.12. Photograph of slurry jig.

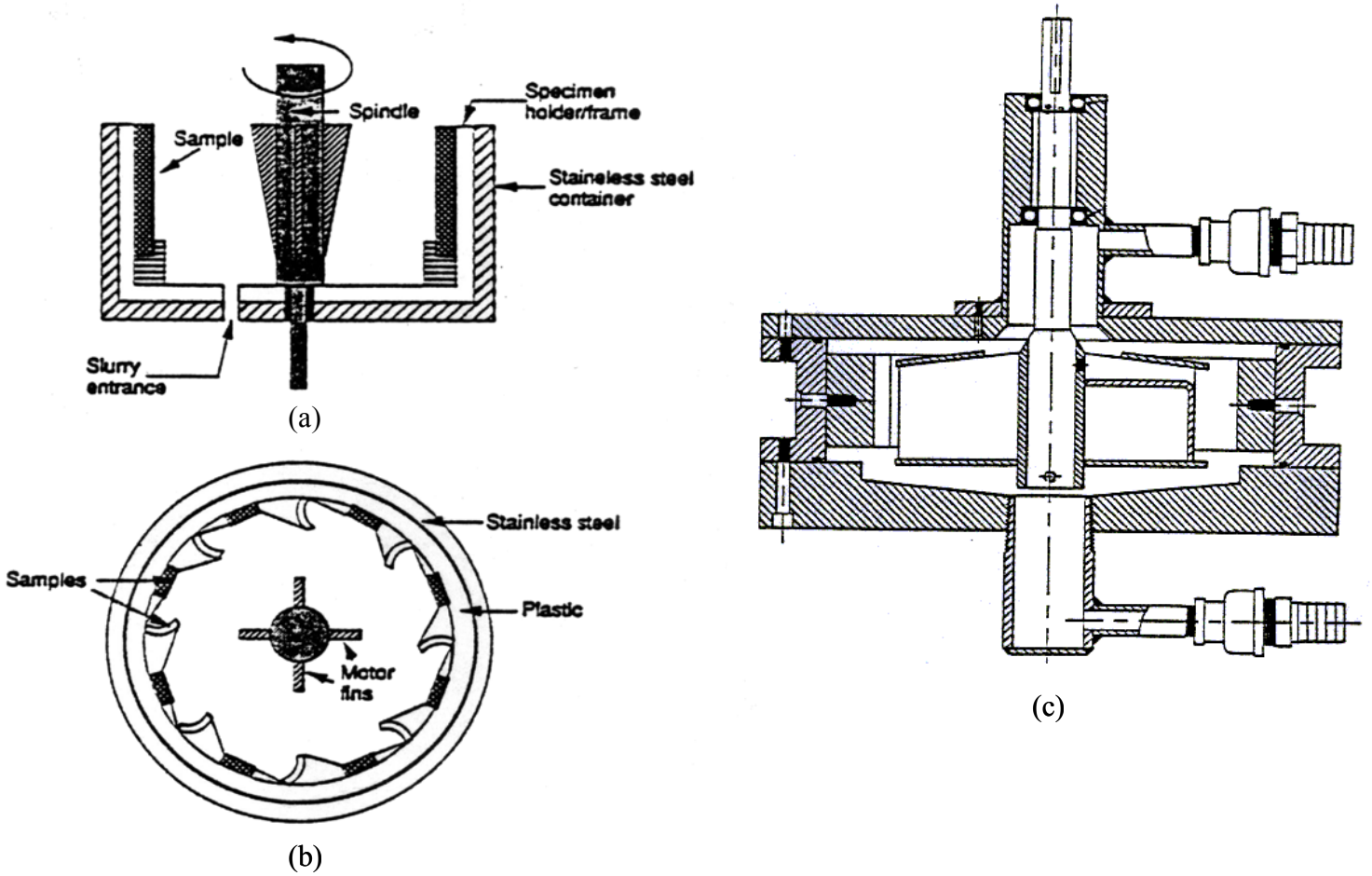

Figure 3.13. Autocad drawings of the slurry tester.

Figure 3.14. Photographs of slurry experimental setup.

Table 3.2. Specimen specifications and parameters for slurry experiment

Particulars	**Values**
Specimen dimensions	$38.1 \times 38.1 \times 6.35$ (mm)
Types of coatings tested	High phosphorus (As and HT) Medium phosphorus (As) Low phosphorus (HT)
The sample holder internal diameter	170 mm
The sample holder external diameter	200 mm
Sample holder height	30 mm
Flow rate into the jig	1-2 liter/s
The jig rotational velocity	115 rpm
The average slurry velocity	1.47 m/s
Particle average size	2 mm
Brine specific weight	1.24

As: as-plated, HT: heat-treated

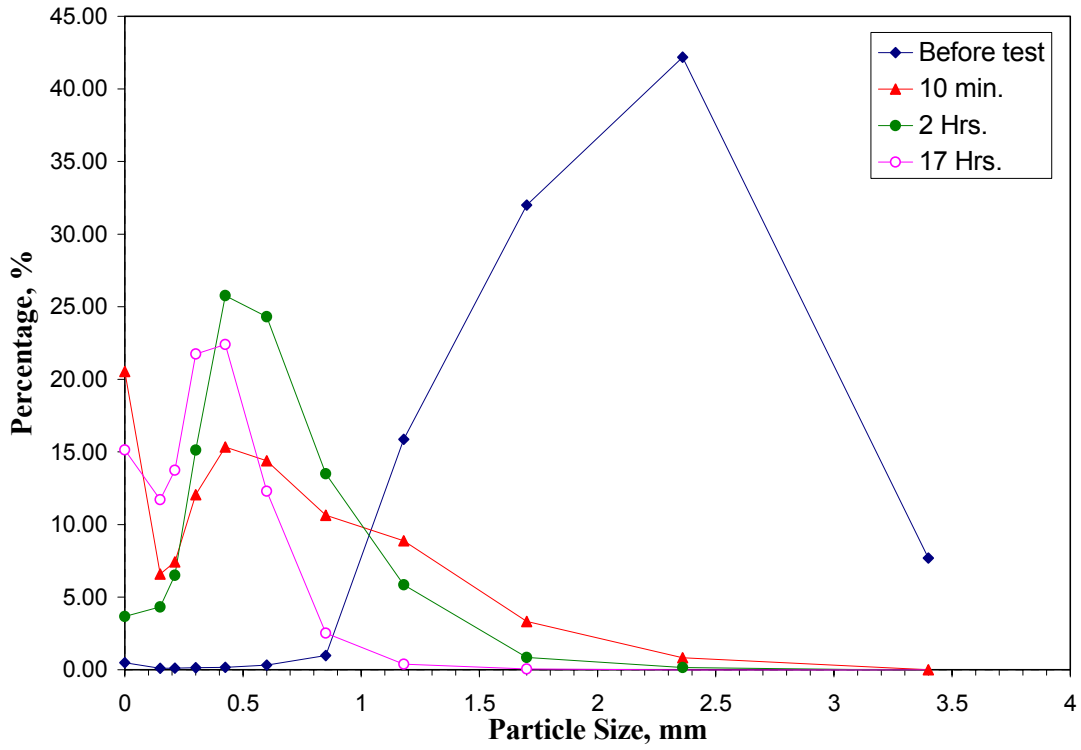

Figure 3.15. Variation of the particle size versus time during the slurry experiment.

3.13 Electron (Microscopy) metallography

As a part of this research, a comprehensive electron microscopic investigation was conducted to study the microstructure of EN coatings as well the effect of heat treatment on microstructural changes. Various microscopic techniques such as EDS spot analysis, X-ray diffraction pattern, X-ray mapping, and X-ray line scanning analysis were employed to complete this segment of the study.

3.13.1 Scanning Electron Microscopy (SEM)

Prior to plating, AISI 1018 plain-carbon steel coupons measuring 20 x 20 x 3 mm were mechanically polished and chemically cleaned using the cleaning and rinsing procedure mentioned in Section 3.2. Heat treatment was carried out in a cylindrical tube furnace. The specimens were enclosed in aluminum foil to prevent phosphorus depletion [Baudrand and Bengston, 1995] and surface oxidation [Weiss, 1992], heat-treated at 400±1 °C for various lengths of time and cooled in air. The specimens were cut to expose the coating-substrate interface, molded in epoxy and polished to 1 μm using a standard metallographic procedure, Figure 3.16.

The phosphorus content of the three types of EN coatings was determined by the X-ray energy dispersive spectrometry (EDS) method in a JEOL JSM-5900LV SEM. Also, elemental X-ray mapping analysis was conducted to study the distribution of nickel and phosphorus throughout the coating layers. All samples were etched using 66 vol.% acetic acid and 33% vol. % nitric acid solution at RT for 15 s prior to examination.

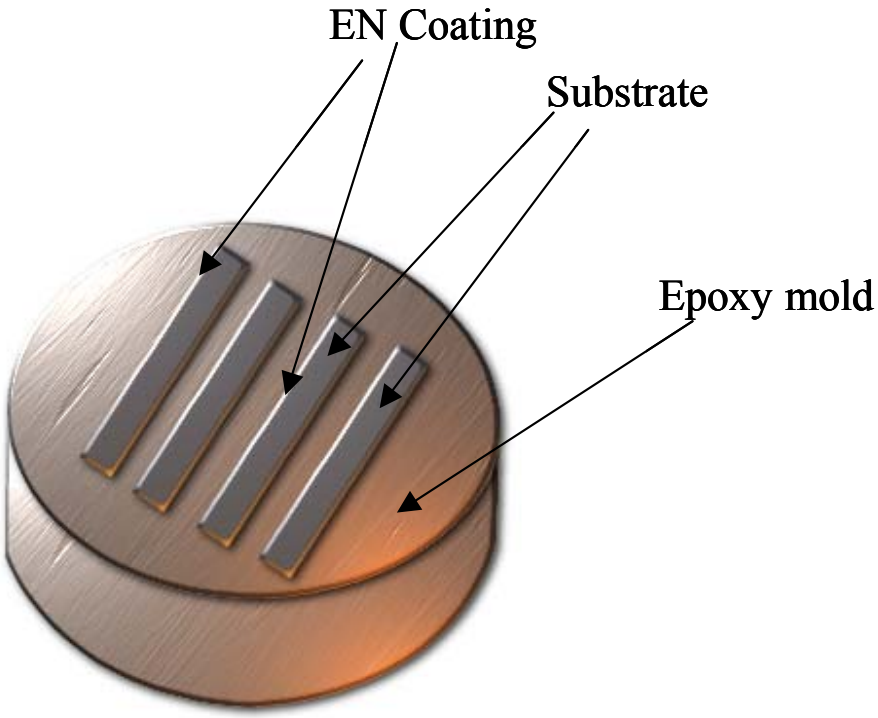

Figure 3.16. Epoxy molded EN coated specimens prepared for the SEM study.

3.13.2 Transmission Electron Microscopy (TEM)

The TEM investigation is an inevitable segment of any detailed microstructure study in general, and in particular where precipitation reactions occur as a result of aging due to heat treatment. The TEM study of EN coatings was conducted in two parts.

Part one was conducted using a JEOL JEM-2000FX transmission electron microscope (TEM) at the Department of Mechanical Engineering, University of Manitoba, in summer 1999. Thin foil specimens for transmission electron microscopy were mechanically polished to about 80 μm and punched into 3 mm diameter disks. The disks were subsequently thinned using a GATAN 656 dimpler grinder using 2-4 μm diamond paste after which they were further thinned to perforation using a GATAN 600 dual ion-miller equipped with a cold stage and cooled continuously with liquid nitrogen. An accelerating voltage of 6 V, a total gun current of 1 mA (0.5 mA/gun) and an incident ion-beam angle of 13 ° were used.

Part two took place in the Department of Mechanical Engineering, University of Saskatchewan (2001-2002) was conducted using a Hitachi HF-2210 scanning transmission electron microscope (STEM). This facility was equipped with 200 kv field emission gun, Oxford EDS elemental analysis, ATM image analysis, 0.5 nm beam size in analysis mode, and a capability of reaching 1.5×10^6 times magnification on the TEM screen and 2.6×10^7 times magnification using digitized camera. It was an excellent tool to conduct a significantly detailed study of the EN microstructures. The 80 μm thick 3 mm diameter disks were thinned using a GATAN 656 dimpler grinder using 2-4 μm diamond paste. Then, specimen disks were further thinned to perforation using a GATAN 690 dual Precision Ion Polisher System (PIPS). An accelerating voltage of 3.5 V, a total gun current, and incident ion-beam angle of ±4 ° were used.

4 Results and Discussion

This chapter discusses the results obtained on the physical, mechanical, corrosion and wear resistance, tribology, and microscopic properties of EN coatings. The results presented follow the same sequence as introduced in Chapter Three.

4.1 Physical Evaluation

4.1.1 Effect of heat treatment on hardness and microstructure of EN coatings

Hardness testing was conducted in order to study the effect of heat treatment on the hardness of EN coatings. Mild steel 1018 AISI flat specimens were coated with 40 μm of three types of EN coatings (as-plated and after heat treatment), namely, low, medium, and high phosphorus content. Figures 4.1 and 4.2 show the effects of aging temperature and time, respectively, on the hardness of EN coatings. Both figures exhibit the typical bell-shape characteristics of an age-hardened material. As expected, the hardness of the coatings increased significantly with heat treatment. As shown in Figure 4.1, the hardness increased with temperature between 300 and 400 °C after which it decreased with further increases in temperature. For samples aged at 320 °C for various lengths of time illustrated in Figure 4.2, the hardness increased with aging time to a maximum and then decreased with further increases in aging time. The increase in hardness has been attributed to fine Ni crystallites and hard intermetallic Ni_3P particles precipitated during the crystallization of the amorphous phase [Park and Lee, 1996; Parker, 1981; Parker, 1990; Hur et al., 1990; Bagley and Turnbull, 1968; and Mahoney and Dynes, 1985]. However, Hur et al. (1990) have reported that the crystallization process of amorphous Ni-P solution involved more than one intermediate phase. The Ni_3P phase has a bct structure with a = 0.835 nm, and c = 0.439 nm [Park and Lee, 1996].

In Figure 4.1, the peak hardness occurred at about 400 °C for the three EN coatings. However, for the medium and high phosphorus coatings a primary peak occurred at about 350 °C. This indicates the precipitation of a phase different from that formed at

around 400 °C. This observation is consistent with DSC results reported in the literature for amorphous EN coatings [Hur et al., 1990], in which it was shown that amorphous EN samples exhibited two transformation peaks. The phase formed at around 400 °C is believed to be the result of Ni_3P particle formation, whereas that formed around 350 °C is believed to be fcc nickel crystallites [Zhang and Yao, 1999]. Figure 4.3 shows the variation of hardness with aging time at 400°C for low and high phosphorus EN coatings in a smaller heat treatment time increment. As shown, the hardness of high phosphorus EN coating shows two well defined peaks. The DSC results conducted as a part of this study are in complete agreement with this observation.

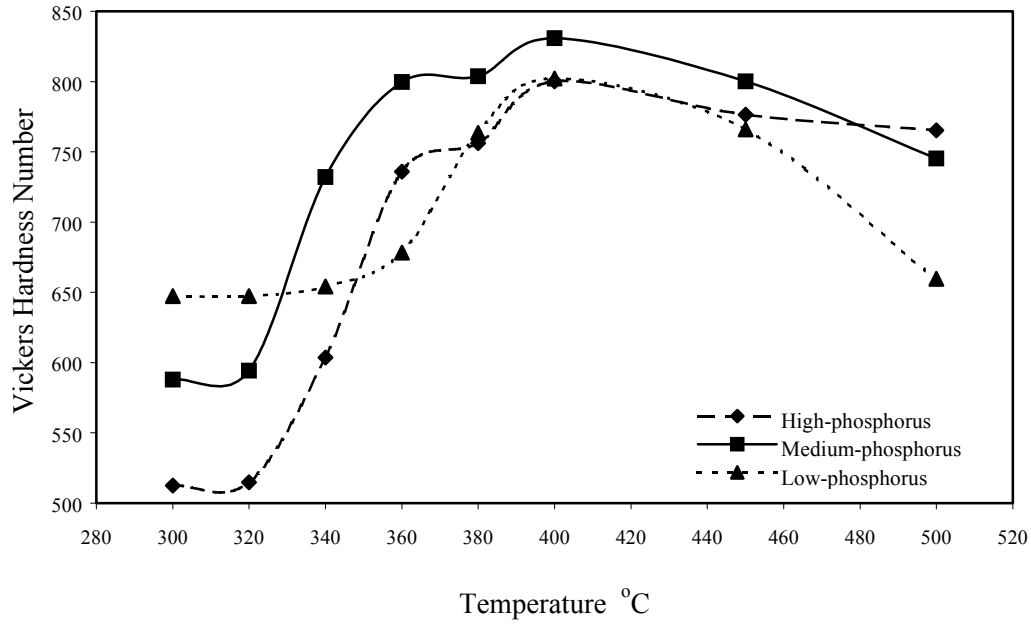

Figure 4.1. Variation of hardness with aging temperature for low, medium, and high phosphorus EN coatings (aging time = 1 hour). Standard deviation of the readings ranged between 4 to 8 (< ± 2% of the read values).

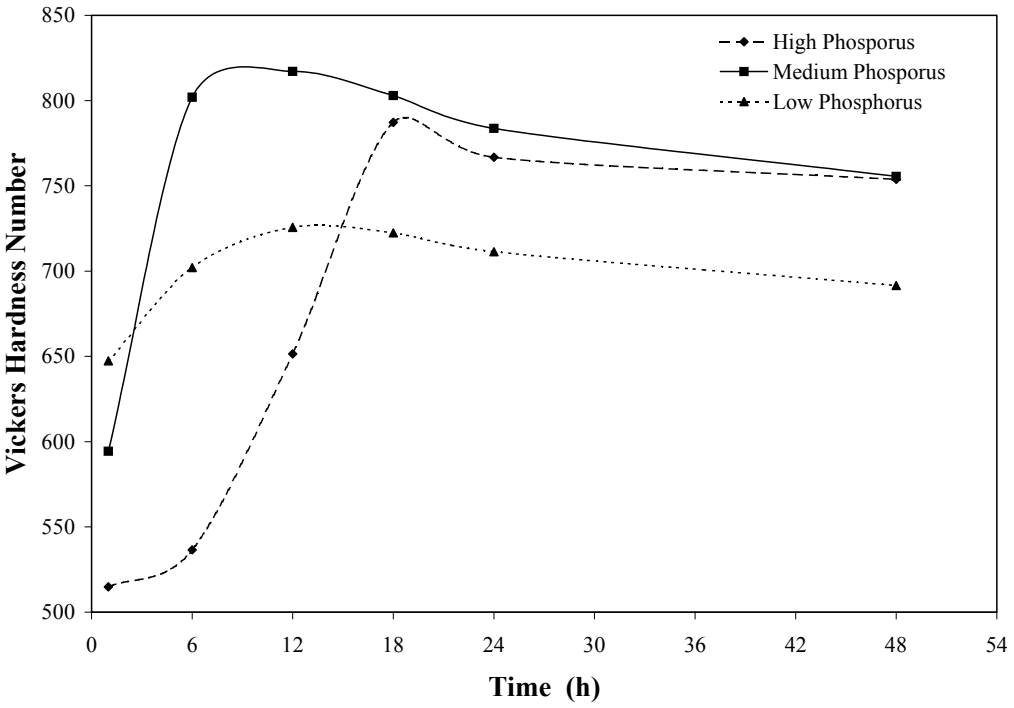

Figure 4.2. Variation of hardness with aging time at 320°C for low, medium, and high phosphorus EN coatings. Standard deviation of the readings ranged between 4 to 8 (< ± 2% of the read values).

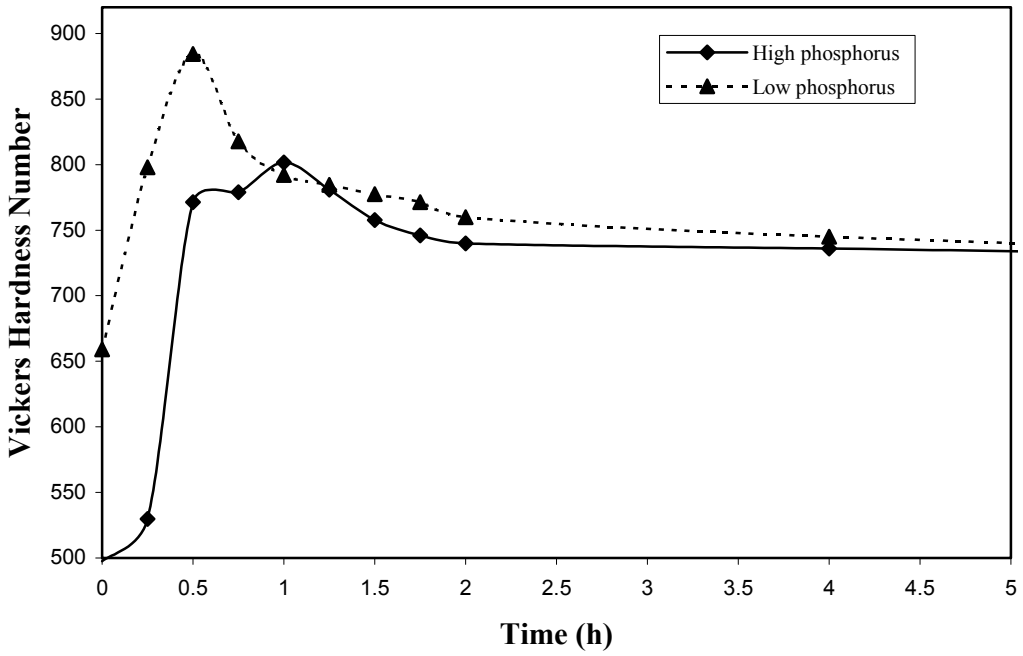

Figure 4.3. Variation of hardness with aging time at 400°C for low and high phosphorus EN coatings. Standard deviation of the readings ranged between 5 to 9 (< ± 3% of the read values).

The effect of heat treatment on microstructure of EN coatings was studied using the DSC method. Figure 4.4 shows the DSC thermographs of as-plated EN coatings. It can be observed that the amorphous or nano-crystalline-to-crystalline transformations taking place in the temperature ranges of 330-355 °C and 380-415 °C are exothermic. The peaks are simple and well defined and correspond to irreversible solid-state reactions since no well defined peak appeared during the rerun or cooling scan. The peak transformation temperatures obtained for each type of EN coating have been summarized in Table 4.1. The as-plated low and medium phosphorus sample results show small DSC peaks at about 403 and 337 °C, respectively, whereas the high phosphorus sample shows a large peak at about 343 °C.

It is interesting to note that the as-plated medium and high phosphorus samples showed one transformation peak each and these peaks do not occur at the same temperature. This is inconsistent with the results reported by Park and Lee [1988]. These authors have reported that the transformation temperature of EN coatings was independent of the phosphorus content (or the EN solution pH). They argued that if EN deposits had an amorphous structure, a change in phosphorus content would change the transformation temperature from amorphous to crystalline. However, the results of other researchers seem to contradict those of Park and Lee [Park and Lee, 1998]. Allen and VanderSande [1982] and Hur et al. [1990] showed that the transformation temperature of EN coatings varied with the phosphorus content. Furthermore, Hur et al. (1990) documented that amorphous EN coatings could show one or two transformation temperature peaks during a DSC scan, depending not only on the phosphorus content but also on the chemical composition of the electroless nickel solutions.

Previous workers [Hur, 1990; Park and Lee, 1988; and Allen; and VanderSande, 1982] have reported that the exothermic reaction peak shown at 403°C by low phosphorus EN deposit is caused by the precipitation of Ni_3P particles from phosphorus-supersaturated nickel solid solution. According to Hur et al. (1990), the exothermic peaks at 337 and 343°C (from medium and high phosphorus EN deposits,

respectively) are due to the decomposition of phosphorus-rich EN matrix into Ni_3P crystallites and nickel crystallites. The single peak reaction temperature exhibited by the high phosphorus EN coating, for example, may be due to co-crystallization of Ni_3P and nickel crystallites. Figure 4.5 shows the DSC curves of EN coatings aged at 300°C for one hour prior to the DSC scan. Here, the decomposition reaction in the high phosphorus sample exhibits a double peak, with the peak at 340°C representing the fcc nickel crystallites precipitated in amorphous matrix and the second peak occurring at 348°C representing Ni_3P precipitation. Such observation is in agreement with the results of hardness tests for high phosphorus EN coating where two well-defined peaks were distinguished. It can also be observed in Figure 4.5 that the peak transformation temperatures of the low and medium phosphorus EN coatings were practically unaffected by heat treatment. Figure 4.6 shows the DSC thermographs of EN deposits heat-treated at 400°C for one hour prior to DSC scanning. It is evident that no decomposition reaction occurred as the samples were scanned. This indicates that the usual commercial practice of heat-treating EN coatings at 400°C for one hour results in equilibrium precipitates.

The extent of reaction at any given temperature during a DSC scan can be controlled by thermodynamic equilibrium or by kinetic limitations [Dollimor et al., 1980]. Figure 4.7 shows the effect of DSC heating rate on the peak reaction temperature of as-plated high phosphorus and low phosphorus EN coatings. It is apparent from the results in Figure 4.7 that increasing the DSC heating rate causes the EN crystallization peaks to occur at systematically higher temperatures. Thus, crystallization of electroless nickel-phosphorus alloys involves a synergism between temperature and time. Therefore, it can be concluded that the precipitation of Ni_3P particles and nickel crystallites is dominated by their reaction kinetics during a DSC scan.

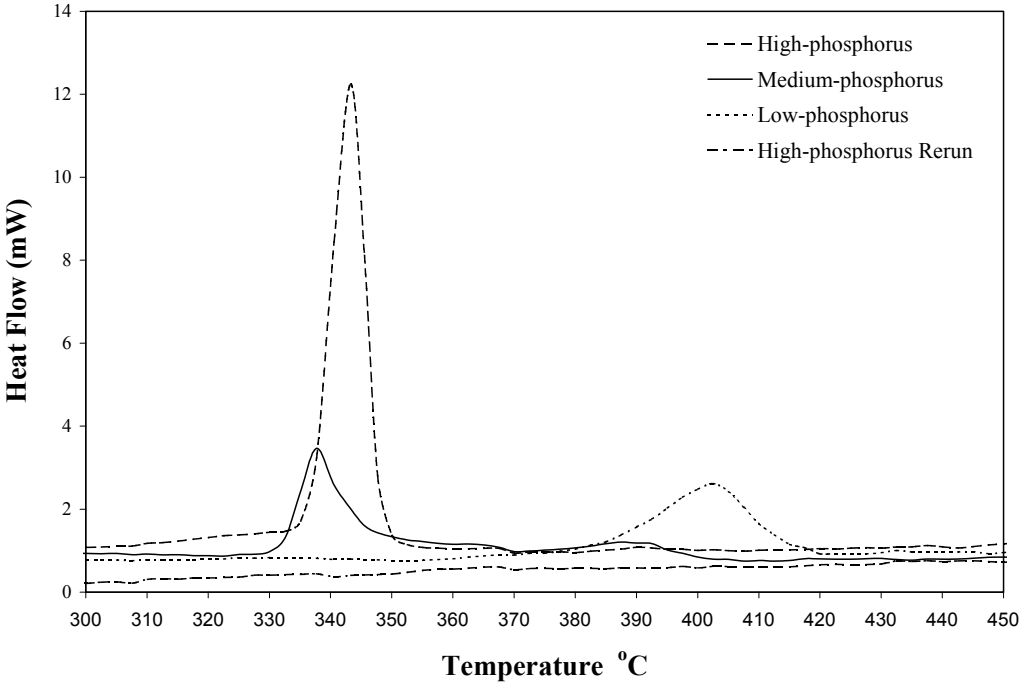

Figure 4.4. DSC thermographs of as-plated EN samples

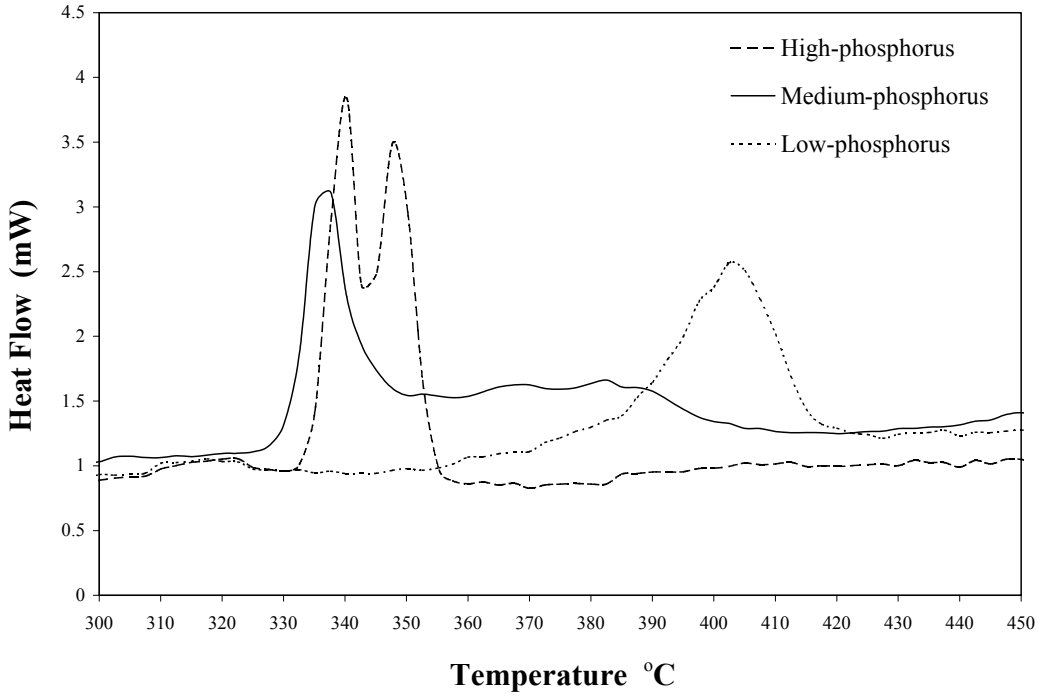

Figure 4.5. DSC thermographs for EN deposits aged at 300 °C for 1 h.

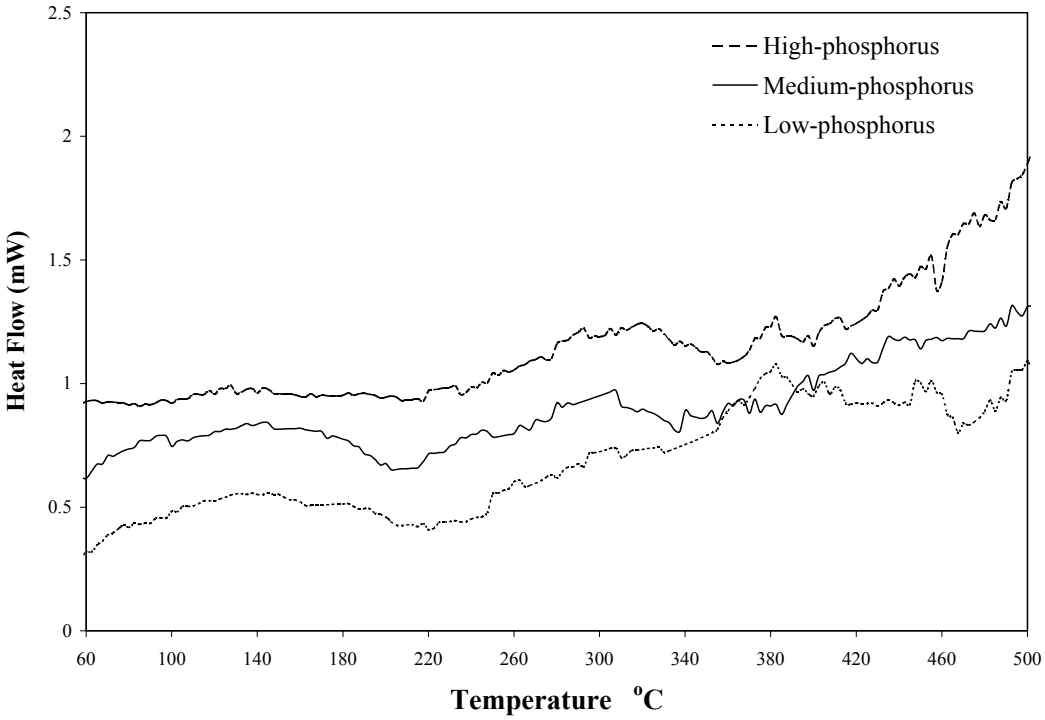

Figure 4.6. DSC thermographs of EN samples aged at 400 °C for 1 h.

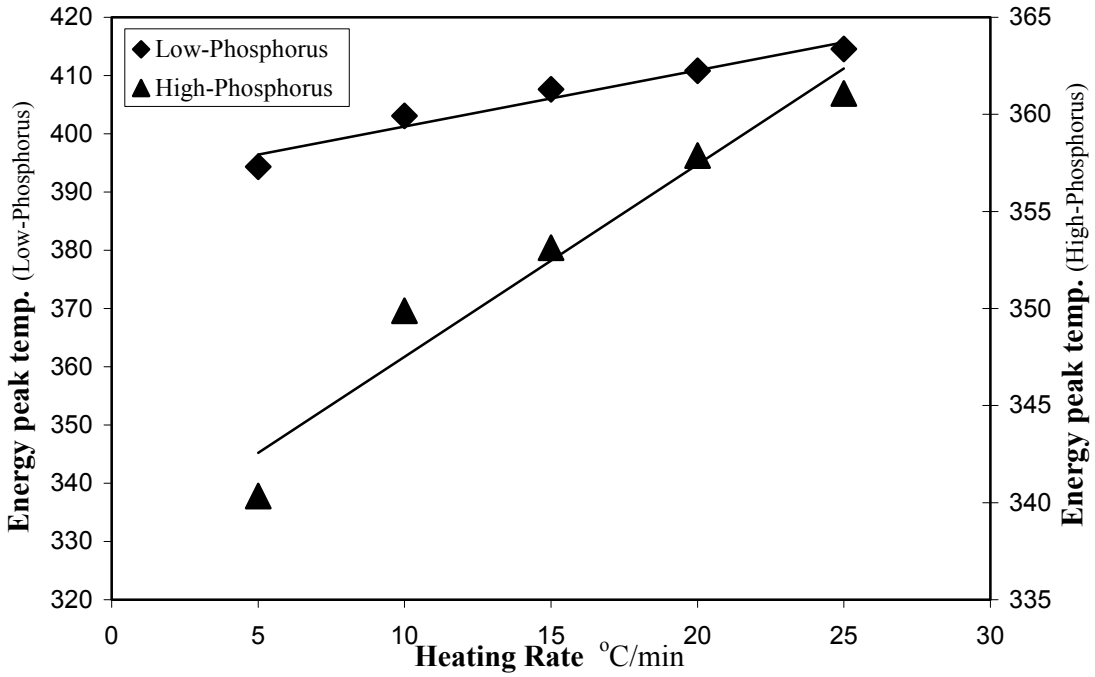

Figure 4.7. DSC thermographs illustrating the effect of heating rate on the crystalline transition temperature.

The activation energy for crystallization (E_C) of EN deposits can be estimated from a relationship developed by Mittemeijer and co-workers (1986 and 1988) which is given as:

$$\ell n \frac{T_p^2}{\Phi} = \frac{E_C}{RT_p} + \text{constant} \qquad (4.1)$$

where Φ denotes the DSC heating rate (K/min), E_C the activation energy for crystallization of EN deposits, R the gas constant (= 8.314 J/Kmol), and T_p the temperature where the maximal transformation rate is experienced during DSC scan (K). In constant-heating rate DSC experiments, T_p is usually taken to be approximately equal to the peak reaction temperature. Hence, the activation energy can be calculated from the slope of the straight line obtained by plotting $\ell n\left(\frac{T_p^2}{\Phi}\right)$ versus $\frac{1}{T_p}$. Figure 4.8 shows a plot of equation (4.1). E_C was calculated to be 258.1 kJ/mol for high phosphorus EN coating. This value is greater than 227.6 kJ/mol reported by Mahoney and Dynes [1985] for EN deposits containing 11 wt.% phosphorus. However, it is significantly lower than the published value of the activation energy for self-diffusion of pure Ni, which is 283.0 kJ/mol [Jena and Chaturvedi, 1992]. The implication of this is that if it is assumed that the activation energy for self-diffusion is the same as the activation energy for crystallization in pure Ni, then increasing the phosphorus content of EN deposits leads to a decrease in the activation energy for crystallization of Ni_3P particles and nickel crystallites. In other words, the higher the phosphorus content the lower is the temperature for crystallization for EN deposits. This hypothesis is fairly consistent with the results of DSC scans shown in Figure 4.4 and Table 4.1.

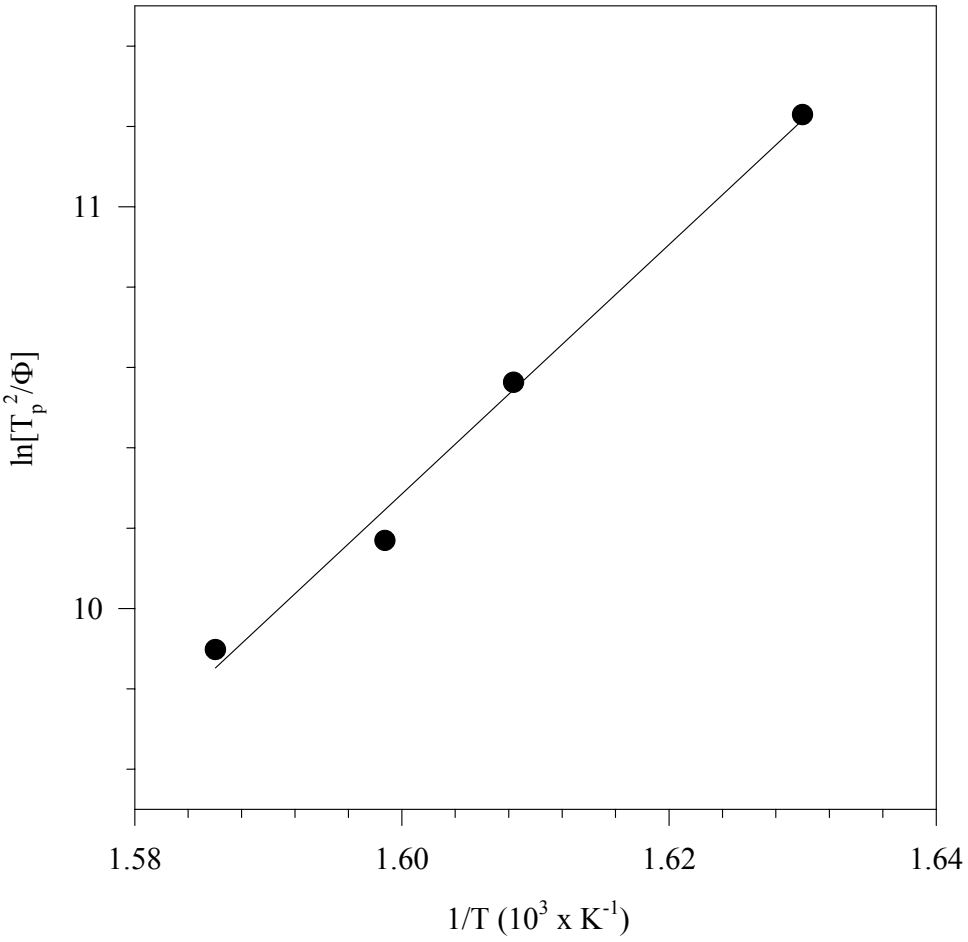

Figure 4.8. Plot after equation (4.1) for the determination of activation energy for crystallization of EN deposits.

Table 4.1. Peak reaction temperatures of DSC samples.

EN Samples	**Peak Temperature (°C)**	
	As-plated	Aged at 300 °C for 1 h
High-phosphorus	343	340 (peak 1), 348 (peak 2)
Medium-phosphorus	337	338
Low-phosphorus	403	403

The significant effect of heat treatment on various properties of EN coatings including hardness is due to the major microstructural changes during the heat treatment of EN coatings. In order to study the crystallographic structure of EN coatings as well as the effect of heat treatment on their microstructure, X-ray diffraction investigation was conducted on three types of EN coatings, namely, low, medium, and high phosphorus in as-plated and heat-treated (at 400 °C for 1 hour) conditions.

Figures 4.9 to 4.14 show the X-ray diffraction analysis of three types of EN coatings. As-plated EN coatings behave similarly to amorphous (nano-crystalline) materials. In the X-ray diffraction of all the as-plated EN samples a broad peak is observed at around 45°C. In terms of heat-treated EN coatings (Figures 4.10 to 4.12) the presence of many peaks evidence the transformation of the amorphous microstructure of as-plated EN coatings to a completely crystalline microstructure after applying heat treatment. Tables 4.2-4.4 show the X-ray diffraction data including the identified peaks and elements. As seen, heat treatment causes the precipitation of various nickel phosphide, Ni_xP_y, particles. As phosphorus content of the EN coating increases the number of identified peaks also increases. Based on the results obtained, X-ray diffraction analysis of low phosphorus EN coating showed 23 peaks identifying $Ni, Ni_{12}P_5, Ni_5P_2, Ni_5P_4, Ni_3P$, and $Ni\ P_2$, whereas in the heat-treated medium phosphorus EN coating 35 peaks were detected identifying $Ni, Ni_7P_3, Ni_5P_2, Ni_5P_4, Ni_3P$, $Ni\ P_2$, and $Ni_{2.55}P$. X-ray analysis of heat-treated high phosphorus EN coating showed 44 peaks identifying $Ni, Ni_{12}P_5, Ni_5P_2, Ni_5P_4, Ni_3P$, and $Ni\ P_2$.

Generally, due to the fact that nickel and phosphorus form several types of intermtallic compounds, Ni_xP_y, some of the peaks were overlapped. As, a result, some of the peaks detected could not be identified.

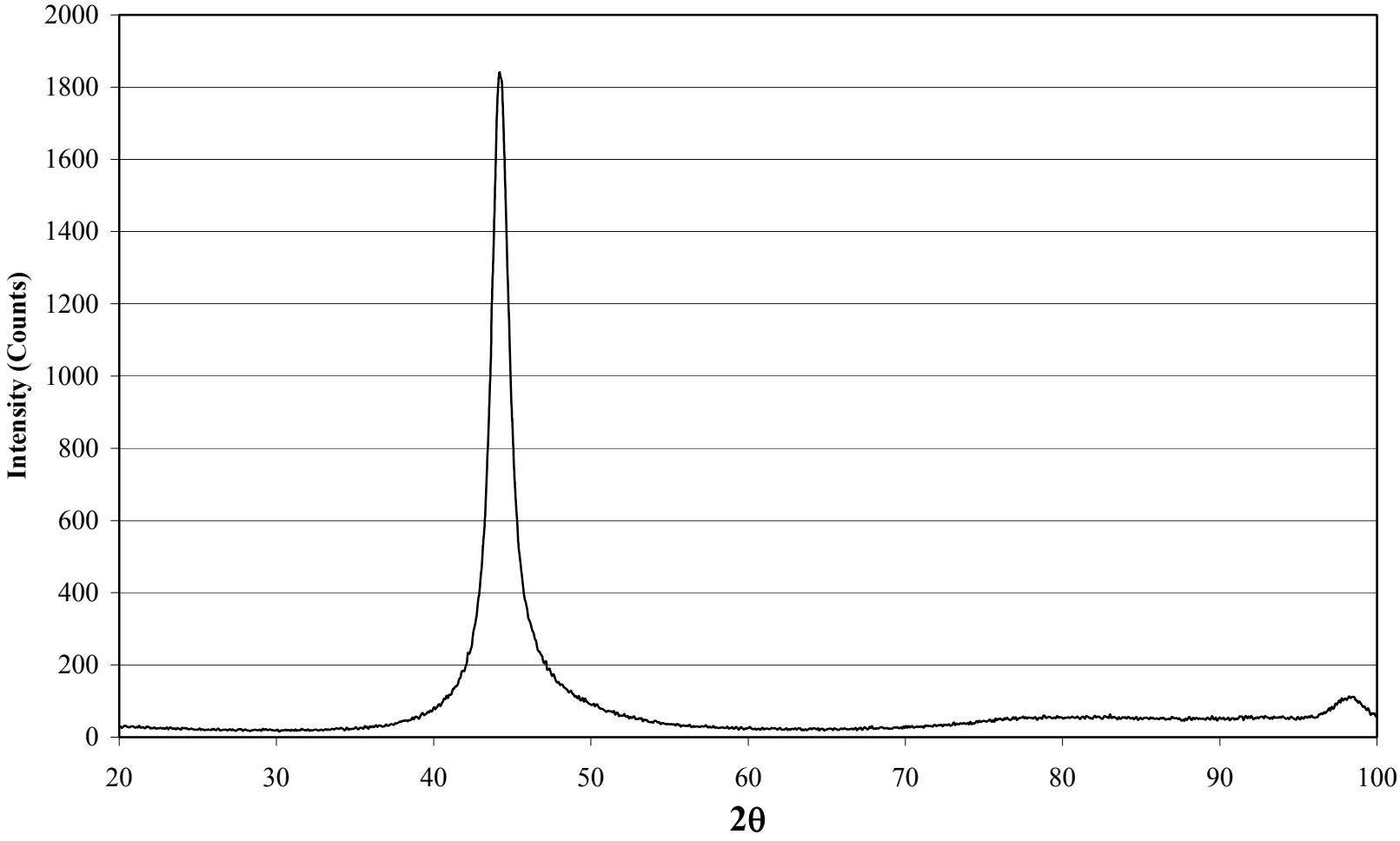

Figure 4.9. X-ray diffraction analysis of low-phosphorus EN coating as-plated.

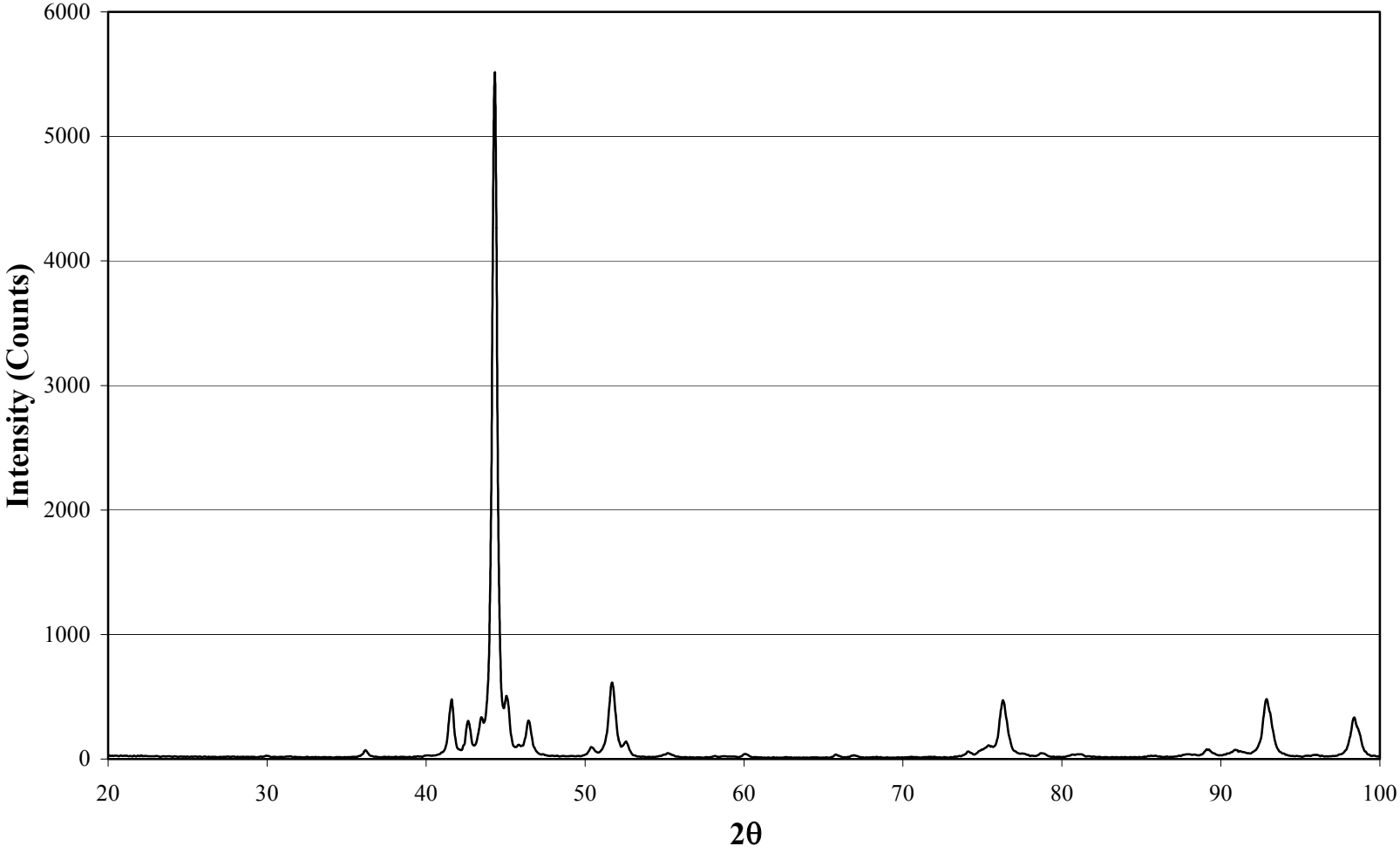

Figure 4.10. X-ray diffraction analysis of low-phosphorus EN coating heat-treated at 400 °C for 1 hour.

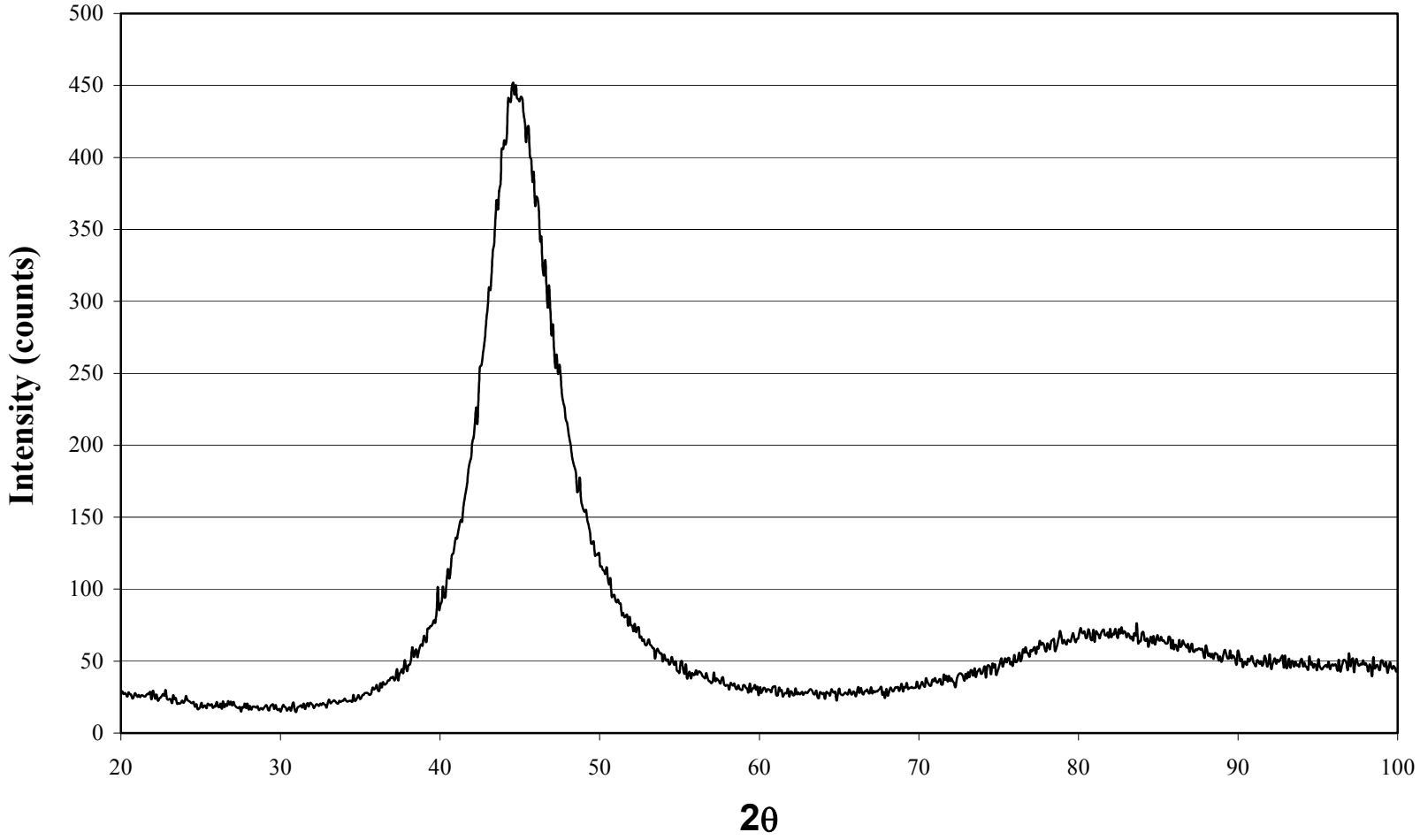

Figure 4.11. X-ray diffraction analysis of medium-phosphorus EN coating as-plated.

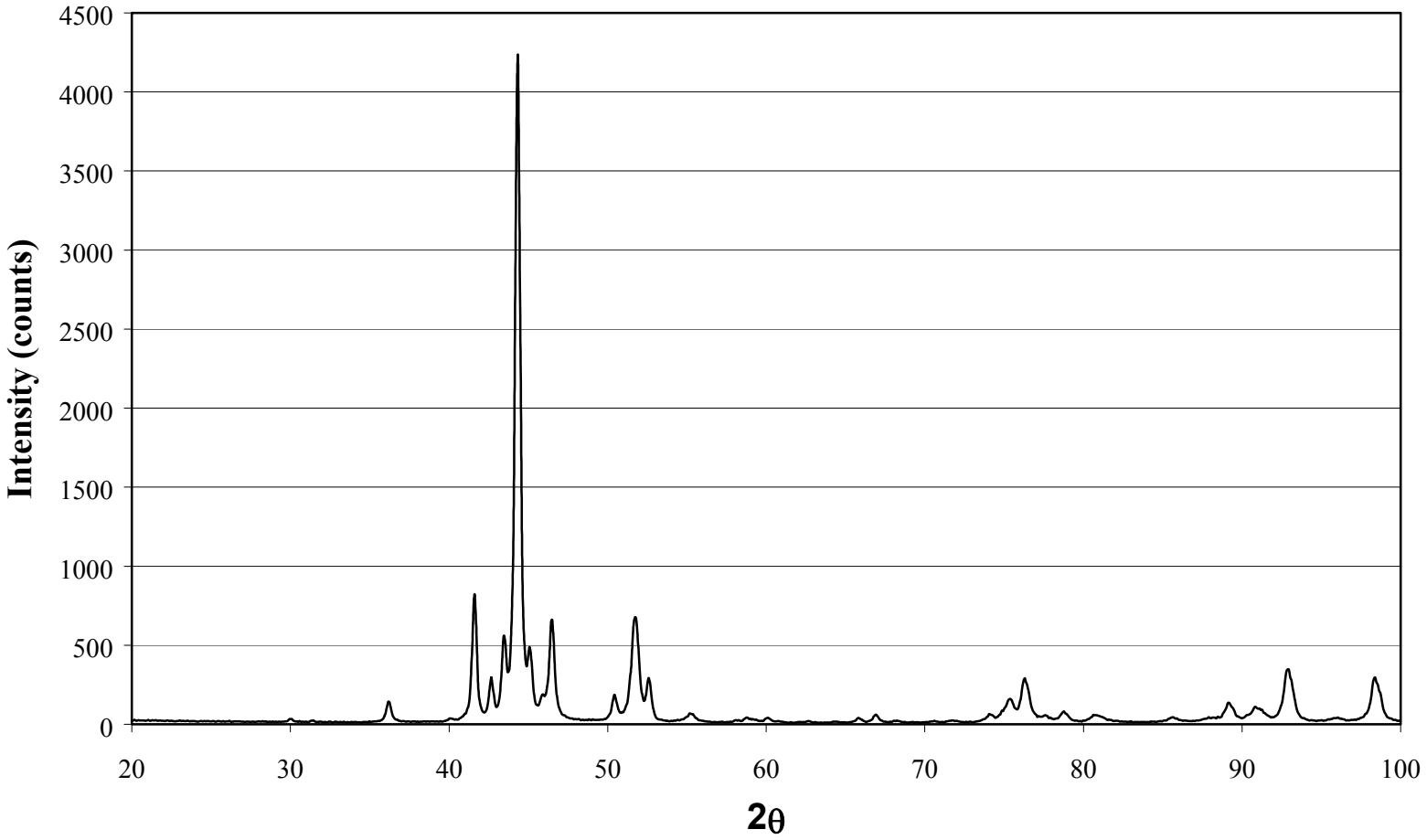

Figure 4.12. X-ray diffraction analysis of medium-phosphorus EN coating heat-treated at 400 °C for one hour.

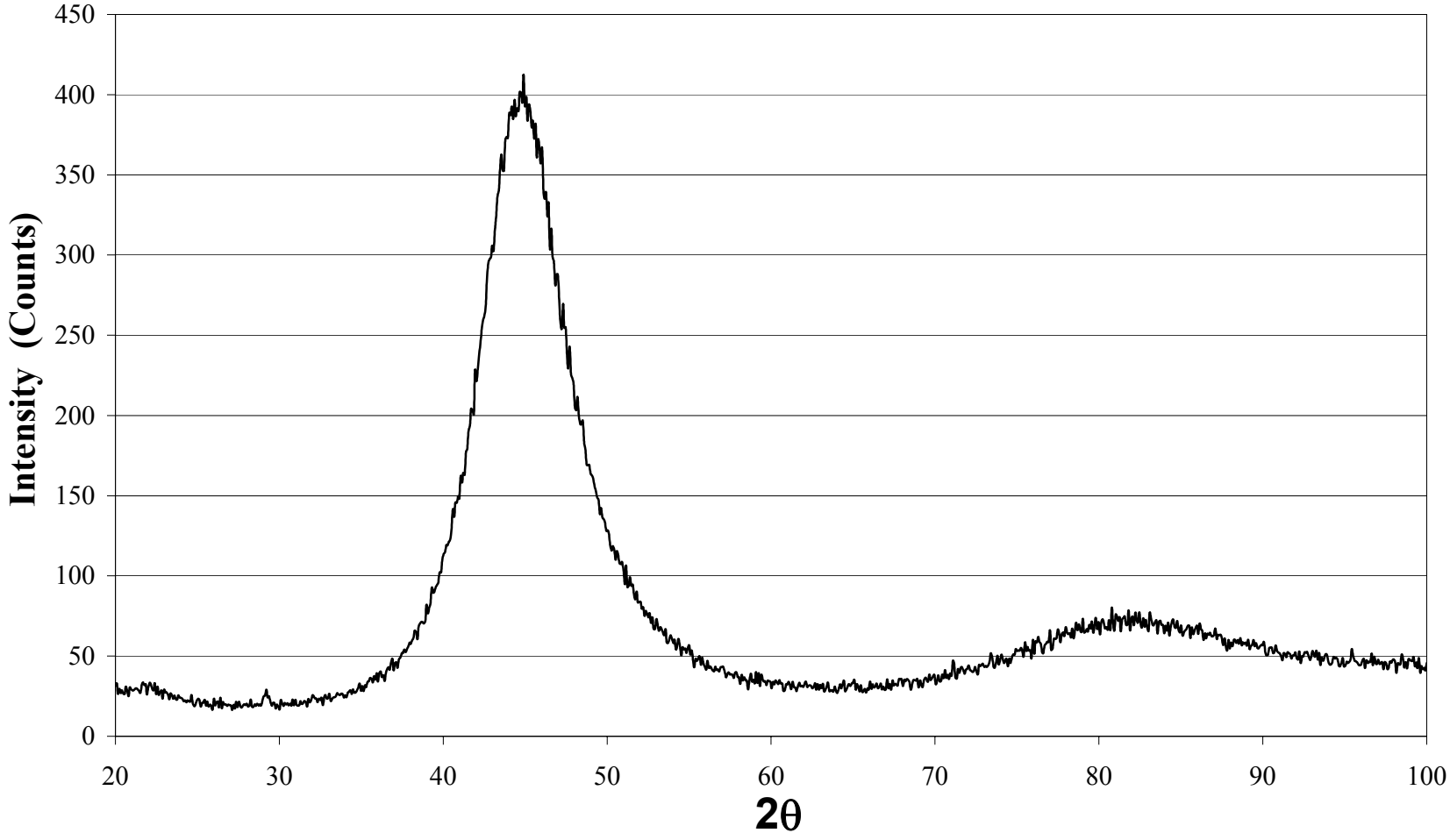

Figure 4.13. X-ray diffraction analysis of high-phosphorus EN coating as-plated.

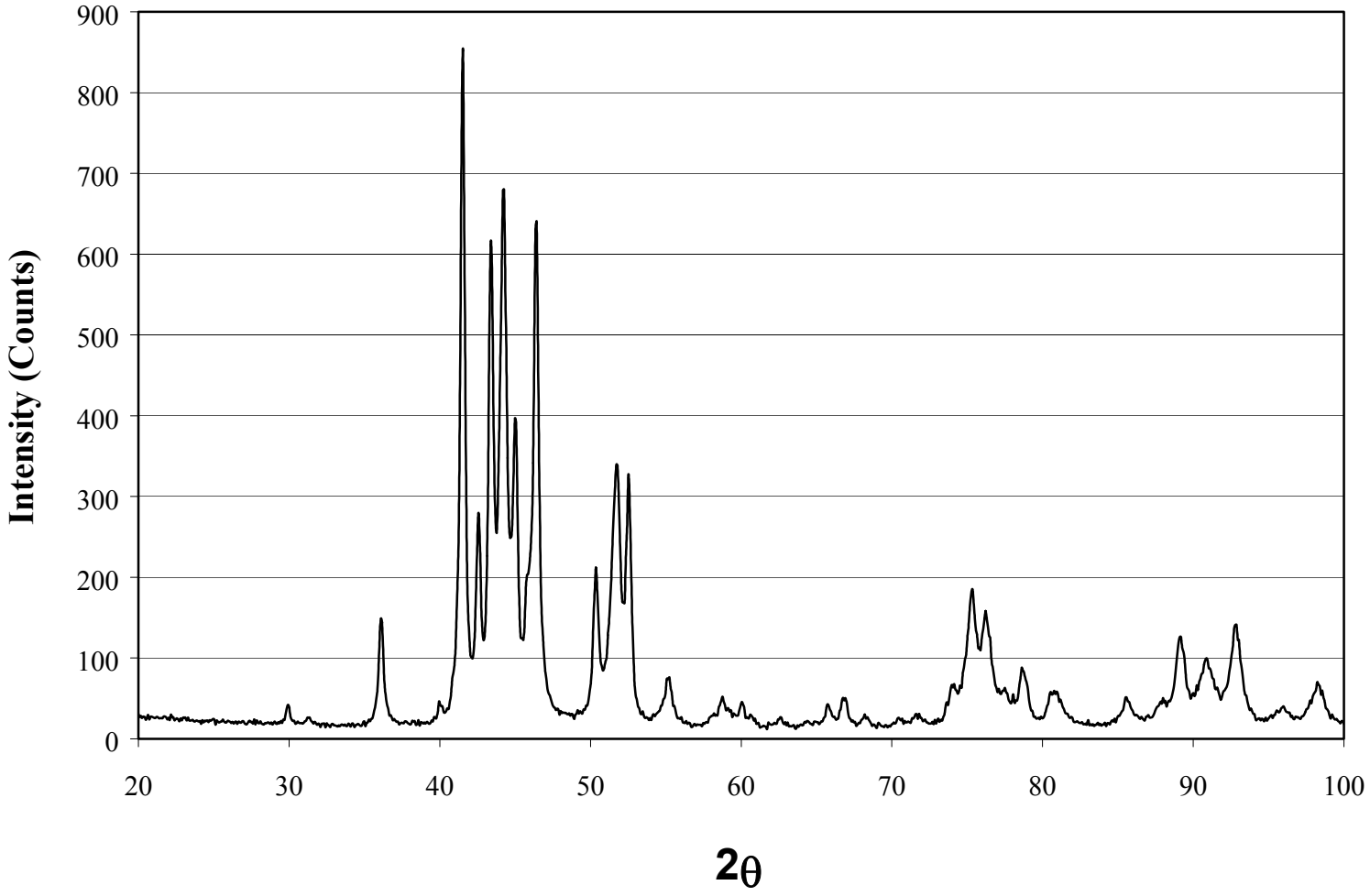

Figure 4.14. X-ray diffraction analysis of high-phosphorus EN coating heat-treated at 400 °C for one hour.

Table 4.2. X-ray diffraction results of low phosphorus heat-treated (1 hr at 400°C) EN coating.

Peak	2-Theta	d(A)	Int.	I%	Phase-ID
1	36.167	2.4815	48	1.2	<>
2	41.602	2.1691	335	8.5	Ni12P5
3	42.606	2.1202	178	4.5	<>
4	42.71	2.1153	128	3.2	Ni5P2
5	43.453	2.0809	183	4.6	<>
6	44.313	2.0424	3941	100	Ni5P2
7	45.056	2.0105	329	8.3	Ni5P4
8	46.081	1.9681	43	1.1	Ni3P
9	46.423	1.9544	139	3.5	<>
10	46.616	1.9467	68	1.7	Ni5P2
11	50.381	1.8098	65	1.6	<>
12	51.651	1.7682	426	10.8	Ni5P2
13	51.808	1.7632	318	8.1	Ni
14	52.56	1.7397	104	2.6	NiP2
15	75.367	1.2601	60	1.5	Ni3P
16	76.237	1.2478	372	9.4	Ni5P2
17	76.758	1.2407	51	1.3	<>
18	87.809	1.1108	31	0.8	Ni
19	92.278	1.0683	50	1.3	<>
20	92.826	1.0634	385	9.8	P
21	93.313	1.0592	75	1.9	Ni12P5
22	97.674	1.0232	32	0.8	<>
23	98.319	1.0182	275	7	<>

Table 4.3. X-ray diffraction results of medium phosphorus heat-treated (1 hr at 400°C) EN coating.

Peak	2-Theta	d(A)	Int.	I%	Phase-ID
1	36.394	2.4666	86	4.7	Ni3P
2	36.743	2.444	30	1.6	NiP2
3	41.161	2.1913	34	1.9	<>
4	41.804	2.1591	448	24.6	Ni7P3
5	42.801	2.111	117	6.4	Ni3P
6	42.889	2.1069	127	7	<>
7	43.717	2.0689	256	14.1	Ni3P
8	44.52	2.0334	1820	100	Ni
9	45.24	2.0027	204	11.2	Ni3P
10	45.337	1.9987	156	8.6	<>
11	46.679	1.9443	292	16	Ni3P
12	46.851	1.9375	188	10.3	
13	47.082	1.9286	58	3.2	Ni5P4
14	50.629	1.8015	118	6.5	Ni3P
15	51.554	1.7713	178	9.8	Ni2.55P
16	51.905	1.7601	513	28.2	Ni5P4
17	52.064	1.7551	323	17.7	NiP2
18	52.8	1.7324	186	10.2	Ni3P
19	55.406	1.6569	44	2.4	<>
20	74.33	1.2751	41	2.3	Ni7P3
21	75.206	1.2624	47	2.6	Ni3P
22	75.474	1.2586	65	3.6	<>
23	76.427	1.2452	262	14.4	Ni
24	76.954	1.238	42	2.3	<>
25	77.386	1.2322	25	1.4	<>
26	80.835	1.1881	32	1.8	Ni2P
27	89.25	1.0965	77	4.2	Ni7P3
28	91.111	1.0789	45	2.5	<>
29	92.49	1.0664	49	2.7	<>
30	92.943	1.0624	313	17.2	Ni
31	93.136	1.0607	193	10.6	<>
32	97.961	1.0209	38	2.1	<>
33	98.112	1.0198	42	2.3	<>
34	98.486	1.0169	181	9.9	Ni
35	98.69	1.0153	79	4.3	<>

Table 4.4. X-ray diffraction results of high phosphorus heat-treated (1 hr at 400°C) EN coating.

Peak	2-Theta	d(A)	In.t	I%	Phase-ID	Peak	2-Theta	d(A)	Int.	I%	Phase-ID
1	29.941	2.9819	21	3.7	<>	23	55.389	1.6574	24	4.2	Ni5P2
2	35.682	2.5142	20	3.5	NiP2	24	58.538	1.5755	17	3	NiP2
3	36.157	2.4822	96	16.7	<>	25	58.736	1.5707	22	3.8	<>
4	40.874	2.206	33	5.7	Ni2P	26	60.046	1.5395	22	3.8	Ni5P2
5	41.53	2.1727	574	100	Ni	27	73.953	1.2806	43	7.5	Ni12P5
6	42.471	2.1267	99	17.2	<>	28	75.27	1.2615	103	17.9	Ni3P
7	42.558	2.1225	137	23.9	<>	29	76.134	1.2493	83	14.5	Ni12P5
8	43.38	2.0842	401	69.9	<>	30	76.499	1.2442	46	8	Ni5P2
9	44.176	2.0485	332	57.8	<>	31	77.052	1.2367	22	3.8	<>
10	44.44	2.0369	120	20.9	Ni12P5	32	77.43	1.2316	26	4.5	Ni5P2
11	44.989	2.0133	249	43.4	Ni5P2	33	78.434	1.2183	21	3.7	<>
12	45.07	2.0099	173	30.1	Ni5P4	34	78.569	1.2165	39	6.8	<>
13	45.736	1.9821	78	13.6	<>	35	78.96	1.2115	20	3.5	<>
14	46.369	1.9566	454	79.1	Ni5P4	36	80.46	1.1926	24	4.2	<>
15	46.892	1.9359	31	5.4	NiP2	37	80.895	1.1873	29	5.1	Ni2P
16	50.354	1.8107	152	26.5	NiP2	38	85.467	1.1351	27	4.7	Ni12P5
17	51.208	1.7824	54	9.4	<>	39	88.583	1.1031	25	4.4	<>
18	51.51	1.7727	161	28	Ni5P2	40	89.05	1.0985	71	12.4	<>
19	51.762	1.7646	159	27.7	Ni	41	90.735	1.0824	47	8.2	<>
20	52.49	1.7419	234	40.8	NiP2	42	92.703	1.0645	86	15	P
21	54.851	1.6724	27	4.7	Ni2P	43	93.433	1.0581	26	4.5	<>
22	55.12	1.6648	58	10.1	<>	44	98.201	1.0191	39	6.8	<>

In order to confirm the microstructural changes caused by heat treatment, a comprehensive TEM investigation was conducted on as-plated and heat-treated high P EN coatings. Also, EDS analysis was conducted to determine the composition of the precipitate particles. It is believed that high phosphorus EN coatings are amorphous (non-crystalline) [Allen and VanderSande, 1983]. Figure 4.15 shows the TEM micrograph of as-plated high phosphorus EN coating. After heat treatment, 400°C for one hour, the microstructure of high phosphorus EN coating becomes completely crystalline, as in Figure 4.16a. This is due to the precipitation of various forms of nickel phosphide particles, Ni_xP_y. The increase in hardness during the heat treatment is attributed to fine Ni crystallites, particle "A" Figure 4.16b, and hard intermetallic Ni_xP_y particles. Particle B in Figure 4.16c, precipitated during the crystallization of the amorphous phase. Tables 4.5-4.8 show the EDS analysis of the as-plated high phosphorus EN coating, particles A and B, and the matrix of heat-treated high phosphorus EN coating (Figure 4.16b and Figure 4.17) respectively. The phosphorus content of the precipitated particles varies due to the changes in stoichometry coefficient, Ni_xP_y, as well as the proportion of nickel and phosphide precipitated within a particle. As shown, the whiter the particle, the higher is the phosphorus content. Figures 4.18 a-e show different particles precipitated after heat treatment. Also, Tables 4.9-4.13 show the EDS analysis of the visible particles in Figures 4.18 a-e respectively. As illustrated, the precipitated particles contain various amount of phosphorus.

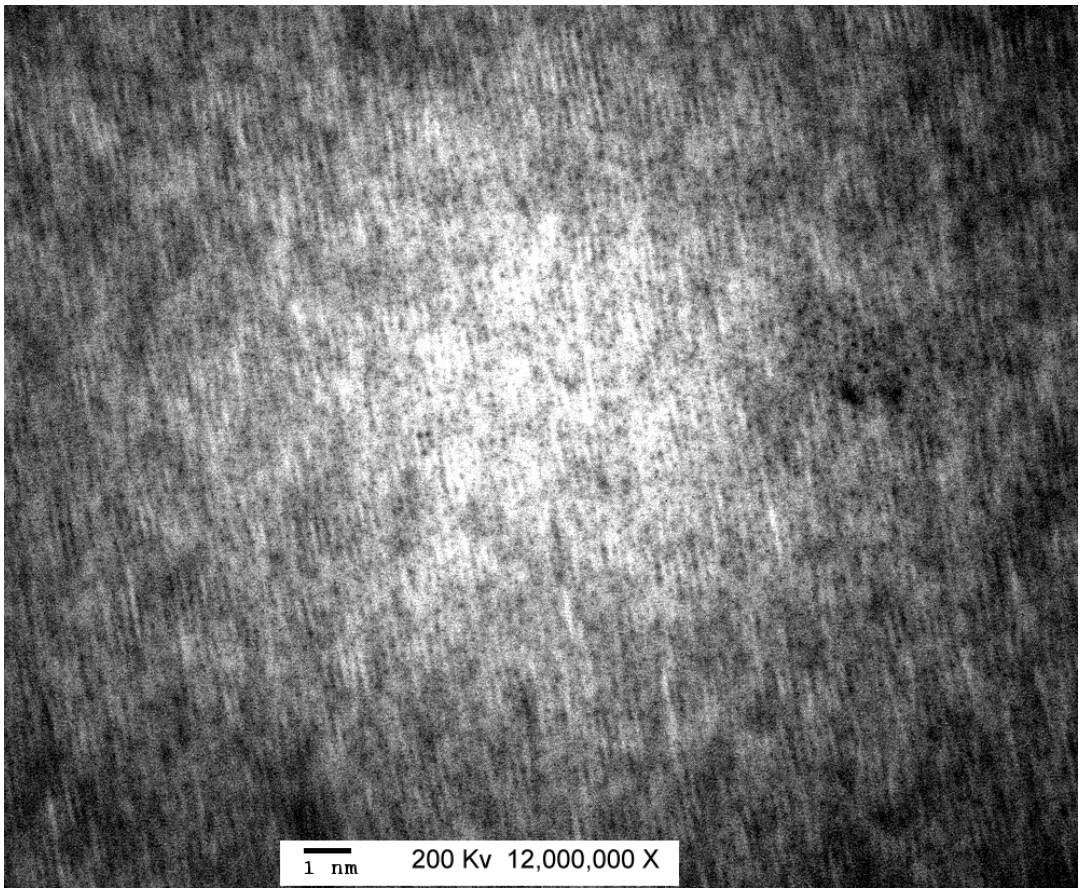

Figure 4.15. TEM micrograph of as-plated high phosphorus EN coating.

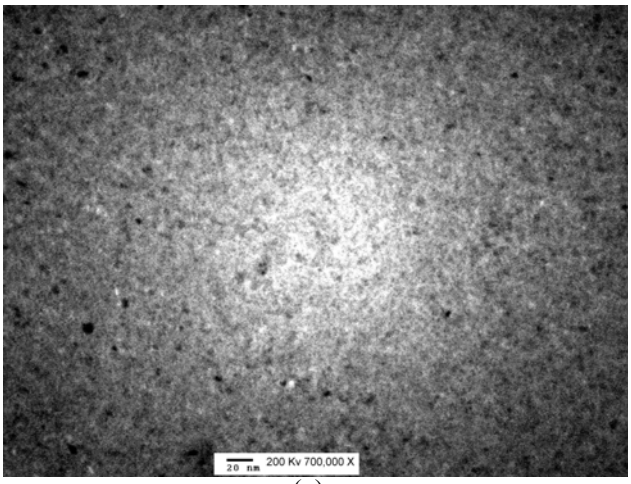

(a)

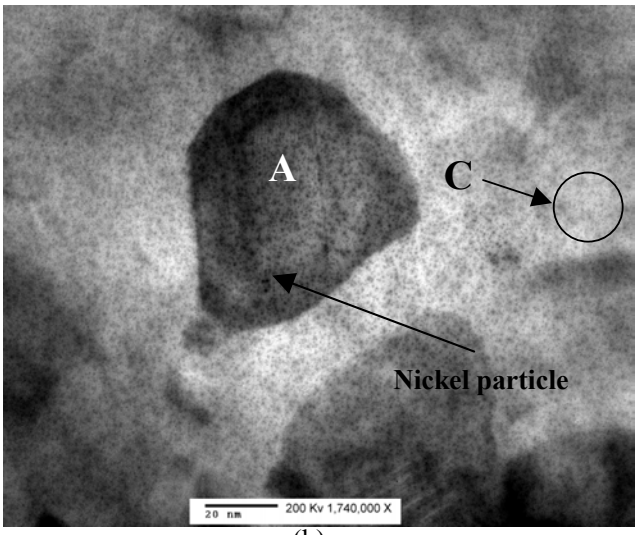

(b)

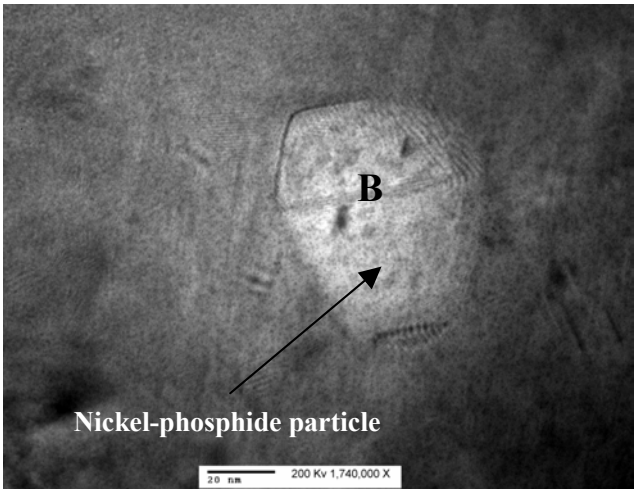

(c)

Figure 4.16. TEM micrographs of heat-treated high phosphorus EN coating.

Table 4.5. EDS Analysis of high phosphorus as-plated EN coating, Figure 4.15.

Element	Peak Area	Weight%	Atomic%
P K	1637	11.56	19.85
Ni K	9977	88.44	80.15

Table 4.6. EDS Analysis of Particle A, Figure 4.16b.

Element	Peak Area	Weight%	Atomic%
P K	52	0.74	1.40
Ni K	5509	99.26	98.60

Table 4.7. EDS Analysis of Particle B, Figure 4.16c and Figure 4.17.

Element	Peak Area	Weight%	Atomic%
P K	1947	5.36	6.60
Ni K	27371	94.64	93.4

Table 4.8. EDS Analysis of high phosphorus heat-treated EN coating, area C Figure 4.16b and Figure 4.17.

Element	Peak Area	Weight%	Atomic%
P K	6675	15.23	25.40
Ni K	29590	84.77	74.60

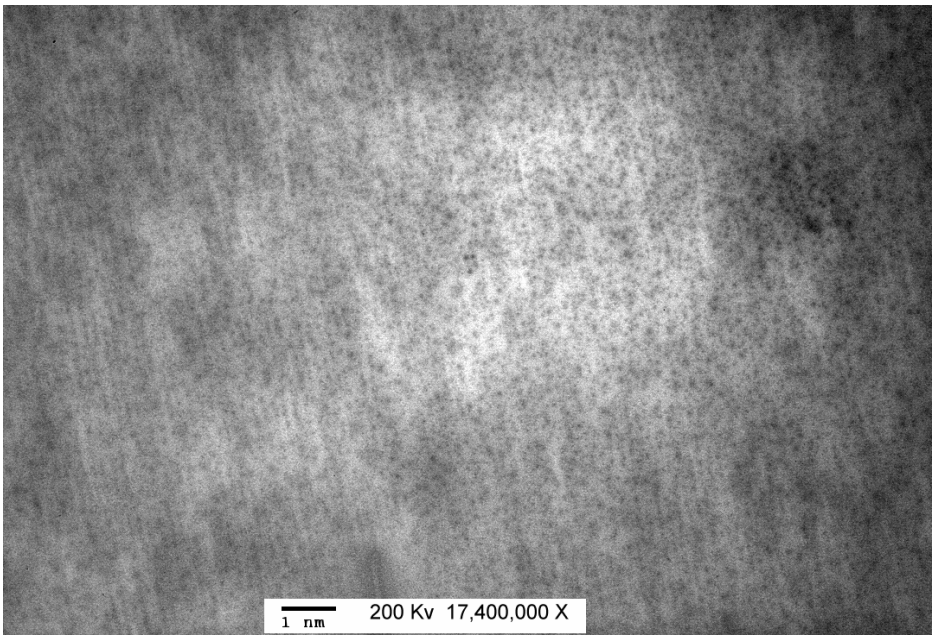

Figure 4.17. TEM micrograph of the matrix of high phosphorus heat-treated EN coating, area C, Figure 4.16.

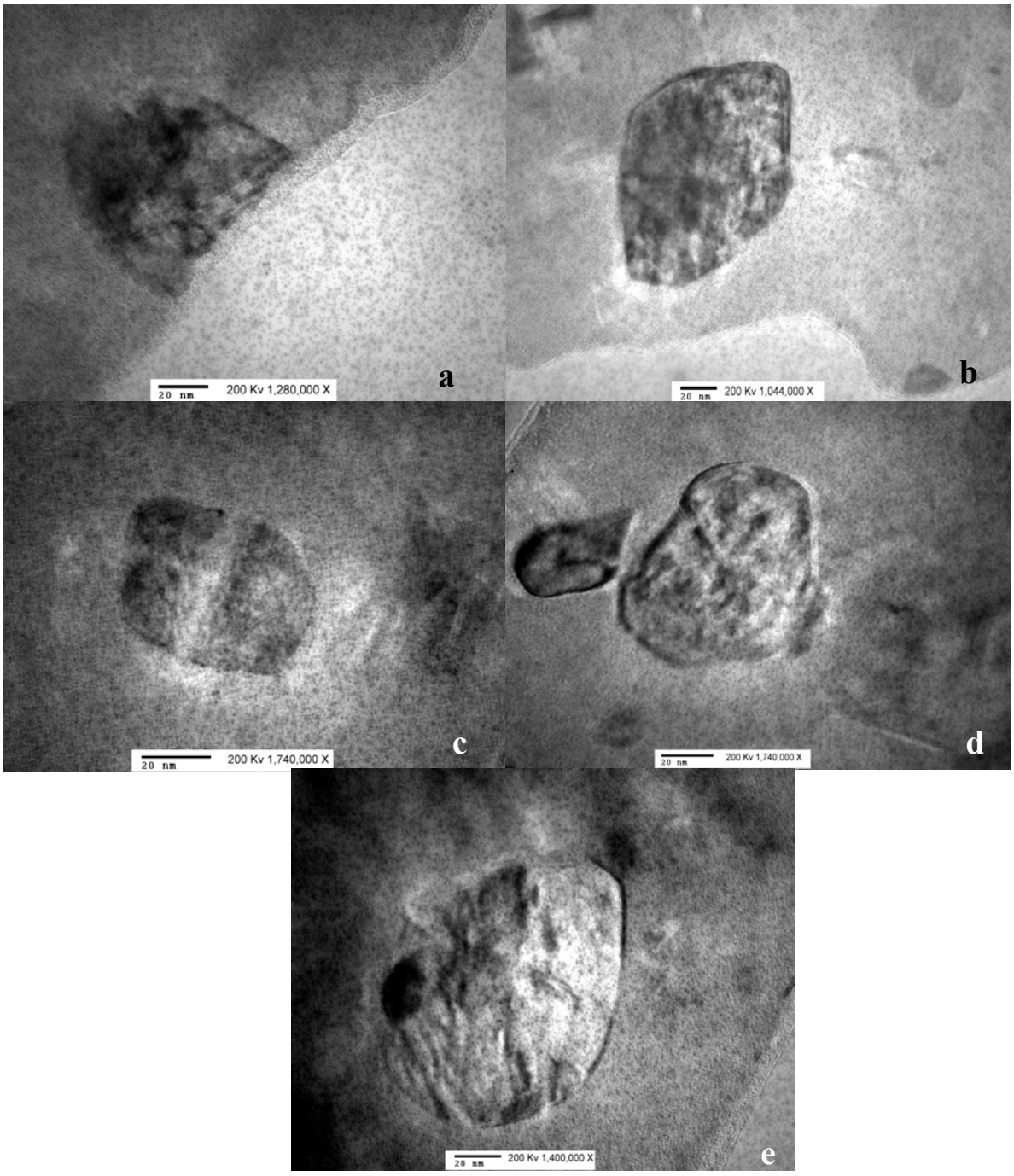

Figure 4.18. Precipitated particles after heat treatment at 400°C for one hour (high phosphorus EN coating).

Table 4.9. EDS Analysis of particle shown in Figure 4.18a.

Element	Peak Area	k Factor	Weight%	Atomic%
P K	184	0.992	1.05	1.98
Ni K	13774	1.245	98.95	98.02

Table 4.10. EDS Analysis of particle shown in Figure 4.18b.

Element	Peak Area	k Factor	Weight%	Atomic%
P K	5	0.992	1.48	2.76
Ni K	252	1.245	98.52	97.24

Table 4.11. EDS Analysis of particle shown in Figure 4.18c.

Element	Peak Area	k Factor	Weight%	Atomic%
P K	454	0.992	1.65	3.09
Ni K	21493	1.245	98.35	96.91

Table 4.12. EDS Analysis of particle shown in Figure 4.18d.

Element	Peak Area	k Factor	Weight%	Atomic%
P K	789	0.992	2.22	4.12
Ni K	27686	1.245	97.78	95.88

Table 4.13. EDS Analysis of particle shown in Figure 4.18e.

Element	Peak Area	k Factor	Weight%	Atomic%
P K	3291	0.992	3.49	6.42
Ni K	72385	1.245	96.51	93.58

Although heat treatment increases the hardness and wear resistance of EN coatings due to precipitation of hard intermetallic nickel phosphide particles, it causes a reduction in corrosion resistance of EN coatings in general and in high phosphorus EN coating in particular. High phosphorus EN coatings (10-13 wt.%) are amorphous (nanocrystalline) with superior corrosion resistance. After heat treatment, the amorphous microstructure of as-plated high phosphorus EN coatings become completely crystalline and prone to various types of corrosion including intergranular corrosion. Corrosion and wear resistance of various types of EN coatings will be discussed in next section.

4.1.2 Tribological properties of EN coatings

The fact that EN coatings are significantly hard makes them good candidates for various applications where superior wear resistance is required. However, hardness is one among many other criteria defining the wear resistance of surfaces in contact with each other. Geometric texture and surface profile of a surface also affect the wear resistance of materials [Williams, 1994]. Furthermore, the coefficient of friction between two surfaces in contact with each other has a significant effect on their wear behavior. As a result, the tribological properties of coatings play important roles in their performance under wear conditions. In addition, surface morphology characteristics of coatings affect their corrosion and fatigue behavior. Several studies comparing the hardness and wear characteristics of EN, hard chromium, and nitriding coatings have been documented [Parker, 1974; L. Wing, 1993; C. Nargi and G. Shawhan, 1983; and N. Tope et al., 1976]. In these studies, well-known wear tests such as the Taber Abraser, Falex Pin, Vee Block, and Crossed Cylinders were used. It was shown that by increasing the hardness of EN coatings through heat treatment, dry abrasive wear resistance (as measured by the Taber Abraser test) may be improved to or beyond the level offered by hard chromium. Another important aspect related to hardness and wear is the coefficient of friction. In a recent study, Hadley and Tulsi [Hadley and Tulsi, 1989] used the Crossed-Cylinder wear test to study the metal-to-metal contact between EN coating, EN-PTFE composite, and mild steel. The least amount of wear occurred in the EN-PTFE composite and this was attributed to the

excellent self-lubricating properties of PTFE. In this section, results obtained from various tribological experiments are presented.

4.1.2.1 Surface Roughness and coefficient of friction

One of the highlighted advantages of EN coatings is that they provide a deposit of uniform thickness that follows all the contours of the substrate, without building up at the edges and corners with the edge receiving the same thickness of the deposit as does a blind hole, unlike electroplating. Therefore, EN plating differs significantly from the conventional electroplating process that depends on an external source of direct current (DC) to reduce nickel ions in the electrolyte to nickel metal on the substrate. Substrate surface morphology and its metallurgical condition can affect the quality of EN coatings. Substrates with passive spots that will not initiate EN coating result in non-uniform deposition and cause porosity. The porosity of EN coatings has been found to depend not only on their surface roughness but also on their surface morphology [Deng and Moller, 1993; Beer, 1981; and Deng and Moller, 1994], which, in turn, can be affected by the pre-coating conditions of the substrate. The effect of substrate surface roughness and coating thickness on the final surface properties of EN coated surfaces was studied by Ernst et al (1997). It was found that the roughness of the coatings increased with the substrate surface roughness.

There is scanty information in the open literature regarding systematic studies of the coefficient of friction (static and kinetic) of EN coatings. In addition, it is often assumed that EN coating does not change the substrate surface morphology when compared with conventional electroplating. The question that arises is: "*Do EN coatings follow exactly the substrate surface profile or do they just seal off surface asperities (the troughs and peaks) like electroplating*?". In the present study, the tribological properties of EN coatings were investigated. These included the effect of EN coatings on surface profile and coefficient of friction of coated EN surfaces and also the effect of heat treatment on the tribological properties of EN coatings.

As was mentioned, the profile of a surface under wear conditions has a significant effect on the wear regime. Generally, smoother surfaces provide a better wear regime. Surfaces under wear conditions can be smoothened during the manufacturing process. However, after coating, the smoothened substrate can be roughened depending on the surface characteristics of the coating. Thus, a more severe wear regime may occur. It is usual for the coating to completely follow the surface profile of the substrate. In other words, it is ideal that the coating does not affect the surface roughness of the substrate before and after coating.

In this part of the study, the effect of EN coatings on the surface profiles of the coated surfaces was investigated. Moreover, the effect of coating thickness on the surface roughness changes of the coated surfaces was studied.

The effect of substrate surface roughness and coating thickness on the surface roughness of the EN coated surfaces (as indicated by Ra and Rz) is shown in Table 4.14. Figures 4.19 and 4.20 embody substrate surface roughness and coating thickness effect on the surface roughness of the EN coated surfaces. As shown, regardless of the initial surface roughness of the substrate and coating thickness the coating surface roughness remains similar to that of the substrate metal. In other words, EN coatings follow the surface profile of their substrates.

Table 4.14. The results of surface roughness measurement for various coating thickness.

	Surface Roughness Ra and Rz (μin)									
	Bare metal		**10 μm coating**		**20 μm coating**		**40 μm coating**		**60 μm coating**	
Specimen	**Ra**	**Rz**	**Ra**	**Rz**	**Ra**	**Rz**	**Ra**	**Rz**	**Ra**	**Rz**
1	235	1090	243	1101	245	1087	258	1123	274	1181
2	97	520	98	527	95	520	100	520	106	539
3	68	364	71	369	70	355	69	355	76	387
4	68	332	63	306	67	332	70	332	64	336
5	57	306	63	309	65	319	63	338	71	337
6	44	244	43	238	44	221	41	235	46	244
7	33	204	35	222	40	210	38	224	38	233
8	15	102	15	109	15	113	17	113	18	117
9	12	79	13	95	14	103	14	98	11	77

Standard deviation of the readings ranged between 0.5 to 8 (< ± 3% of the read values)

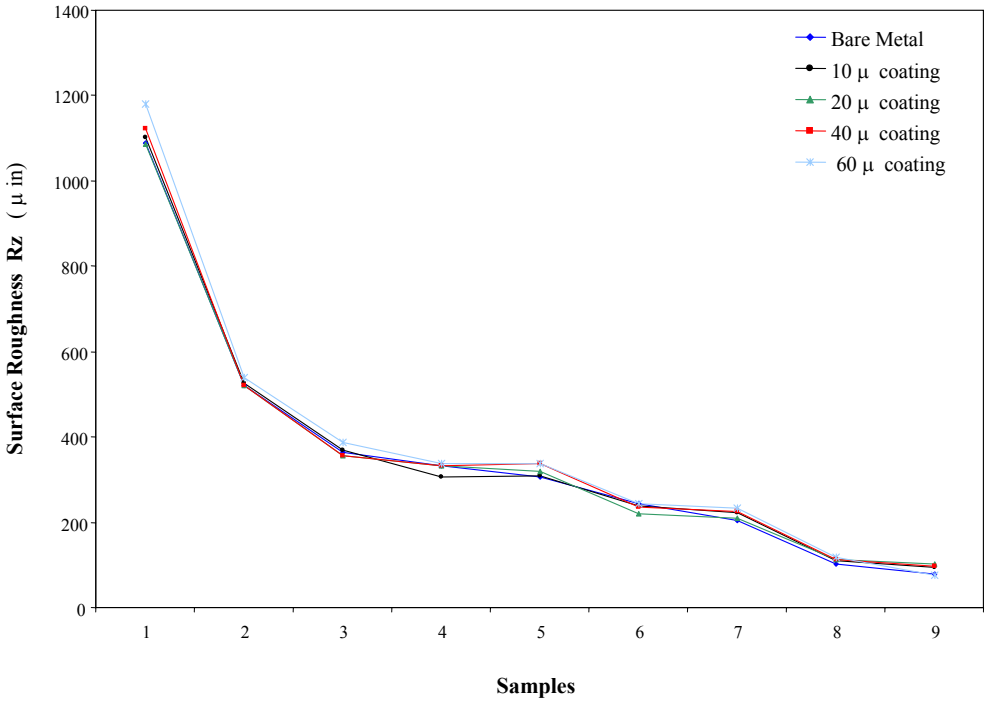

Figure 4.19. The effect of high-phosphorus EN coating thickness on the Rz.

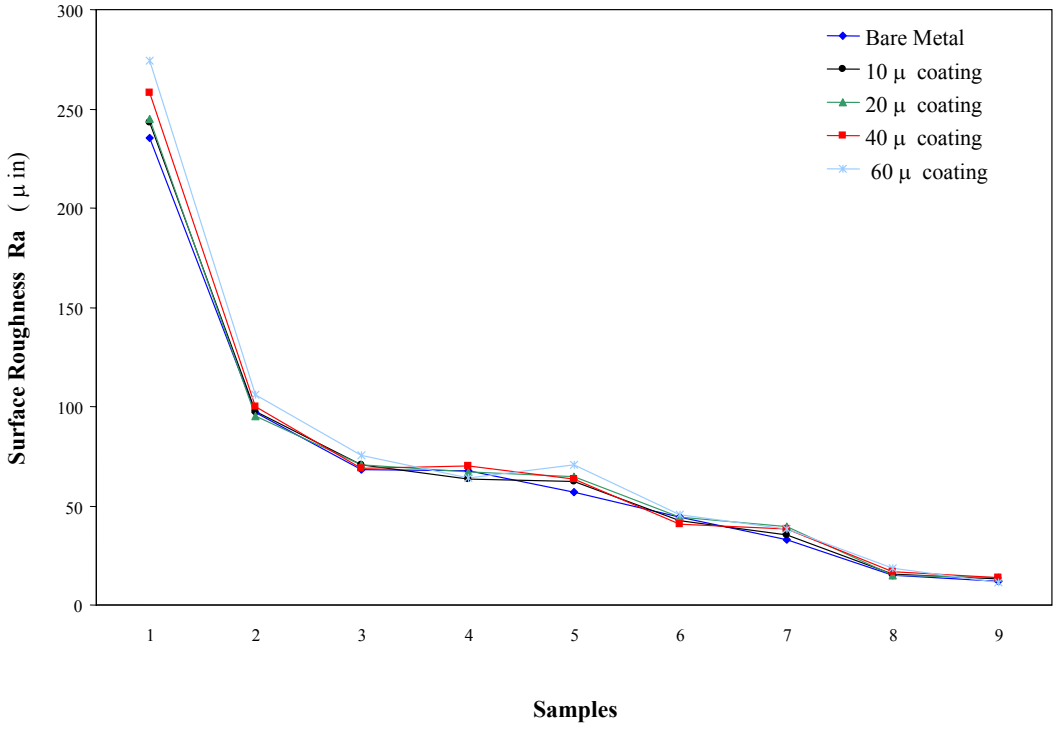

Figure 4.20. The effect of high-phosphorus EN coating thickness on the Ra.

The results of this work are in several ways different than those of Ernst et al. [1997]. These authors have studied the effect on the substrate surface roughness prior to and after EN coating and found that a transition or critical substrate Ra exists. That is, on rough substrate surfaces, EN coatings decrease the Ra value, whereas on very smooth surfaces, the Ra value increases. Therefore, a critical Ra value was defined where below that value, EN coating has a detrimental effect on the smoothness of the coated or final surface. However, the Ra data obtained in the present work did not exhibit any critical substrate Ra, probably due to differences in the initial substrate surface roughness and lubrication characteristics of the samples used in the two investigations. Also, the bath conditions used in the present work were not the same as those used by Ernst et al. Moreover, different filtration systems were used in these two research studies. In the present work, the substrate Ra and the EN coating Ra are practically identical, indicating that the EN coating follows the profiles of surface asperities rather than just filling them. Figures 4.21-4.23 show the optical micrographs of samples of the 1018 carbon steel substrate (Ra = 2.47 and 5.97 μm, respectively) coated with 20-μm thick high phosphorus EN deposit. It is apparent from these figures that the EN coating follows the profile of the substrate surface waviness rather than trying to fill it as usually found in conventional electroplating. This is a very significant characteristic of EN coatings distinguishing them from conventional electroplating.

Aside from surface profile, the coefficient of friction between two surfaces in contact subjected to relative motion has a great impact on wear behavior of the surfaces. Ideally, the lower the coefficient of friction, the more desirable the wear behavior will be. In other words, surfaces with lower coefficients of friction provide a better sliding wear behavior. Therefore, it will be beneficial if a coating can reduce the coefficient of friction of a surface due to its self-lubricating characteristic. As a part of the tribological investigation on EN coatings, the effect of EN coatings on the reduction of coefficient of friction of coated surfaces was investigated.

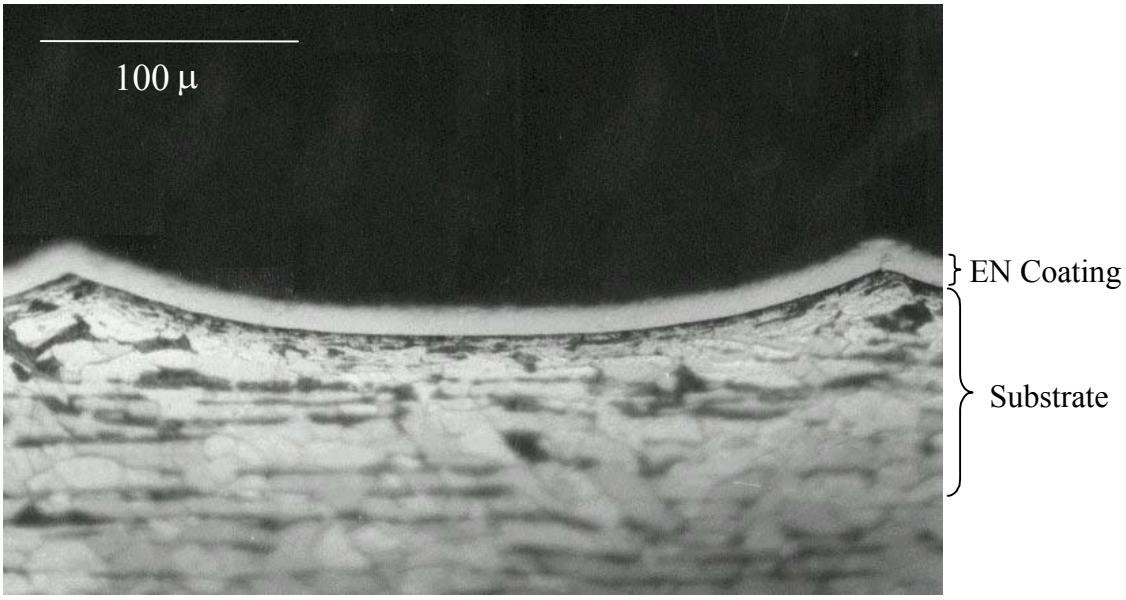

Figure 4.21. Optical micrograph of 20-μm thick high phosphorus coating (Ra = 5.97 μm).

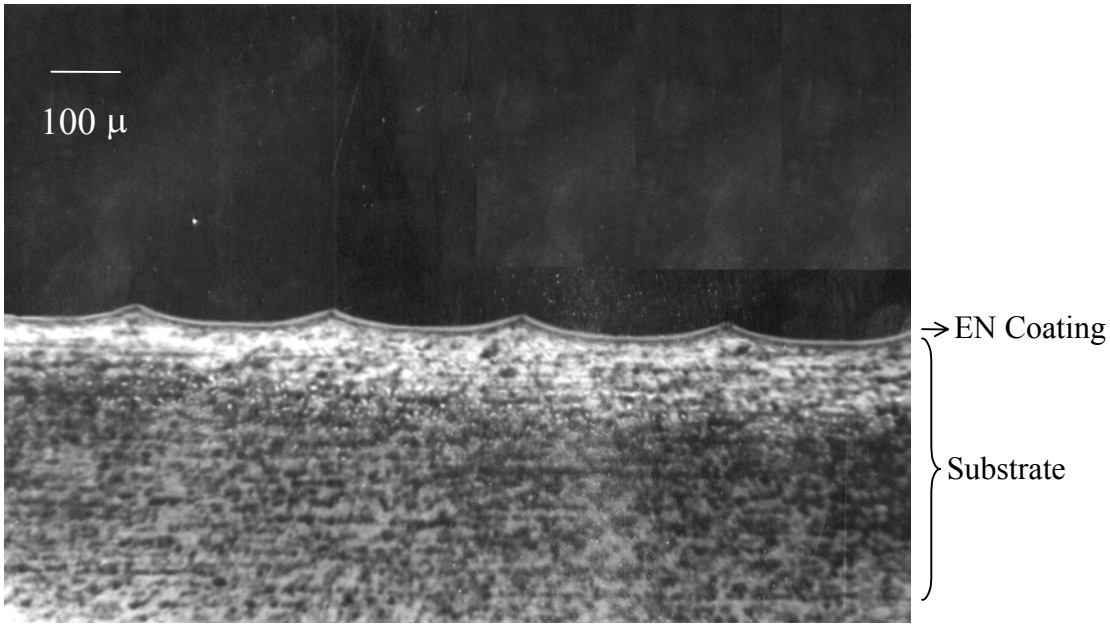

Figure 4.22. Optical micrograph of 20-μm thick high phosphorus coating at a low magnification (Ra = 5.97 μm).

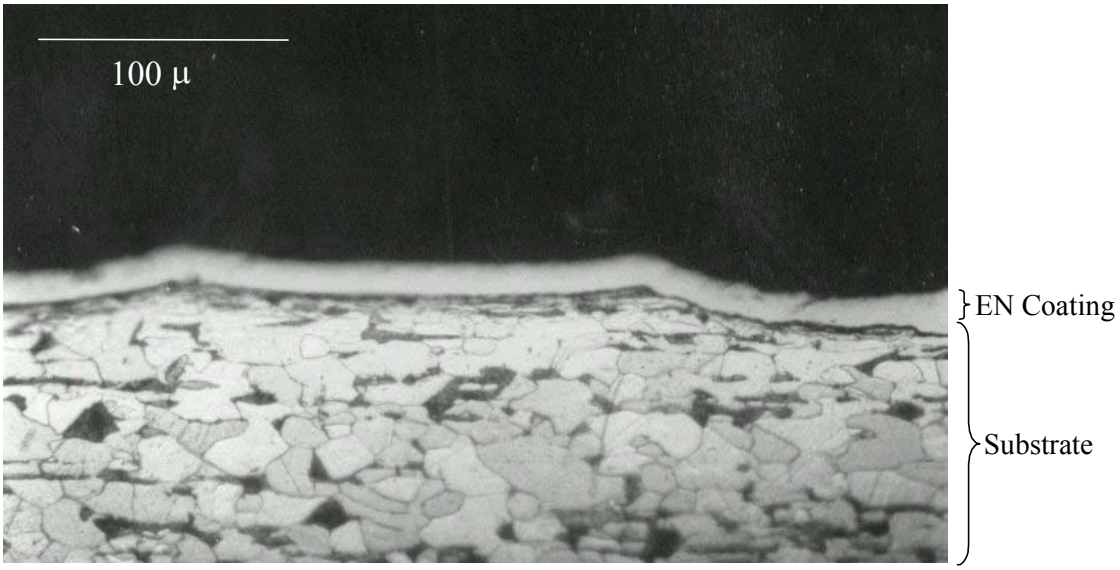

Figure 4.23. Optical micrograph of 20-μm thick high phosphorus coating (Ra = 2.46 μm).

The kinetic coefficients of friction[1], COFs, of EN coatings and bare substrate were determined under different conditions using a sliding ramp (Figure 3.7, Section 3.8).

A summary of the results obtained from the friction experiment is shown in Table 4.15. As shown, the EN coated surfaces had lower kinetic COF than that of the bare substrate. Figure 4.24 and 4.25 show the effect of surface roughness on the COF of as-plated and heat treated EN coatings, respectively. As expected, the COF of EN coatings increases with increasing Ra of the test surface, Figure 4.24 and Figure 4.25. For example, the COF of as-plated high phosphorus EN coating is 0.764 for Ra = 0.254 μm, whereas it is 0.828 for Ra = 13.157 μm. The same trend is obtained for other classes of EN coatings. The relation between the surface roughness and coefficient of friction is shown in a more profound manner in Figure 4.26. As seen, the rougher the surface, the larger the COF values are.

Certain interesting results can be deduced from Figures 4.24 and 4.25 and Table 4.15. At low substrate surface roughness, Ra, the friction of EN coatings tends to decrease with decreasing phosphorus content, whereas at high Ra, the friction seems to be independent of phosphorus content. Also, although heat treatment is known to increase the hardness of EN coatings substantially [Berkh et al, 1996, Barker, 1993, and Parkinson, 1995], the results obtained in this study show that it does not have any significant effect on the kinetic COF. The COFs of as-plated and heat treated samples are practically identical.

Figure 4.26 shows a comparison of percentage reduction in COFs due to EN coatings and lubrication. Although lubrication improves the wear properties of two sliding surfaces in most of the cases, it does not necessarily reduce the COF of the surfaces in contact. This is due to the fact that a lubricant may create an adhesive bond between two sliding surfaces. As a result, the kinetic COF between two sliding surfaces may increase as depicted in Figure 4.26. For example, applying lubricanting oil between the specimen with smoother surfaces, Ra=9.7 μin, and the sliding ramp increased the

[1] In tribology, the dimensionless ratio of the friction force (F_f) and normal force (F_n) between two bodies.

COF compared with dried surfaces with the same surface roughness value. On the other hand, EN coatings can increase the wear resistance and reduce the COF at the same time. It can be seen in Figure 4.26 that the effectiveness of EN coatings in reducing the COF is more significant than that of lubrication. This suggests that coating a steel substrate with an EN deposit may be more effective than lubrication.

The unique combination of the superior hardness and low friction offered by EN coatings explains their excellent wear resistance. [Nargi et al., 1984, Tope, et al., 1976, and Wing, 1993]. Furthermore, since heat treatment causes a significant increase in the hardness of EN coatings without a reduction of the COF, it may be very beneficial in improving the wear resistance of EN coatings. The results of reciprocating corrosion and wear tests, presented in the next section completely agree with the previous statement.

Table 4.15. Coefficients of friction (μ_k) obtained for EN coatings and bare substrate.

Material	**Coefficient of Friction†, μ**		
Ramp Surface Roughness(μm)	Ra= 13.157	Ra = 4.928	Ra = 0.254
As-plated high phosphorus EN coating	0.828	0.800	0.764
Heat treated high phosphorus EN coating	0.807	0.812	0.768
As-plated medium phosphorus EN coating	0.843	0.783	0.725
Heat treated medium phosphorus EN coating	0.840	0.807	0.728
As-plated low phosphorus EN coating	0.829	0.786	0.723
Heat treated low phosphorus EN coating	0.810	0.774	0.744
Bare substrate	0.930	0.846	0.776
Bare substrate (oil)	0.865 (wet)	0.844 (wet)	0.798 (wet)
Bare substrate (silicone)	0.871 (wet)	0.889 (wet)	0.741 (wet)

† Unless otherwise stated, value is for dry kinetic friction. Standard deviation of the readings ranged between 0.002 to 0.004 (< ± 3.5% of the read values)

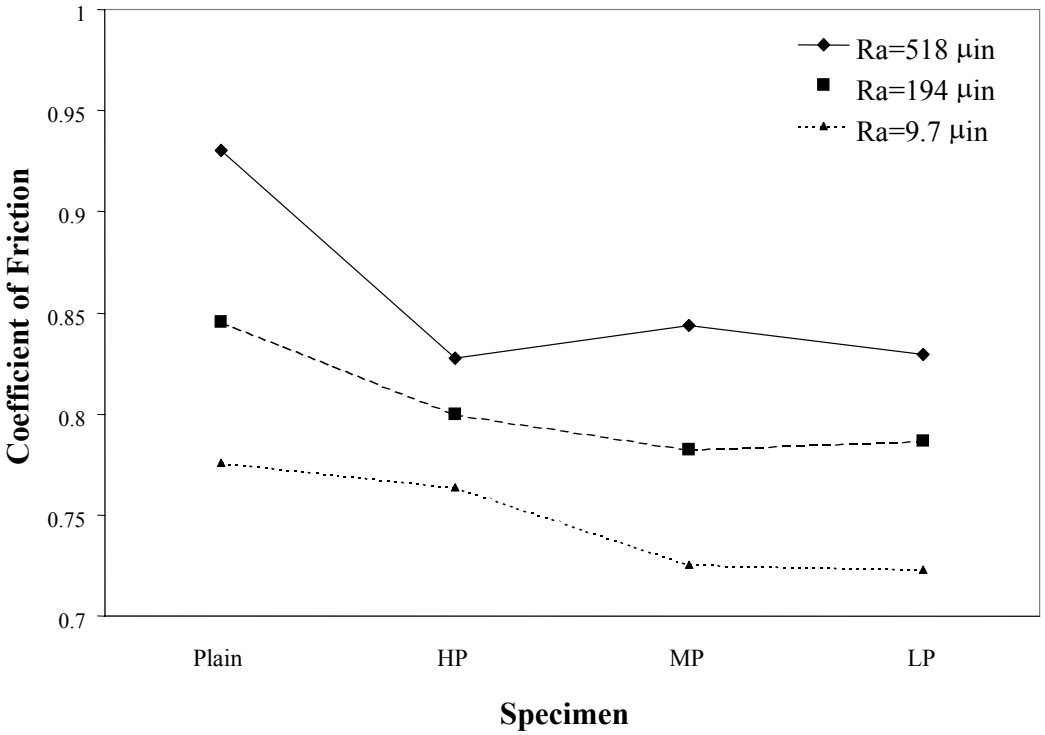

Figure 4.24. Effect of phosphorus content of as-plated EN coatings on the coefficient of friction for various ramp surfaces.

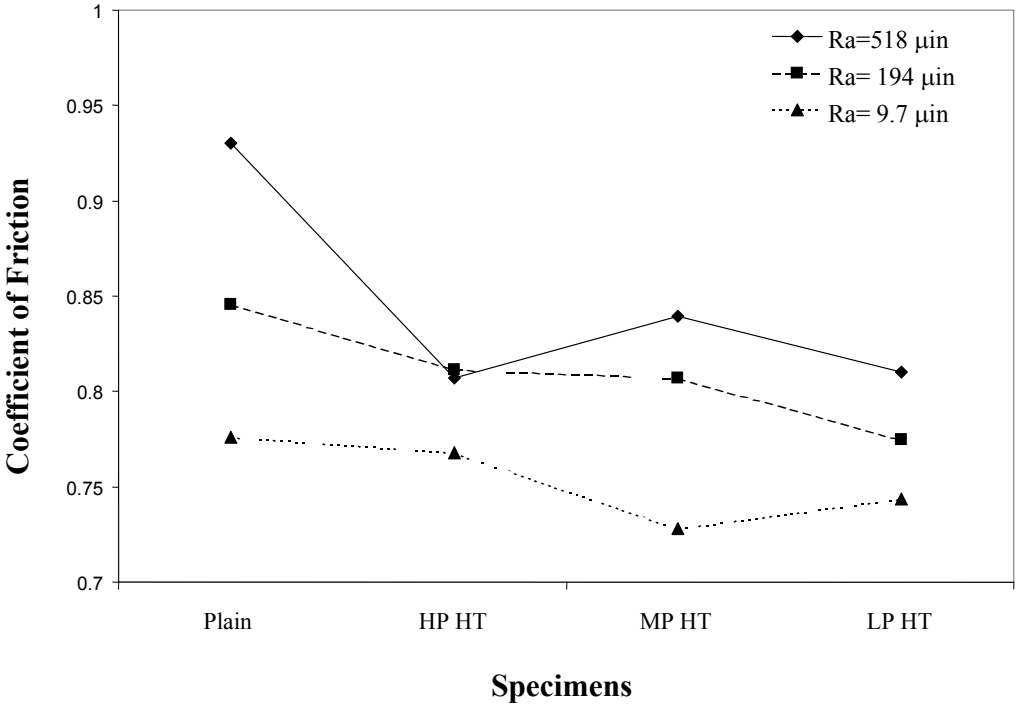

Figure 4.25. Effect of phosphorus content of Heat-treated (at 400 °C for one hour) EN coatings on the coefficient of friction for various ramp surfaces.

.

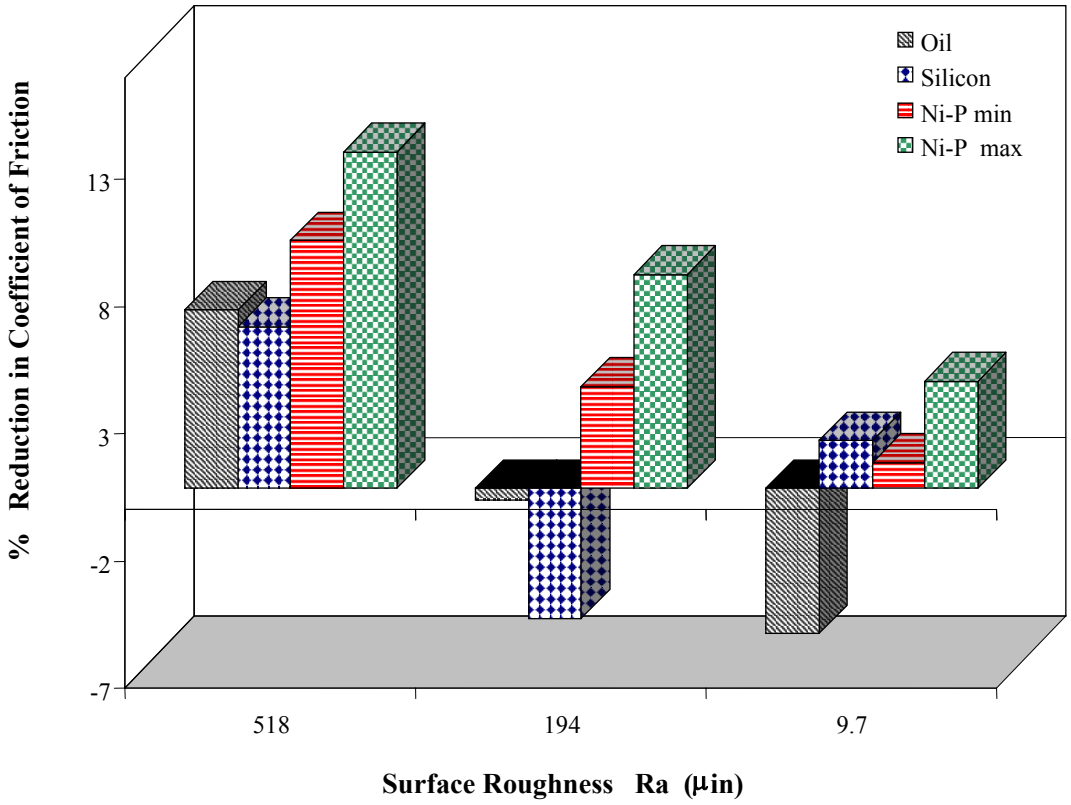

Figure 4.26. Effect of EN coatings on reduction of the coefficient of friction of various surfaces.

4.2 Mechanical Evaluation

4.2.1 Adhesion properties of EN coatings

The adhesion properties of coatings are important characteristics affecting the quality of coatings. The quality of a coating is determined by the extent of bonding with the substrate. Coatings with superior adhesion resist the chip and peel defects under wear conditions. As a result, they show a better wear resistance. In order to study the adhesion properties of EN coatings a comprehensive investigation was conducted. In this section, the results obtained on the adhesion performance of two types of EN coatings, low phosphorus (4.5 wt.% P) and high phosphorus (11.3 wt.% P), are discussed. The effects of several coating parameters such as phosphorus content, coating thickness, heat treatment, and substrate mechanical properties on the adhesion properties of EN coatings were investigated by mean of three-point bending test. Figure 4.27 and Table 4.16 show the effect of coating thickness on the crack initiation deflection value (CIDV). As shown, thicker EN coatings crack at lower mid-span deflection values. This is due to the fact that thicker coatings are more brittle and consequently more prone to cracking as a result of their layered structures, Figure 4.28. This effect of coating thickness on the adhesion properties of EN coatings is more pronounced in high-phosphorus EN coatings. As shown in Figure 4.27, the CIDV for the high phosphorus EN coating shows 25% decrease as the coating thickness increases from 13.5 to 45 μm. This is attributed to the fact that high phosphorus EN coatings are relatively soft and ductile compared with low phosphorus EN coating [Allen and VanderSande, 1982; Vafaei-Makhsoos, 1978; Graham , 1965; and Goldstein et al., 1972]. As coating thickness increases, the high phosphorus EN coating becomes more brittle and prone to delamination and cracking. Thus, the bending cracks in these coatings appear at lower deflection values.

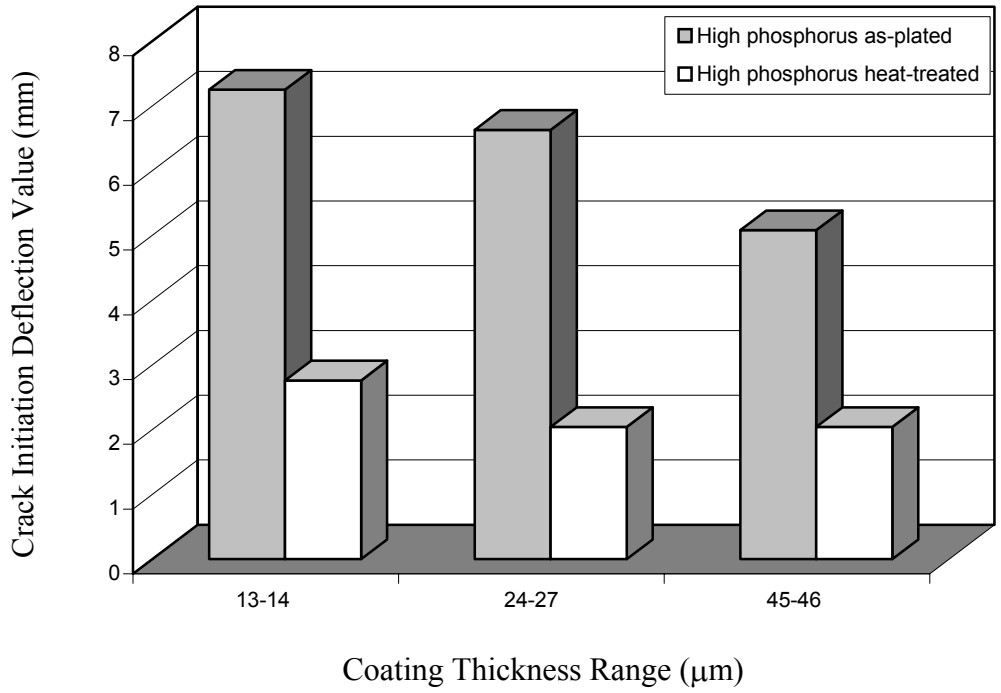

Figure 4.27. Variation of crack initiation deflection value with coating thickness for 1018 steel coated with high phosphorus EN coatings.

Table 4.16. Crack initiation deflection value (CIDV) for various coating conditions.

Type of Coating	Type of substrate	Thickness (μ)	CIDV (mm)
HP	1018	13.5	7.25± 0.3
HP	1018	27.5	6.63± 0.2
HP	1018	30.5	5.79± 0.2
HP	1018	45	5.08± 0.2
HP HT	1018	13.5	2.76± 0.2
HT HT	1018	24	2.04± 0.2
HP HT	1018	35.5	2.08± 0.2
HP HT	1018	45.5	2.04± 0.2
LP	1018	14	3.87± 0.1
LP	1018	24.5	4.11± 0.1
LP	1018	35	4.08± 0.1
LP	1018	38.5	4.23± 0.4
LP HT	1018	12	2.51± 0.2
LP HT	1018	27.5	2.17± 0.2
LP HT	1018	35	2.17± 0.2
LP HT	1018	44	2.17± 0.2
HP	1045	16	10.06± 0.2
HP	1045	28.5	9.62± 0.3
HP	1045	39	9.50± 0.2
HP	1045	47	7.99± 0.2
HP HT	1045	13	9.20± 0.4
HP HT	1045	29.5	7.90± 0.2
HP HT	1045	40	7.60± 0.2

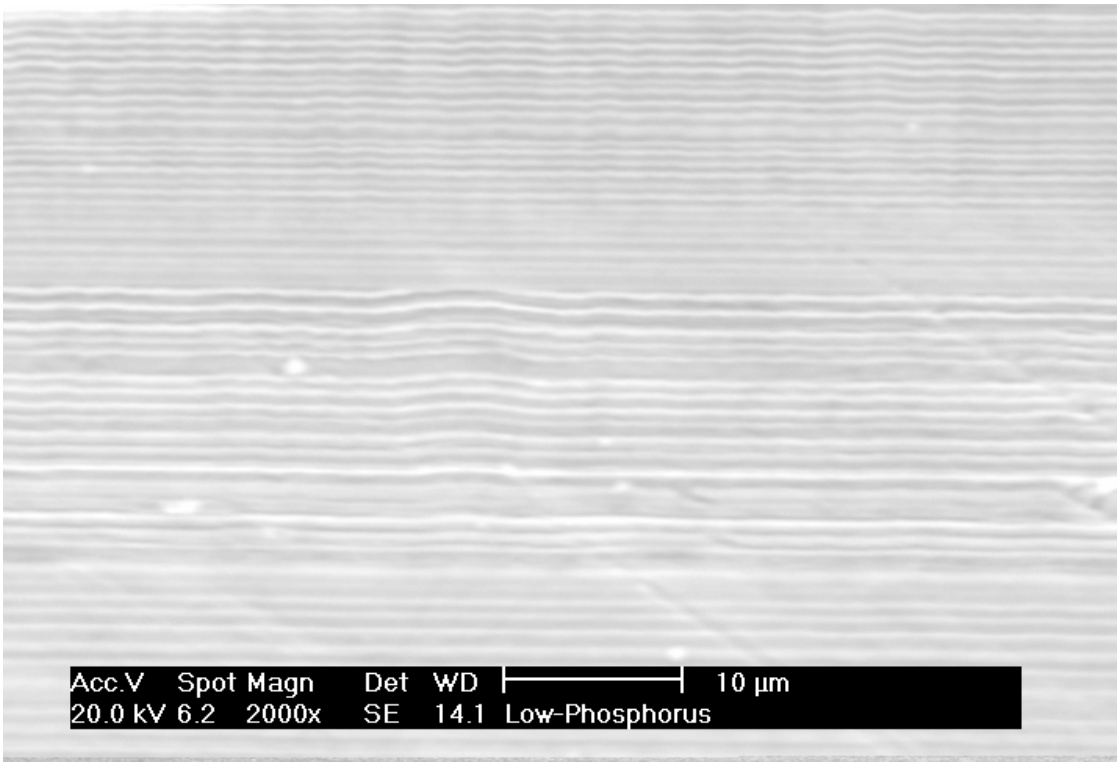

Figure 4.28. Cross-sectional SEM Micrograph (cross section) of low phosphorus EN coating after etching (etching solution; 30 vol. % nitric acid 60 vol.% acetic acid for 10 seconds).

In terms of low phosphorus EN coatings, the effect of coating thickness on the CIDV is insignificant, Figure 4.29. This is due to the fact that low phosphorus EN coatings are substantially hard and brittle even at lower thickness. Thus, bending cracks were initiated and propagated at lower deflection values regardless of the coating thickness, implying that the brittle nature of low phosphorus EN coatings undermines the effect of coating thickness on the CIDV. The variation of CIDV for low phosphorus EN coating with the coating thickness lies within a narrow range of ±5%, Figure 4.29. As shown in Figure 4.30, heat treatment reduces the CIDV of EN coatings. This is attributed to the effect of heat treatment on causing significant changes in the microstructure and therefore the mechanical properties of EN coatings. The hardness of EN deposits increases as a result of heat treatment. It has been found that heating an EN deposit to temperatures of 300-400 °C for one hour causes the hardness and brittleness to increase due to the formation of nickel phosphide (Section 4.1.1). As a result, cracks appear at lower deflection values for heat-treated EN coatings compared with as-plated coated specimens. Once again, the detrimental effect of heat treatment on CIDV is more pronounced for high phosphorus EN coating compared with that of low phosphorus EN coatings, Figure 4.30. For example, heat treatment of a 1018 specimen coated with a 13.5 μm high phosphorus EN coating causes a 62% reduction in CIDV whereas the CIDV reduction for low phosphorus EN coating with a similar coating thickness after heat treatment is only 35%. This is attributed to the substantially brittle structure of both high and low phosphorus EN coatings after heat treatment, indicating that the effect of phosphorus content on CIDV after heat treatment becomes insignificant, Figure 4.31.

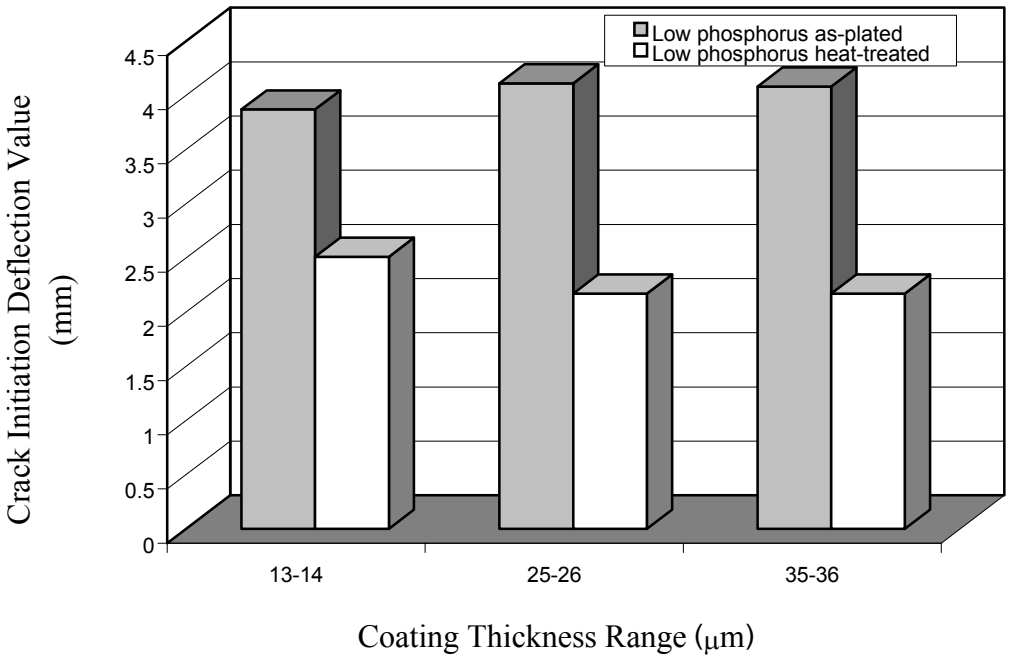

Figure 4.29. Variation of crack initiation deflection value with coating thickness for 1018 steel coated with low phosphorus EN coatings.

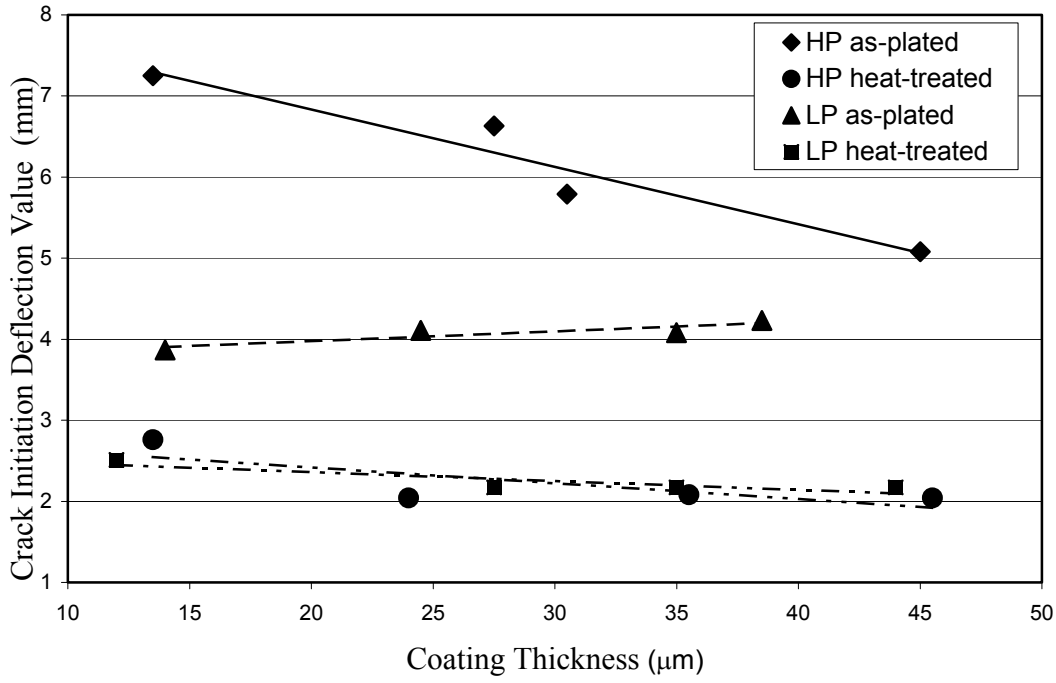

Figure 4.30. Variation of crack initiation deflection value with coating thickness for 1018 steel coated with low and high phosphorus EN coatings.

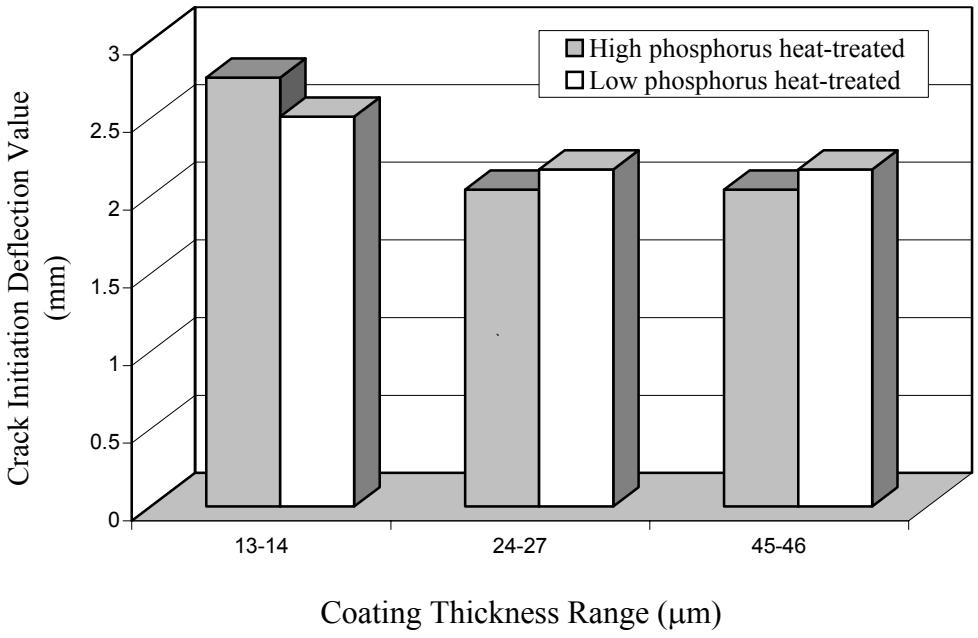

Figure 4.31. Variation of crack initiation deflection value with coating thickness for 1018 steel coated with heat-treated high and low phosphorus EN coatings.

The effect of substrate ductility on CIDV was studied by means of using two different substrates, namely, AISI 1018 and 1045. As shown in Figure 4.32 and Figure 4.33, 1045 EN coated specimens cracked at substantially higher deflection values than 1018 specimens. For example, CIDV for 1045 substrate coated with 47 μm high phosphorus EN coating is 57% higher than that of the 1018 substrate. This is attributed to the fact that 1045 is a harder and less ductile material compared with 1018. Thus, there is more similarity between the ductility of EN coatings and 1045 than that of EN coatings and 1018 alloy. Ideally, when a coating and substrate have identical ductility, they behave as a single material (assuming perfect bonding at the interface). Thus, the maximum CIDV can be obtained. Figure 4.34a shows a schematic illustration of a coating with substantially lower ductility than its substrate. In such a case, the excessive shear stress existing at the interface of the coating-substrate, due to significant differences between the tensile behavior of the coating and substrate, causes the bending cracks to initiate at a lower deflection value than in a system where the coating and substrate have similar ductility, as illustrated in Figure 4.34b. In the latter case, both substrate and coating act as a single material, assuming that a high degree of adhesion exists. Thus, there is no excessive shear stress at the coating-substrate interface to cause the separation of coating from its substrate. Consequently, the coating cracks at higher CIDV.

Figure 4.35 shows the optical micrographs of cracks propagated on the surface of a specimen coated with a heat-treated low phosphorus 44 μm thick EN coating after an 8 mm deflection. As shown, bending cracks initiated on the surface of the coating travel across the specimen in the form of straight parallel lines. No signs of separation, branching, chip off, delamination, or other superficial defects were found. This shows the superior adhesion properties of EN coatings. A coating with poor bonding properties does not resist the shear stress at the interface. As a result, the bending cracks are diverted from a coating causing various superficial defects such as chip off and delamination, Figures 4.36. Figures 4-37(a) and (b) show a schematic illustration of the crack propagation in two coated samples, one with poor adhesion properties (Figure 4.37a) and the other one with superior adhesion properties (Figure

4.37b). As shown, in a coating with poor adhesion properties, Figures 4.36 and 37a, the excessive shear stress during the bending causes the separation of the coating from its substrates (chip off and delamination effect). On the other hand in the case of a coating with superior adhesion properties, the bending cracks do not cause the separation of the coating from the substrate (Figure 4.35 and Figure 4.37 b). As a result, no sign of chip off or delamination would be detected.

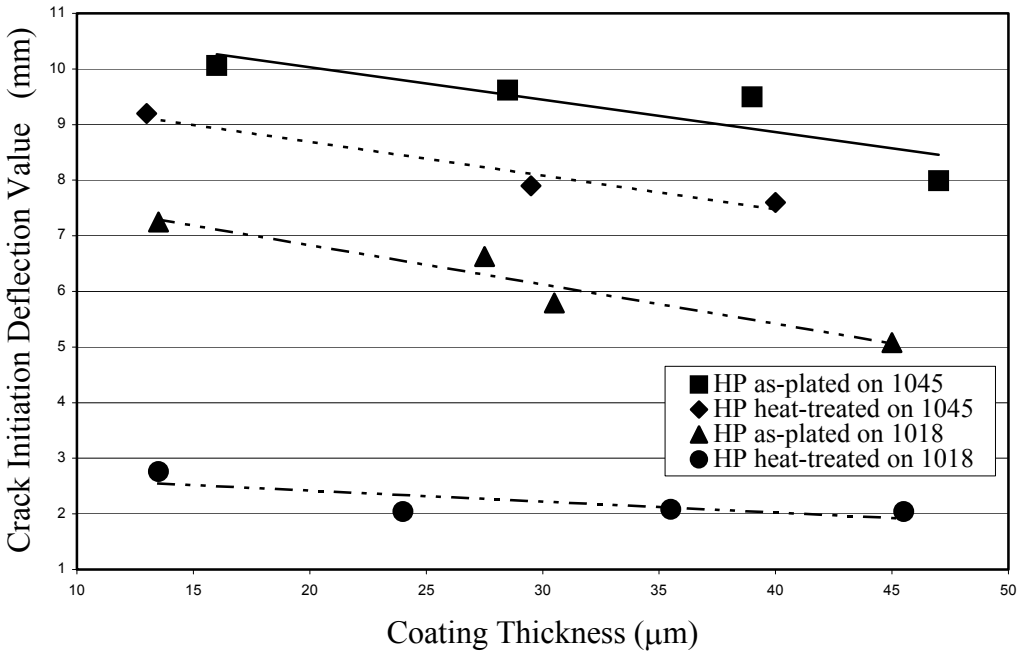

Figure 4.32. Variation of crack initiation deflection value with coating thickness for 1018 and 1045 steels coated with high phosphorus EN coating.

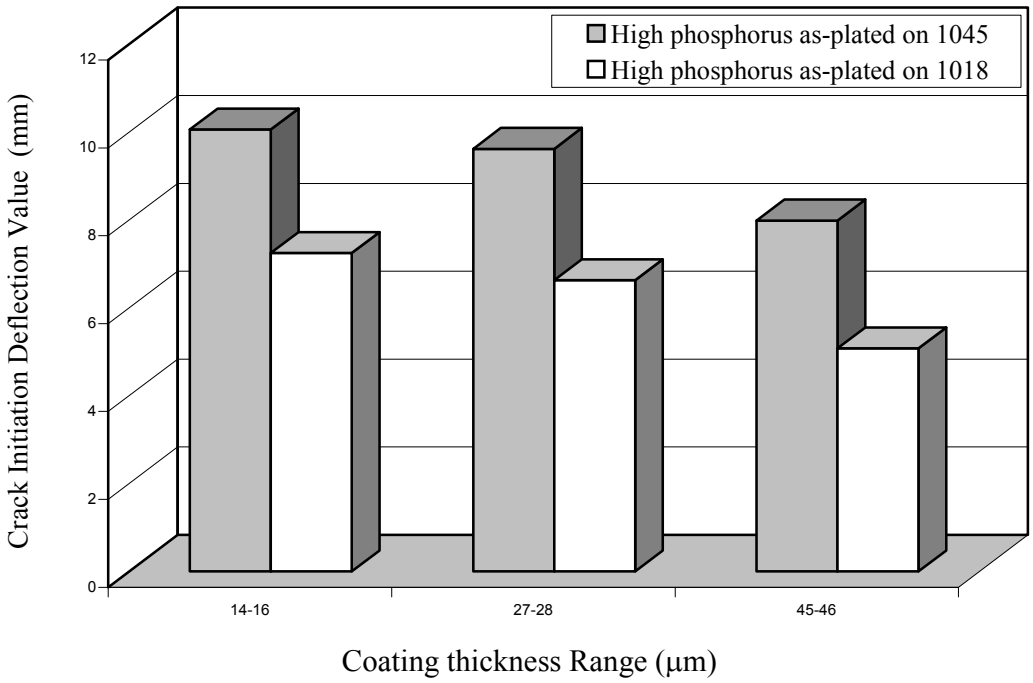

Figure 4.33.Variation of crack initiation deflection value with coating thickness for 1018 and 1045 steels coated with high phosphorus EN coating.

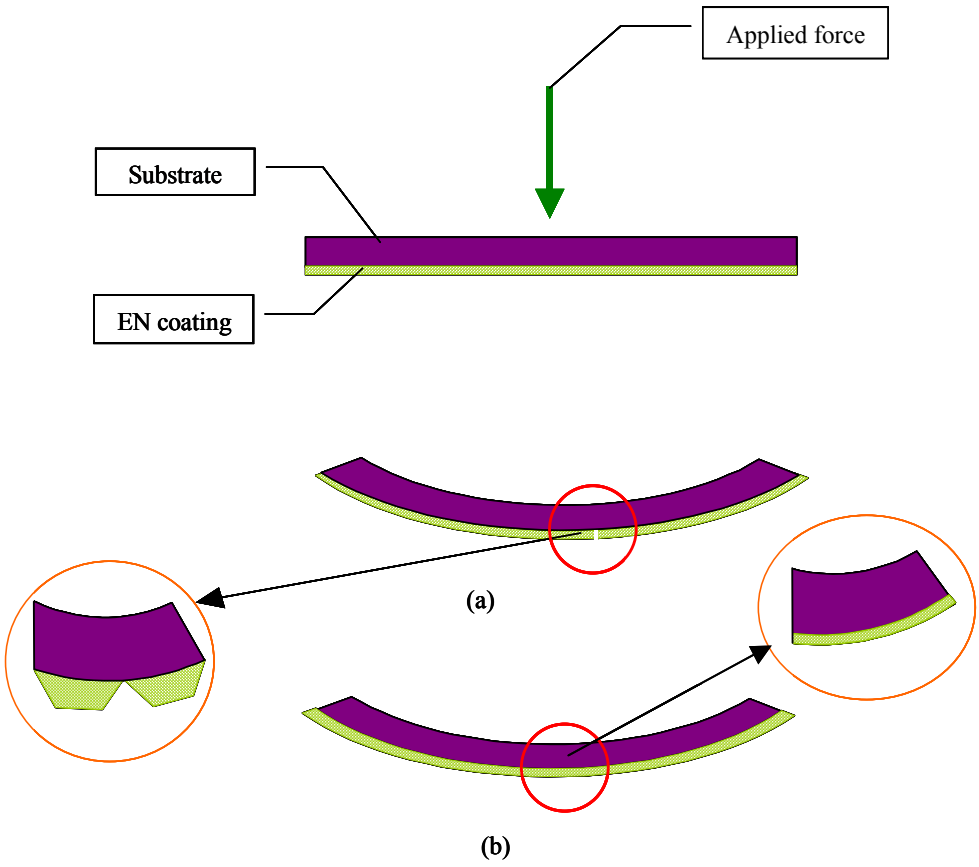

Figure 4.34. Illustration of the effect of mechanical properties of the substrate on the adhesion properties of EN coating, (a) substrate with higher ductility compared with the EN coating; (b) substrate with similar ductility to the EN coating.

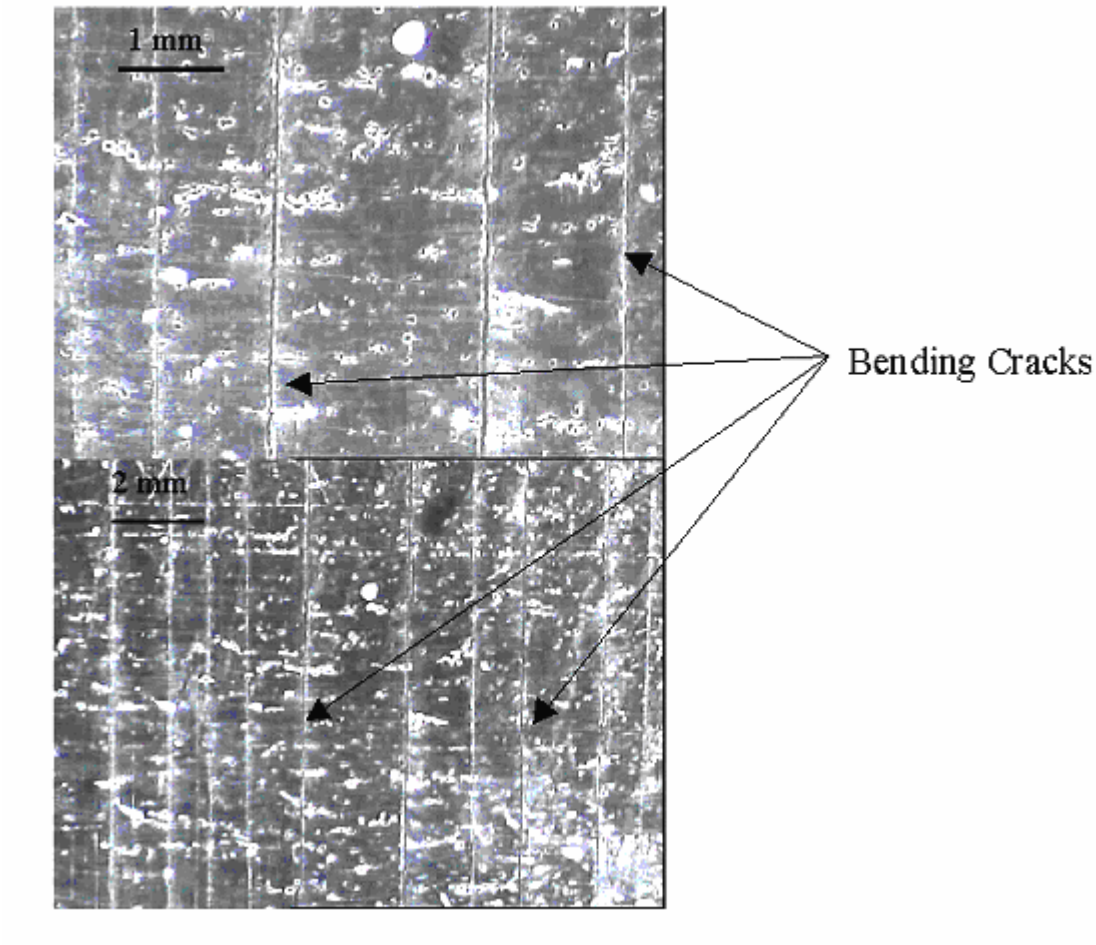

Figure 4.35. Optical micrograph of cracks propagated on the surface of three-point bending test specimens along the specimen width.

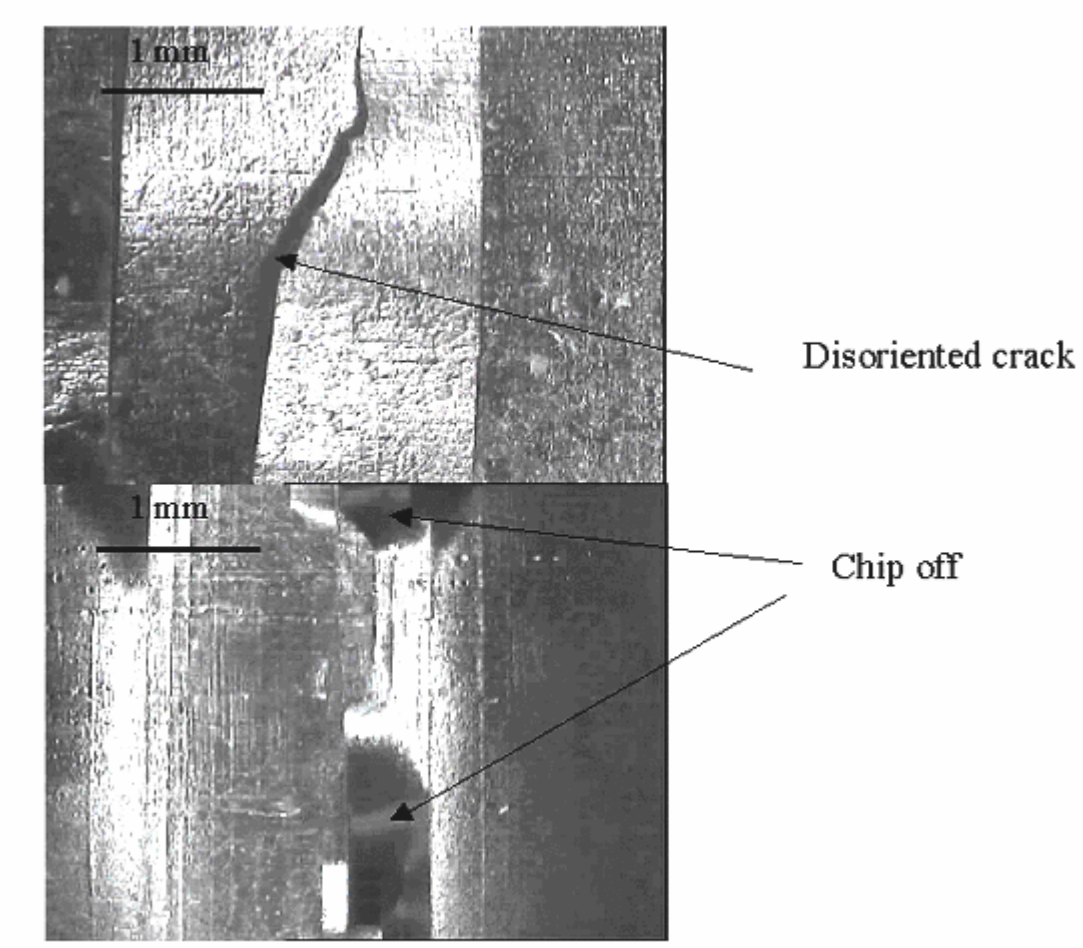

Figure 4.36. Optical micrograph of bending cracks propagated along the specimen width on the surface of a coating with poor adhesive properties.

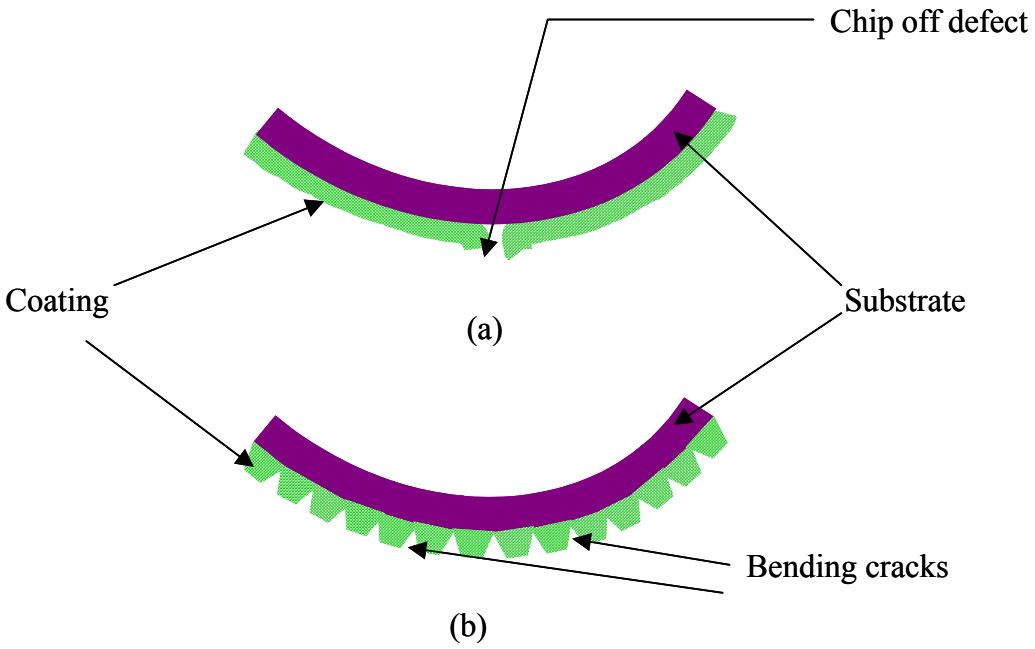

Figure 4.37. Schematic illustration of the deformation of coating during bending tests, (a) coating with poor adhesion properties ; (b) coating with superior adhesion properties .

4.2.2 Fatigue behavior of EN coatings

The fatigue properties of EN coatings were studied by means of the Krouse rotational fatigue test. As was previously mentioned, Section 3.10, controversial results have been reported in explaining the effect of EN coatings on fatigue behavior of the substrate. This is due to the fact that there are several effective parameters involved in studying the fatigue properties of EN coatings. First of all, the sample preparation and the initial substrate surface roughness play a very important role. Secondly, coating conditions including bath type, filtration and agitation system can significantly affect the EN coatings, and various properties including their fatigue behavior. Based on the results presented in section 4.1.2.1, the surface roughness of the coated surfaces before and after EN coatings is generally the same. However, such a desirable outcome depends on various coating parameters including the filtration system. In baths with poor filtration systems, the coated surfaces can be rougher than those of the substrates. This causes a detrimental effect on fatigue properties of the coated specimens. Various superficial defects can lead to initiation and propagation of premature fatigue cracks. Furthermore, the mechanical properties (fatigue behavior) of the substrate play a significant role on the fatigue properties of EN coated specimens. EN coatings are hard and brittle in general and in particular after applying post heat treatment as illustrated in Figure 4.2. Therefore, the fatigue properties of a hard and brittle substrate, similar to the EN coatings can be less affected by the EN coating than that of a soft and ductile substrate. Similar finding were reported in Section 4.2.1 dealing with the adhesion properties of EN coatings. The combination of the mentioned parameters makes the comparison of the results on the effect of EN coatings on fatigue properties of EN coated substrates obtained through several studies difficult.

In this section, the effect of EN coatings on fatigue and tensile properties of carbon steel substrates is presented. The effect of various parameters including coating thickness, post-coating heat treatment, and phosphorus content on fatigue properties of the EN coated specimens was investigated. Furthermore, the effect of EN coatings on the tensile properties and fracture behavior of the low carbon steel substrates has been investigated.

Table 4.17 shows the results of the fatigue test of various types of EN coatings (as-plated and heat treated condition) with different thickness levels. Figure 4.38 shows the effect of various types of EN coatings (40 μ thickness) on the number of the cycles to failure at 448 MPa (65ksi) recorded stress. As shown, in general the EN coated specimens show inferior fatigue behavior compared with the bare specimens. In particular, the heat-treated low phosphorus EN coated specimen has the shortest fatigue life compared with other specimens. This is attributed to the brittle nature of EN coating making it prone to fatigue crack initiation and propagation. Furthermore, as the phosphorus content decreases, the fatigue resistance is reduced. EN coatings with lower phosphorus content are more crystalline, harder, and consequently more brittle compared to high phosphorus EN coatings [Broszeit, 1975 and Taheri et al., 2001]. As a result, failure occurs at a lower number of cycles, Figure 4.39. In addition, as shown in Figure 4.39, heat treatment adversely affects the fatigue properties of an EN coating.

The deleterious effect of heat treatment on the fatigue strength of EN coated specimens is more pronounced when high phosphorus EN coatings are used, as shown in Figure 4.40. As the phosphorus content decreases, the effect of heat treatment on reducing the fatigue resistance of EN coated specimen becomes less pronounced. This is due to the fact that heat treatment has a greater effect on the microstructure and consequently on mechanical property changes of EN coatings, as phosphorus content increases. As-plated high phosphorus EN coating has a softer structure compared with that of low phosphorus coating. However, due to precipitation of various types of nickel-phosphides (during the heat treatment, Figures 4.16 to 4.18) the high phosphorus coating undergoes a more significant phase transformation compared with low phosphorus coating. Thus, the effect of heat treatment on various properties of high phosphorus EN coatings (including the fatigue properties) is more pronounced than that of low and medium phosphorus EN coatings. Similar results were obtained on the effect of heat treatment on CIDV presented in Section 4.2.1

Table 4.17. Number of the cycles undergone by the various EN coated specimens.

Specimens	**Heat treatment**	**Coating thickness (μ)**	**No. of Cycles @ 448 MPa**
Plain	NA	NA	234,833± 8,000
HP	No	40	209,300± 8,000
HP	Yes	40	75,133± 4,000
HP	No	60	146,500± 3,000
HP	Yes	60	59,012± 2,000
HP	No	80	90,400± 5,000
HP	Yes	80	55,167± 3,000
MP	No	40	121,050± 6,000
MP	Yes	40	69,367± 4,000
LP	No	40	72,433± 3,000
LP	Yes	40	51,600± 2,000

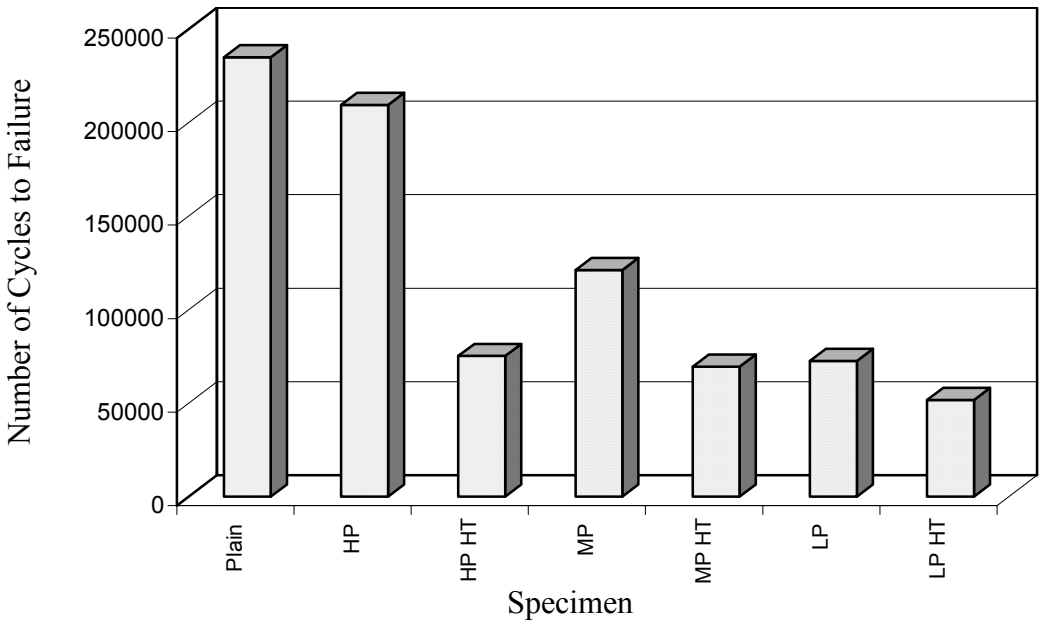

Figure 4.38. Variation of number of cycles to failure for samples of as-plated and heat-treated AISI 1018 steel coated with 40 mm thick EN coatings with different phosphorus content. Stress applied= 65 ksi

Notes: HP= High phosphorus as-plated, HP HT= High phosphorus heat-treated , MP= Medium phosphorus as-plated, MP HT= Medium phosphorus heat-treated , LP= Low phosphorus as-plated, LP HT= Low phosphorus heat-treated

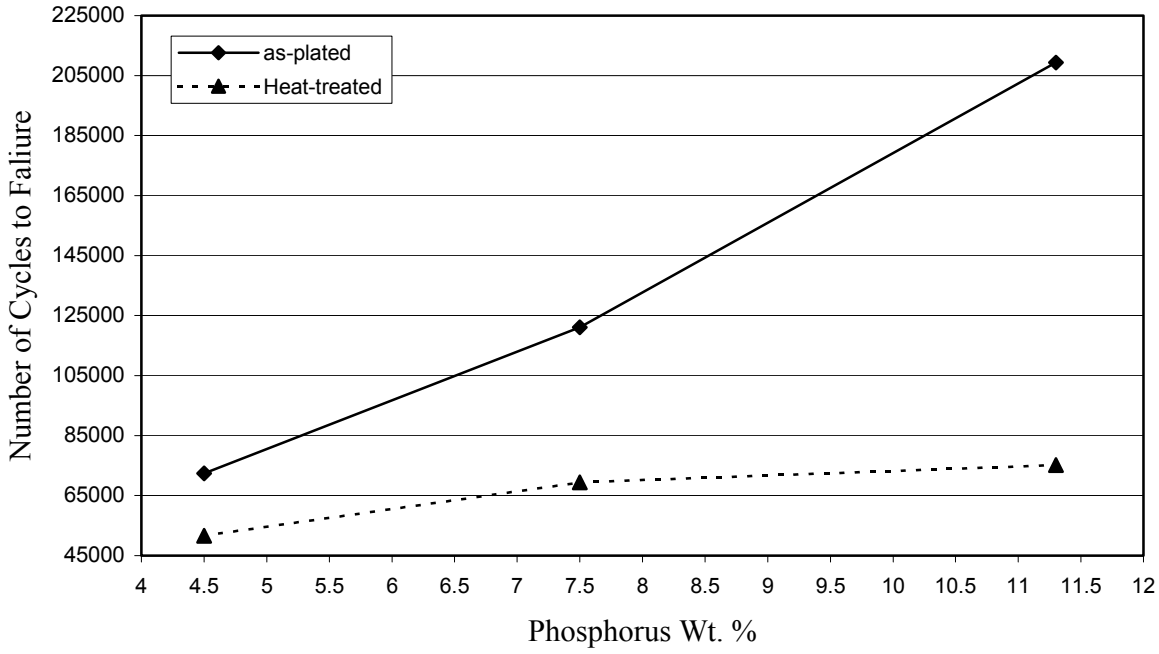

Figure 4.39. Effect of phosphorus content of EN coating (40 μm) on the fatigue properties of EN coated 1018 steel.

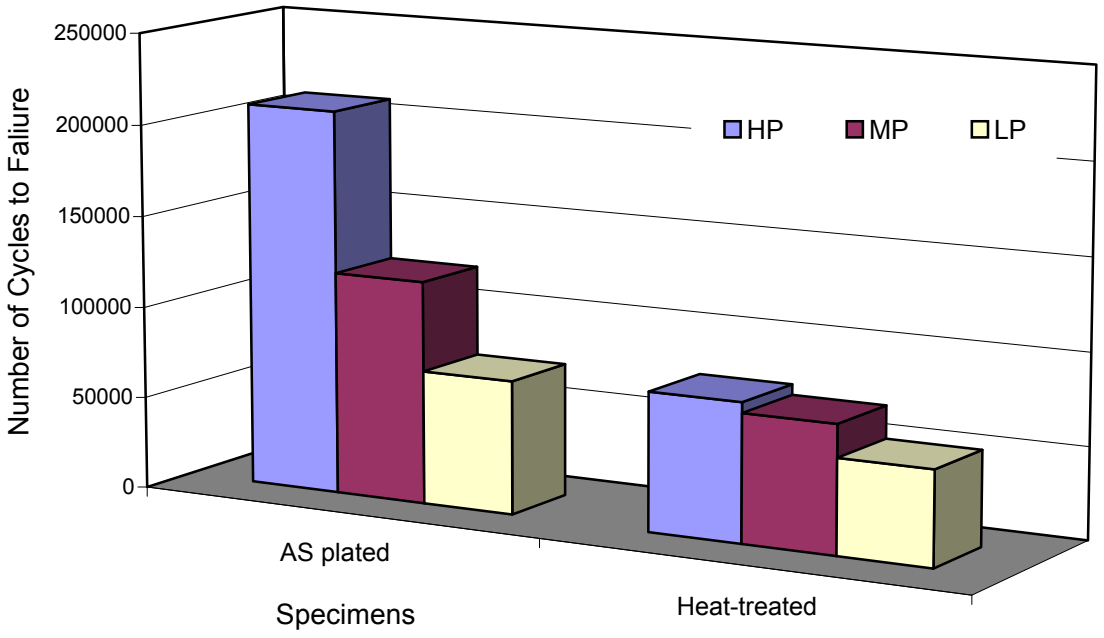

Figure 4.40. Comparison between fatigue properties of as-plated and heat-treated (400^{o} C for one hour) of various types of EN coatings.

Figure 4.41 shows the effect of coating thickness on fatigue properties of high phosphorus EN coating. As shown, by increasing the coating thickness, the fatigue resistance of EN coated specimens drops substantially. This is also due to the effect of coating thickness on coating brittleness. In general, thicker coatings are more brittle and prone to delamination due the layered structure of EN coatings, as shown in Figure 4.28. Due to precipitation hardening during the heat treatment, EN coatings become very brittle, Section 4.1.1. Thus, the effect of thickness on fatigue properties of EN coatings becomes less pronounced. In other words, the brittle nature of heat-treated EN coating undermines the detrimental effect of coating thickness on the fatigue strength of low carbon substrates.

Figure 4.42 shows a fatigue crack which has propagated through the coating-substrate interface without causing any damage to the coating at the coating-substrate interface. As shown, the fatigue crack started on the coating surface and propagated through the substrate. No sign of delamination, chip-off effect, or superficial defects was detected at the coating-substrate interface. Such a finding is a good indication of the superior adhesion of EN coatings. Figure 4.43 shows a schematic illustration of the difference between a coating with superior and poor adhesion during fatigue crack propagation. Figure 4.43a shows that in a coating with superior adhesion properties, the fatigue crack initiated at the coating surface passes through the interface and into the substrate. On the contrary, in a coating with poor adhesion resistance, Figure 4.43b, the fatigue crack travels along the coating-substrate interface and causes separation of the coating and results in a chipped off defect. In such a case, the presence of the coating does not have a significant influence on the fatigue properties of the substrate simply because the propagation of the crack stops at the coating substrate interface.

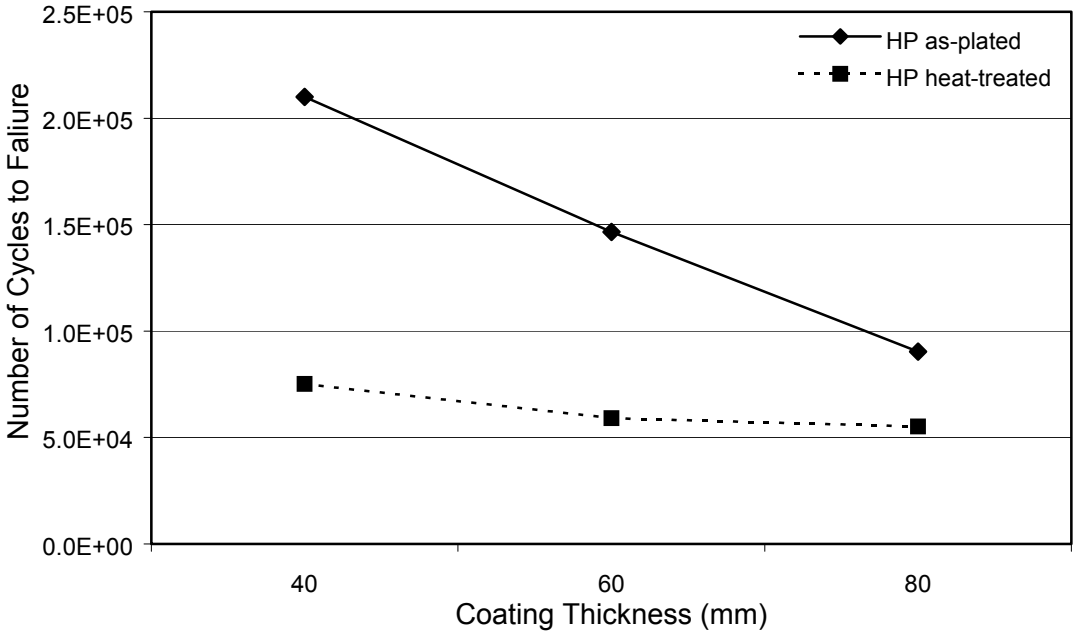

Figure 4.41. Effect of coating thickness on the fatigue properties of AISI 1018 samples coated with high phosphorus EN coatings.

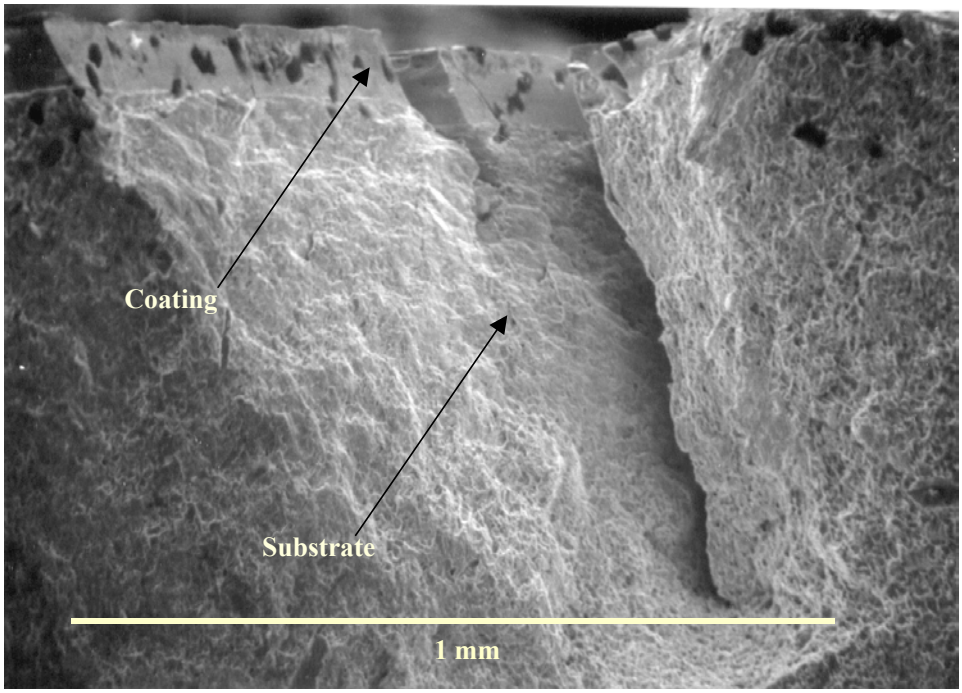

Figure 4.42. SEM micrograph of rupture cross section of fatigue specimen coated with LP HT EN coating

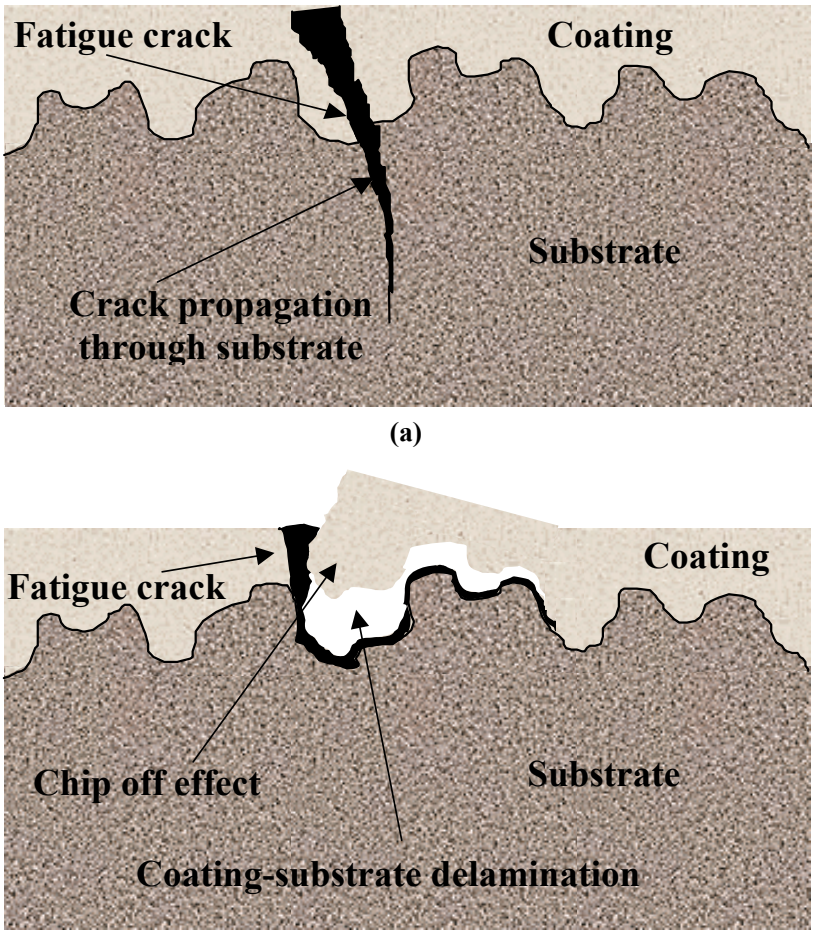

Figure 4.43. (a) Schematic illustration of fatigue behavior of a coating with superior adhesion properties , (b) Schematic illustration fatigue behavior of a coating with poor adhesion properties .

The results obtained show that EN coatings have a deleterious effect on the fatigue properties of the substrate. However, the fact that EN coatings have such a significant effect on the fatigue properties of their substrates is a strong indication of their excellent adhesion to their substrates.

Moreover, the effect of three types of EN coatings, namely low, medium, and high phosphorus, in as-plated and heat-treated, forms on tensile properties of 1018 substrates was studied. Also, the effect of phosphorus content and heat treatment on the fracture behavior of the substrate was investigated. Surprisingly, it was found that although a thin layer of EN coating (10-50 μm which is 1.5 to 8.5 percent of the specimen diameter) had negligible effect on the actual yield or tensile strength of the coated specimen substrates, it had significant effect on the fracture behavior of the low carbon steel substrates during the tensile test. The results obtained showed that EN coatings can alter the fracture behavior of the substrates from a completely ductile (cup and cone) failure, observed in heat-treated un-coated 1018 specimen, to a less ductile failure, sharp 45° angle shaped, which occurred in 50 μm thick low phosphorus heat-treated EN coated specimens, Figure 4.44. This very interesting phenomenon was evidence for the fact that the EN coatings have excellent adhesion to their substrates. The bonding of the coating to the substrate had such a high strength that even at the point of fracture the coating still was completely attached to the substrate. As a result, cracks initiated on the surface of the coating readily propagated through the coating-substrate interface and into the substrate. Thus, it changed the fracture behavior of the substrate. Figure 4.44 shows the comparisons of the fractured cross sections among low, medium, and high phosphorus EN coatings. As shown, the lower the phosphorus content, the more brittle is the manner in which the specimen fails. As a result, the fracture cross section of specimens coated with high phosphorus EN coating did not appear sharp and diagonal, unlike those of low and medium phosphorus coated specimens. Instead, they had a star pattern shape, Figure 4.44d. This may be attributed to the fact that high phosphorus EN coatings are softer and less brittle compared to that of low and medium phosphorus EN coatings.

Figure 4.45 is a SEM micrograph of a fracture cross section. As shown, no sign of delamination or partial loss of bonding was detected at the coating-substrate interface. This observation is in complete agreement with what was previously stated in describing the effect of EN coatings on fatigue behavior of the 1018 substrate.

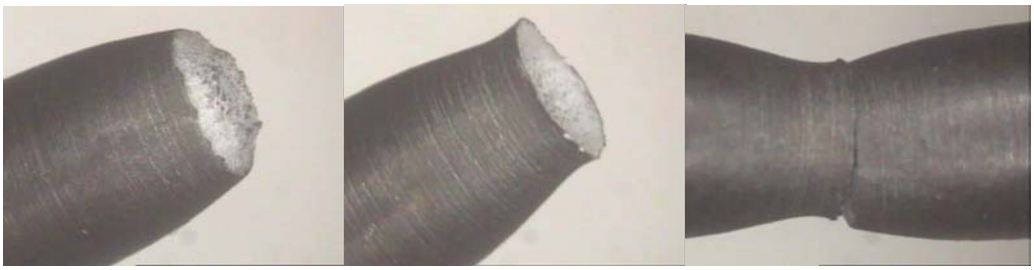

(a)

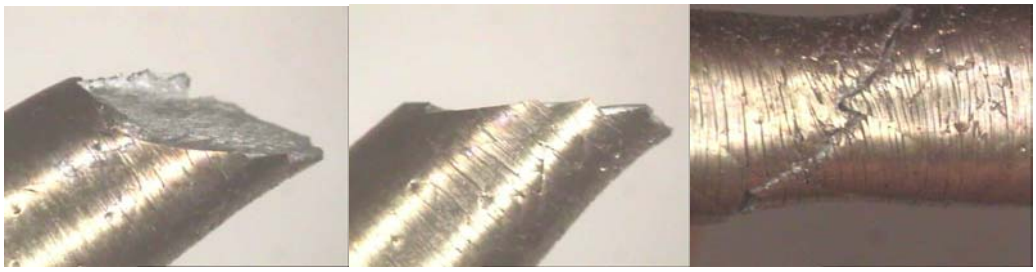

(b)

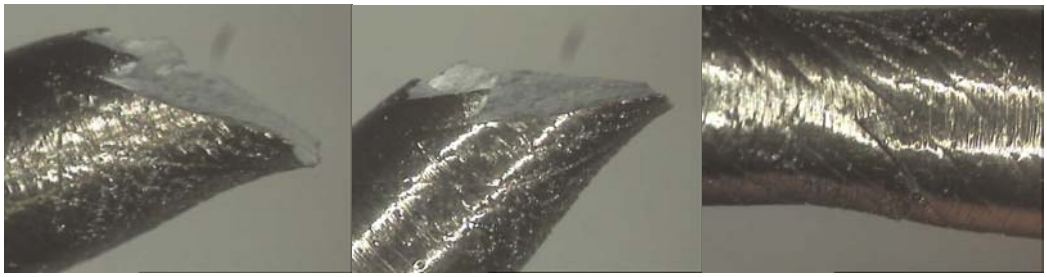

(c)

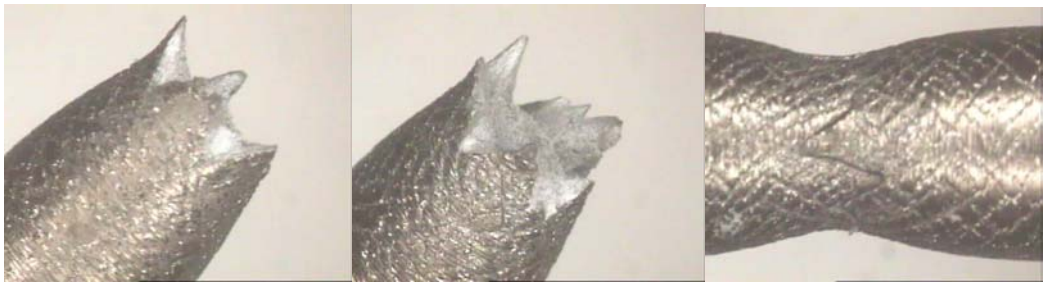

(d)

Figure 4.44. Rupture cross section during after tensile test. (a): 1018 heat-treated un-uncoated sample, (b): heat-treated low phosphorus coated samples (50 μm), (c): heat-treated medium phosphorus coated samples (50 μm), (d): As-plated high phosphorus coated samples (50 μm).

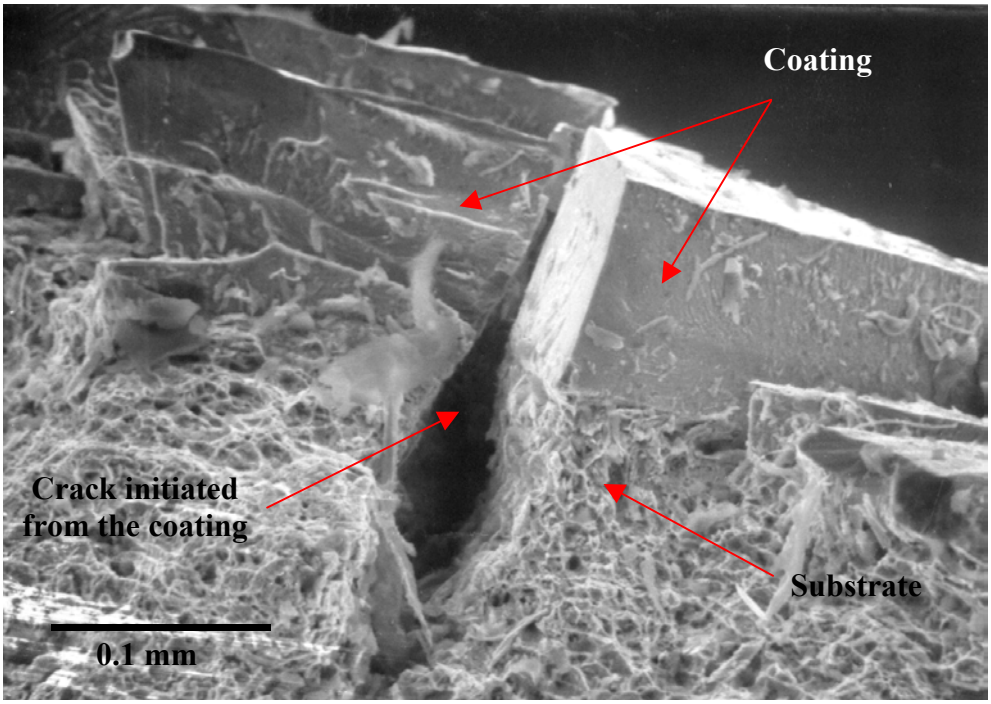

Figure 4.45. SEM micrograph of failure cross section of tensile specimen coated with 50 μm LP HT EN coating.

Figure 4.46 shows the effect of EN coatings on the stress-strain curve. As shown, the heat-treated coated specimens show a less ductile behavior compared with bare specimens. The ductility values are shown by the colored arrows in Figure 4.46. As the tensile stress increases on the surfaces of EN coated specimens and reaches ultimate tensile strength, UTS, of the coating, the tensile crack initiates and propagates through the coating-substrate and into the substrate. In such a case, the tensile crack acts as a stress riser (a notch, Figure 4.45) at the coating-substrate interface causing the substrate to fail in a brittle manner. As a result, the fracture behavior of coated specimens has been significantly affected by the EN coatings. In other words, EN coating has altered the fracture behavior of the 1018 substrate from a completely ductile to a less ductile failure. Such a phenomena can be observed only if a superior adhesion exists at the coating-substrate interface.

Furthermore, the effect of heat treatment on fracture behavior of EN coated specimens is shown in Figure 4.47. As shown, the heat-treated EN coated specimens show less ductility compared with as-plated ones. This is due to the fact that the precipitation of various types of nickel-phosphide particles during heat treatment makes the EN coatings even harder and more brittle.

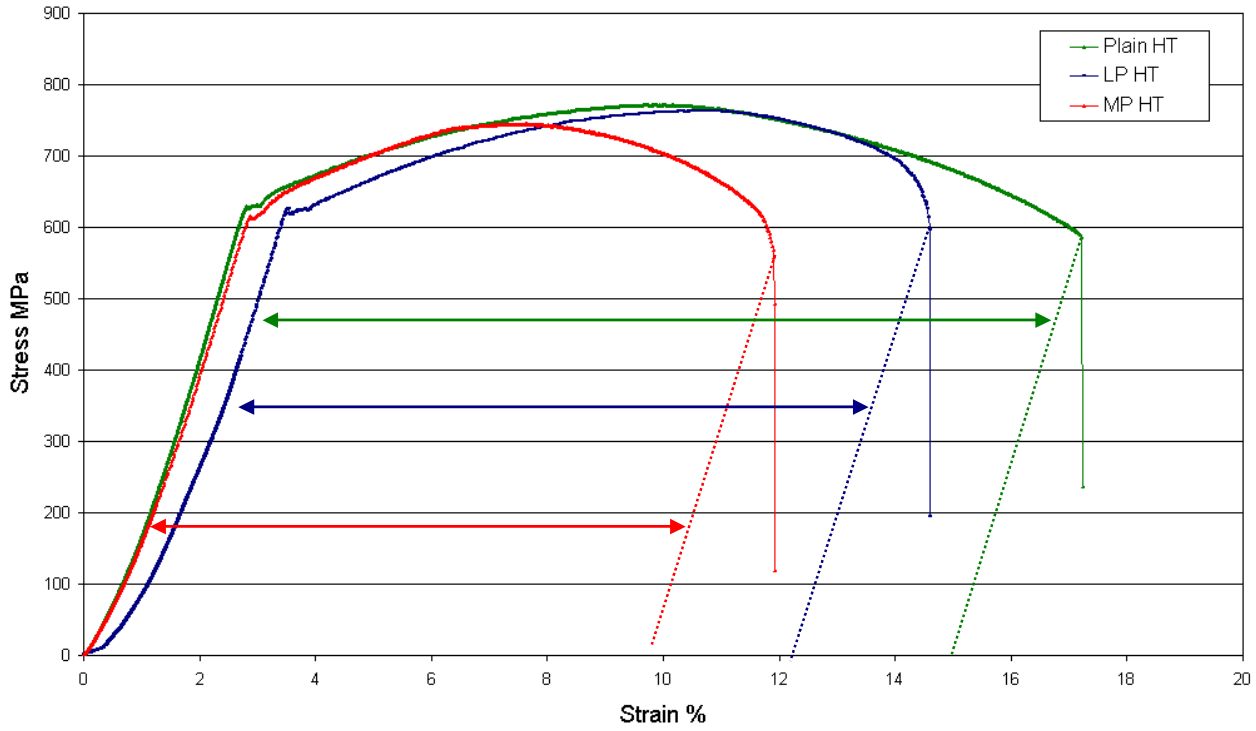

Figure 4.46. Stress-Stain plot for various samples tested.
Notes: Plain HT= Un-coated heat-treated samples, LP HT= 50 µm heat-treated low phosphorus EN coating , MP HT=50 µm heat-treated low phosphorus EN coating.

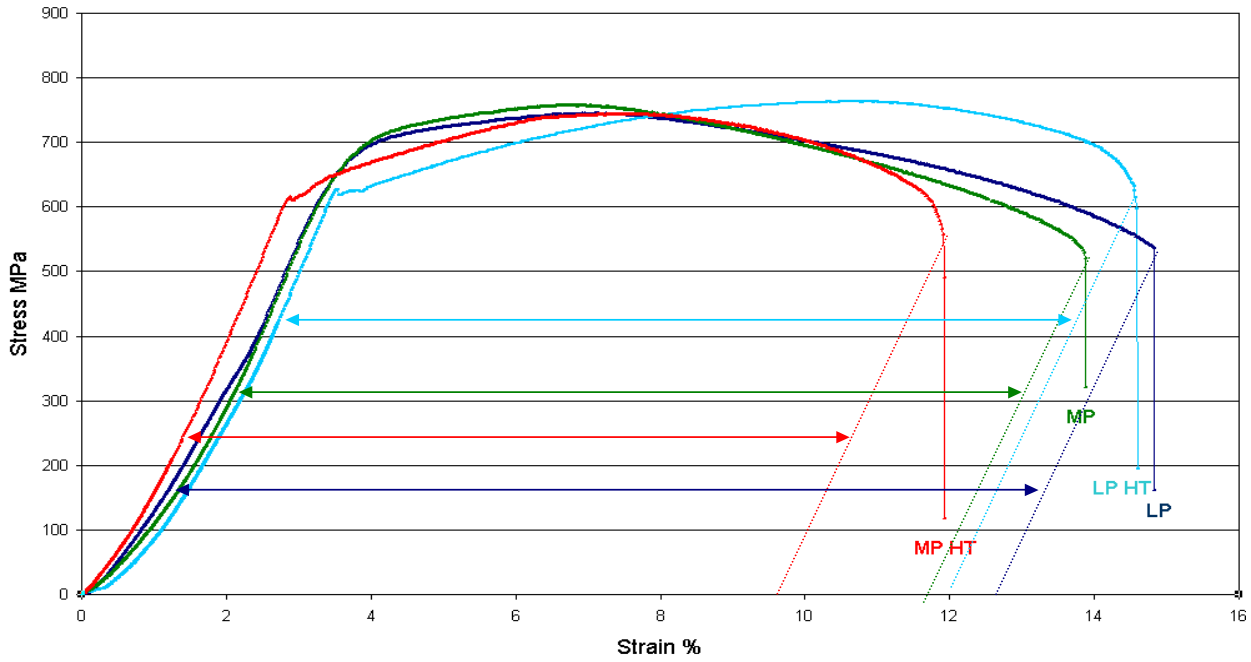

Figure 4.47. Stress-Stain plot for various samples tested.
Notes: LP = 50 µm low phosphorus, LP HT= 50 µm heat-treated low, MP = 50 µm medium phosphorus, MP HT= 50 µm heat-treated medium phosphorus

4.3 Corrosion and Wear (C&W) Evaluation

EN coatings are hard and corrosion resistant. The combination of these two characteristics makes EN coatings excellent candidate materials for applications where severe corrosion and wear elements exist. A good example of such a harsh environment can be found in various processes in the potash industry. Therefore, as a part of this study the corrosion and wear resistance of three types of EN coatings in a potash environment was studied. A reciprocating C&W experiment was conducted to study the corrosion and wear resistance of EN coatings under severe wear conditions. The depth and area of the wear scars were measured periodically. Furthermore, erosion-corrosion experiments were conducted in the potash brine at the Potash Corporation of Saskatchewan (PCS) pilot plant for a period of several weeks.

4.3.1 Reciprocating corrosion and wear testing

The experimental details are outlined in Section 3.12.2. Table 4.18 and Table 4.19 show the variation of wear scar areas and depths during the reciprocating C&W experiment. Figure 4.48 shows the variation of wear scar area with number of the cycles. As shown, during the first 30000 cycles there is a linear increasing trend (with sharp slope) in scar areas. This is due to the excessive stress developed by the small contact area between the indenter (ball) and specimen surface at the beginning of the experiment. After the stage of high stress regime, the contact area increases, due to the ball wear, resulting in a decrease in the contact stress. As a consequence, the slope of the scar area versus number of cycles curve is reduced. In general, the heat-treated EN coatings showed better wear resistance. Heat-treated EN coatings are harder due to the precipitation of various nickel phosphide particles. The same conclusion can be obtained in analyzing the results of depth measurement, Figure 4.49. As seen, heat-treated EN coatings showed better wear resistance in terms of the depth of the wear scars.

Among the six EN coated specimens, the high phosphorus as-plated EN coated specimen was the only one that failed after 15000 cycles (the coating was damaged at the center of the wear scar and the substrate became visible), Figure 4.50. However,

as shown in Figure 4.50, the failure was caused by excessive wear not localized chip off, unlike commercially EN coated surfaces, an example of which is shown in Figure 4.51. This showed the superior adhesion resistance of EN coated specimens at the University of Saskatchewan in comparison with a commercially made counterpart.

Table 4.18. Scar area for different types of EN coatings at various numbers of cycles.

	Scar Area (mm^2) at the numbers of cycles						
Type of Coating	15000	30000	45000	60000	90000	180000	540000
HP	75.903	-	-	-	-	-	-
HP HT	17.386	37.003	38.419	-	42.862	61.416	84.883
MP	34.614	44.111	46.732	61.189	68.654		
MP HT	26.715	40.421	41.442	-	53.922	70.512	80.060
LP	42.034	49.577	60.624	-	71.356	75.546	90.798
LP HT	41.184	47.850	57.141	-	72.805	78.568	80.510

Standard deviation of the readings ranged between 2 to 4 (< ± 5% of the read values)

Table 4.19. Scar depth for different types of EN coatings at various numbers of cycles.

	Scar depth (μ)at the numbers of cycles						
Type of Coating	15000	30000	45000	60000	90000	180000	540000
HP	125						
HP HT	4	6	7	-	8	10	30
MP	20	38	42	47	53		
MP HT	5	7	8		10	13	34
LP	9	16	20		26	29	58
LP HT	8	15	17		25	28	54

Standard deviation of the readings ranged between 1 to 5 (< ± 8% of the read values)

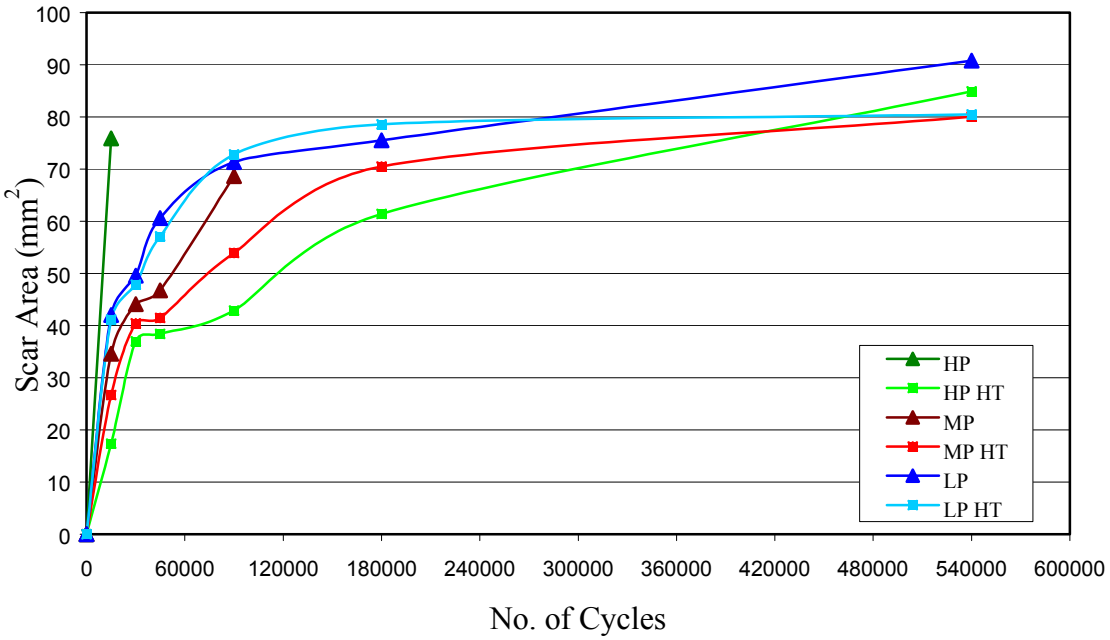

Figure 4.48. Variation of scar areas vs. number of cycles during the C&W experiment.

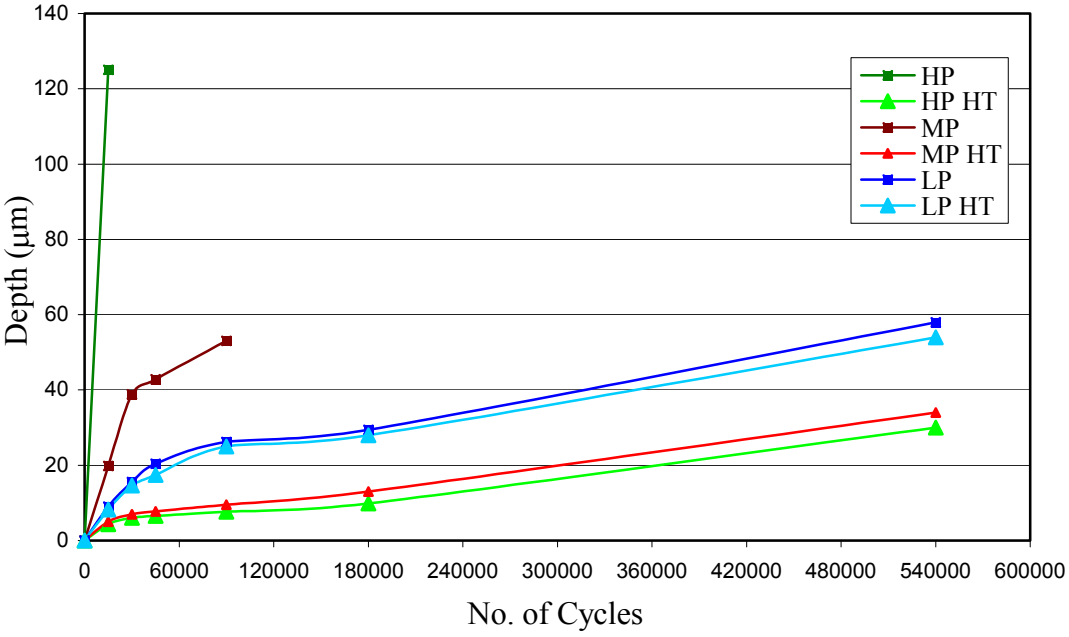

Figure 4.49. Variation of scar depth vs. number of cycles during the C&W experiment.

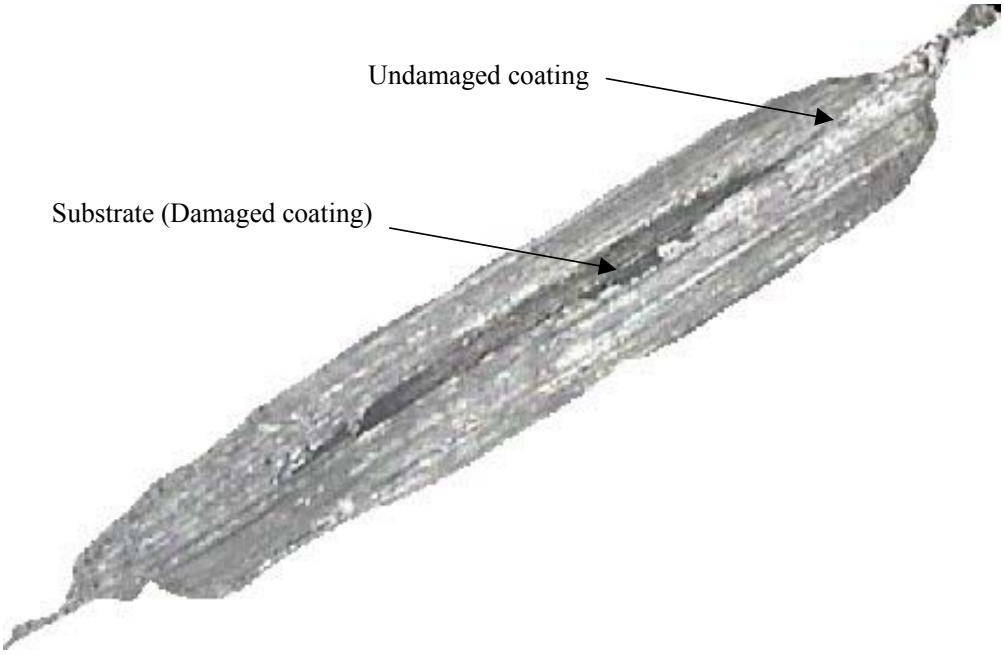

Figure 4.50. High-phosphorus EN coated specimens after 15000 cycles.

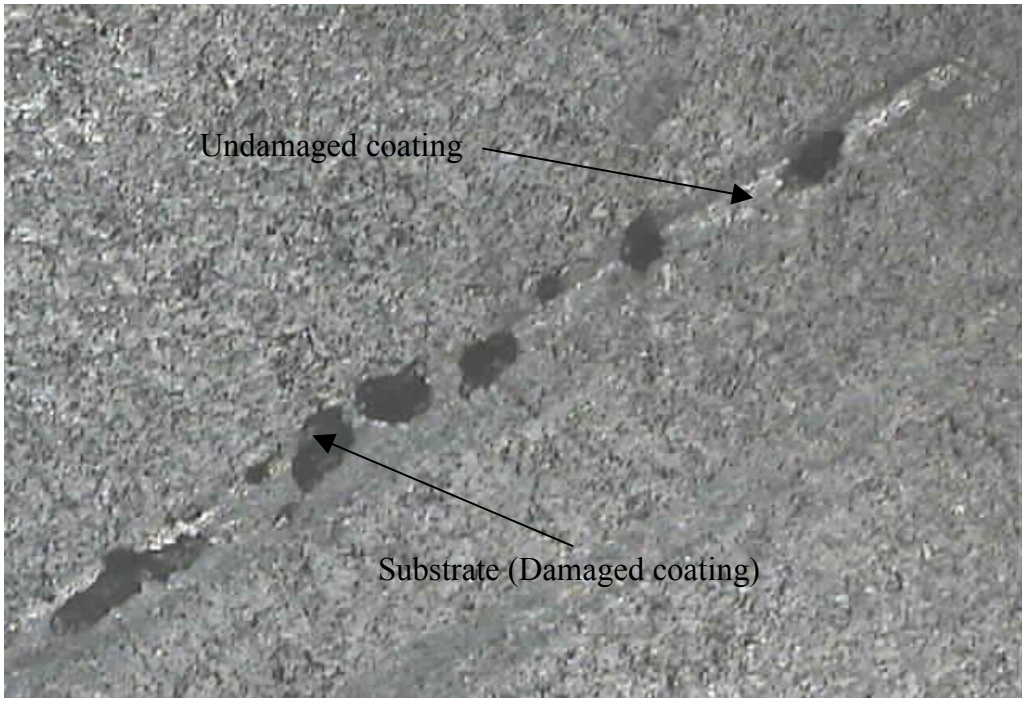

Figure 4.51. Commercially EN coated.

Figures 4.52 through 4.54 show the progression of the wear scar during the reciprocating C&W experiment. As seen, heat-treated specimens showed better corrosion and wear resistance compared with as-plated ones. This is directly related to the effect of heat treatment on the hardness of EN coatings.

In order to compare the C&W resistance of EN coatings with that of high corrosion resistant alloys, reciprocating experiments were conducted on various alloys. Although a complete discussion of the results obtained is the topic of another broad study, a simple comparison between the corrosion and wear resistance of the EN coatings and that of some other superior alloys can be beneficial. Figure 4.55 shows a comparison among wear scars of Hastaloy C, titanium grade 7, Inconel, and high-phosphorus heat-treated EN coating. As indicated by scar size, the high-phosphorus heat-treated EN coating showed far superior resistance compared with other test materials.

The results obtained in this segment of EN evaluation showed that EN coatings in general and high phosphorus heat-treated in particular are highly wear resistant. As a result, EN coatings can be excellent candidates for materials working under severe corrosion and wear conditions.

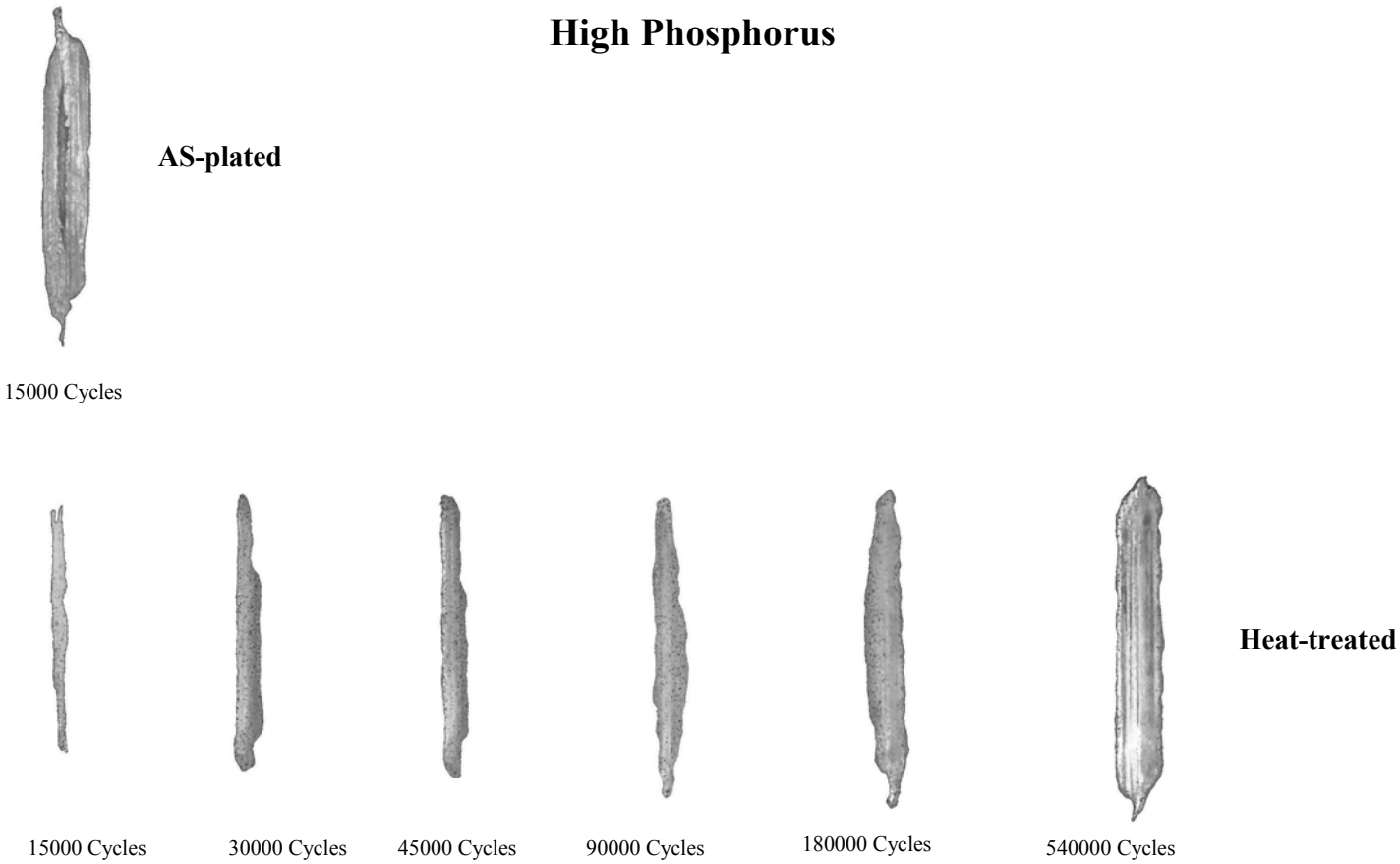

Figure 4.52. Photograph of the progressive wear scars of the high-phosphorus EN coated specimens.

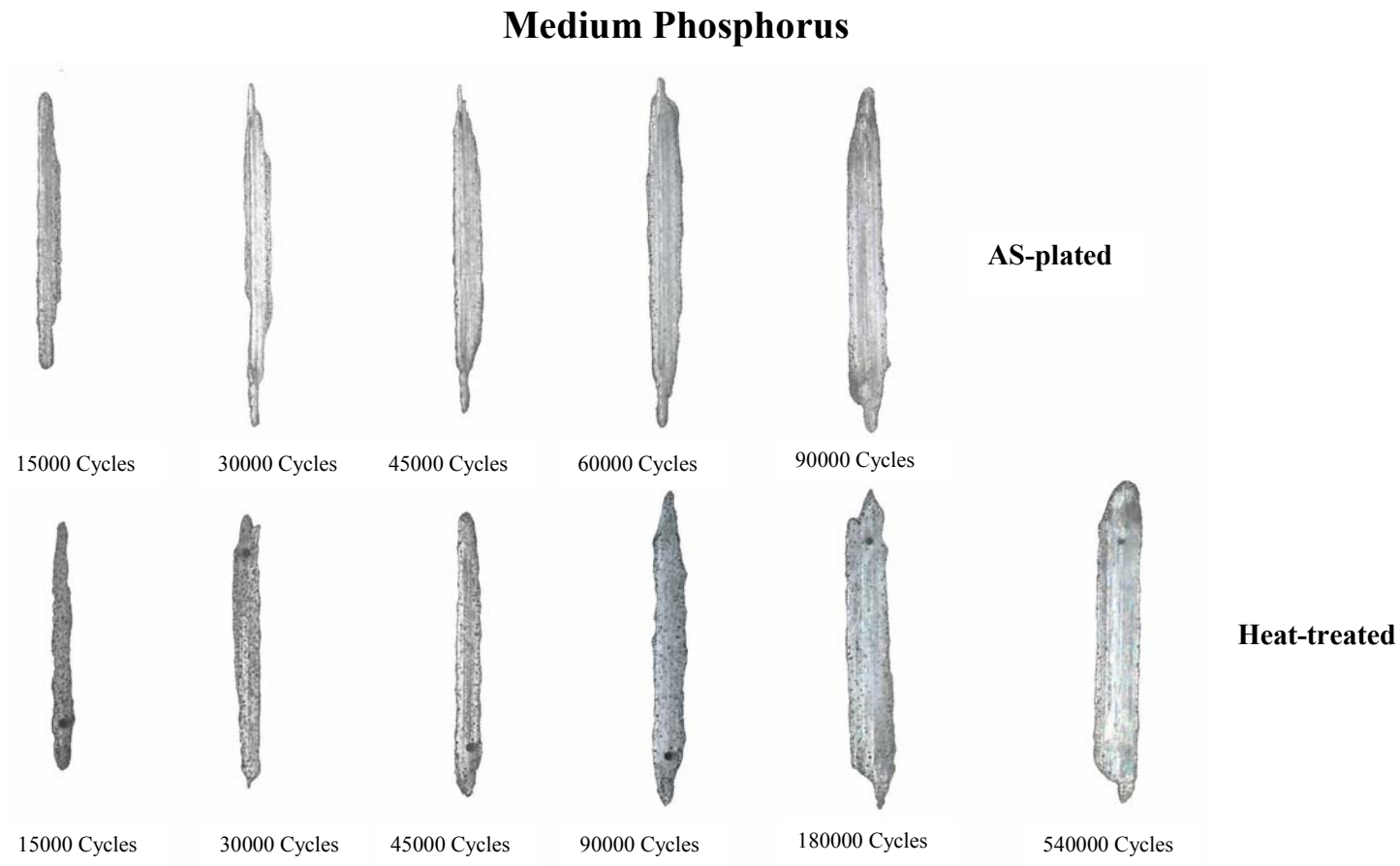

Figure 4.53. Photograph of the progressive wear scars of the medium-phosphorus EN coated specimens.

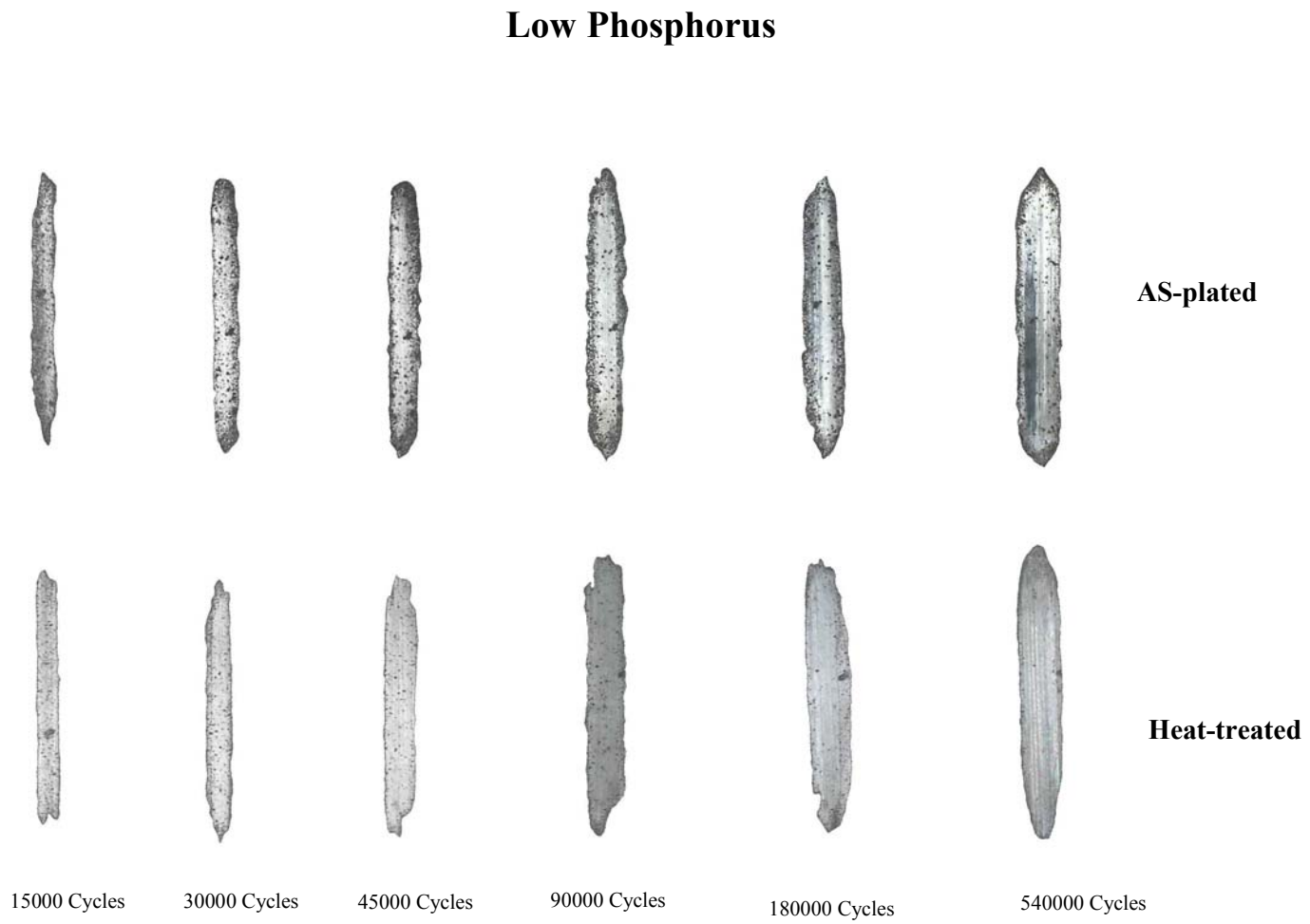

Figure 4.54. Photograph of the progressive wear scars of the low-phosphorus EN coated specimens.

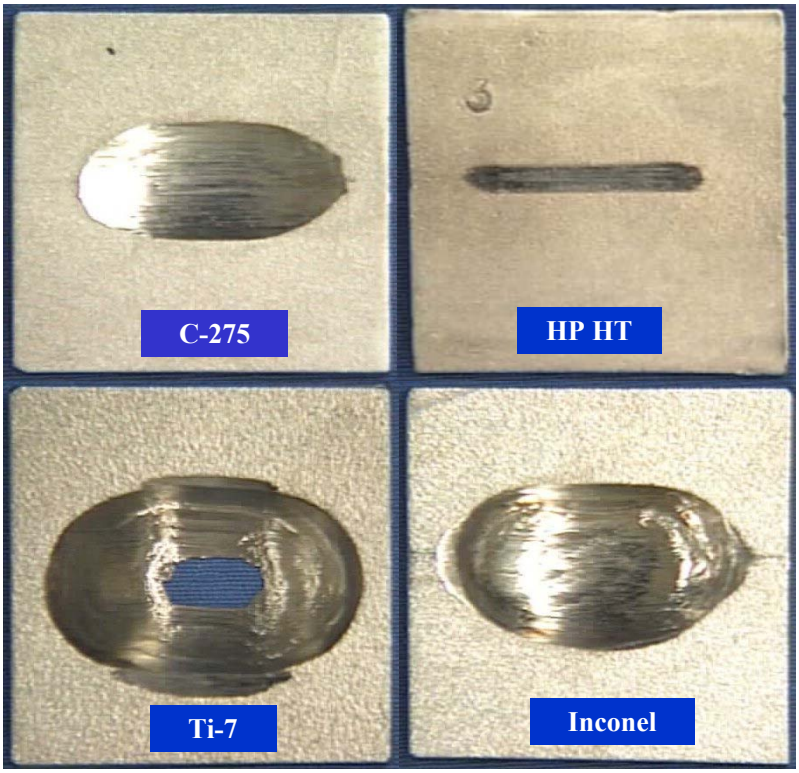

Figure 4.55. Photograph of scars on various specimens after reciprocating C&W test for 540000 cycles .

4.3.2 Erosion-corrosion Evaluation

Although the reciprocating corrosion and wear experiment revealed valuable information about the corrosion wear behavior of EN coatings it does not represent an actual simulation of the working environment in the potash industry. As a result, the erosion-corrosion experiment was conducted in order to evaluate the erosion and corrosion behavior of EN coatings in a simulated potash slurry environment.

The test was conducted in 4 periods of 240 hours. In order to detect any superficial defects after each period of the experiment, the surfaces of the coated specimens were inspected using an optical microscope at 50X magnification. After the fourth run, for a total of 960 hours of exposure, the Ferroxyl test, described in Section 3.12.3, was conducted on the exposed surface to detect the presence of any microcracks or pits.

Figure 4.56 shows the surface of high-phosphorus as-plated EN coated specimen exposed after each period of run. As shown, there is no indication of any superficial defects including delamination, pits, cracks, or chip off. Also, Figure 4.57 shows the results of the ferroxyl test. As shown, there is no sign of any superficial damage on the coating since no blue spots were revealed. A similar conclusion can be obtained for all other EN coatings tested, namely, high-phosphorus heat-treated, medium phosphorus as-plated, and low phosphorus heat-treated, Figure 4.58, 4.60, and 4.62. Also, Figure 4.59, 4.61, and 4.63 show the ferroxyl test results for various EN coated specimens. As shown in the latter figures, no sign of failure was detected after the ferroxyl test. Figure 4.62 shows the exposed surface of a low-phosphorus heat-treated EN coating. The large pit was caused by mechanical damage to the surface of the coating prior to exposure (the last photograph from left on the first row is distinguished with a red circle). However, study of the pit after each period of the slurry experiment indicated that the pit was growing in a circular manner rather than an irregular shape. Also, the fact that no superficial damage was detected around the circumference of the pit evidenced the superior adhesion of these EN coatings.

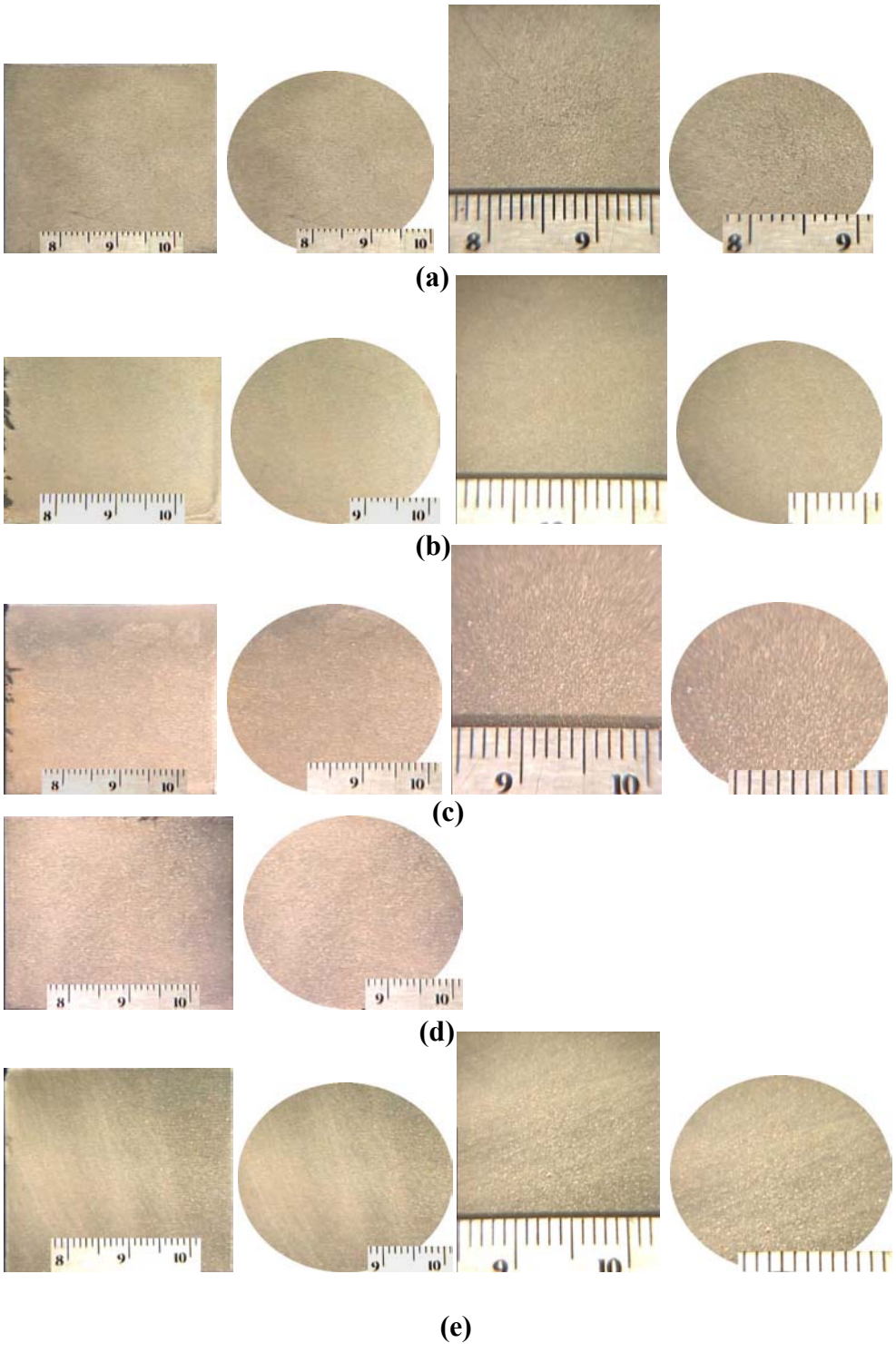

Figure 4.56. Photographs of as–plated high-phosphorus EN coating before and after slurry experiment. (a) before, (b) 240 hr, (c) 480 hr, (d) 720 hr, and (e) 960 hr.

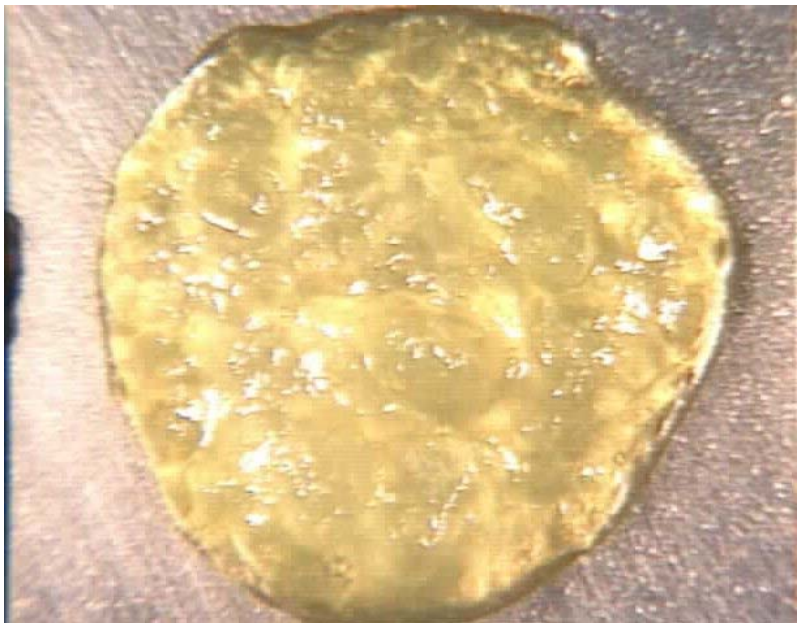

(a)

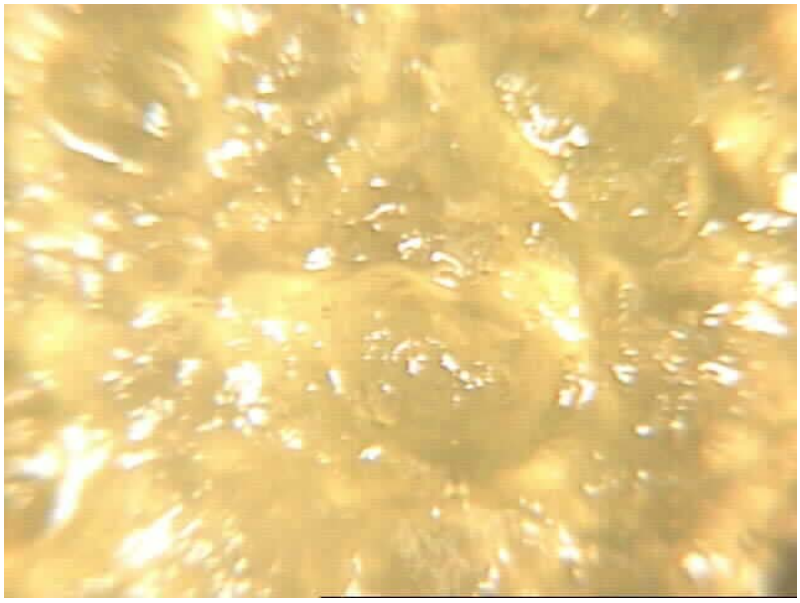

(b)

Figure 4.57. Photograph of ferroxyl result of high Phosphorus as-plated EN coated specimens after slurry experiment. (a) 5 X, (b) 20 X.

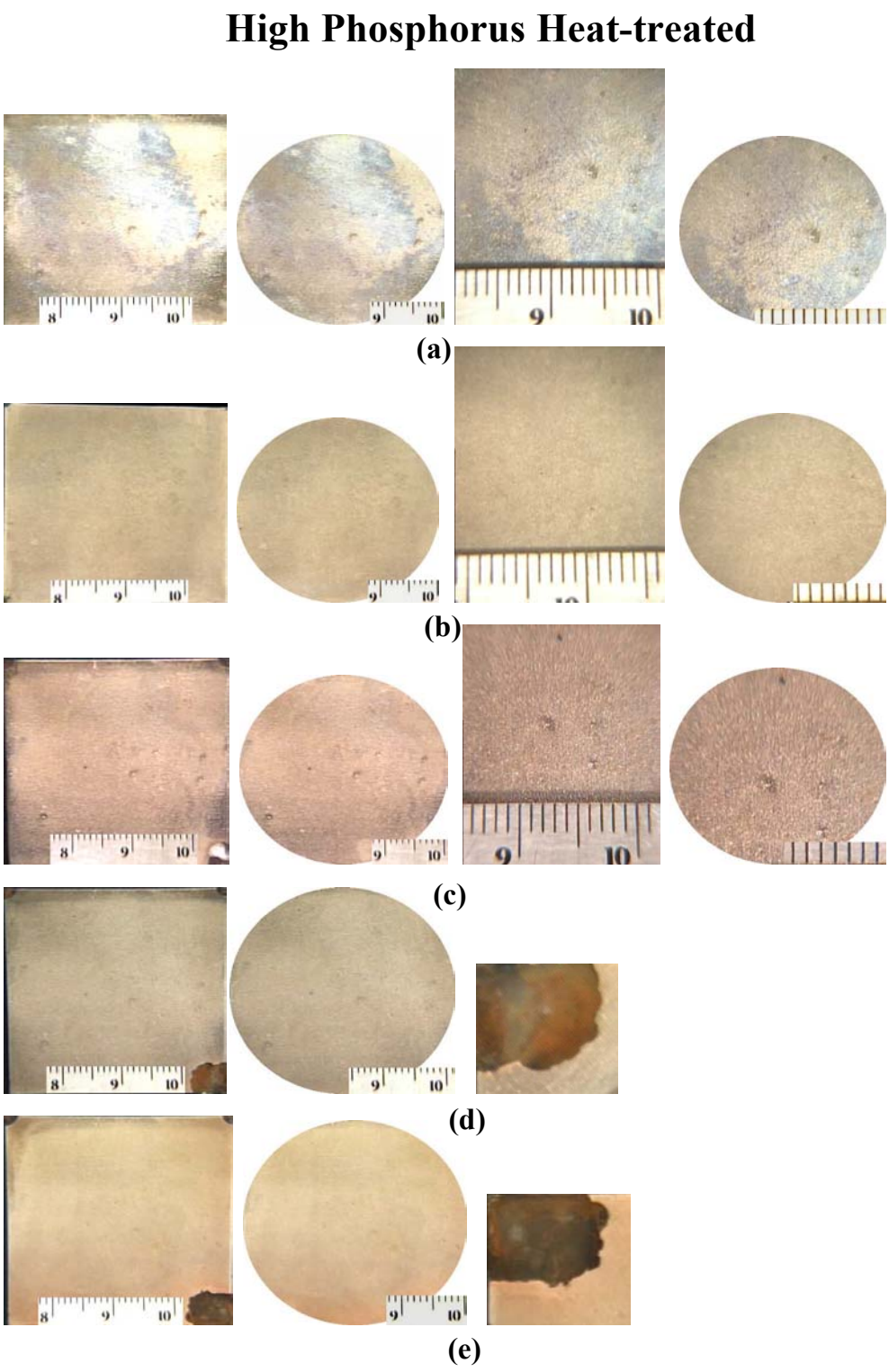

Figure 4.58. Photographs of heat-treated high-phosphorus EN coating before and after slurry experiment. (a) before, (b) 240 hr, (c) 480 hr, (d) 720 hr, and (e) 960 hr.

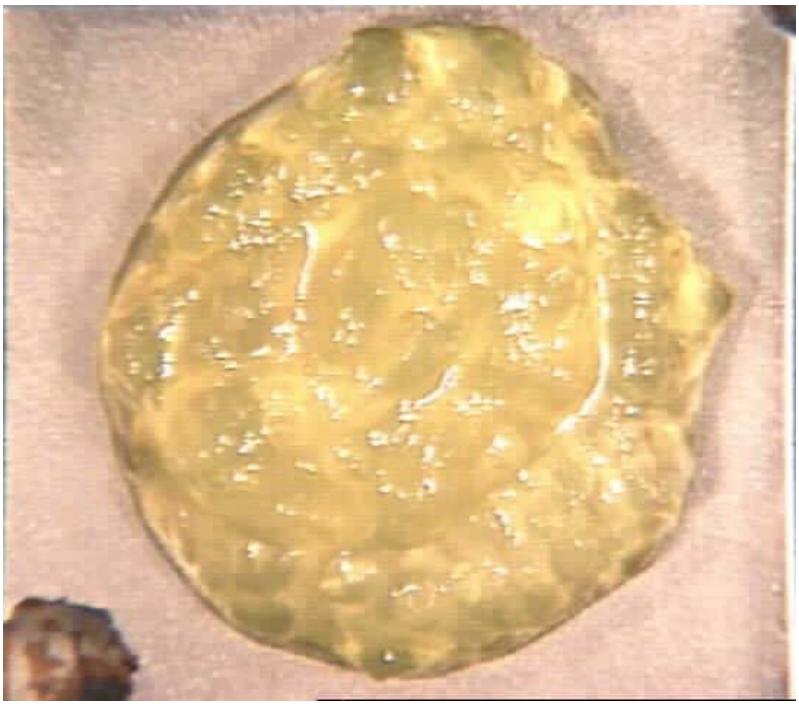

(a)

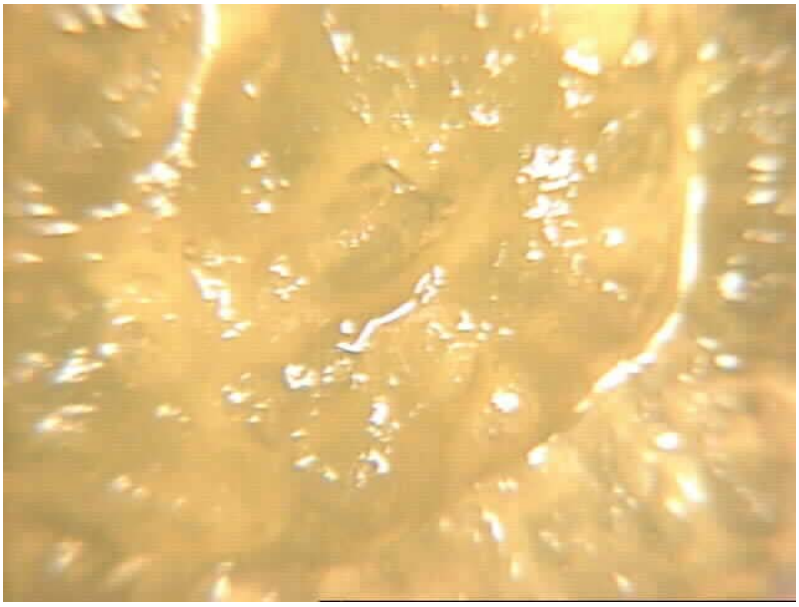

(b)

Figure 4.59. Photograph of ferroxyl result of high phosphorus heat-treated EN coated specimens after slurry experiment. (a) 5 X, (b) 20 X.

Medium Phosphorus As-plated

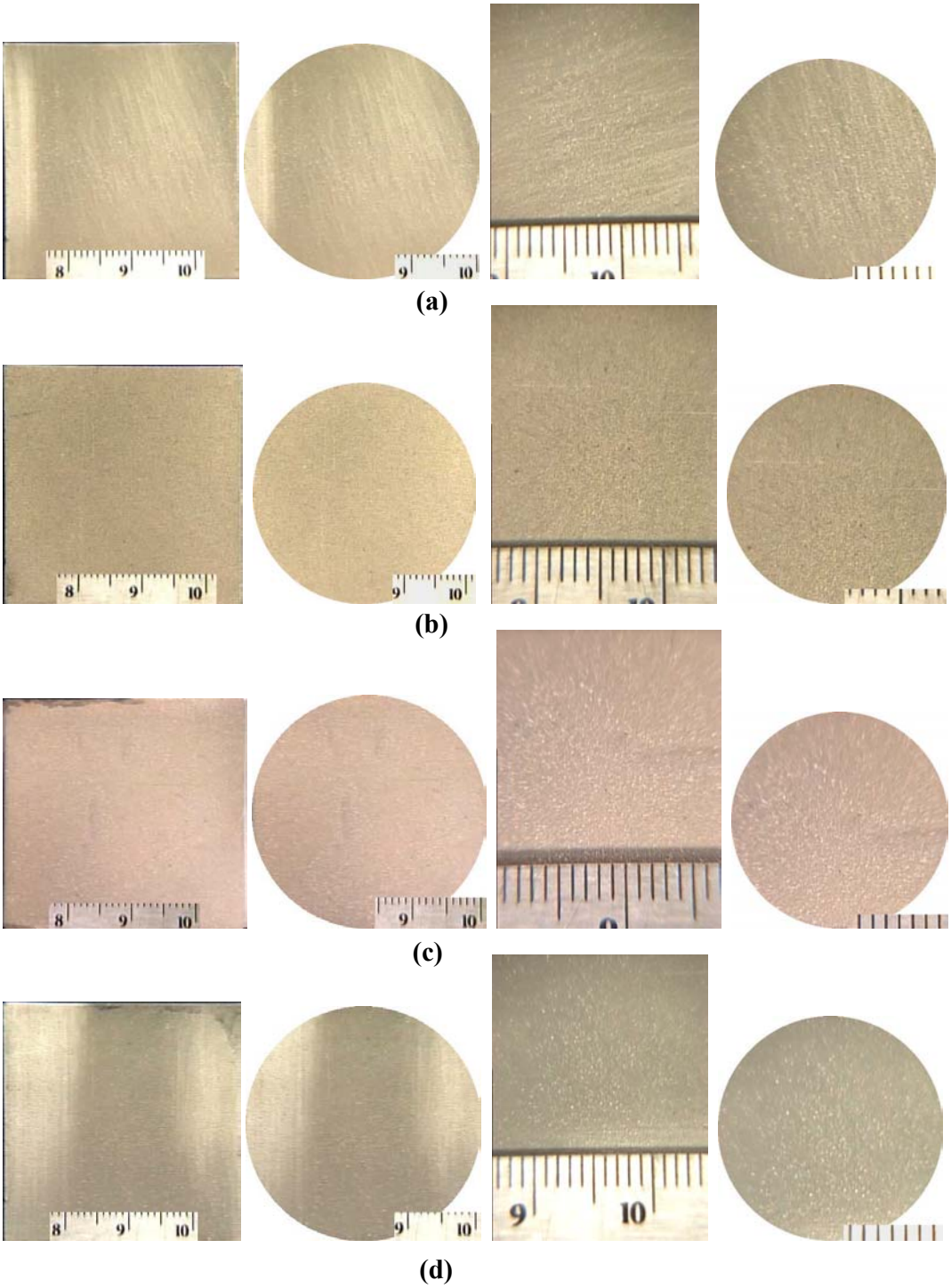

Figure 4.60. Photographs of as–plated medium-phosphorus EN coating before and after slurry experiment. (a) before, (b) 240 hr, (c) 480 hr, and (d) 720 hr.

(a)

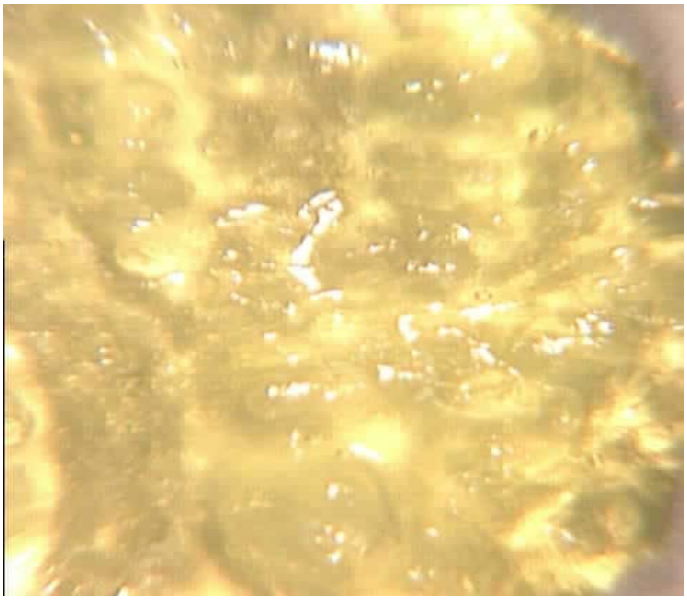

(b)

Figure 4.61. Photograph of ferroxyl result of medium phosphorus as-plated EN coated specimens after slurry experiment. (a) 5 X, (b) 20 X.

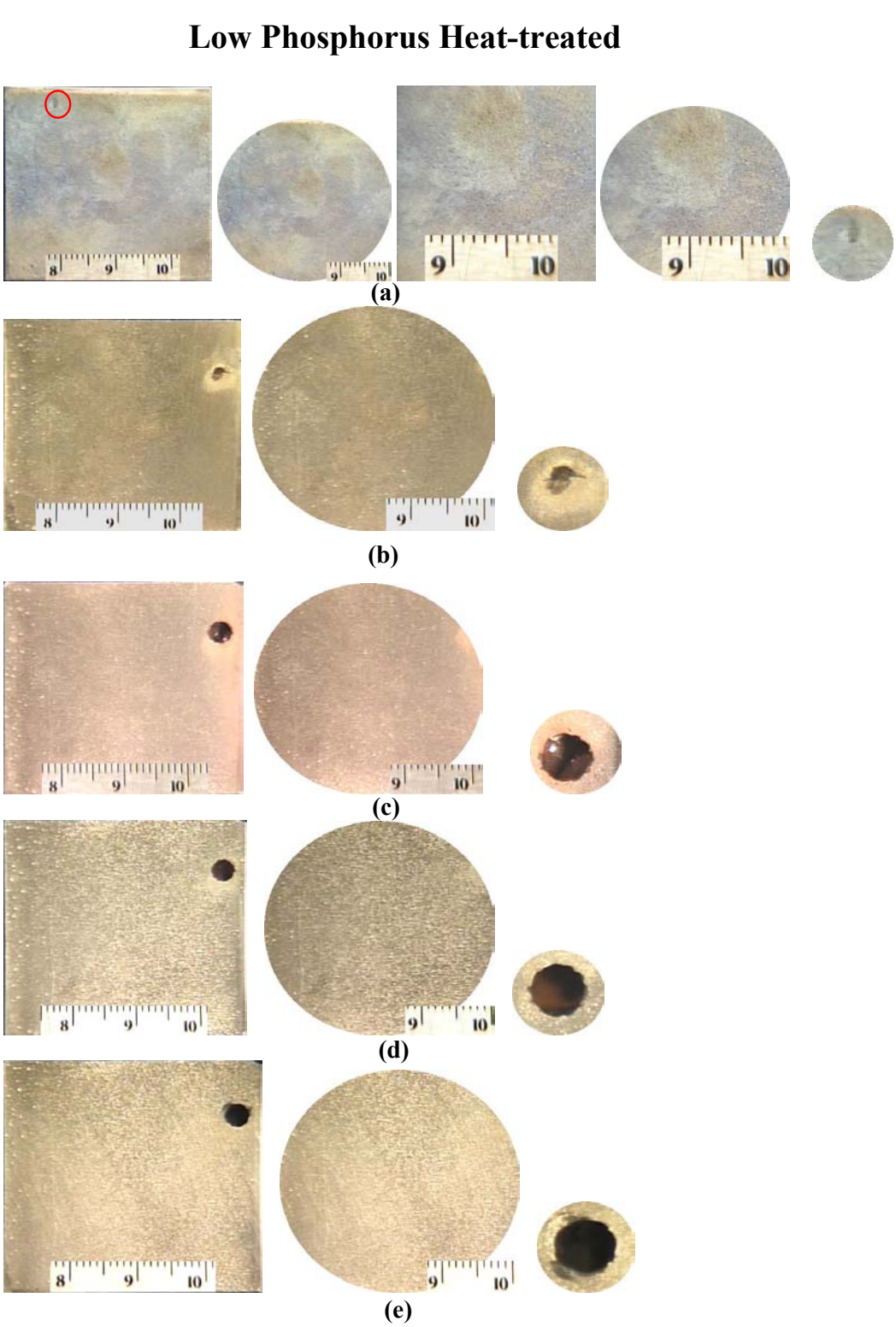

Figure 4.62. Photographs of heat-treated low-phosphorus EN coating before after slurry experiment. (a) before, (b) 240 hr, (c) 480 hr, (b) 720 hr, and (e) 960 hr.

(a)

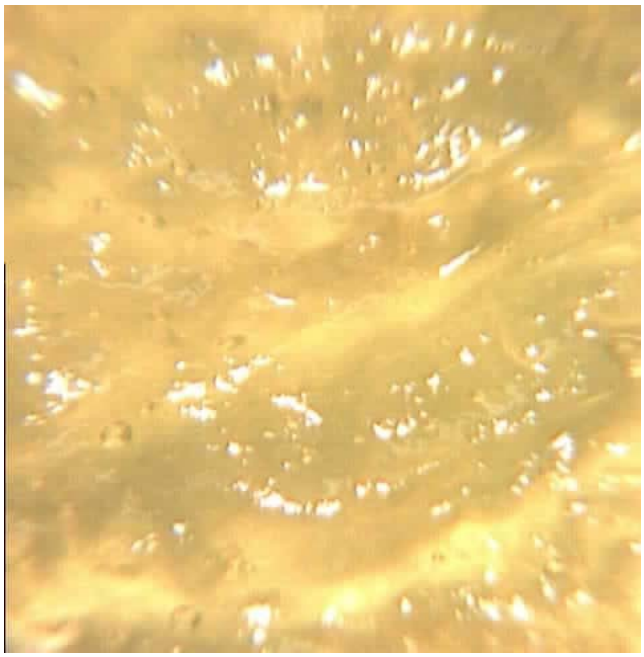

(b)

Figure 4.63. Photograph of ferroxyl result of high phosphorus heat-treated EN coated specimens after slurry experiment. (a) 5 X, (b) 20 X.

The results of these slurry experiments showed that EN coatings have excellent erosion-corrosion resistance even in severe environments. Therefore, EN coating in general, and heat-treated high phosphorus EN coating in particular, are excellent candidates where significantly high wear resistance at high temperature (around 100 °C) is the main criterion.

4.4 Summary

In this chapter, the results obtained from the evaluation of the various properties of three types of EN coatings; namely, low, medium, and high phosphorus, are presented. The evaluations were conducted in five different areas; physical, tribology, mechanical, corrosion and wear, and microscopic examination.

In evaluating the physical properties of EN coatings, the effect of heat treatment on hardness was studied. Changes in physical properties of EN coatings during heat treatment were due to the precipitation of various nickel phosphide particles. Furthermore, the effect of various parameters such as phosphorus content, time and temperature of the heat treatment process were investigated. Various qualitative and quantitative techniques such as microhardness, DSC, X-ray elemental analysis, and X-ray powder diffraction were employed to conduct this segment of the study. Furthermore, in evaluating the physical properties of EN coatings their tribological behavior (surface roughness and coefficient of friction) was investigated. The results of the latter study showed that unlike conventional electroplating, EN coatings completely follow the surface profile of the substrates. Also, it was found that EN coated samples exhibit a lower coefficient of friction compared to that of a bare substrate. This characteristic of EN coatings is very important when rough metallic surfaces are subjected to excessive sliding wear.

In evaluating mechanical properties of EN coatings, bending, adhesion, fatigue, and tensile behavior of EN coatings were investigated. It was shown that EN coatings, in general, significantly change the mechanical behavior of their substrates. The adhesion properties of EN coatings were studied using three-point bending testing. In general, EN coatings have excellent adhesion characteristics. Moreover, it was shown that the adhesion of EN coatings was a function of many variables including phosphorus content, heat treatment process, thickness, and the properties of the substrates. In terms of fatigue behavior, it was found that EN coatings had a detrimental effect on the fatigue behavior of the 1018 substrate. This was attributed to the brittle nature of EN coatings. The effect of various coating parameters, including

phosphorus content, heat treatment and coating thickness on fatigue behavior of 1018 coated specimens was investigated. Finally, the effect of EN coatings on tensile fracture behavior of 1018 substrate was studied. It was found that EN coatings (even a very low thickness, 10 to 50 μ) altered the fracture behavior of the 1018 coated specimens from a ductile failure to a brittle failure.

The study of the corrosion-wear properties of EN coatings was conducted by means of reciprocating wear experiments. It was shown that EN coatings, in general, had excellent corrosion and wear resistance under severe wear conditions. Furthermore, the results of erosion-corrosion experiments showed that EN coatings had superior erosion-corrosion resistance at a high temperature, 100°C, in a potash brine environment.

5 Conclusions, Recommendations, and Future Work

In this chapter, the conclusions obtained as a result of a comprehensive evaluation conducted on EN coatings are briefly discussed. The conclusions are presented in the same sequence as introduced in Chapters Three and Four. Also, based on the study conducted, several recommendations are made in order to improve the quality and performance of EN coatings. As a continuation of this study, suggestions for future work are also presented in this chapter.

5.1 Conclusions

5.1.1 Physical evaluation

1. Heat treatment at 300-400°C for one hour significantly affects various properties of EN coatings. For example, the hardness of EN coatings can be increased up to 60% after heat treatment at 400^{o}C for one hour. As a result, the heat treatment temperature, rather than the pH of the coating solution, is the dominant factor in determining the final deposit hardness.

2. The results of the DSC study showed that the crystallization of EN deposits is kinetically controlled. In other words, the precipitation of various types of nickel phosphide particles during heat treatment is a time-temperature controlled process. Also, the results obtained through TEM and X-ray diffraction investigation agreed with the DCS results showing the precipitation of various nickel phosphide particles during the heat treatment

3. The surface profile study of EN coatings showed that unlike electroplating (EP), EN coatings follow the substrate surface profile rather than just filling up the spaces between surface asperities. Furthermore, it was found that at a constant substrate roughness, the surface roughness of EN coatings is independent of coating thickness.

4. The results of the tribological study on the EN coatings showed that these coatings lower (up to 15%) the kinetic coefficient of friction of their substrate, irrespective of their heat treatment condition. As a result, EN coatings can significantly improve the dry wear resistance of their substrate.

5.1.2 Mechanical evaluation

1. The results of the three-point bending experiment showed that EN coatings have excellent adhesion properties. Also, the study on the parameters affecting the adhesion properties of EN coatings showed that due to their layered structure, increasing the EN coating thickness causes bending cracks to appear at lower deflection values during the three-point bending test. This effect was more pronounced for high phosphorus EN coatings. Furthermore, CIDVs of EN coatings are significantly dependent on the mechanical properties (ductility) of the steel substrates. Substrates with ductility values similar to the EN coatings provide a better support for these coatings. In such a case, bending cracks appear at higher deflection values.

2. The results of the bending test showed that bending cracks travel transversely across EN coatings in straight and parallel lines. No sign of separation, branching, chip off, or delamination of the coatings was observed. This indicates the superior adhesion properties of EN coatings.

3. EN coatings have deleterious effects (up to 80% reduction) on the fatigue behavior of their 1018 substrates. Furthermore, the lower the phosphorus content, the higher this detrimental effect is.

4. Heat-treated EN coatings show lower fatigue resistance compared with as-plated EN coatings. Moreover, the detrimental effect of heat treatment is more pronounced in higher phosphorus content coatings. Furthermore, coating thickness has an adverse effect on fatigue behavior of EN coated specimens. This is attributed to the layered structure of thick EN coatings which may cause coating delamination.

5. The fact that EN coatings have such a significant effect on the fatigue behavior of their substrates can lead to the conclusion that EN coatings exhibit such an excellent adhesion with their substrates that cracks initiated on the coating surface propagate into the substrate without damaging the coating at the coating-substrate interface.

6. The EN coatings, even at low thickness (50 μm), have a significant effect on the fracture behavior of the substrate subjected to a tensile test. It was found that 50 μm thick low phosphorus EN coatings change the nature of failure under tensile stress from ductile (bare metal) to brittle (coated specimen).

5.1.3 Corrosion and wear evaluation

1. EN coatings in general have excellent corrosion and wear resistance under severe wear conditions. In particular, high phosphorus EN coating shows better corrosion resistance (due to its nano-crystalline microstructure) whereas low phosphorus EN coating shows better wear resistance (due to its high hardness value)
2. The results of erosion-corrosion experiments showed that EN coatings had excellent erosion-corrosion resistance at a high temperature, 100°C, in a potash brine environment.

3. The combination of superior adhesion properties and excellent hardness characteristics makes EN coatings excellent candidate materials for applications where severe corrosion and wear elements exist.

5.2 Recommendations

Based on the results of the present study, the following recommendations are deemed to be significant in improving both the deposition process and EN coatings' applications.

5.2.1 Recommendations for the EN coating process

1. Using distilled water rather than tap water during the rinsing stages is beneficial since various existing impurities in tap water may act as barriers for the EN deposition process. However, due to economic factors, using distilled water through all of the rinsing stages might not be feasible. In such a case, using distilled water in the last rinsing stage after electrocleaning is desirable.

2. For more complex shapes, it is important to provide a uniform current density during the anodic and cathodic electro-cleaning. Using a single electrode does not provide a homogeneous hydrogen or oxygen evolution on the entire exterior surface of the work piece. It was found that the best way to provide such a uniform current is by immersing the specimen(s) in a conductive container and using the body of the container as the cathode (in an anodic cycle) or as the anode (in a cathodic cycle).

3. Minimizing the lag time between each stage is crucial since the specimen immersed in the acid is very susceptible to oxidation in the presence of air. The oxide film formed in air deleteriously affects the properties of the EN deposit. Therefore, an appropriate setting is required for industrial capacity plating shops.

4. It is very important to use distilled water in making up the electrocleaning solution. The presence of contaminants and debris drastically affects the adhesion and porosity properties of EN deposits. It was found that the best result can be obtained when distilled or de-ionized water with very high resistivity (30 MΩ-cm or higher) is used for make-up solution.

5. Application of agitation during rinsing is very beneficial in removing the remaining acid trapped inside the pores on the surface of the specimen.

5.2.2 Recommendations for application of EN coatings

1. Generally, EN coatings are very corrosion and wear resistant. However, whenever corrosion is the main criterion, the high phosphorus EN coating is a better

candidate. On the other hand, wherever wear resistance is the dominant criterion, low phosphorus or high phosphorus heat-treated (@ 400 °C) EN coatings are recommended .

2. Since EN coatings are usually deposited with less than 100 μm of thickness, it is recommended to avoid using EN coatings to coat sharp edges in direct contact with abrasive surfaces or high velocity flows. Instead, the sharp edges should be moderately chamfered.

3. Whenever the EN coating is deposited on substrates under deflections or bending loads, it is recommended to choose, if possible, a substrate with closer mechanical properties (tensile strength and ductility) to those of EN coatings. For example, in such a scenario AISI 1045 is a better candidate substrate than AISI 1018.

4. EN coatings are porous in nature. As a result, the EN coated surfaces always include some porosity. The smoother the substrate surface, the more pronounced are the EN pores. Therefore, whenever the surface smoothness is not a major concern, it is recommended to sandblast the substrate with fine glass beads. This not only helps the removal of any contamination from the surface of the substrate, but also results in a better adhesion due to the increase in contact area between coating and substrate.

5. Although EN coatings have superior adhesion, they are not recommended for surfaces under impact. This is due to the brittle nature of EN coatings in general, and heat-treated EN coatings in particular.

6. EN coatings are usually applied up to 100 μm in thickness. It has been observed that thicker EN coatings are prone to delamination under relatively low deflection. Therefore, wherever a coating with higher thickness is required to protect a substrate under load (deflection), EN coatings are not recommended. In such cases, polymer coatings are better candidates.

7. EN coatings are lubricous. As a result, EN coated surfaces are recommended wherever the reduction of kinematic friction needs to be accomplished.

5.3 Future Work

The following are only a few among many aspects of EN study that the author would like to investigate in the future:

1. A more comprehensive TEM study on EN coating microstructures including the effect of heat treatment on the phase transformation of EN coatings (in progress).

2. Using TEM to investigate the mechanism of EN coating. There has been a long debate on whether EN coating deposition is a diffusion controlled process or simply the result of a series of chemical reactions. Using the available STEM equipment provides the opportunity of conducting an elemental analysis at the interface of coating and substrate at the atomic scale. Although such a study requires excruciating sample preparations, the results will be very rewarding.

3. Electrochemical Impedance Spectroscopy (EIS) is a powerful tool to study the corrosion resistance of coatings. Using EIS, a simulated model of corrosion in EN coatings can be made. As a result, the effect of various coating parameters such as phosphorus content, heat treatment, and coating thickness can be investigated through modeling (in progress).

4. Using EN techniques for depositing composite coatings is a very new nevertheless fast growing area in EN coatings. Using aluminum and silicon oxides, diamond, and PTFE particles in the coating bath has been studied briefly. Since the method is fairly new, any study on such coating systems will be very original and promising.

References

1. Allen R. M. and VanderSande J. B., "Structure Of Electroless Ni-P Films As a Function of Composition". Scripta Metall. Vol. 16, 1(982), 1161-1164.

2. Annual Book of ASTM Standard, Vol. 8.01, Designation D790, (1998), 145-156.

3. Annual Book of ASTM Standards vol. 03.01, , Designation E466, (1998), 471-487

4. Annual Book of ASTM Standards vol. 1.03, , Designation 380, (1998), 471-487

5. Apachitei, Duszczyk J., Katgerman L., and Overkamp P. J. B., "The Effect of Heat Treatment on the Microhardness of Substrate and Coating" Scripta Mater., Vol. 38 No. 9, (1998), 1347-1353.

6. ASTM Standard B 735-84, (1984).

7. Bagley B. G. and Turnbull D., " The Preparation and Cyrstalization Bhavior of Amorphous Nickel-Phosphrous Thin Flims", Journal of .Appl. Phys., Vol. 39 (1968), 5681-5685.

8. Bangwei Z., Zhaosheng T., Heng Z., Jueqi Y., and Xiaolin S., "Effect of Cerium CuPNiSn on Properties of Cupnisn Amorphous Alloys "Journal of the Chinese Rare Earth Society (English Edition), Vol. 11, No. 1, (1993), 41-45.

9. Barker D., "Electroless deposition of metals ", Trans. Inst. Metal Finish., Vol. 71 No. 3, (1993), 121-125.

10. Barker D., "Electroless Deposition of Metals", Trans. Inst. Metal Finish., Vol. 7 (1993), 121.

11. Baudrand D. W. and Bengston J., "Electroless Plating Processes Developing Technologies For Electroless Nickel, Palladium, and Gold ", Metal. Finish. (September 1995), 55-57.

12. Baudrand D. W., Metals Hand book, 8th edition, (1978).

13. Baudrand D., Proceedings of the SPIE - The International Society for optical Engineering, Los Angeles vol. 2649, (1995). 142

14. Beck J. and Arnold K., Parameter Estimation in Engineering Science, John Wiley & Sons, (1977).

15. Beer C. F., Surface Tech., Vol. 12 (1981), 89-92.

16. Berkh O., Bodnevas A., and Zahavi J., “Electrodeposited Ni-P-SiC Composite Coatings “, Plating Surf. Finish., Vol. 82 No. 11 (1995), 62-66.

17. Berkh O., Eskin S., and Zahavi J., “Properties of Electrodeposited NiP-SiC Composite Coatings “, Metal Finish., (march 1996), 35-40.

18. Bozordat R.M., Phys. Rev., 26, 1925, 390

19. Broszeit E., Heinke G., and Wiegand H., Metall, 25 (1975), 1110-1114

20. Burke Jr. J. T., “Corrosion Protection of Steels in Contact with Nitrogeneous Fertilizers and Solutions”, US Patent 2 901 439 (August 1959).

21. Carbajal J. and White E., J. “Electrochemical Production and Corrosion RTesting of Amorphous Ni-P “, Journal of the Electrochemical Society, Vol. 135 No. 12 (1988), 2952-2956.

22. Chen Y., Duh J., and Chiou B., “Effect of Substrate Surface Roughness on the Wettability of Sn-Bi solders “, Journal of Materials Science: Mater Electron, Vol. 11, (2000), 279-283.

23. Chitty J.A., Pertuz A., Hintermann H., and Puchi E.S., “Influence of Electroless Nickel-phosphorus Deposits on the Corrosion-fatigue Life of Notched and Un-notched Samples of an AISI 1045 Steel “, Journal of Materials Engineering and Performance, Vol. 8, (1999), 83-86

24. Chow Y., Lau W., and Karim Z., “Surface properties and Solderability Behaviour of Nickel-phosphorus and Nickel-boron Deposited by Electroless Plating “, Surface and Interface Analysis, Vol. 31, (2001), 321-327.

25. Dang H. and Moller P., Proceedings of the 80th AESF Annual Technical Conference Proc., Anaheim, CA, USA, (June 21-24 1993), 979-988.

26. Das L., Chin, D.T., “Electrochemical Porosity Measurement of EN Coating”, Plating and Surface finishing, Vol. 84, (1996), 66-68.

27. Data A., Robinkin A., and Bose D., Journal of welding, Vol. 63, No. 10, (1984), 14.

28. Deng and Hong, “Effect of the Substrate Surface Morphology”, Trans. Inst. Of Metal Finishing, 71(4), (1993).

29. Deng H. and Moller P., “Effect of the Substrate Surface Morphology on the Porosity of Electroless Nickel Coatings “, Trans. Inst. Metal Finish., Vol. 71 (1993), 142-148.

30. Deng H. and Moller P., “Effects of Pre-treatment on the Structure and Properties of Electroless Nickel Coatings “, Plating Surf. Finish., Vol. 81 (1994), 73-77.

31. Dickinson T., Sheet metal Ind., (1954), 312, p. 19

32. Dini, J.W. " Shear ring Adhesion", Metal Finishing, 25, (1972), 692-696

33. Dollimor D., Menis O., Rook H., and Garn P.D., "The State-of-the-Art of Thermal Analysis", Stand. (USA), Special Publcation, 580, U. S. Government Printing Office, Washington DC. (1980), 1-31.

34. Donahue F. and Yu C., Electrochem Acta, Vol. 15 (1970), 237.

35. Doong, J.C. , Duh, J.G., and Tsai, S.Y., "Corrosin Behaviour of EN Plating Modified TiN coating" Surface & Coating Technology, Vol. 27, No.1 Jan. (1986).

36. Duncan R. N., "Effect of Solution Age on Corrosion Resistance of Electroless Nickel Deposits ", Plat. Surf. Finish. Vol. 83 (1996), 65.

37. Duncan R. N., "Metallurgical Structure of EN Deposit, Plating and surface finishing, vol. 83, 1996, 65 R. Parkinson, Properties and applications of EN, NIDL, (1997)

38. Duncan R. N., "Metallurgical Structure of EN Deposit, Plating and surface finishing, vol. 83, (1996), 65.

39. Duncan R.N., "Effect of Solution Age on Corrosion Resistance of EN Plating", Surface Finishing, Vol. 10, (1983), 64-68

40. Duncan R.N., "Properties and Application EN". Finisher's management, Vol. 26, (1981), April.

41. Eggers W. J., "Evaluation of Organic Coatings by Electrochemical Impedance Spectroscopy" , EG&G Princeton Applied Research, CN 2565, (1998).

42. Ernst P., Wadsworth I. P., and Marshall G. W., "Porosity of Electroless Nickel Coatings Investigated Using Different Porosity Tests and Their Application ", Trans. Inst. Metal. Finish., Vol. 75 No. 5 (1997), 194-199.

43. Feldstein N., "Electroless Composite Plating. ", Metal Finishing, Vol. 81(8), (1983), 35-41.

44. Fields W., and Zickearff J.R., Electroless, Publication of ASM committee on EN-platting, (1984).

45. Fildes J. M., Chen P., and Zhan X., "Application of Electrochemical Impedance Spectroscopy, Color visible , and Infrared Imaging For Non-destructive Evaluation of Anti-corrosion coatings", Sensors Expo conference, Boston, (May 1995).

46. Fils J. and Duquette D.J., "Effect Of Phosphorus On Anodic Dissolution And Passivation of Nickel in Near-Neutral Solutions. ", Corrosion, Vol. 41, No. 12, (1985), 700-706.

47. Fitzsimmons T. and Henry N., "Corrosion Prevention in the Process industries", R. N. Parkins (ed.), Houston Texas, NACE (1990) 313.

48. Fontana M., Corrosion Engineering, 3rd Ed., McGraw-Hill, New York, (1986).

49. Gallory G. and Hajdu JB., "Fundamentals and Applications of Electroless Plating" American Electroplaters and Surface Finishers Society: Orlando, (1990).

50. Gawne D. T. and Ma U., "Structure And Wear of Electroless Nickel Coatings ", Mater. Sci. and Tech., Vol.3 (1987), 228-238.

51. Gawrilw G. G., Chemical EN plating. Protcullis press Ltd. (1979); p 101

52. Gemmler A., Zbolch T., Gut H., and Keller W.: "Mechanism of Electroless Nickel Deposition and Its Utilization in Expert Systems", Proc. 77th AESF Annual Tech. Conf., Boston, MA, (9-12 July 1990), 595-608.

53. Goldstein A. W., Rostoker W., and Rezek J., J. "Electron Microscope Study Of The Nucleation And Growth Of Electroless Cobalt And Nickel ", Electrochem. Soc., Vol. 119 No. 12, (1972), 1614-1619.

54. Graham H., Lindsay R. W., and Read H. J., J. Electrochem. Soc., Vol. 112 (1965), 401.

55. Grunwald P., Galvanotechnik, Vol. 74, (1983), 1286-1290.

56. Gutezit G., and Kring A., US Pat., 2.658.841, (1953).

57. Hadley J. and Tulsi, S. EN '89 Conference (1989).

58. Hammond R.A.F., Symposium on EN in engineering industry, London, (1963).

59. Hansen M., Der Aufbau der Zweistofflegierungen, Edward brothers, Ann Arbor, MI, 1943

60. Haowen X., Bangwei Z., Qiaoqin Y., "Preparation, Structure and Corrosion Properties of Electroless Amorphous Ni-Sn-P Alloys", Trans. IMF, vol. 77, No. 3, (1999), 99-102.

61. Hedayat A., Yannacopoulos A., Postletwaite J., " Wear and CO2 Corrosion of the Steel Couplings and Tubing in Heavy Oil Screw-pump Wells", Wear Journal, Vol. 209, (1997), 263-273.

62. Hedgecock N., N. Schlesinger, and M. Rezek, J., "Electron Microscope Study of The Nucleation and Growth of Electroless Cobalt And Nickel", Electrochem. Soc., Vol. 119 (1972), 1614-1619.

63. Herny J., Metal finishing, Guidebook and Directory, Vol. 88(1A), (1990), 367-382.

64. Heymann K.,and Doner Ch. in Brockmann W., "Haftung Als Basis Stoffverbunde und Verbundwerkstiffe", Deutshe ges. Fur Metallkunde, (1983).

65. Hickling A. and Johnson D., Electroanal. Chem., Vol. 13 (1967), 100.

66. Horne J. R. and Houlle L. S., "Advances in Phosphate Fertilizer technology", Gordon F. Palm (ed.) AIChE Symp. Ser. 89 (1993), 38.

67. Hosthersall, A.W. Inst. Metals, 107, (1948)

68. Hur K., Jeong J., and Lee D., J., "Microstructures and Crystallization of Electroless Ni-P Deposits", Mater. Sci., Vol. 25 (1990), 2573-2584.

69. International Standard ISO 4536 "Metallic and non-organic Coatings on Metallic Substrates -- Saline Droplets Corrosion Test (SD test)", (1985).

70. International Standard ISO 4541, "Metallic and Other Non-organic Coatings Corrodkote Corrosion Test (CORR test)", (1978).

71. International Standard ISO 9227 "Corrosion Tests in Artificial Atmospheres Salt Spray Tests", (1990).

72. Izumi H., Paper presented 18. Jap Conf. On Materials Research, (March 1975).

73. Jafar M.I. et al., "Some Factors Affecting Corrosion Resistance of EN", British corrosion journal, vol. 31, No. 3, (1996).

74. Jena A. K. and Chaturvedi M. C., Phase Transformations in Materials, 103; (1992), New Jersey, Prentice-Hall.

75. Kalantary M., Holbrook K. A., and Wells P. B., "Optimisation of a Bath for Electroless Plating and Its Use for the Production of Nickel-phosphorus-silicon Carbide Coatings" , Trans. Inst. Metal Finish., Vol. 71 (1993), 55-61.

76. Kehrer H.P., Ziese J. and Hoffmann F., HM, 37, (1982), 174-179.

77. Kerr C., Barker D., and Walsh F.C., "Physical and Electrochemical Characteristics of EN on Carbon Steel", Proceedings of the International Conference on Computer Methods and Experimental Measurements for Surface Treatment Effects, (1997), 47-59.

78. Khoperia T. N., Tabatadze T. J., and Zedgenidze T. I., "Formation of microcircuits in microelectronics by electroless deposition ", Electrochemica Acta, Vol. 42 No. 20-22, (1997), 3049-3055.

79. Koeneman J. and Metcalfe A. G., Trans. Metallurgy. Soc. Of AIME, 571, (Aug. 1958).

80. Konstantinov N., Anorg Z.. Chem. 60, 405, (1908).

81. Lashmore D. S. and Weinroth J. F., "Pulsed Electrodeposition Of Nickel-Phosphorus Metallic Glass Alloys", Plating Surf. Finish., Vol. 69 No. 8 (1982), 72-76.

82. Leisner P. and Benzon M.E., "Porosity Measurement of Coatings", Trans IMF, 75(2), (1997), 88-92.

83. Linka, and Riedel, "Corrosion Resistance of Nickel-Phosphorus Alloy Coatings Deposited by Chemical-Reduction", Galvanotechnik, (1986), 568-573

84. Luke D. A., "Nickel-Phosphorus Electrodeposits", Trans. Inst. Metal Finish., Vol. 64 No. 3, (1986), 99-104.

85. Lukes R., Plating, Vol. 51 (1964), 969.

86. Lyons V. C., "Proc. Seminar Fertilizer Plant Maintenance", New Delhi, India: U. S. Agency for International Development (1979), 243.

87. Mahoney M. W. and Dynes P. J., "Effects Of Thermal History And Phosphorus Level On The Crystallization Behavior Of Electroless Nickel ", Scripta Metall., 19, (1985), 539-542.

88. Mainier F. B. and Araujo M. M., "On the Effect of the Electroless Nickel-Phosphorus Coating Defects on the Performance of This Type of Coating in Oilfield Environments", IPE Advanced Technology Series, Vol. 2 No.1, (1994), 63-67

89. Mandich V. and Krulik A., "Fundamentals Of Electroless Copper Bath Operation For Printed Circuit Boards ", HBM Electrochemical & Engineering Co Metal Finishing, Vol. 91, No. 1 (Jan 1993), 33-41

90. Mansfeld F., Kending M., Tsai S., "Evaluation of Corrosion Behavior of Coated Metals With AC Impedance Measurements", Corrosion, Vol. 38, (1982), 478-485.

91. MFPP-Process Guide, 11, Sept/Oct. (1975), 144-152.

92. Mittemeijer E. J., Cheng Liu, Van der Schaaf, P.J., C. M. Brakman, and B. M. Korevaar, “Analysis Of Nonisothermal Transformation Kinetics; Tempering Of Iron-Carbon And Iron-Nitrogen Martensites” Metallurgy Trans. A, (1988), 19A, 925-932.

93. Moonir-Vaghefi S.M., Saatchi A., “Deposition and Properties of Elecetroless Nickel-Phsophsorus-Molybdenum Disulfide Composite”, Metal Finishing, Vol. 95, No. 11, (1997), 46-53.

94. Munemass J. and Kumakiri T., “Effect of the Surface Roughness of Substrates on the Corrosion Resistance Properties of Thin Films Coated by Physical Vapour Deposition, (1991).

95. NACE Publication 6A287, “Electroless Nickel Coatings”, National Association of Corrosion Engineers, Houston, Texas, 1987.

96. Nahle H., Kerr, D. Barker, and F.C. Walsh, “A Rapid Electrochemical Test for Porosity in EN Coating on Carbon Steel Substrates”, Trans IMF, 76(1), (1998).

97. Narcus H., Plating, Vol. 54, No. 4, (1967), 381.

98. Nargi C. and Shawhan G., “Electroless Nickel For Engineering Applications: It's Not Always The Best Choice “, AES Second Electroless Plating Symposium Orlando, FL, USA, E, 8p Sponsored by: American Electroplaters' Soc (1983)

99. Nicholls R. V. V., "Two Hundred Years of Canadian Potash", Phosphorus and Potassium, No. 201 (1996), 22-26.

100. Nishira, Masayoshi; Takano, and Osamu, “Friction and wear characteristics of electroless Ni-P-PTFE composite coatings”, Plating and Surface Finishing, Vol. 81, No. 1, Jan, (1994), 48-50.

101. Okinaka Y., Osaka T., Gerischer and C. W. Tobias (ed.), “Advances in Electrochemical Science and Engineering”, Weinheim, Germany H., Vol. 3 (1994), VCH, 55.

102. Padget J.C. and Moreland P. J., “Use of AC Impedance in Study of the Anticorrosion Properties of Chlorine-Containing Vinyl Acrylic Latex Polymers” Coating Technology, Vol. 55 No. 698, (1983), 39-51.

103. Park S. H. and Lee D. N., “A Study on the Microstructure and Phase Transformation of Electroless Nickel Deposits”, J. Mater. Sci., Vol. 23 (1988), 1643-1654.

104. Park S. H. and Lee D. N., “Study on the Microstructure and Phase Transformation of Electroless Nickel Deposits”, Journal of Mater. Sci., Vol. 23 (1988), 1643-1654.

105. Parker K. and Shah H., “Residual Stresses in Electroless Nickel Plating”, Plating, 58 (1971), 230.

106. Parker K., "Recent Advances in Electroless Nickel Deposits”, 8th international conference, Sep 5-9, Basel, Switz, Publisher: Forster-Verlag, Zurich, Switz (1972), 202-207.

107. Parker K., “State of Art”, The Proc. 77th AESF Annual Tech. Conf. (1990), Boston, MA, 1425-1441.

108. Parker K., Platin, “Hardness and Wear Resistance Tests of Electroless Nickel Deposits “, Vol. 61, No.9, (September 1974), 834-841.

109. Parker K.,” Effects of Heat Treatment on The Properties of Electroless Nickel Deposits”, Plating and Surface Finishing, v 68, n 12, Dec, 1981, p 71-77

110. Parkinson R., “Nickel Development Institute Technical Series No. 10081”, (1995), 1-37.

111. Parkinson R., Properties and applications of EN, Nickel Development Institute, NiDI Techenical Series No. 10081, (1997),

112. Pertuz A., Chitty J.A., Hintermann H., and Puchi, E.S., “Corrosion-fatigue Behavior of an Annealed AISI 1045 Carbon Steel Coated With Electroless Nickel-phosphorus**”,** Journal of Materials Engineering and Performance”, Vol. 8, (1999), 424-428.

113. Prabhu-Gaunkar G. V., Corrosion Reviews, Vol. 16 (1998), 393-416.

114. Prasad, P.B.S.N.V, Ahila, S.; Vasudevan, R.; Seshadri, S.K., “Fatigue Strength of Nickel Electrodeposits Prepared in Ultrasonically Agitated Bath “Journal of Materials Science Letters, vol. 13, No. 1, Jan 1, 1994, 15-16.

115. Puchi E.S., Staia M.H., Hintermann H., Pertus A., and Chitty J., “Influence of Ni-P electroless coating on the fatigue behavior of plain carbon steels “, Thin Solid Film, Vol. 290-291, (1996), 370-375.

116. Puipee J.C. and Tobias J.P., Surface Modification Technology, (1989), 707-708

117. Queau, G., Stremsdoerfer, G., Martin, J.R., and Clechet, “Electroless Metal Deposition as a Useful Tool for Microelectronics and Microstructures “, Plating and Surface Finishing, Vol. 81, No. 1, Jan, 1994, 65-69.

118. Reddy V.V.N., Ramamoorthy, B., Nair P., Kesavan, “Study on the wear resistance of electroless Ni-P/diamond composite coatings”, Wear, Vol. 239, (2000), 111-116.

119. Reidel W., “Electroless Nickel Plating”, ASM international, Metals Parks, Oh. (1991), 68-69

120. Reidel W., Electroless Nickel plating, ASN International, (1997).

121. Reinhardt G, Paper presented at EN-Conf., Cincinnati, 6 and 7, Nov. (1979).

122. Riedel W., Electroless Nickel Plating, Finishing Pub. Ltd., Stevenage, Hertfordshire, England (1991).

123. Safranek W.H., ASTM-Spec. Techn. Publ., Vol. 265, (1959), 41-49.

124. Salvago G., and Cavalotti P., Plating and Surface Finishing, (July 1972), 665-671.

125. Simon H. and Thoma M., Konstruktion, Vol. 37, No.6, (1985), 235-241

126. Simon J., Zakel E., Reich H., “Electroless Deposition of Bumps for TAB Technology”, Proceedings of the 40th Elec. Components and Technology Conference, Vol. 1. New York, 412, (1990), 412-417.

127. Singh D., Balasubramaniam R. and Dube R.K., “Effect Of Coating Time On Corrosion Behaviour Of Electroless Nickel-Phosphorus Coated Powder Metallurgy Iron Specimens”, Corrosion vol. 51, No.8, (1995).

128. Solowjewe N.A., J. Prikladnoj Chimnij, (1959), 556

129. Spähn H., Trans. Inst. Metal finishing, Vol. 42, (1964), 365-379.

130. Stevenson M., “EN, No Longer a Coating”, Anoplate Corporation, 1996).

131. Stevenson M., Technical report, Anoplate Corporation, (1992).

132. Strathdee G., "Performance of Materials in Potash Production", Phosphorous and Potassium, No. 205 (1996), 33-40.

133. Taheri R., Ogucha I.N.A., Yannacopulos S., “Effect of Heat treatment on the Age Hardening Behavior of Electroless Nickel-Phosphorus Coatings”, Materials Science and Technology, Vol. 17, March (2001), 278-284.

134. Tallet A., “Corrosion Resistance of EN in Food Acid Environments”, Metal finishing, 9, (1988).

135. Tulsi S.S., “Properties Of Electroless Nicke“, Transactions of the Institute of Metal Finishing, Vol. 64, No. 2, (May 1986), 73-76.

136. Tomlison W. and Mayor J. P., “Microstructure and Surface Roughness and Porosity of EN”, Surface Engineering, (1988).

137. Tope N., Baker E., and Jackson B., "Evaluation Of The Wear Properties Of Electroless Nickel", Plating and Surf. Finish. (October, 1976), 30-37.

138. Tracy R.P. Colaruotolo, Joseph, Misercola, Anthony, Chuba, and Barry R., "Corrosion And Economics of Electroless Nickel Coatings in Chemical Process Environments." Materials Performance, Vol. 25, no. 8, (1986), 21-29.

139. Tulsi S., "Electroless Nickel-Ptfe Composite Coatings", Transactions of the Institute of Metal Finishing, Vol. 61, (1983), 142-149.

140. Vafaei-Makhsoos E., Thomas E. L., and Toth L. E., "Electron Microscopy Of Crystalline And Amorphous Ni-P Electrodeposited Films: In-Situ Crystallization Of An Amorphous Solid ", Metallurgical Transactions, Vol. 9A (1978), 1449-1460.

141. Walter G.W., "Application of Impedance Measurements to Study Performance of Painted Metals in Aggressive solutions", Electroanal. Chem., Vol. 118, (1981), 259-273.

142. Weil R. and Parker K., G.O. Mallory, and J.B. Hajdu, "Electroless Plating Fundamentals and Application", American Electroplating and Surface finishers Society, Orlando, Florida, USA, (1990), Chapter 4, 111.

143. Weil R., Lee J.H., Kim I., and Parker K. "Comparison of Some of Mechanical and Corrosion Properties EN and Eectroplating Nickel-Phosphorus Alloys", plating and surface finishing, Vol. 76, No. 2, (1989), 62-66

144. Weiss Z., "High-temperature Oxidation of Iron Covered by Electroless Ni-P Coating: A GDOS Depth Profiling Study ", Surface and Interface Analysis, Vol. 18 (1992), 691-694.

145. Wesley A. W. Plating, vol. 7, 1950, 732 .

146. Williams J. A., "Engineering Tirbology", Oxford University Press, (1994).

147. Wing L. M., Linda M., "Use of Electroless Nickel on Automotive Components", Trans. Inst. Metal Finish., Vol. 75 No. 1 (1997), B11-B14.

148. Wing L., EN '93 Conference, November, (1993).

149. Wong K., Chi K., and Rangappan A.. Plat. Surf. Finish. 75, 70, (1988).

150. Wronkowska A.A., J., "In situ and Ex Situ Characterization of Passive Layers on Ni1-xPx alkaline Solution", Electrochem. Soc. Vol. 140, No. 4, (1993), 995-1005.

151. Wu Y., Zhang Y., and Yao M., "Effect of Electroless Nickel Plating on Fatigue Strength of 30CrMoA steel ", Plating and Surface finishing, (1995), 83-85.

152. Xam-Hua Z. et al. Wear, Vol. 157, (1992), 381-387.

153. Xinmin H.and Zongang D., Trans. Inst. Metal Finish., Vol. 70 (1992), 84.

154. Yamasaki T., Izumi, H and Sunada H., "Microstructure and Fatigue Properties of Electroless Deposited Ni-P Alloys ", Scripta Metallurgica, Vol. 15, (1981) ,177-181.

155. Young B., Duh J., and Chiou B., "Wettability of Electroless Ni in the Under Bump Metallurgy With Lead Free Solder "Journal of Electronic Materials, Vol. 30, No. 5, (2001), 543-553.

156. Yu X., Wang H., Yang Z., Yin P., and Xin X., "XPS and AES investigation of two Electroless Composite Coatings ", Applied surface Science, Vol. 158, (2000), 335-339.

157. Yusis Z. Z., Yu Y., Laynkaitene I., and Lunyatskas A. M., "Reaction of Phosphorus Formation During Chemical Nickel Plating", Plenum publishing corporation, (1889). molybdenum disulfide

158. Zhang Y.Z. and Yao M., "Studies of Electroless Nickel Deposit With Low Phosphorus Content", Trans IMF, Vol. 77, No. 2, (1999), 78-83.

159. Zhang, Bangwei, Xie, and Haowen, "Effect of Alloying Elements on the Amorphous Formation of Corrosion Resistance of Electroless Ni-P Based Alloys", Elsevier Science, Vol. A 281, (2000), 286-291.